Urbanergy WindVine

Final Report

DSE Group 03

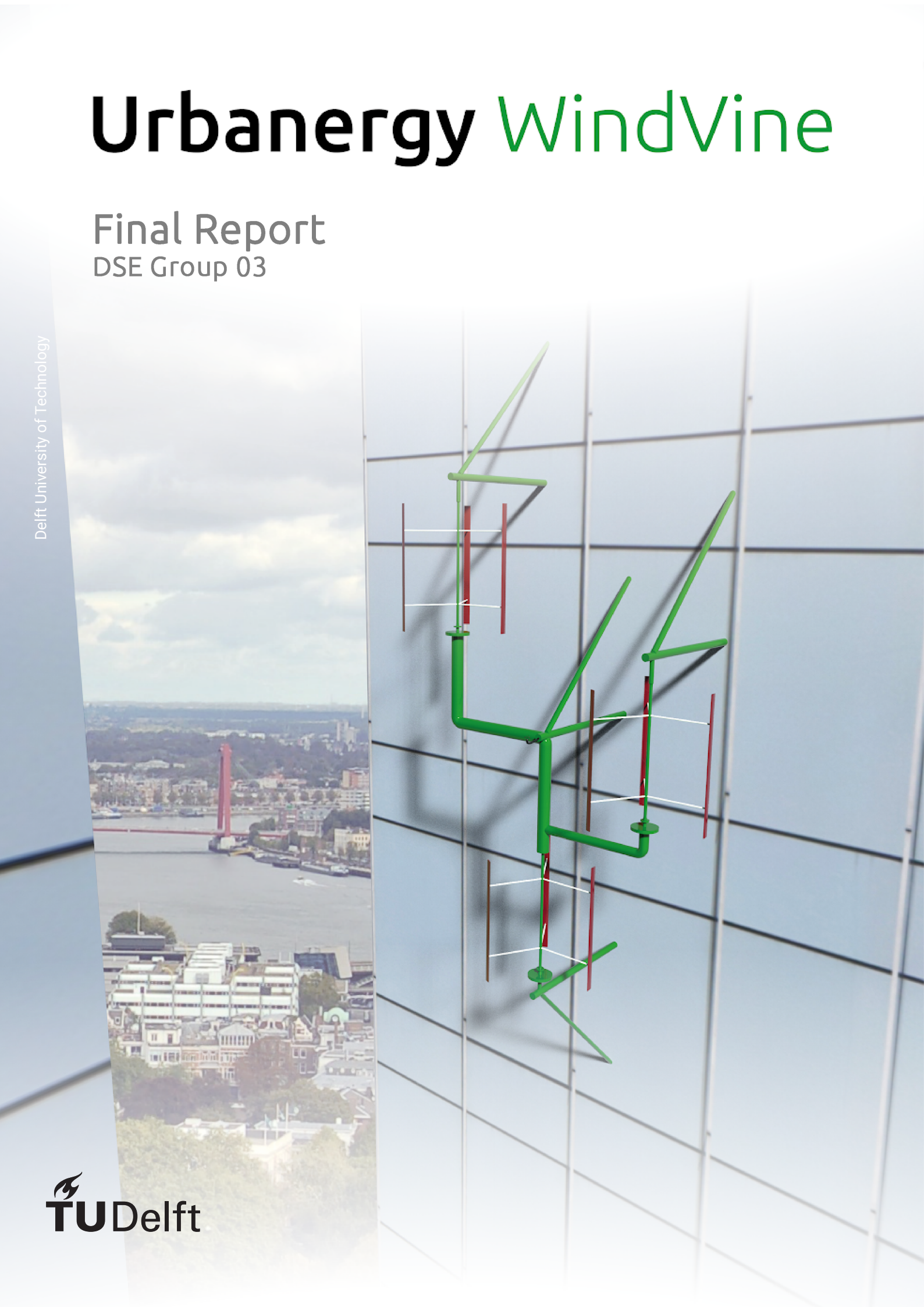

Delft University of Technology

TU Delft

This page is intentionally left blank.

DSE: FINAL REPORT

WIND ENERGY SYSTEM INTEGRATED BETWEEN HIGH-RISE BUILDINGS

BY

DSE GROUP - 03

FACULTY OF AEROSPACE ENGINEERING, DELFT UNIVERSITY OF TECHNOLOGY

Group Member	Fayt, Vladimir	4673301	
	Follet, Arthur	4548329	
	Loonen, Martijn	4666615	
	Norbruis, Rogier	4556658	
	Postma, Thies	4558359	
	den Ridder, Luc	4543165	
	Schrijver, Koen	4538315	
	Schwarzpaul, Levin Waitangi	4545230	
	Stensen, Jari	4666380	
	Vleeschouwer, Kjell	4557107	
Tutors	Avallone, Francesco	Asst. Prof.	Wind Energy
	Eleftheroglou, Nick	Researcher	Structural Integrity & Composites
	Kootte, Luc	PhD Student	AE Structures & Computational Mechanics

Table 1: Change log

issue	date	pages affected	Description of change
1	June 22, 2020	all	Full draft
2	June 30, 2020	all	General feedback on all chapters was implemented and diagrams improved. The market analysis extented. Directivity function included. Noise & aero model explanation improved. Serration sizing explanation improved. Shaft & Connectors designed without thin-walled assumption. Clearer assumptions for vibrations of support structure. Data handling diagram improved to also include hardware/software. Drawings updated.

TU Delft

JUNE 30, 2020

Preface

This report is the result of the combined effort of 10 students working for 10 weeks towards one goal: creating an urban renewable wind energy option. This report is part of the Design Synthesis Exercise and thus forms the final report of these students' Bachelors of Science in Aerospace Engineering. This being the last report, it tries to exemplify the knowledge gained during this Bachelors program.

The Design Synthesis Exercise has been an educative experience for us and provided us with hands on know how of the design process. Not only a lot of technical knowledge was obtained but also expertise in Project Management and Systems Engineering. Additionally, a look into the world of wind energy was intriguing from the aerospace perspective. Although initially hindered by the limitations caused by the COVID-19 pandemic, the team soon learned to work around these, and used the situation as an opportunity to get experience in working in a team remotely.

The team would like to thank Francesco Avallone, Nick Eleftheroglou and Luc Kootte for their knowledge, guidance and support throughout this project, which helped us a lot throughout the entire Design Synthesis Exercise.

The team would additionally like to thank Livia Brandetti for supplying us with verification data from her vertical-axis wind turbine model and help with improving our noise model.

Furthermore, the team would like to thank the Teaching Assistants, especially Thomas Hunter, for their feedback, ready availability and first hand experience throughout the Design Synthesis Exercise. Their input primarily on the project management and systems engineering side of the project was of great value in performing the design process.

Lastly, the team would like to thank the DSE Organising Committee for the opportunity and the facilities to perform the Design Synthesis Exercise from home.

Group 03
June 22, 2020

Executive Overview

The demand for renewable energy has increased significantly over the past years. During the last decades it became clear that the main source of renewable energy will be wind energy. The wind turbines, still growing in size every year, are almost all located in either remote rural or offshore areas. However, there lies a huge opportunity in implementing wind harvest systems in urban areas.

The aim of this project is to create a wind harvest system integrated in between two high-rise buildings and providing the generated energy locally. The system should be able to be implemented in the Netherlands, complying with all local regulations, and be within a budget of €75,000 unit cost. This resulted in the following mission need statement:

"Provide a local sustainable wind-energy harvesting source for urban usage"

This mission need statement ensues in the following more detailed project objective statement:

"Design an integrated wind energy harvesting system in between two high-rise buildings, by ten students within ten weeks."

To be able to come up with the most efficient design, first an extensive concept sizing for five different design options is done. These concepts were: Horizontal axis wind turbines(HAWT), vertical axis wind turbines(VAWT), pressure based systems(AeroMINE), the hummingbird turbine and kite systems. These five concepts have been compared in a first trade-off, using weighted criteria. The HAWT, VAWT and AeroMINE came out as the best concepts. A second trade-off had been done not only comparing the harvesting type, but also the location of the turbine, namely either at the side of the building or in between the buildings. The VAWT at the side of the building and the HAWT in between the buildings came out as the best options. The VAWT was chosen as the final concept, mainly because it has a higher efficiency at lower/more turbulent wind conditions, thus matching the urban environment better.

Before starting with the design, a market analysis and sustainability approach was created, both being crucial during the entire design process. The market analysis concluded that the first system will be placed in Rotterdam, a city with a good infrastructure and the widest high-rise vision of The Netherlands. Sustainability both includes the materials used and having an environmental friendly production. The foundation of our sustainability approach is maintaining a circular economy, where the production of waste is minimized and a continual use of resources is applied. All sustainability goals are met except for the social economic goals, since the noise regulations are not met in the proximity of the turbine.

With market analysis and the sustainability approach in mind, the final design could be started. The system will be integrated between two 200-meter high-rise buildings generating over 50 MWh a year. The design consists of three vertical axis lift driven wind turbines each with a rated output power of 11 kW. The turbines are supported by an organically looking support structure, resembling a vine growing on the building. The urban environment in which the system is placed brings up a lot of challenges that need to be tackled regarding both the aerodynamic and structural integration.

When it comes to aerodynamics, mainly two coherent problems were encountered; making the rotor as efficient as possible while keeping the emitted noise within the regulations. For the efficiency it needs to be taken into account that the average wind speed will be 10 m/s Gaussian distributed. To ensure an optimal aerodynamic performance it chosen to make the system with three blades. Although, two blades have the highest efficiency, having three blades has the advantage that the torque and aerodynamic forces are more constant during the rotation. Another crucial factor for the efficiency is the airfoil of the blades. Only symmetric airfoils were considered in a trade-off, since they have power coefficients at tip speed ratios higher than three. The NACA0018 was chosen because of its high C_p and structural advantages over thinner airfoils. In order to fulfill the given power requirement of 50 MWh a year, an iterative design process was done. This resulted in the dimensions presented in Table 2.

Table 2: Main dimensions and parameters for one turbine.

Parameter	Value	Unit	Parameter	Value	Unit
Swept area	27.97	m^2	Rotational speed	151	RPM
Height	5.55	m	$V_{tip_{max}}$	40	m/s
Radius	2.52	m	Airfoil	NACA0018	-
Solidity	0.33	-	Power control	Passive stall	-

The regulations in the Netherlands allow for a maximum noise output of 47 dB(A) during the day and 41 dB(A) during the night. Taking these requirements into account it was determined that the system should have a lower average noise than 45.5 dB(A). A BPM model was generated to analyze the most critical noise of the VAWT, the airfoil self-noise. The model gave an average noise output of 56.9 dB(A) which means that the noise requirements are violated. To meet the requirements, the maximum tip speed was set at 40m/s and serrations were applied. When implementing this, the noise requirements are reached at a distance of 13 meters. It should be kept in mind that the system is integrated at 4 meters from the building. This means that only within a radius of 9 meters too much noise is generated. To mitigate the noise, several mitigation methods were researched: including a noise panel, facade optimization and active noise control. The latter is the most promising method, which could be implemented in the design in the future, but needs further investigation.

To generate electricity the wind harvest system uses a permanent magnet synchronous generator, which converts mechanical energy to electrical energy. This is a direct drive generator, which means a gearbox is not needed. The poor self-starting ability of the vertical axis wind turbine is conquered by using the generator as an engine to drive the turbine. A brake system guarantees safety in case of failure or planned maintenance. The blades are connected to the generator by the main shaft and smaller connectors, that are designed to withstand the aerodynamic and gravitational loads as well as the torque created by the turbine.

The support structure of the turbines will be a tree structure made of low-carbon steel and supports the total weight of all three turbines combined, 2,110 kg. The system is placed outside of the 4 m boundary layer of the building. A polymer coating was applied to protect against corrosion. Since the natural frequency of the the structure is higher than the operating frequency of the turbine, the support structure will not experience any problems due to vibrations. The total weight of the support structure is 4,675 kg.

The system will be controlled by one central unit, getting input from both external and internal sensors. The external measurement units consists of wind direction and speed meters. The internal measurement unit is added to detect possible failures and includes strain gauges, accelerometers, connectivity and current sensors. The control unit makes sure safety is guaranteed during operations and risks of failures are being kept low. A step-down transformer converts the 380V output of the generator to the 230V needed for the energy grid.

This resulted in our final design: the "Urbanergy WindVine". It is an aesthetically pleasing, innovative system that can be applied in any city worldwide. In total 52 Mwh will be produced on a yearly basis, thus meeting the requirements. The total cost of the system is €62,000 and return of investment takes 16 years. The way people think about urban wind energy harvesting is about to change drastically. Not only will it make cities greener, it will also make the people aware of the possibilities of wind technology.

Contents

Abbreviations vi

Symbols vii

1 Introduction 1

2 Project Setup 2
- 2.1 Project Objective . . . 2
- 2.2 User Requirements . . . 2
- 2.3 Market Analysis . . . 3
- 2.4 Location and Environment Analysis . . . 12
- 2.5 Resource Allocation Class I . . . 14
- 2.6 Sustainability Approach . . . 15

3 Design Approach 19
- 3.1 Conceptualization . . . 19
- 3.2 System Sizing . . . 24

4 Wind Harvesting System 25
- 4.1 Functional Analysis . . . 25
- 4.2 Functional Requirements . . . 25
- 4.3 Rotor sizing . . . 26
- 4.4 Power Train . . . 35
- 4.5 Airborne Noise . . . 39
- 4.6 Structural Analysis . . . 51
- 4.7 Resource and Sustainability Overview . . . 66

5 Structural Support System 68
- 5.1 Functional Analysis . . . 68
- 5.2 Functional Requirements . . . 68
- 5.3 Support Structure . . . 69
- 5.4 Structural Analysis . . . 70
- 5.5 Vibrations in Structure . . . 80
- 5.6 Resource and Sustainability Overview . . . 82

6 Electrical and Control System 84
- 6.1 Functional Analysis . . . 84
- 6.2 Functional Requirements . . . 86
- 6.3 Control Unit . . . 86
- 6.4 External Measurement Unit . . . 88
- 6.5 Internal Measurement Unit . . . 88
- 6.6 Grid sizing . . . 89
- 6.7 Resource and Sustainability Overview . . . 93

7 Final System 94
- 7.1 Performance Analysis . . . 95
- 7.2 Sensitivity analysis . . . 95
- 7.3 Validation Process in Further Development Phase . . . 96
- 7.4 RAMS and Risks . . . 97
- 7.5 Final Design Summary . . . 105

8 Project Development 110
- 8.1 Project Design and Development Logic . . . 110
- 8.2 Production Plan . . . 114
- 8.3 Operation and Logistic Concept . . . 117
- 8.4 Resource (Class II) and Financial Analysis. . . . 118
- 8.5 Sustainability Score Final Design . . . 123
- 8.6 Compliance Matrix . . . 126

8.7 Future Vision 128
9 Conclusion and Recommendation 130
9.1 Conclusion 130
9.2 Recommendation 130
Bibliography 132
A Functional Breakdown Structure 136
B Material Overview 137
C Catia Drawings of Final Design 138

Abbreviations

ANC	Active Noise Cancellation	50, 51
BMWT	Building Mounted Wind Turbine	81, 82
BPM	Brooks, Pope and Marcolini	40–44
CFRP	Carbon Fiber Reinforced Polymer	53, 54, 137
DOT	Design Option Tree	20, 21
DSE	Design Synthesis Excercise	16, 110
DSM	Double-Multiple Streamtube	26, 27, 31
ECS	Electric and Control System	15, 16, 84, 89, 93, 116
FBS	Functional Breakdown Structure	20
FEA	Finite Element Analysis	78–80
FFD	Functional Flow Diagram	19, 20, 84
GDP	Gross Domestic Product	4, 5
GFRP	Glass Fiber Reinforced Polymer	53, 137
GWA	Global Wind Atlas	12
HAWT	Horizontal Axis Wind Turbine	15, 20–22, 35, 38
LCOE	Levelized Cost of Energy	122, 123
MAI	Manufacture, Assembly and Integration	114
MNS	Mission Need Statement	2
NDT	Non-Destructive Testing	115
OASPL	Overall Sound Pressure Level	40, 43, 46, 82
PLA	Polylactic Acid	137
PMSG	Permanent Magnet Synchronous Generator	35, 46, 105
PNC	Passive Noise Cancellation	47
POS	Project Objective Statement	2
PPP	Purchasing Power Parity	4
RoI	Return on Investment	17
RPM	Revolutions per Minute	34, 35, 38, 39
SPL	Sound Pressure Level	41, 43, 44, 46
SSS	Structural Support System	15, 16, 68, 76, 83, 88, 89, 101, 116, 117, 120, 124
SWOT	Strength, Weaknesses, Opportunities, Threats	3, 6, 7, 11
tpPVC	Thermoplastic Polyvinyl Chloride	76, 116
TSR	Tip Speed Ratio	27–30, 32, 34, 37
VAWT	Vertical Axis Wind Turbine	15, 17, 18, 20–24, 26–29, 31, 33, 35–40, 42, 43, 49, 69–73, 81, 97, 101, 105–107
WES	Wind Energy System	3–16, 18, 19, 24, 25, 36, 38, 50, 51, 82, 87, 89, 90, 92, 94, 95, 100–102, 106, 118, 120, 121, 128
WHS	Wind Harvesting System	6, 12, 15–17, 19, 21, 22, 24, 25, 37–39, 43, 47, 49, 51, 53–55, 65, 66, 68–71, 73, 75, 88, 99, 106, 116–120, 124, 137
ZPII	Zoning, Permitting, Inspection, and Incentives	119, 120

Symbols

Symbol	Description	Units
α	Angle of attack	$[degrees]$
δ	Boundary layer thickness	$[m]$
δ	Displacement	$[m]$
δ_p^*	Boundary layer displacement thickness pressure side	$[m]$
δ_s^*	Boundary layer displacement thickness suction side	$[m]$
θ	Twist angle	$[degrees]$
λ	Tip speed ratio	$[-]$
ρ	Air density	$[kg/m^3]$
σ	Rotor solidity	$[-]$
σ_{normal}	Normal stress	$[Pa]$
$\sigma_{bending}$	Bending stress	$[Pa]$
σ_{vms}	Von Mises stress	$[Pa]$
$\sigma_{allowed}$	Allowable stress	$[Pa]$
$\sigma_{fatique}$	Fatique stress	$[Pa]$
τ_{shear}	Shear stress	$[Pa]$
$\tau_{torsion}$	Torsional stress	$[Pa]$
ϕ	Azimuth angle	$[degrees]$
ω	Angular velocity	$[rad/s]$
ω_n	Natural frequency	$[Hz]$
A	Area	$[m^2]$
A	Spectral shape function	$[-]$
$A(f)$	A-weighting	$[dB]$
A_b	Blade area	$[m^2]$
A_H	Fraction of total area occupied by nearby buildings	$[-]$
A_p	Panel area	$[m^2]$
a	Amount of hours in a year	$[h]$
b	Spacing	$[m]$
B	Spectral shape function	$[-]$
c	Chord length	$[m]$
c_0	Speed of sound	$[m/s]$
CF	Capacity factor	$[-]$
C_d	Drag coefficient	$[-]$
C_n	Normal coefficient	$[-]$
C_p	Power coefficient	$[-]$
C_t	Tangential coefficient	$[-]$
D	Diameter	$[m]$
DT	Downtime	$[h]$
D_h	High frequency directivity	$[-]$
D_l	Low frequency directivity	$[-]$
d	Blade span	$[m]$
E	Young's modulus	$[GPa]$
E_{req}	Energy required	$[Wh]$
F	Force	$[N]$
FR	Failure rate	$[-]$
f	Frequency	$[Hz]$
f_n	Eigenfrequency	$[Hz]$
f_0	Perceived frequency	$[Hz]$
f_{bl}	Block forces	$[N]$
G	Shear modulus	$[Pa]$
$G_{BB}(f)$	Overall acoustic pressure signal,	$[Pa]$
$G(f)$	Acoustic pressure at the observer location	$[Pa]$
H	Height	$[m]$

$\overline{H}$	Average height of surrounding buildings	$[m]$
H_{stg}	Stagnation height	$[m]$
H_{sys}	Possible system placement height range	$[m]$
I	Second moment of inertia	$[m^4]$
I	Current	$[A]$
J	Polar moment of inertia	$[m^4]$
K	Amplitude correction factor	$[dB]$
k_{eq}	Spring stiffness	$[N/m]$
L	Length	$[m]$
L_{den}	Day-evening-night sound pressure level	$[dB(A)]$
L_{day}	Day sound pressure level	$[dB(A)]$
L_{evening}	Evening sound pressure level	$[dB(A)]$
L_{night}	Night sound pressure level	$[dB(A)]$
l	Distance	$[m]$
M	Mass	$[kg]$
M_p	Panel mass	$[kg]$
$M_{x/y/z}$	Moment in x/y/z direction	$[Nm]$
M_0	Mach number	$[-]$
N	Number of blades	$[-]$
n	Factor related to Reynolds number	$[-]$
n_{phi}	Amount of angular discretization points in a revolution	$[-]$
n_s	Rotational speed	$[rpm]$
P	Power	$[W]$
P	Number of poles	$[-]$
P_{rated}	Rated power	$[W]$
p	Fixed pitch angle	$[degrees]$
q_s	Shear flow	$[N/m]$
R	Radius	$[m]$
R	Resistance	$[ohm]$
$R_A(f)$	Input function for the A-weighting	$[W/m^2]$
r	Radius	$[m]$
r_p	Panel radius	$[m]$
s_t	Strouhal number	$[-]$
s	Spacing	$[m]$
T	Torque	$[Nm]$
t	Thickness	$[m]$
t_{op}	Operation time	$[h]$
u	Wind velocity	$[m/s]$
U_0	Local velocity of the blade	$[m/s]$
U_∞	Free stream wind velocity	$[m/s]$
U_r	Relative velocity of observer to noise source	$[m/s]$
U_s	Relative velocity of noise source to observer	$[m/s]$
u_{max}	Wind velocity outside boundary layer	$[m/s]$
V	Speed	$[m/s]$
V	Shear force	$[N]$
v_b	Operational velocity	$[m/s]$
W	Weight	$[N]$
W_p	Pressure side noise	$[dB]$
W_s	Suction side noise	$[dB]$
W_α	High angle of attack noise	$[dB]$
W_{bpm}	Noise from bpm model	$[dB]$
y	Location in y-direction	$[m]$
$Y^T_{C,cb}$	Mobility matrix	$[-]$
z	Distance to observer	$[m]$

1 Introduction

Climate change is one of the biggest issues our society faces at the start of the 21^{st} century.[1] To tackle climate change, it was necessary to take a good look at the energy industry. In the past years, the demand for renewable energy has been growing constantly.[2] Wind energy is one of the most universally applied, due to the fact that it runs on a cheap and easy accessible energy source: wind.[3] While most of the existing wind turbines are located in rural areas, the potential of urban wind energy is often ignored. This report will tackle the perceived issues with low efficiency, safety and noise.[4] Still, the rapid increase of energy needs of cities as well as prospect of a source of renewable energy so close to home, has created the need for urban wind energy. One of the possible solutions is the integration of wind harvest system onto high-rise buildings, as they experience higher wind loads with increasing heights [1].

The main goal of this report is thus to perform a preliminary design of a renewable wind energy system that could be integrated in-between two high-rise buildings. To do so, both a technical and non-technical approach will be needed. A technical approach is required to get the optimal design for the given requirements set by the client. The non-technical part will, throughout the design process, consider the economic, social and environmental impacts of such a system. Combining the two will allow for a fully developed design concept that will satisfy the need of the client.

In order to start-off this design process, the project setup with the various analysis, that allow for a preliminary sizing, are discussed in Chapter 2. Following this, Chapter 3 conceptualizes the project and by using multiple trade-offs an initial design is determined. Chapter 4 goes more into detail with all the subsystems of the harvesting system itself. The technical capabilities of Urbanergy will be utilized, such as aerodynamic and noise analysis, to create the current final turbine design. Next, the support structure is determined in Chapter 5 by doing an extensive structural analysis taking vibrations into account. Furthermore, the electrical systems are designed and documented in Chapter 6. The whole system is then showcased in Chapter 7 , to be followed by the possible future and timeline of this project in Chapter 8. Finally the report is concluded concisely with its last section: Chapter 9.

This report is the final report of this project and succeeds the previously written Baseline and Midterm Report, which can be solicited for more details.

[1] https://www.ipcc.ch/sr15/ [cited 19 June 2020].
[2] https://www.iea.org/reports/renewables-2018 [cited 19 June 2020].
[3] https://www.ge.com/renewableenergy/wind-energy/what-is-wind-energy [cited 19 June 2020].
[4] https://www.buildinggreen.com/feature/folly-building-integrated-wind [cited 19 June 2020].

2
Project Setup

This chapter gives the general project setup. In Section 2.1 the project objectives are given, followed by the user requirements in Section 2.2. Then a market analysis and environmental analysis is performed in Section 2.3 and Section 2.4 respectively. Finally, the resource allocation is given in Section 2.5 and the sustainability approach is explained in Section 2.6.

2.1. Project Objective

To keep a clear overview of the project, it is essential that the project has clear objectives. These objectives drive both the project team, as well as the design process. In this section the project objectives are elaborated starting from the Project Objective Statement (POS) and Mission Need Statement (MNS). Over the course of the project the team had as MNS :
"Provide a local sustainable wind-energy harvesting source for urban usage"

In order to fulfil this need, the team had as clear objective to:
"Design an integrated wind energy harvesting system in between two high-rise buildings, by ten students within ten weeks."

During the project the team will not only focus on just achieving the required design. The team set specific goals that would drive the design to get the best possible solution for the client.

System specific objectives

1. Circular economy
2. Cost objective
3. Innovation
4. Aesthetics
5. Low noise
6. Safety

Other objectives

1. Personal skills
2. Turn disadvantages into opportunities (COVID-19)

As the project mainly focuses on implementing a sustainable energy system in an urban environment, designing for sustainability over the life-cycle of the design is crucial. As a starting point, a circular economical mindset is set as goal. The first step is to create an affordable renewable energy option in cities producing 50 MWh a year for a unit cost of €75,000. As wind energy between high-rise buildings is a relatively unexplored market, innovation is key throughout the design. The design should thrive to promote building integrated wind harvesting technology, which can be achieved by implementing novel ideas and interesting concepts. As the design will be implemented in a city, the wind energy system should be aesthetically pleasing and safety has a high importance. Therefore, special attention will be given on avoiding damage of the building from vibrations and ensuring safety for people in case of a failure. To get a certified system that satisfies noise regulations, designing for low noise emissions is required.
This project is also a personal exercise and this should be reflected in our goals over the duration of the project. The team intends on improving its professional attitude by improving its communication, project management and team working skills. In addition, gaining first hand experience in the development of wind energy systems is a driving motivation for the team. As a closing remark, this project takes place in very unusual circumstances. Not being able to work on campus comes with disadvantages, but also with opportunities. It is thus crucial during this project to explore those opportunities and capitalize on them to their greatest extent [2].

2.2. User Requirements

The user requirements are stated in Table 2.1. Requirement WES-A17 was previously removed and changed to WES-A20, which stated that the unit cost was increased to €100,000. However, WES-A20 was again removed due to the removal of the energy storage from the design as explained in Subsection 2.3.7 and WES-A17 was added to the user

requirements again. This removal also preceded WES-A06 and WES-A07 being deleted. Furthermore, some small changes were made to requirements WES-A02 and WES-A03, which were therefore given the new codes of respectively WES-A21 and WES-A22. The changes are explained in Subsection 2.4.3 and Subsection 2.4.2 respectively. The final list in Table 2.1 gives the user requirements after the removal and addition of requirements. In the chapters explaining the design methodology of the various subsystems, the most important user requirements and other important (subsystem) requirements to which is designed are stated. User requirements "WES-A15: The system, excluding structural components, shall be made of lightweight materials with a minimum specific strength of <tbd> Nm/kg." and "WES-A19: The system, excluding structural components, shall be made of lightweight materials with a minimum specific stiffness of <tbd> Nm/kg." were removed from the list of user requirements. The reason for this is, that no values for these requirements were specified by the client and there are no exact values for the specific strength and specific stiffness above which materials are considered lightweight. The client just required the use of lightweight materials. Since no proper requirement could be stated on this, it was decided to include the use of lightweight materials as a design consideration and not as a requirement. This use of lightweight materials is taken into account in sustainability approach and the material selections addressed in Section 2.6, Subsection 4.6.3 and Subsubsection 5.4.1.3.

Table 2.1: User requirements.

Requirement code	Requirement
WES-A01	The system shall have a cut-on velocity of 3 m/s.
WES-A04	The system shall be within standard noise regulations for conventional wind turbines.
WES-A05	The system shall absorb the turbine generated vibrations in a way that they will not be noticeable to the high-rise buildings.
WES-A08	The system shall have a minimum lifetime of 10 years.
WES-A09	The system shall not require a technical inspection before 5 operating years.
WES-A10	The system shall not damage the high-rise buildings in case of failure.
WES-A11	The system shall not damage the area in between the high-rise buildings.
WES-A12	The system shall not damage people in case of failure.
WES-A13	The system shall stop working automatically in case of failure.
WES-A14	The system shall be controlled by a mechanical safety system.
WES-A16	The system, excluding structural components, shall be made of recyclable materials.
WES-A17	The system shall have an overall unit cost below €75,000.
WES-A18	The mechanical safety system shall be controlled by software.
WES-A21	The system shall provide 50 MWh at a rated velocity of 10 m/s with a free-stream turbulence distributed with Gaussian law at a standard deviation of 2.5.
WES-A22	The system shall be integrated into a 30-meter space between two buildings of which the parallel sides have a rectangular shape with a height of 200 meters and a width of 30 meters.

2.3. Market Analysis

In this chapter the market analysis will be done. Kicked of by a city analysis that results in the preferred market to attract new clients. This will be followed up with a section where all the considerations, that need to be kept in mind during the design phase, are explained. The chapter will be finalized by having a Strength, Weaknesses, Opportunities, Threats (SWOT) analysis and an analysis of the competitors.

2.3.1. Rotterdam

Rotterdam is allocated to be the city with the first operational Wind Energy System (WES) in [3]. In order to analyze the specific environmental characteristics at the location of the building (done in Section 2.4), the building site was determined to be 'Kop van Zuid'. The city of Rotterdam has allocated this space for skyscrapers and the tallest buildings are located here. The maximum building height of Rotterdam is 250 meters, while the tallest buildings are significantly smaller.[1] Requirement WES-A03 states that the building will have a height of 300 meters and is in

[1] https://www.stichtinghoogbouw.nl/wp-content/uploads/2019/10/Hoogbouwvisie-2019.pdf [cited 10 June 2020].

violation with the regulations set by the city. The requirement has to be revisited and advantage shall be taken of this opportunity by analysing the flow characteristics at different heights within the city. Then a comparison to the characteristics described in WES-A02 shall be carried out in Section 2.4. In addition, the client has commented that they do not feel the need to build a tall building, when the harvesting system can be placed, while fully operational, at lower heights.

2.3.2. City Analysis

After completing the WES installation for the current client, in Rotterdam (The Netherlands), the WES concept will be sold to new clients. The strict regulations and small size make Rotterdam a shallow market. Therefore, a new target market should be realized by investigating the potential of other markets. For this a trade-off is performed between the ten most suitable cities from the baseline report[2] and six cities that just did not make it into that report. The team also recognizes that the current client will not be able to keep producing multi billion-dollar building projects like this, therefore it is a good idea to look at other markets with new potential clients. The market should contain many potential clients and integration possibilities. To determine this market a trade-off will be performed by using four criteria that express important factors the new market should contain.

Number of twin skyscrapers: The number of twin skyscrapers is the first criterion that is evaluated. As the WES is initially designed to be between two high-rise buildings, it is necessary to know the number of skyscrapers that are in close proximity to another skyscraper. In the baseline report a rough estimation was made on the amount of suitable premises per city[2]. This was done using the database of The Skyscraper Center [2] and manually looking at buildings with a height exceeding 200 meters. As the results from obtaining data this way are are sensitive to estimation errors, the cities will be divided into four categories. If the amount of suitable premises is below 20 it is considered Medium, if this is between 20 and 30 it is considered Med-High, if this is between 30 and 50 it is considered High and if it is higher than 50 it is considered Very High.

Gross domestic product: The Gross Domestic Product (GDP) of a country is a good indication of how big the economy of the respective country is. This criterion is chosen as it is recognized that the transfer to renewable energy sources will need big initial investments. Compared to large wind turbines the WES will not be as efficient in generating energy. Which means that the investor wants to go the extra mile to showcase their contribution to green energy generation. Thus it is preferred if the market that is targeted has a big economy. The data is available on DataBank.[3] The Purchasing Power Parity (PPP) per capita was chosen as the metric to measure as this reflects the value of money in a country. A PPP below $15,000 is considered Low, a PPP between $15,000-$30,000 is considered Medium and a PPP higher than $30,000 is considered High.

Wind speed: Wind speed is another criterion on which different cities will be compared on. Requirement WES-A21 states that the rated velocity for which the WES will be designed for is 10 m/s. Higher wind speeds will result in more energy generated, while lower wind speeds will generate less energy. Due to the many buildings in cities, the wind will stagnate and accelerate based on building orientations. The average wind speed also increases with an increase in height. An optimal orientation and taller building could make cities more interesting than the average wind speed would make it seem. Wind speeds are obtained from Weather Spark which measures wind speeds at a height of 10 meters.[4]

Shortwave solar energy: Solar energy is a direct competitor of wind energy. Therefore it is researched if the relevant cities have a lot of shortwave solar energy available. Wind energy becomes more viable in cities that have a low shortwave solar energy level, because using solar energy will not be as efficient. To simplify this relationship it is assumed that cities with high shortwave solar energy available will choose solar energy over wind energy and cities with a low shortwave solar energy available will not. This weather data is also obtained from Weather Spark.

The cities and their trade-off results can be seen in Table 2.2. The cities with the best results are: New York, Hong Kong, Shenzhen, Busan and Shenyang. As can be seen in Figure 2.1 these cities except for New York are geographically speaking located near each other. As the market would be too broad by including New York, it was decided that the optimal market will be around the East China Sea. Hong Kong, Shenzhen, Busan and Shenyang will be specifically targeted in this region.

[2] http://www.skyscrapercenter.com/compare-data [cited 29 May 2020].
[3] https://data.worldbank.org/indicator/NY.GDP.PCAP.PP.CD [cited 18 June 2020].
[4] weatherspark.com [cited 18 June 2020].

Table 2.2: Trade off between cities. [5]

	New York	Moscow	Abu Dhabi	Dubai	Mumbai
Twin towers	High	Medium	Medium	Very High	High
GDP per capita	High	Medium	High	High	Low
Solar energy	2.8 - 5.8 kWh	1.5 - 4.9 kWh	4.9-7.2 kWh	4.9 - 7.2 kWh	5.3 - 6.7 kWh
Wind speed	2.9 - 4.6 m/s	3.4 - 5.5 m/s	3.4 - 4.5 m/s	3.1 - 4.2 m/s	3.0 - 6.5 m/s

	Chongqing	Hong Kong	Shanghai	Shenyang	Shenzhen
Twin towers	High	High	Medium	High	Very High
GDP per capita	Medium	High	Medium	Medium	Medium
Solar energy	3.2 - 5.3 kWh	4.3 - 5.3 kWh	3.5-5.4 kWh	2.9 - 5.6 kWh	4.3 - 5.3 kWh
Wind speed	2.0 - 2.6 m/s	4.1 - 5.9 m/s	4.6 - 5.4 m/s	3.4 - 5.5 m/s	3.8 - 5.1 m/s

	KL	Singapore	Jakarta	Manila	Busan	Seoul
Twin towers	High	Medium	High	Med-High	Med-High	Medium
GDP per capita	Medium	High	Low	Low	High	High
Solar energy	4.4 - 5.5 kWh	4.0 - 5.0 kWh	4.7 - 5.9 kWh	4.5 - 6.2 kWh	3.5 - 5.7 kWh	3.1 - 5.7 kWh
Wind speed	1.5 - 2.1 m/s	2.3 - 4.5 m/s	2.2 - 3.4 m/s	2.6 - 4.5 m/s	4.0 - 6.1 m/s	3.0 - 4.2 m/s

Figure 2.1: The selected cities after comparing the amount of twin skyscrapers, GDP and weather.

2.3.3. Configuration Selection Considerations

In this section, the different considerations are explained that need to be kept in mind while designing the WES. These considerations are based on what the current client would like to see in our product and will help broaden the pool of potential future clients. These considerations will consistently be taken into account, especially when an important design choice has to be made. When designing, the following thoughts are taken into consideration:

- Design freedom
- Risk of failure
- Aesthetics
- Scalability
- Sustainability

First it is important to have a design that is easy to tweak for a market with other wind conditions or even regulations. It speaks for itself that different places on earth have other environmental conditions as well as regulations, it is thus important that there is still some freedom in the design, for easy adaptations to other markets. The design should of course have a low risk of failure. As the clients want to sell as many apartments or office space as they can, it is important to take the aesthetics into consideration. The building will be more desired if it is aesthetically pleasing,

[5] see footnotes 2, 3 and 4

original and really stands outs in comparison with other buildings. Lastly it is a big advantage if the design is scalable. This means that it is possible to place multiple Wind Harvesting System (WHS) next to each other, which means that larger scale system can be sold to clients with more building space and budget, while down scaling is also possible. The scalability of the design is important in the sense that it broadens the pool size of possible future clients.

Previous paragraph mainly talked about the looks, use and adaptability of the design. This paragraph will discuss the performance of the design. The clients, of course, want the best possible design available, this means that during the design phase the loads on the structure, the vibrations, the noise, the efficiency and the cut-on velocity are aspects that need to be taken into consideration. The loads on the structure need to be minimized as this opens up the possibility to lower the cost of the support structure and thus lowering the cost of the WES. The vibrations need to be minimized to a level where they do not form a disturbance inside the building. This is also a user requirement, "WES-A05: The system shall absorb the turbine generated vibrations in a way that they will not be noticeable to the high-rise buildings". The noise is another consideration that has to be accounted for. Every market has different noise regulations, as a result, it is important to have a design where the noise level can still be lowered if the regulations are stricter than in the Netherlands. The efficiency is something that is desired to be as high as possible. As increasing the efficiency means increasing the available power for the high-rise buildings. The last aspect, sustainability, will be discussed in Section 2.6

The aspects that were listed in these paragraphs are important to the clients and will therefore be considered every time a design choice needs to be made. By doing this the design will be made with a market analysis perspective in mind, which will result in a product that can be more effectively implemented into other markets.

2.3.4. SWOT Analysis

The SWOT analysis from the baseline report[2] is updated to show a clear picture of the value proposition of the WES. The SWOT analysis determines the strengths and weaknesses of the WES from a market perspective. Opportunities and threats to the position of the system in the market are also discussed. The perspective mainly focuses on the influence of the region the system is in, the development of similar technologies and how a world crisis would change the market.

Table 2.3: SWOT analysis based on market analysis.

Strengths	Weaknesses
What sets the new design apart from others. Assets within the design that should be taken advantage of.	*Properties of the design that should be avoided or taken care of.*
Applicable to existing buildings: One of the biggest strengths is that the two high-rise buildings do not need to be designed around the WES. The system could be made suitable for many existing skyscraper pairs. The design is therefore easily adaptable to other high-rise buildings. Because the WES is only on one high-rise building the possibility exists to use the design for a single high-rise building. As will be discussed in Section 2.4, the building height of a single building has to be 50 %, however the market of single buildings is also significantly bigger than those of twin buildings. **Highly visible:** The proposed solution will be integrated in-between two high-rise buildings and therefore it will be highly visible throughout the entire city. The visibility will be such that all the local people will form an opinion about it. This opinion will generate awareness about the importance of sustainability. This will stimulate people to think more actively about an environmentally friendly existence. **Wind energy is getting cheaper:** Wind turbines continue to develop and the price per MWh will drop further. This, in combination with the fact that there is a lack of urban wind turbines creates a very promising market position. So the customer could become an early adopter, which means that if these types of projects take off they could profit from these investments. **Europe is a good testing market:** An advantage of designing and manufacturing the system on the European market in general and the Dutch market specifically is that the logistics and organisation are easy to set up. The jurisdiction is clear and legislation is detailed and complete. **Scalable:** The WES is a very scalable and adaptable design. This means it is possible to easily use the system in other market with different building heights. The minimum height is 148m as will be discussed in Section 2.4, the system can also be used on lower heights than this but the efficiency of the system will become lower. **Wind is often available:** In comparison with solar panels, wind is on average more available. It does not have the problem where it does not generate power for a certain period.	**Regulations:** Height restriction laws are amongst the most notorious laws in cities. In Saint Petersburg, buildings cannot exceed the height of the Winter Palace [4]. While in the central area of Rome buildings cannot be taller than the dome of St. Peter's Basilica. Besides Europe, North America and Australia have a lot of zoning codes. Such as rules that required buildings to step back as they rose to enable sunlight to reach the streets.[6] The analysis to establish the target market showed enough potential however. **Safety:** The WES will be integrated between two residential high-rise buildings and will therefore cause safety issues. A large installation will hang more than a hundred meter up in the air above a road or public area, which in case of any external failures can be very dangerous. This was already one of the main issues with the implementation of the building integrated wind turbines. **Wind availability:** The energy production depends on the wind availability, meaning that there will be seasonal differences in the energy generated. **Energy demand of buildings:** The harvesting system does not meet the energy demand of the two high-rise buildings and therefore a connection to the grid is needed.

Opportunities	Threats
Events that happen outside of the design processes that can lead to progression, if handled carefully.	*Changes that can lead to more difficulties while realizing the product.*
High density of high-rise buildings in target markets: As discussed in Subsection 2.3.2 the market around East China Sea will be the main area where the design will be sold to other clients. This brings an extra opportunity because these cities are all densely populated and the amount of high-rise building is therefore very high. This means selling the design in this market will be easier than in the Netherlands.	**Possibility of a recession:** A global financial crisis could occur, especially as a result of the current COVID-19 pandemic. Therefore investors might be more conservative to invest in a project like this.
Environmental sentiment of possible clients: A lot of governments and companies altered their resources to a more sustainable approach because of there own initiative or because regulations made them do it. The fact that some big banks have announced that they will only finance new high-rise buildings if they are labeled "environmental friendly" will only increase companies to have green solutions like the WES. [7]	**Political instability:** Political instability is something that can have an influence on investors. Currently two, Hong Kong and Busan, of the four cities that are targeted are notably unstable politically, which can cause possible clients to halt the development of new buildings with the WES or to make new investment in the WES to add to already existing buildings. [8,9]
Noise regulations of target markets: Noise regulations are another aspect that needs to be taken into account. In both North America and Europa, there are a lot of regulations in place to make sure that noise levels in the city are comfortable. Whereas in China, which is one of the target markets, noise regulations are much less strict [5]. This gives the opportunity that because the product is designed for a much stricter market, it will be easier to implement in markets where they are less strict	**Solar energy:** The increase in solar panel development could cause a lower demand of wind harvesting systems, as both of these products have overlap in their market. The possibility exists of a long term future where cities will be supplied exclusively by solar farms or that developers prefer to go with solar energy on their own building.
Demand for renewable energy: The decreasing supply of fossil fuels increase the demand for sustainable alternatives.	**Noise regulations in the future:** The possibility exists that in the future the noise regulations in the target markets become a lot stricter than they are now. This would mean that the WES will need to be redesigned in order to comply with the noise regulations.
Combination of solar and wind in urban usage: The perfect combination of wind energy harvesting systems and solar panels could soon cause a solution to start generating carbon-neutral buildings.	

2.3.5. Competition

In this section the competitors for the WES are discussed. More specifically those who provide green energy and can supply to the urban environment.

Solar energy: An important trend nowadays is to implement solar panels on the roof of large buildings, generating a small percentage of the total energy usage. This could be done on either a flat or inclined rooftop to increase the efficiency. The significance and effect of these implementations vary widely and some companies mainly do this to show a goodwill in favor of sustainable development instead of really making a difference. Other companies really advocate for a sustainable future and try to show this by implementing as many solar panels as possible. [10] The

[6] https://www.ing.nl/nieuws/nieuws_en_persberichten/2016/12/ing-financiert-na-2017-alleen-kantoorpanden-die-voldoen-aan-voorwaarden_groen_label.html [cited 17 June 2020].
[7] https://www.bbc.com/news/world-asia-53074095 [cited 17 June 2020].
[8] https://www.bbc.com/news/world-asia-china-49317695 [cited 16 June 2020].
[10] https://interestingengineering.com/skyscraper-covered-solar-panels-europes-largest [cited 29 april 2020].

biggest potential for solar energy to serve the urban market is by completely covering skyscrapers with transparent solar panels. Only one example of this is found today, namely the CIS Tower in Manchester. It was renovated in 2004 and covered in 7000 individual solar panels generating 575.5 kW. [11] With the current technological development and the increase of importance of sustainable energy, the solar panel market can expect to grow rapidly. Large solar parks are built in order to generate enough energy to supply surrounding villages.[12] This technology could also be implemented in larger cities and therefore the expectations are that by 2022, skyscrapers could generate 2500 MWh per year with an average area of 8 football fields per skyscraper covered by solar panels. This could be enough to create a zero-carbon building.[13,14] These solar parks are also recognised as a threat for the design as real estate developers who can create zero-carbon buildings without adding their own green energy solution to a building.

Wind energy: While looking at the wind energy market it can be concluded that it is a rising market. In the past fifteen years the market quadrupled and it was able to generate 591 GW in 2018. The biggest investors are China and the US, overseeing together around 50% of the entire market. However, Denmark is the country with the highest dependency on wind energy as 46.9% of their energy comes from wind energy harvesting.[15]

As discussed earlier, solar farms are competitors that need to be accounted for, same as for wind farms. The latter farms consist out of individual wind turbines, which are connected to the electric power transmission network. There are two types of wind farms, either onshore or offshore. Onshore wind farms are an efficient and cost effective method of producing green energy for the neighbouring surroundings. However, they impact the landscape and therefore have to be spread out over land more than other power stations. Offshore wind farms are more efficient as the wind flow is stronger and steadier. While they do not suffer from any visual impact on society, the construction and maintenance costs are much higher as the wind turbines are placed on sea. The three biggest wind energy companies are Siemens, Vestas and GE Renewable Energy. Looking at those companies it is important to address that Siemens starts looking at producing wind energy solutions for cleaner and affordable wind power for residential and commercial purpose.[16] In comparison to the development and growth of the onshore and especially offshore wind energy parks, the urban usage of wind energy is lacking. Some small turbines are installed on the roofs of a few large skyscrapers, however large improvements have to be made as they make up a handful of projects. Some examples of the implementation of wind energy on buildings can be seen in the Baseline Report [2]. The goal of the WES is therefore to have a cost efficient wind harvesting system that can be adapted to more buildings and therefore increase the technological development of the small wind turbines.

2.3.6. Cost Trends and Market Price

In Subsection 2.3.5, the competition the team will have to deal with for the deployment of the WES was discussed. In this section the market price of the competition is described and compared. As well as how the cost of renewable energy is expected to behave the coming years.

The current decreasing trend, in the cost of renewable energy sources, is high. The prices for utility-scale solar photovoltaics fell 13% last year reaching 0.07 $/kWh. Which results in a total fall of 82% over the past 10 years. This is the sharpest decline in comparison with other renewable energy technologies. Whereas onshore and offshore wind energy fell 9% over the year and averaged a decline around respectively 40% and 29% over the past ten years. The cost thus fell to a level of 0.053 $/kWh for onshore and 0.115 $/kWh for offshore wind energy [6].

IRENA also recognises in the report, that by 2021 up to 1,200 GW of coal-fired production would cost more to operate than to install a new utility-scale solar photovoltaics [6]. The prediction for the coming year is that the price of electricity could fall below 0.049 $/kWh for onshore wind and 0.055USD/kWh for solar photovoltaics by 2020.[17] As this trend will keep on going for the coming years, this means that at a certain time the cost of renewable energy will be low enough that not a single company will have doubts that investing in renewables will be cost effective.

[11] https://interestingengineering.com/skyscraper-covered-solar-panels-europes-largest [cited 29 april 2020].
[12] https://www.smart-energy.com/renewable-energy/total-wins-french-ground-based-solar-parks-tender/ [cited 29 April 2020].
[13] https://www.power-technology.com/news/solar-panel-glass-turn-skyscrapers-power-stations/ [cited 29 April 2020].
[14] https://www.sciencemag.org/news/2018/06/skyscrapers-could-soon-generate-their-own-power-thanks-see-through-solar-cells [cited 29 April 2020].
[15] https://renewablesnow.com/news/wind-meets-record-47-of-denmarks-power-demand-in-2019-682219/ [cited 30 April 2020].
[16] https://www.windml.org/top-15-wind-energy-companies-around-the-world/ [cited 30 April 2020].
[17] https://www.reuters.com/article/us-renewables-costs/solar-onshore-wind-costs-set-to-fall-below-new-fossil-fuel-energy-report-idUSKCN1SZ1ML [cited 18 June 2020].

2.3.7. Energy Storage Device Addition

Having a storing device was one of the user requirements and it was decided to go with the vanadium redox flow battery, as this came out on top during the trade-off. At the beginning of the design phase the team realized that even at the minimum usage of the building, there might not be a need for this battery. This realization was confirmed by an analysis of the energy usage of a 200 meter apartment building. This meant that requirement WES-A20: “The system shall have an overall unit cost below €100,000" changed back to WES-A21: “The system shall have an overall unit cost below €75,000.", which was the original project objective. Due to the lack of this subsystem, requirements WES-A07 and WES-WF-EN-06 are discarded which are respectively “The system shall store over-night generated energy” and “The system shall have an energy storing device”.

The reasoning why the energy storage device should be removed from the design is as follows. To start off, one apartment is assumed to be the same as the average household in the Netherlands which uses 3,000 kWh of energy per year. This would correspond to an energy-consumption of 8.22 kWh per day.[18] An example of a 215 m building with 200 apartments was found, multiplying this by 2 would lead the total energy consumption of the 2 buildings to 1,200 MWh per year and 3.29 Mwh per day. Figure 2.2 shows the daily pattern of the average household, from this graph it can be derived that at the lowest peak, the power requirement is still around 250 W. Which means at the lowest peak the buildings will still require 100 kW. In Subsection 4.3.4, the power production of the WES will be calculated at which can produce a maximum of 33 kW without accounting for losses. This means that the first conclusion of this analysis is that, even at minimal power usage, there is still a higher usage than production by the harvesting system.

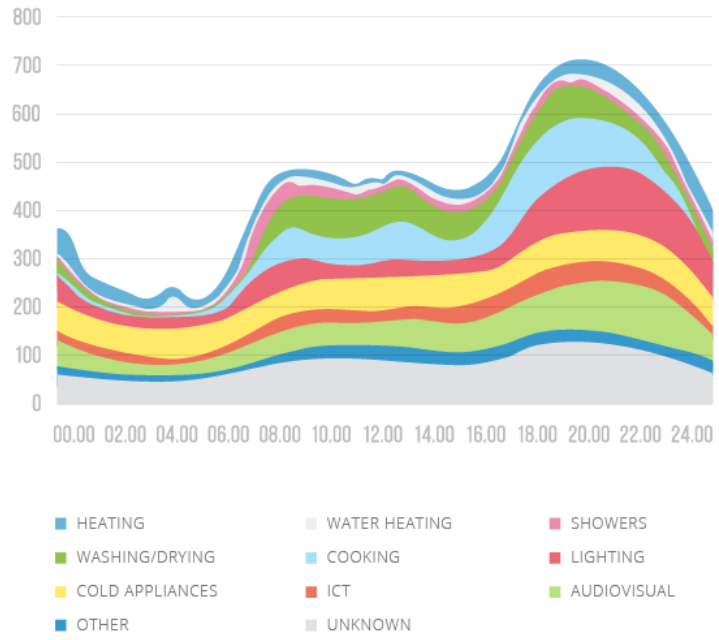

Figure 2.2: Daily power usage pattern of an average household. [19]

Before fully discarding the battery, the aspect of cost is looked at. It can be the case that charging the battery during off-peak hours and using this off-peak energy during peak hours can save money on the long term. For this analysis four different markets were considered, they can be seen in Table 2.4 with their corresponding peak and off-peak energy prices. These currencies are then converted to euro for the analysis.[20]

[18] https://www.essent.nl/kennisbank/energie-besparen/inzicht-in-verbruik/gemiddeld-energieverbruik [cited 15 June 2020].
[19] https://www.ovoenergy.com/guides/energy-guides/how-much-electricity-does-a-home-use.html [cited 16 June 2020].
[20] The following currency conversion rates are cny/eur = 0.12, gbp/eur = 1.11 and usd/eur = 0.9. These conversion rates are used throughout the entire report. Source: https://uk.finance.yahoo.com/currencies [cited 29 May 2020].

Table 2.4: Cost of energy for different markets during peak and off-peak hours.

	Peak Hours	Off-Peak Hours
United Kingdom [2]	0.121 £/kWh	0.08 £/kWh
Netherlands [3]	0.0947 €/kWh	0.0796 €/kWh
United States [4]	0.0704 $/kWh	0.0134 $/kWh
China [5]	1.51 ¥/kWh	0.35 ¥/kWh

As can be seen in Table 2.4, there are different prices for peak and off-peak hours, which thus opens up the possibility to store the cheaper energy and use it during peak hours. As the battery would have cost €25,000, this is the break even point. In Figure 2.3a, it can be seen that investing in the battery would only save money in China. This is an important aspect because as was discussed in Subsection 2.3.2, the Chinese market will be the main focus to try and sell this design. Figure 2.3b shows that the battery in the Netherlands will not break even after 25 years. It is therefore now possible to conclude that including a storing device will not have a financial benefit thus the battery is discarded in the design.

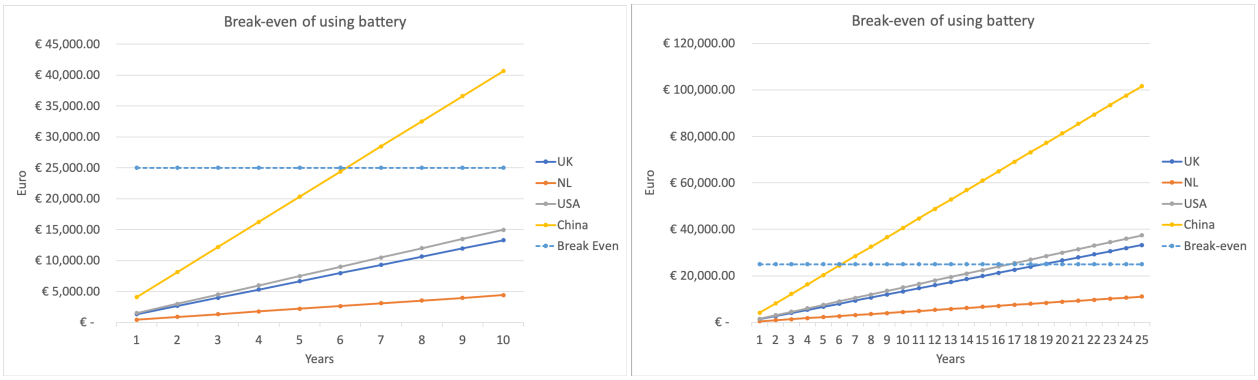

(a) Model for first 10 years.

(b) Model for first 25 years.

Figure 2.3: Break even model of including battery into design.

2.3.8. Market Analysis Future Vision

In Subsection 2.3.2 the target market was selected. After doing a trade-off between different markets, the East China Sea was selected as the target market. This region consists of the cities Busan, Shenyang, Shenzen and Hong Kong which are all cities where the pool of possible new clients is really high. These cities do not only have a high amount of high-rise buildings where the WES can be adapted on, but also have a high rate of new high-rise buildings in development. When looking at Hong Kong there are currently 355 buildings above 150m while in Rotterdam there are 5, there are also ten skyscrapers planned to be developed in Hong Kong whereas only two in Rotterdam, while these are the buildings where the WES will be implemented on. [21] [22] Busan, Shenyang and Shenzen respectively have 62 , 85 and 289 buildings that are higher then 150m and have 10 , 30 and 79 buildings planned to be constructed, which is a lot more then Rotterdam. [23] [24] [25] If you compare these amounts with the amount of twin tower locations for all cities, 80, it shows that targeting the market for single buildings instead of twin tower buildings will result in a bigger pool of possible clients. This is something that is desired when selling the WES design.
The possible clients will have different needs than the current clients, this means the user requirements will be different. It is therefore important that the WES is scalable as this was recognized and identified as a strength of the WES in the SWOT analysis in Subsection 2.3.4. The scalability of the WES will be further analyzed and explained in Subsection 5.4.1.

The team recognizes that the total harvested energy per year will differ from client to client. It is also expected that on average the required energy per year will be higher in the target market. It can be expected that the unit cost will

[21] https://www.deopenbareruimte.nu/nieuws/dit-zijn-de-5-hoogste-gebouwen-in-nederland/ [cited 30 June 2020].
[22] https://www.skyscrapercenter.com/city/hong-kong [cited 30 June 2020].
[23] https://www.skyscrapercenter.com/city/busan [cited 30 June 2020]
[24] https://www.skyscrapercenter.com/city/shenyang [cited 30 June 2020].
[25] https://www.skyscrapercenter.com/city/shenzhen [cited 30 June 2020].

rise with the increase in required energy. This is something that is expected because 200m high-rise building developments are considered normal in the target market whereas a 200m building in Rotterdam is considered unique. Meaning the availability of higher and more buildings of this kind gives reason to expect an higher required amount of harvested energy. The addition of the battery, as discussed in Subsection 2.3.7 is something that could be included in a future version of the WES to attract possible clients. This is of interest as this holds financial advantages, as is shown in Figure 2.3a and Figure 2.3b, where this system would have a break even point after 6 years. Having a break even point after 6 years can be consiered normal as most renewable energy products have break even points of 6 to 8 years. [26]

2.4. Location and Environment Analysis

In this chapter the environmental conditions are addressed in which the WHS will operate. For that, first the building and system location had do be determined, which are dependent on the wind characteristics (speed and direction), as they determine the building orientation and specific heights. In the following, the procedure is given for how the local wind characteristics were obtained.

2.4.1. Analysis of Height and Wind Speed

The average yearly wind speed of the past 10 years were analyzed by Global Wind Atlas (GWA) [27] and compared to the data of Rotterdam Airport [7]. The GWA model includes precise roughness lengths, based on geographic data and hence is more realistic than the commonly used wind profile power law [8]. For the location of the building in Rotterdam, the average wind speeds were obtained for different altitudes (10-200 meters). As the flow will be accelerated between the two high-rise buildings, this effect was added. In the research of Lu and Ip [9] on enhancement methods of wind power utilization in high-rise buildings, very similar buildings were analyzed. Their findings for the velocity profile between the two buildings and boundary layer characteristics resulted in an updated velocity profile for different heights. An acceleration factor of 1.85 was obtained through extrapolation of the incoming flow vs building spacing [9]. A 33% wind speed loss between the buildings was assumed, as inefficiencies due to wind direction variation and shading effects are not accounted for in a later stage. With a fitting curve, the average wind speed profile for different altitude was determined and can be seen in Figure 2.4a. From the plot a minimum system height H_{min} of 148 meters was determined for a turbine placement. If the system would not have taken advantage of the speed increase due to two buildings, but instead was built on the side of a skyscraper and the same method would be applied but this time with a wind speed loss of 17% due to direction, the system would have to be placed at least 250 meters in the air. Further research has to be done to analyze the flow characteristics around a single building in more detail.

In a next step, the velocity profile between the building was analyzed to obtain the minimum space between the building and the outer diameter of the WHS. A fully developed turbulent boundary layer thickness δ of 4 m was estimated and is slightly higher than the results obtained by Lu and Ip. Outside of this layer, it was assumed that the wind speed is constant. This is an important assumption as it does not take into account the difference in wind loads on the blades (further discussed in Section 4.6). As a first design process, this estimation is valid but should be further analyzed in a later design phase. The velocity profile in the turbulent boundary layer was calculated by using the power-law velocity profile expression shown in Equation 2.1 [10].

$$u = u_{max}\left(\frac{y}{\delta}\right)^{\frac{1}{n}} \qquad or \qquad u = u_{max}\left(1-\frac{y}{\delta}\right)^{\frac{1}{n}} \tag{2.1}$$

The velocity outside the boundary layer is denoted as u_{max} and the location in the boundary layer as y. δ is the boundary layer thickness and the factor n is related to the Reynolds number. For many flows in practice the profile can be approximated with $n = 7$ and was therefore assumed [10]. The resulting velocity profile between the two buildings at a height of 148 meters is shown shown in Figure 2.4c. For the system placement it means that the turbine should be placed outside of this region to ensure turbine efficiency and avoid fluctuating loads bad for fatigue on blades.

[26] https://www.powersystemsdesign.com/articles/the-elusive-break-even-point-for-alternative-energy/34/11533 [cited 30 June 2020].
[27] https://globalwindatlas.info [cited 08 July 2020].

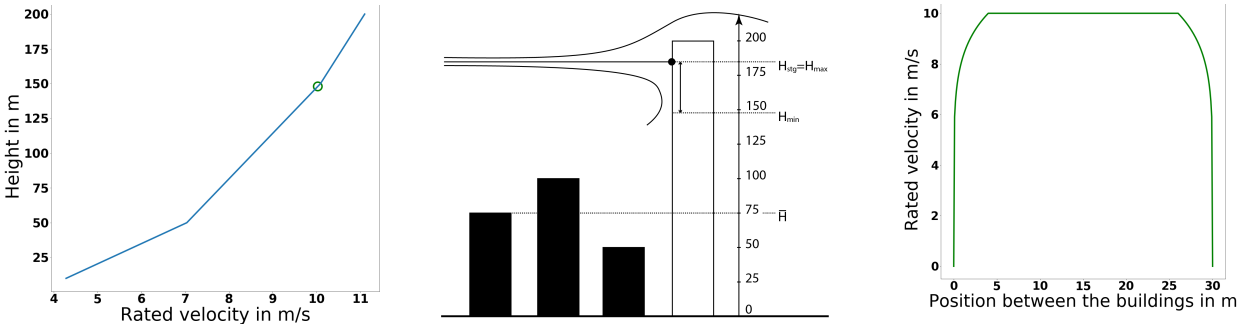

(a) Building height versus the local rated wind speed between the high-rises.

(b) Visualization of the different characteristic heights: $\overline{H}$, H_{stg}, H_{max}, H_{min} and H_{sys}.

(c) Velocity profile between the two high-rises at a height of 148 meters.

Figure 2.4: Plots to determine characteristic heights and local wind condition.

2.4.2. Stagnation Height

Another relevant aspect to consider with airflow around buildings is the location of the stagnation point at the building[11]. At a specific height, there will be a stagnation point at the facade facing towards the wind. Separation of the flow is inevitable and from the stagnation point, the airflow will separate into a flow going over the building, one pressured flow downwards and one around the building as shown in Figure 2.4b. If wind is not coming from SW (as explained in Subsection 2.4.3), the stagnation point will move between the two buildings and hence a system placement at this location is undesired, as it would lower the turbine efficiency. The height of the stagnation point is close to the building top. Since there is not much space between the stagnation height and the building top to place a system, it should be placed below the stagnation height. Therefore the upper limit or maximum system height will be the stagnation height H_{stg} of 185 m with a building height of 200 m. The stagnation height was calculated by making use of Equation 2.2 [11].

$$\frac{H_{stg}}{H} = 0.9 + 0.15\frac{\overline{H}}{H}(1 - 1.25A_H(1 - A_H)) \tag{2.2}$$

The equation is based on statistical data. $\overline{H}$ is the average height of surrounding buildings and was assumed to be 75 meters for the urban area of Rotterdam. A_H is the percentage of total area occupied by nearby buildings and this value for a city is typically 0.42[12]. The constant of 0.9 in Equation 2.2 depends on the slenderness of the buildings. 0.9 is the result of a slenderness ratio of 1:1:8. This means that the width of the building is one-eights of the length of the building. This is assumed to be the case for the WES.

Knowing the maximum and minimum system height, the possible placement height range H_{sys} of 37 meter was obtained, also shown in Figure 2.4b. This means that a building height of 200 meters would fulfill the need of the client and of the developers. As such, WES-A03 was replaced by WES-A22. Since the system should function for winds coming from both directions (SW and NE), the system should be placed in the middle of the building length. This is also beneficial, as the flow will be most accelerated here[9].

2.4.3. Wind Direction Variation

Finally, the predominant wind direction of Rotterdam was analyzed using the data of meteoblue.[28] Historic data of the past 30 years of four different stations were synthesized for Rotterdam in a respective wind rose shown in Figure 2.5.

[28] https://www.meteoblue.com/en/weather/historyclimate/climatemodelled/rotterdam_netherlands_2747891 [cited 08 July 2020].

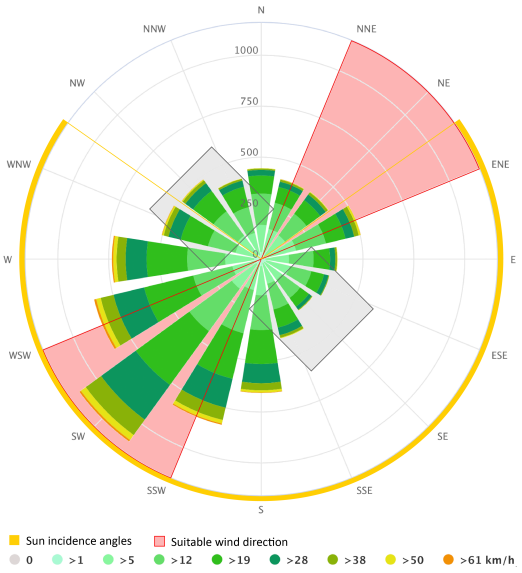

Figure 2.5: Wind rose for Rotterdam[29]: also indicating the building orientation, suitable wind direction (red area) and sun incidence angles (yellow area).

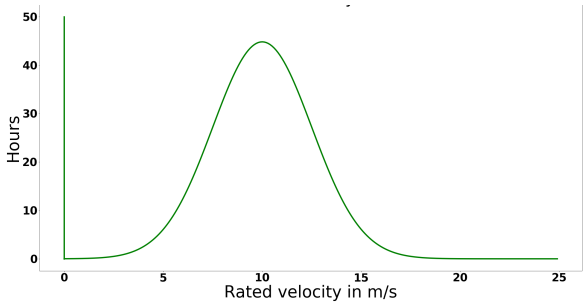

Figure 2.6: Rated wind speed variation, normal distributed with $\sigma = 2.5$ and $\mu = 10 m/s$.

As can be seen, the main wind direction is SW. This resulted in the according building orientation, the building gap is lying on the SW-NE axis. Furthermore, the wind directions of NNE to ENE and SSW to WSW were considered as suitable directions for wind harvesting. WES-A02 was ambiguous and was therefore changed to WES-A21, which states "The system shall provide 50MWh at a rated velocity of 10 m/s with a free-stream turbulence distributed with Gaussian law at a standard deviation of 2.5." Resulting, a normal distributed wind speed variation with $\sigma = 2.5$ around a rated wind speed of 10 m/s, a speed variation was obtained, which shown in Figure 2.6. This figure only shows the speed when there is wind speed due to suitable directions. 5955 hours per year the wind direction will not be suitable and therefore the wind speed will be zero. From the given variation of the rated wind speed at a suitable system placement, the turbine sizing was derived as explained in Table 4.2. The wind characteristics were simplified in this chapter for this design phase. However, these should be revisited and further investigated in later design phases.

2.4.4. Sun and Shadow

Shadow flickering due to wind turbines is a health issue that needed to be considered in an urban environment. It can cause photosensitive epilepsy if the flicker frequency is above 3 Hz [13]. Therefore the sun hours and incidence direction for Rotterdam were analyzed in order to find a suitable placement location for the WES. On average there are 1623.8 sun hours per year for Rotterdam[7] resulting in approximately 4.4 sun hours per day. Looking at the sun path the maximum sun angle is from 55° to 305° [30] and is also indicated in Figure 2.5. Due to the building orientation, it is therefore best to place the WES onto the south-east building, as here the system will be most of the time in shadow – avoiding shadow flickering.

2.5. Resource Allocation Class I

In this section estimations will be provided for the power, cost and mass budget. These will later on be revisited. Further rated power calculations are performed in Subsubsection 4.3.4.2, while improved cost and mass budgets are shown in Section 8.4.

2.5.1. Power and Energy

From the wind data used before in Section 2.4, also the average hours per direction could be obtained. Considering the NE-SW axis plus minus 22.5 degrees, the average amount of possible operation time is t_{op} 2808 hours. Taking into account the energy requirement (WES-A21) , also the capacity factor CF as well as rated power output P_{rated}

[29] see footnote 21
[30] http://solardat.uoregon.edu [cited 17 June 2020].

for the system could be determined through Equation 2.3 and 2.4 respectively.

$$CF = \frac{t_{op}[h]}{a[h]} = \frac{2808[h]}{365.25 \cdot 24[h]} \approx 0.32 \tag{2.3}$$

$$P_{rated} = \frac{E_{req}[Wh]}{a[h] \cdot CF} = \frac{50 \times 10^6[Wh]}{365 \cdot 24[h]0.32} \approx 17.8\,[kW] \tag{2.4}$$

Hence, the system needs to provide at least 17.8 kW on average over the year, taking into account wind availability dependent on suitable direction and speed, as described in Section 2.4.

2.5.2. Costs

For the cost allocation, it is assumed that the cost structure of the WES will be similar to that of a Horizontal Axis Wind Turbine (HAWT) of similar size[14]. For the unit cost only the wind turbine system equipment, the foundation and electrical infrastructure were considered. Besides the commercial cost structure was selected as this is most similar to the branch our client operates in. During this phase of the project setup a Class 5 estimation is done to determine the cost estimation [15]. This means that the estimate should have an accuracy of -30 % to 50 %.

Table 2.5: Class I Cost Allocation of WES.

Subsystem	**Cost of small HAWT**	**Cost of WES**		
WHS	4,393 $/kWh	€78,000		
Structural Support System (SSS)	591 $/kWh	€11,000		
Electric and Control System (ECS)	458 $/kWh	€8,000	+	
Unit Cost		**€97,000**		
Contingency (-30% to 50%)		*-€29,000*	-	*€48,000*
Total Unit Cost		***€68,000***	-	***€145,000***

2.5.3. Mass

It is assumed that the size of a Vertical Axis Wind Turbine (VAWT) does not have an effect on the ratio between the mass of structural components and the mass of the generator of a turbine. The ratio for a 5 MW VAWT is 1:2 respectively [16]. The ratio between the mass of the blades, connectors and shafts was also assumed to be similar for different sizes. It was found that for a 1.2 kW VAWT, the blades make up 10% of the structural mass, the connectors make up 5% of the structural mass and the shaft the other 85% [17]. The mass of a 10 kW VAWT[31] and the mass of the control box of a 20 kW HAWT[32] are used to determine the mass of the WHS and the mass of the ECS. As there is no indication of the mass of the SSS it is assumed to be as heavy as the rest of the system combined. Resizing this to a rated power of 17.8 kW yields Table 2.6. A contingency of 25 % was chosen, based on aerospace industry standards [18].

2.6. Sustainability Approach

In order to create a market feasible and profitable design, it is required that the design scores very high with respect to sustainability. As a society we have to switch to a more eco-friendly and zero-carbon lifestyle, this design should be a step in right direction. The main goal of this design is to give a kick start to the use of green energy in urban areas. Therefore, it should not only be producing clean energy but also consist out of recyclable materials and have a transparent design philosophy. Which was also the desire of the client, expressed in WES-A16 as stated in Section 2.2 . A more detailed explanation for each different strategies and how the ratings are chosen can be found in the midterm report [3].

[31] https://www.renugen.co.uk/content/small_wind_turbine_brochures/small_wind_turbine_brochures/Aeolos%20Wind%20Turbine/Aeolos-Aeolos-V-10kW-10kW-Wind-Turbine-Brochure.pdf [cited 18 June 2020].
[32] https://www.enair.es/descargas/Manual/E200_UserManual-en.pdf [cited 18 June 2020].

Table 2.6: Class I Mass Budget of WES.

Subsystem	**Relative mass**	**Mass**
Blades	3 %	20kg
Connectors	2 %	15kg
Shaft	30 %	205kg
Generator	65 %	445kg
WHS	38.5 kg/kW	685kg
ECS	35 kg/kW	625g
SSS	73.5 kg/kW	1,310kg
System Mass WES		**2,620kg**
Contingency	25 %	*660kg*
Total System Mass		***3,280kg***

2.6.1. Sustainable Design Philosophy

From day one of Design Synthesis Excercise (DSE) a clear sustainable design philosophy has been applied to every phase. Since a circular economy is becoming more important with the day, it was decided that this should be the foundation of the philosophy. A circular economy means that the production of waste is minimized and a continual use of resources is applied. From the design phase until the moment the system is dissembled the use of energy should be minimized. This can be done by reducing transportation matters, using smart electric tools and designing in a modular way. This approach will be carried in 6 different strategies addressed below, based on the "Design4sustainability" method.

2.6.2. Sustainable Strategies

The "Design4sustainability" (D4S) method is created due to an urge for smart redesigning of existing products [19]. A lot of very interesting products have been brought to the market over the years, however many of these products are designed with a lack of sustainable interests. The D4S applies this sustainable interest by creating key strategies and evaluating the existing products with respect to those. Due to the broad vision it can also be applied for this specific design, however instead of using it to evaluate afterwards, it is already used from the beginning. These strategies provide an insight and a step wise approach to assure a go to market strategy and a sustainable design. Six strategies have been created based on the philosophy and requirements. Each strategy will be assigned with a different rating based on impact and feasibility. These ratings scale from - - to ++, a ++ meaning very feasible and high impact design and a - - meaning not feasible and low impact. The ratings in between, namely -, o, + form the middle ground, correspond to almost feasible, a neutral and feasible option respectively. Each strategy will get a rating which should be aimed for during the design, in Table 2.7 these aims are stated per strategy and their accompanying criteria. After every design phase these aims will be evaluated and checked whether they are reached. It is believed that this is a good way to approach a sustainable design process as an aim can be set what needs to be achieved and by the use of a radar diagram it can visualize at which stage the current design is.

Table 2.7: Sustainable Strategies goals.

Strategy	**Rating**	**Attributes**
Manufacturing	+	Recycled, medium and clean energy consumption, many steps, high flexibility, medium waste, low material use
Transportation and integration	-	Energy inefficient transport, inefficient logistics, few local supplies, low clean energy use
Social-economic impact	+	Intriguing shape, low shadow impact, noise level at WES-A04, quick ROI
Environmental impact	++	High clean energy output, no (toxic) emissions
Initial lifetime	+	High reliability, medium Durability, highly modular design, normal maintenance
End of life	+	Some components re-used or recyclable, low energy use

Manufacturing: The first strategy, optimization of the manufacturing techniques, is the starting point of every pro-

duction process. This part includes the material choice. The WHS has to be made out of recyclable materials but the structural components do not. For the structural component the strength and performance is the driven factor but trying to implement as much as possible recyclable components is important. The amount of energy used during the manufacturing procedures shall be minimized and it is important to apply techniques which assure a low waste policy. The system shall be designed such that a lightweight structure is created in order to reduce the material requirement and to decrease the amount of steps for the manufacturing process. The amount of steps required in manufacturing the design is highly dependent on the level of flexibility that can be implemented during the design phase. In Table 2.7 the aim for all the strategies is shown. The aim for the manufacturing techniques is a "+", as it is believed that is the minimum rating that should be achieved in order to achieve a sustainable design.

Transportation and integration: The next strategy concerns the transportation and integration techniques. After all the materials are chosen and produced, they need to be transported to the building site. The transportation route should be as short as possible with a low use of energy. This can be achieved by making use of mostly local suppliers and good logistics. If everything is safely delivered at the construction side, the integration can start. This integration should be executed with few and clean energy. However, this step is mainly executed by third party companies and therefore transparency is difficult to assure. Thus, the aim for this strategy is set at a "-". This has mainly to do with the fact that it is beyond control.

Social and economic impact: Moving on to the strategy which addresses the social and economic impact of the design on the society. If an intriguing shape is created which is embraced by the local people it will raise awareness with respect to sustainable living. The design will be integrated in the flourishing city of Rotterdam, which is a very international orientated city mainly due to its harbor. Millions of people will see it over the years. As it is going to be highly visible, negative effects such as shadow and noise should be mitigated at all costs. Lastly, it should be interesting for investors. This can be achieved with a quick Return on Investment (RoI) and this will benefit the market position. If the product can enter the market, it will be a pioneer with respect to urban energy harvesting systems. Therefore, a "+" rating is chosen, since the social and economic impact is the main thing the residents and the outside world is going to see.

Environmental impact: But it must be noted that the most important strategy for the design is the environmental impact. This is the strategy what the people do not see but need to start caring about. The design should have a high clean energy output of 50 MWh as stated in WES-A21, and no (toxic) emissions. This combined ensures an optimization of the environmental impact. It is chosen that the aim for this strategy should be "++", which means that the energy requirement needs to be met and while doing that not producing any emissions. Once this aim is achieved the most important goal of the system is reached.

Initial lifetime: The fifth strategy is the optimization of the initial lifetime of the design. This has mainly to do with a reliable, durable and modular design. The system should be designed modular in order to be able to implement future developments for specific components. The impact of a modular design is can not be quantified at this stage as future technology is unknown, however with the current developments it is believed that a lot of new technology is coming to our society. Furthermore, it should designed such that easy maintenance at all times is possible. Since all these aspect influence the sustainability of the design significantly it is chosen to go for a "+" aim.

End of life: The last strategy has to do with the optimization of the end of life of the design. As already mentioned the circular economy has to be taken into account from the start of the design, and its impact can be measured once the system is being dissembled. Therefore, it is required that once the system functioned for more than 10 years every part of the WHS is recyclable, and preferably also a large part of the structural component. Moreover, it is important that the system is designed and integrated such that not much energy usage is required to remove the structure from the building. Thus, an aim of "+" has been chosen for this specific strategy.

2.6.3. Preliminary Sustainability Score

During the design a preliminary sustainable score has been applied to both the WHS and the battery. The red line in both diagrams shown in Figure 2.7, display the aim that has been chosen to assure a sustainable design. For the VAWT the blue line indicate till what extend the sustainability was taken into account at that stage. However, as explained in Subsection 2.3.7 the battery was discarded and therefore will not be used anymore for further analysis however it was used for the the preliminary sustainability score and therefore also displayed below.

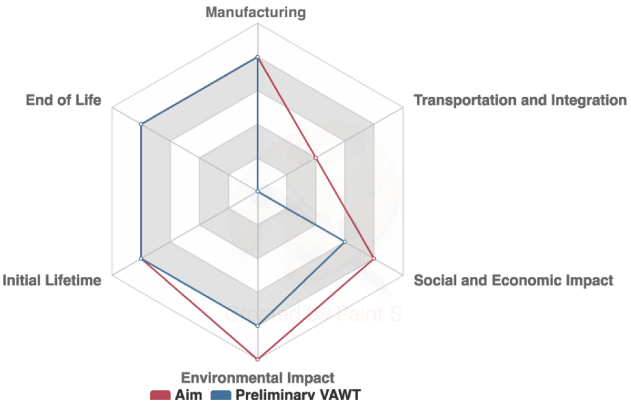

Figure 2.7: Radar diagram visualizing the preliminary score of VAWT.

Figure 2.8: Radar diagram visualizing the preliminary score of VRFB.

For the upcoming detailed design phase these six strategies will be taken into account at all moments, and design chosen will be based on it. In Figure 8.9 a final score will be applied to the sustainability of the WES. This final score will be a combined score for the electrical control system, structural support system and the harvesting component.

3
Design Approach

In the previous chapter the main guidelines are defined as approaches which the system needs to comply with. There are six strategies created to ensure a sustainable design. Furthermore, a mass, cost and energy allocation has been made and the addressable market is identified. Combined it can used to generate the first concept of the WHS. This process starts with analyzing the functions and requirements. Once the main goals are identified a design option tree will be made, stating the possible solutions. The next step is to apply a trade-off between five possible wind harvesting solutions. Once a system is chosen some detailed information on the system should be acquired before the real designing of the concept can start. First the selected design concept is summarized in Section 3.1. The systems functions will be analyzed in Subsection 3.1.1. The design option tree is explained in Subsection 3.1.2 and the trade-off between those design options is summarized in Subsection 3.1.3. Lastly, the main characteristics of the chosen concept are addressed in Subsection 3.1.4. In Section 3.2 the first sizing of the system is explained, resulting in the amount of turbines.

3.1. Conceptualization

The design conceptualization encompasses the early steps in the design of the wind energy harvesting system. The design commenced with the functional analysis, which allowed for understanding of the scope of this project. This was followed by the creation of a design option tree, in which many ideas for this project were thought up. Finally, the different alternatives from the design option tree were traded off to arrive at a final choice for the design.

3.1.1. Functional Analysis

Based on the mission statement and project objective the top level functions for the WES were determined. An overview of the top level functions is given in the Functional Flow Diagram (FFD) shown in Figure 3.1. It shows not only the different functions that the system should provide, but also the order in which they are performed. Usually this is done consecutively, but sometimes also in parallel as shown in Figure 3.1 as all of those functions need to be performed at the same time. In rare cases also only alternative functions will be performed in case of an "or" diversion.

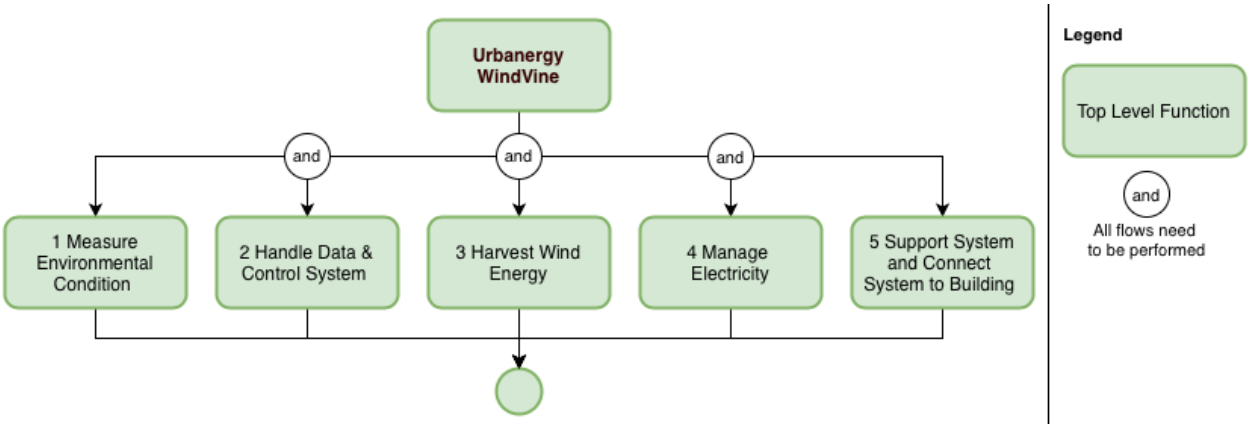

Figure 3.1: Functional Flow Diagram of the WES on top level.

The five main functions are; Measure Environmental Condition, Handle Data & Control System, Harvest Wind Energy, Manage Electricity and Support System & Connect System to Building. The first, second and fourth functions are contained in the electrical and control subsystem. Note that the focus of the FFDs in Figure 3.1 and subsequent chapters lies on the operational phase of the system, as most technical functions are associated to those. Other functional considerations are included in the project logic diagrams presented in Subsection 8.1.1.

In Section 4.1, Section 5.1 and Section 6.1 more detailed FFDs are shown for each subsystem. Furthermore, a full Functional Breakdown Structure (FBS) is available in Appendix A. It gives an overview of all the system functions on multiple levels and is structured as an hierarchical "AND"-tree. This means that lower system functions support each other, to fulfill higher level functions.

3.1.2. Design Decisions Summary

In order to choose the final design several new and proven concepts have been investigated. Various types of energy storage concepts, support structures and methods for wind energy harvesting were taken into consideration. In this section only the last two will be discussed since the energy storage was discarded during the design process, see Subsection 2.3.7. For both parts of the design, a Design Option Tree (DOT) was constructed. The tree is an "OR" tree, which means all branches are alternatives to each other [2]. The tree included creative solutions and also proven concepts.

After all options were written down, infeasible options were discarded. If the technical readiness level was too low and the amount of information on the system was limited, it would not be realistic for the team to pursue in the design process. In the tree these options were given the color red. Options in the tree that would not follow the constraints on safety and environmental were also discarded, and assigned to the color yellow. The last option that could be given to any of the design proposals of the tree for deleting out of the tree is when the efficiency would be too low. The efficiency comes together with other parameters such as cost and sustainability. However, if the desired system would not be able to stay below the requirements on cost and sustainability the efficiency was too low, and therefore not of proper use. This DOT is visualized in the midterm report [3].

3.1.2.1. Design Option Tree for Wind Harvesting System

The harvest wind energy tree was divided into passive and active wind usage, where active wind usage was then subdivided into blade-less and blade systems. For the passive wind usage three design options were considered. Generating energy with temperature differences, but these design options were discarded because it would not be efficient since there are no real large wind temperature differences. Then generating energy with pressure based options was considered. This could be further split into Piezoelectric Nanogenerator and pressure difference. However, making use of pressure differences was something that would be something to look further into. The last design option for passive wind usage was the power fence. An application of this is EWICON. However, after looking further into this, this option was discarded as well because the efficiency was not high enough [20].

The next step was to subdivide the blade systems into the Hummingbird Turbine, the VAWT and the HAWT. The Hummingbird Turbine[1] was something that would be looked into more detail as it was promising to have more then one turbine. The same was true for the VAWT options; the flower [2], the Savonius [3] and the Darrieus turbine were all viable options because of this.[4] Then for the HAWT only the 1 blade turbine was eliminated because this was considered to be not efficient enough. On the other side, the blade-less systems were subdivided into the following categories: rigid, semi-rigid and non-rigid. All the rigid design options were considered not viable. The options moving turbine, coil driven system, moving wings and Saphonian turbines were not considered because for options like these there was not a lot of research and therefore also not used in many applications. Then Oscillating Pillars [5], flaps and Magnus effect windmills were not considered because they would not be efficient enough.

Lastly the non-rigid options were investigated. Here the sail system was not considered viable because the probability of it lasting five years without maintenance was almost non existing. The kite system [6] could be considered as viable design option, but only by making use of one kite. The moment that more kites should be needed, the safety around the building could not be guaranteed, since there was not enough space to make sure they were not able to cross each others path [2].

[1] http://www.tyerwind.com/ [cited 4 May 2020].
[2] https://flowerturbines.com/ [cited 4 May 2020].
[3] http://www.reuk.co.uk/wordpress/wind/savonius-wind-turbines/ [cited 4 May 2020].
[4] https://www.powerelectronics.com/technologies/alternative-energy/article/21851777/small-wind-turbine-improves-on-darrieus-design [cited 18 June 2020].
[5] https://vortexbladeless.com/ [cited 4 May 2020].
[6] https://kitepower.nl/ [cited 4 May 2020].

3.1.2.2. Design Option Tree for Building Integration

Besides the question on whether the system would be integrated during the building phase or added later, the real design options were how the system would be integrated from a structural point of view. The different options for the integration to the building were a rigid connection or hanging cables which would result in a floating or fling structure. The system could then be integrated directly into the buildings or on a fixed support structure between the buildings. Another option would be to make the system deployable and retractable. Another set of design options was associated with the system layout. For example the system could be comprised of only one big wind harvesting system (mono layout) which would need to be integrated or out of multiple turbines (farm layout). In case of a farm layout, there were again different design options. The main options were: have the turbines connected (e.g. through panels) or diverted/spaced, have them in one line, parallel to each other or rather shifted and more distributed. These options were however already quite detailed. A non-rigid system integration in the limited area between the high-rises was rated a too high risk and hence discarded from the feasible design options [2].

3.1.3. Trade-off Summary

After discarding a large amount of options from the DOT, multiple options on the design were still valid for the final design. To create separation between all of the last designs, a trade-off was performed. This section will discuss all the criteria and weights that were given to the trade-off and design respectively. Five designs entered the trade-off which were the HAWT, VAWT, AeroMINE, MagnusBalloon and Hummingbird Turbine. At this point, a better judgment could be made based on more detailed information of the respective technology [3]. All designs were researched, especially on the criteria that were used in the trade-off.

The trade-off for the WHS consisted of two parts. After the first trade-off two options were discarded and the last three options entered the second trade-off. In each trade-off different criteria were looked at, and all options were given a rating. The rating scheme is shown in Table 3.1.

Table 3.1: Ratings and their respective descriptions for the trade-off.

Rating	Description		Color
5	Excellent	Able to exceed requirements	Dark green
4	Good	Meets requirements	Light green
3	Neutral	Barely meets requirements	Yellow
2	Poor	Corrections are required	Orange
1	Unacceptable	Will not meet requirements	Red

3.1.3.1. First Trade-off for Wind Harvesting System

Criteria is being be placed in two different classes, quantitative and qualitative. It was preferred that these were quantitative, as one could compare exact numbers, which were based on calculations. If they were not, a good explanation of the qualitative score was given. Once these criteria were finalized, each criterion is assigned a weight. The first five criteria used for the trade-off were:

- Noise
- Reliability
- Impact in case of failure
- Development Readiness

With the weights and the rating, every system received their product as a score. All scores were then summed together determining a total score for each system and lead to the final ranking as shown in Table 3.2. From the total scores, it can be seen, that the HAWT and VAWT received the best result, closely followed by the AeroMINE. Both, the MagnusBalloon and the Hummingbird did not even reach a total score above '3', indicating, that these technologies are not suitable and mature enough for the intended use case. For that reason, they were eliminated and also rejected from the DOT [3].

Table 3.2: First trade-off for the WHS.

		HAWT		VAWT		AeroMINE		MagnusBalloon		Hummingbird	
Criteria	**Weight**	Rating	Score	Rating	Score	Rating	Score	Rating	Score	Rating	Score
Noise	15%	2	0.30	4	0.60	4	0.60	3	0.45	4	0.60
Reliability	25%	5	1.25	4	1.00	5	1.25	2	0.50	2	0.50
Impact in Case of Failure	25%	2	0.50	3	0.75	4	1.00	3	0.75	3	0.75
Development Readiness	35%	5	1.75	4	1.40	2	0.70	2	0.70	1	0.35
Final Score	100%		**3.80**		**3.75**		**3.55**		**2.40**		**2.20**
Rank			**1**		**2**		**3**		**4**		**5**

3.1.3.2. Second Trade-off for Wind Harvesting System

Only the HAWT, VAWT and AeroMINE were considered in the following trade-off. The focus of this trade-off was on the kind of integration of the WHS. The distinction was made whether the system should be placed between the two high-rises and connected to both, or only attached to the side of a high-rise. Next to this, the older criteria were kept and a few were added:

- Accessibility
- Power efficiency
- Wind direction dependency

With the new ratings, every system received their specific scores and are shown in Table 3.3. From the total scores, it can be seen, that the VAWT placed on the side of a building received the best result, followed by the HAWT placed in the middle of the two high-rises. The AeroMINE received the lowest scores for both integration options and was therefore considered as not suitable for the intended use case. In the end, both design concepts, the HAWT between the building and the VAWT at the side of the building are well feasible and suitable solutions for the given mission need and project objective [2]. All other options would not be the best choice and were eliminated. For further explanation of the design trade-off, refer to [3].

Table 3.3: Second trade-off for the final three WHSs.

		HAWT				VAWT				AeroMINE			
		side		middle		side		middle		side		middle	
Criteria	**Weight**	Rating	Score	Rating	Score	Rating	Score	Rating	Score	Rating	Score	Rating	Score
Accessibility	10%	3	0.30	2	0.20	4	0.40	3	0.30	4	0.40	3	0.30
Power Efficiency	15%	2	0.30	5	0.75	4	0.60	3	0.45	2	0.30	4	0.60
Wind Direction Dependency	8%	2	0.16	2	0.16	5	0.40	5	0.40	2	0.16	2	0.16
Noise	8%	2	0.16	2	0.16	4	0.32	4	0.32	4	0.32	4	0.32
Reliability	20%	5	1.00	5	1.00	4	0.80	4	0.80	5	1.00	5	1.00
Impact in Case of Failure	13%	2	0.26	2	0.26	3	0.39	2	0.26	4	0.52	4	0.52
Development Readiness	26%	5	1.30	5	1.30	4	1.04	4	1.04	2	0.52	2	0.52
Final Score	100%		**3.48**		**3.83**		**3.95**		**3.57**		**3.22**		**3.42**
Rank			**4**		**2**		**1**		**3**		**6**		**5**

3.1.3.3. Sensitivity Analysis

To verify the final design a sensitivity analysis was performed. The weights of each criterion were revised and the underlying relationship between the designs was found. Afterwards it was concluded that indeed the VAWT on the side of one of the buildings would be the most optimum design. The type of VAWT that was chosen is the H-rotor, Darrieus type. Moreover, the reasoning for that choices are further explained in Subsection 3.1.4.

3.1.4. VAWT Characteristics

As explained in Subsection 3.1.3 the chosen concept is a VAWT H-Darrieus rotor. VAWTs have an axis transverse to the wind in contradiction of the axis parallel to the wind direction as for HAWT. An important characteristic of wind turbines is the power coefficient. The power coefficient indicates the efficiency of the turbine. The Betz limit is a theoretical maximum efficiency of a wind turbine. The limit is based on the principles of the conservation of mass and the momentum of the air stream going through an idealized actuator disk, as shown in Figure 3.2.

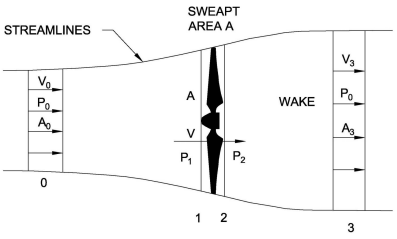

Figure 3.2: Visual representation of Betz limit theory.

According to the law it is impossible for a turbine to capture more than 59.3% of the kinetic energy in wind. Efficient wind turbines achieve at peak performance 75-80% of the Betz limit.

The VAWTs can work based on two different principles, drag or lift. The most developed types are shown in Figure 3.3 and are the Savonius, Darrieus with curved blades and H-Darrieus rotor.

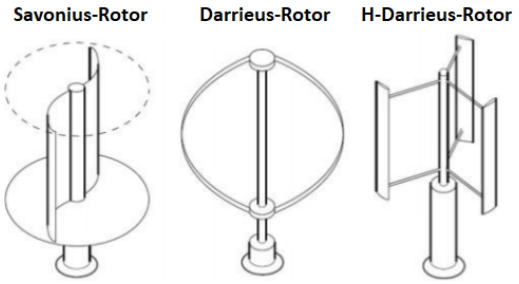

Figure 3.3: Main types of VAWT [21].

The Savonius rotor is a drag driven turbine and the other two are lift driven. Drag driven VAWT rotate due to the difference in drag created on the swept area. The Savonius rotor as shown in Figure 3.4 is one of many examples. The upwind side of the Savonius has the lowest drag and therefore it starts rotating counter clock wise. The big advantage of a drag driven VAWT is that it start operating at very low cut-on velocities which enhances a self-starting capabilities and a higher power output at low-wind speeds. However drag driven VAWT have low efficiency and can only convert about 11% of the kinetic energy available in wind, which is about 18.5% of the Betz limit [11].

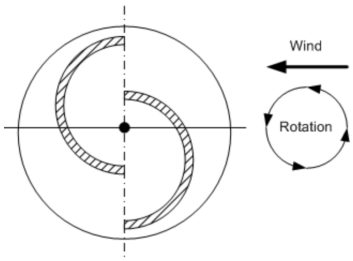

Figure 3.4: Schematic top view of a rotating drag driven VAWT.

A lift driven VAWT rotates due to the lift created over the blades. The resultant lift force moves the first blade it encounters into a counterclockwise direction as can be seen in Figure 3.5. A problem arises with respect to the cut-on velocity of the lift driven VAWT, since this is much higher then for a drag driven VAWT. Therefore, a lift driven VAWT requires a kick start which costs energy. On the other hand, the maximum theoretical power output of a VAWT is much higher than a drag driven one. Theoretically speaking, the lift driven VAWT could reach at peak performance 100% of the Betz limit. However, in reality is this never possible and this result was derived from some idealization and assumptions. But it must be noted that the performance of a lift driven VAWT is much higher.

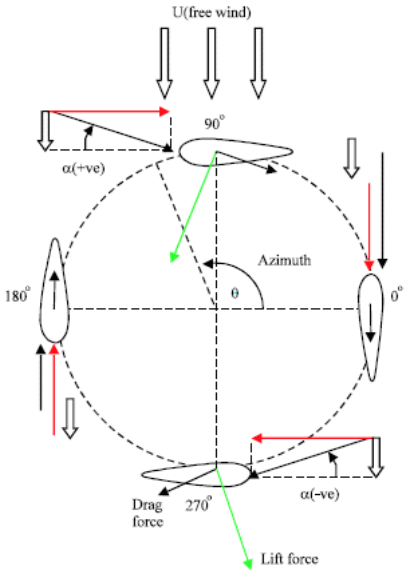

Figure 3.5: Schematic top view of a rotating lift driven VAWT [22].

Since the H-Darrieus rotor is more efficient than a Savonius rotor and more reliable and cheaper than the normal Darrieus rotor, the H-Darrieus rotor was selected for the design [23–25]. An other important design aspect that has to be taken into account is the poor self-starting capability of lift driven VAWTs. Savonius rotors can start and operate at lower wind speeds and therefore Savonius rotors were considered for a potential hybrid solution between the H-Darrieus and Savonius rotor.

3.2. System Sizing

In the previous chapter, a more detailed technology concept for the WES was selected and described. This was the starting point for a more detailed subsystem sizing. In the next coming three chapters, first the WHS is addressed (Chapter 4), dealing with the aerodynamic and structural turbine sizing, as well as the power train. In Chapter 5 the process for the structural support system is presented, being the connection of the turbine and the building. Lastly, the electrical and control subsystems are described in Chapter 6.

One first big design decision was the determination of the number of turbines. After multiple considerations during the design process [3], including all different departments, the total number of VAWTs was determined. In the end it was a compromise between one large turbine and multiple small ones. The benefit of one large system is that it will have less components to be integrated and more importantly, that it would have a higher efficiency [26]. Multiple turbines on the other hand would be easier to be integrated to already existing buildings as the load would be distributed to multiple locations of the building. Furthermore, if the turbine is smaller, multiple units are required of smaller size. Production, logistics, installment and maintenance will therefore be easier and the costs of the system and for operation will be reduced. Furthermore having several turbines makes the design more easily scalable with respect to the power production required. The influence of the turbine number is not directly related to a performance reduction caused by turbulent flows that get generated. The layout however could have an influence, for example if multiple turbines are placed horizontally in a line, which is why their spacing needed to be considered (see Chapter 5).

The usage of three turbines was a good compromise resulting from multiple iterations in different subsystems, mainly from the power optimization explained in Subsection 4.3.4.

4

Wind Harvesting System

The upcoming chapter discusses every aspect of the design of the turbine. Three turbines are involved in the complete WES system, as explained in Section 3.2. The functional analysis is given in Section 4.1 followed by the functional requirements in Section 4.2. and the aerodynamic rotor design process in Section 4.3. Section 4.4 addresses the design of the power train, including the design of the generator, brake system and an analysis of the starting performance. After that an analysis of the noise is given in Section 4.5 and Section 4.6 goes into depth of the structural design of the turbine. Finally, the mass, cost and sustainability aspects of the turbine are discussed in Section 4.7.

4.1. Functional Analysis

As already mentioned in Subsection 3.1.1, in Figure 4.1 a more detailed functional flow for the wind harvesting subsystem is presented and reaches three levels down. An extensive functional break down structure with one more lower level can also be found in Appendix A.

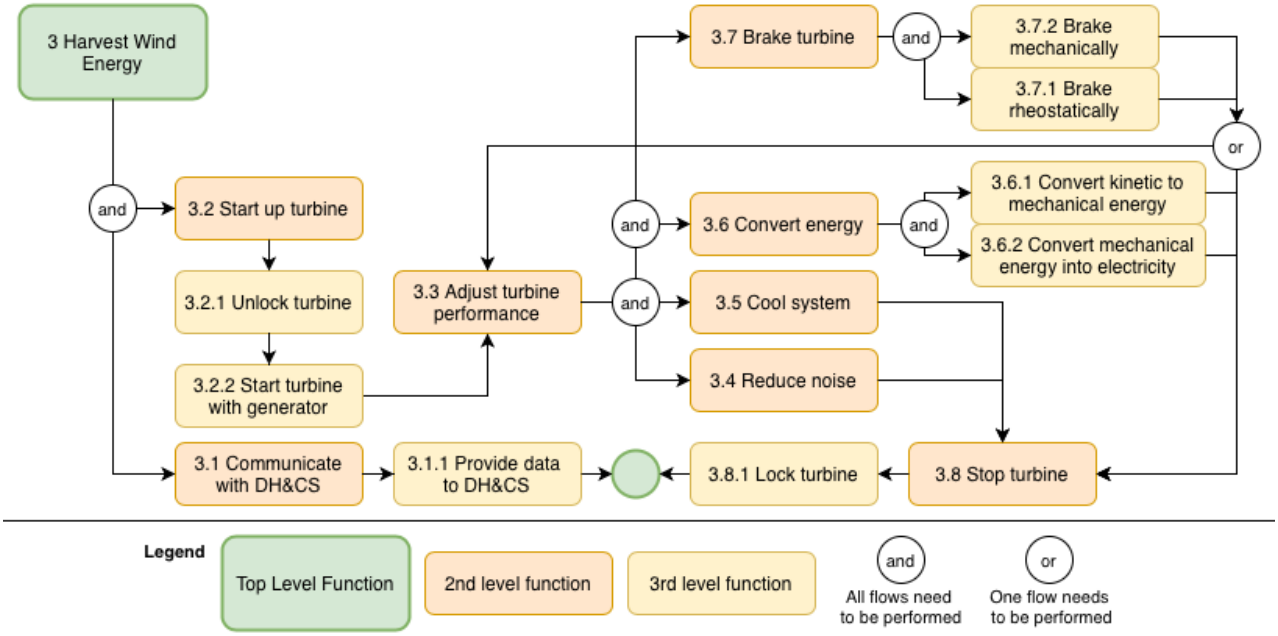

Figure 4.1: Functional Flow Diagram of the WHS.

4.2. Functional Requirements

The most important requirements for the turbine design are shown in Table 4.1. These are off course not all the requirements, but give an indication of the main requirements on which the turbine sizing and designing was based.

Table 4.1: Main requirements for turbine design.

Requirement code	Requirement
WES-A01	The system shall have a cut-on velocity of 3 m/s.
WES-A04	The system shall be within standard noise regulations for conventional wind turbines.
WES-A08	The system shall have a minimum lifetime of 10 years.
WES-A09	The system shall not require a technical inspection before 5 operating years.
WES-A10	The system shall not damage the high-rise buildings in case of failure.
WES-A11	The system shall not damage the area in between the high-rise buildings.
WES-A12	The system shall not damage people in case of failure.
WES-A13	The system shall stop working automatically in case of failure.
WES-A14	The system shall be controlled by a mechanical safety system.
WES-A16	The system, excluding structural components, shall be made of recyclable materials.
WES-A17	The system shall have an overall unit cost below €75,000.
WES-A21	The system shall provide 50 MWh at a rated velocity of 10 m/s with a free-stream turbulence distributed with Gaussian law at a standard deviation of 2.5.
WES-A22	The system shall be integrated into a 30-meter space between two buildings of which the parallel sides have a rectangular shape with a height of 200 meters and a width of 30 meters.
WES-OP-MU-03	The system shall have an absolute noise limit of 47 dB L_{den} (Dutch absolute noise power limit [27–29]).
WES-OP-MU-04	The system shall have an absolute noise power limit at night, L_{night} (23.00-7.00 local time), of 41 dB. [28, 29]

4.3. Rotor sizing

In this section, the aerodynamic design of the turbine is explained. Firstly, the numerical model used for the aerodynamic design is presented in Subsection 4.3.1 and its limitations are discussed in Subsection 4.3.2. Then the design considerations and optimization process for the aerodynamic performance is discussed in Subsection 4.3.3 and Subsection 4.3.4 respectively. Finally, verification is performed in Subsection 4.3.5.

4.3.1. Aerodynamic Model

To analyze and size the VAWT turbine, the open source software QBlade was used. QBlade uses the Double-Multiple Streamtube (DSM) model, developed by Ian Paraschivoiu [30]. Several sources state that QBlade is a suitable tool for preliminary designing and optimizing wind turbines [31], however it is not the most accurate model as explained later in this section. Nevertheless, in this stage of the design process QBlade is appropriate to size and optimize parameters of the turbine, which can be refined in a more detailed design phase. A more accurate model would be the actuator cylinder model, however this model is not available in third party software and is therefore not feasible to implement in the current preliminary design phase [32]. It is advised to be used for more accurate analysis of the design in a later stage of the design.

The DSM model is based on the actuator disk theory and blade element theory. The flow over the turbine is divided into multiple streamtubes, which are parallel and aerodynamically independent. Since for a VAWT the blades pass the air stream twice each revolution, two actuator disk are used in the DSM model. For every streamtube at both actuator disks the one-dimensional momentum conservation theory is applied to calculate the upstream and downstream wind velocities around the blade by calculating the induced velocity through the rotor blade. The induced velocity is the velocity of the air after the interaction with the blade, which is lower due to the energy extraction of the blade. An extra set of equations is then derived from the blade element theory, which calculates the aerodynamic forces on the blade based on the airfoil lift and drag polars. These two sets of equations are solved simultaneously by means of an iterative algorithm. This procedure is performed for every azimuth angle (rotational position of the blade) and for every height position of the blade. Using the result of the DSM model, the performance of the turbine can be summarized [30, 33].

The first step in QBlade is loading the selected airfoil and doing a two-dimensional analysis. This is performed using the integrated XFoil software. The analysed (4-digit NACA) airfoils can be loaded in directly. XFoil is validated several times to perform accurate estimations on the airfoil characteristics [34]. However, the software is limited to perform

accurate estimations for angles of attack before and slightly after stall. For very high and low angles of attack, where a lot of flow separation occurs, XFoil is unable to do accurate predictions due to the fact that the used algorithm does not converge. This results in XFoil not being able to analyze the airfoil for these angles of attack. For VAWTs very high and low angles of attack can occur due to the circular movement which causes the XFoil analysis to be insufficient (since the data for very high and low angles of attack is missing). The lift and drag polars should therefore be extrapolated to 360° angle of attack to assure correct performance of the DSM model. For this the Montgomery extrapolation method was used. Another model able to perform the extrapolation is Viterna. Montgomery is a more complex method but is proven to have a higher accuracy. Since both these extrapolation methods were available in QBlade and the accuracy of the Montgomery method is higher, this method was selected [35].

The Montgomery method uses the assumption that there exists a potential flow behaviour at an angle of attack of 0°. For high angles of attack, the performance of the airfoil is modeled, as if it would be a thin plate. An interpolation between the two behaviours is then used to obtain the lift and drag coefficient for all angles of attack [35]. In QBlade this method is performed and the results were optimized by manually changing parameters creating a close fit of the extrapolation with the part of the graph created by XFoil. Changing the parameters mainly changes the transition region between the XFoil generated data and the extrapolated data. Great care was taken in the extrapolation procedure, by comparing the extrapolation with available 360° plots in literature, since the extrapolation can have significant influence on the accuracy of the further performed analysis of the turbine [30].

The final step was to estimate the amount of energy the system produces per year. This was calculated by using a weighted average over the different wind speeds using the distribution as explained in Subsection 2.4.3.

4.3.2. Limitations of QBlade and DMS Model

The main limitations of the application of QBlade (and the DSM model) lie in very high solidities and high Tip Speed Ratios (TSRs) [30]. The rotor solidity is defined by $\sigma = \frac{Nc}{R}$, where N is the number of blades, c is the chord length and R is the rotor radius. TSR is defined by $\frac{R\omega}{V}$ and is the ratio between the velocity at the tip and the free stream velocity [33]. At very high solidities and high TSRs backflow can occur, which is not implemented in the model, causing the results to be inaccurate. For this reason the results for high TSRs should not be used or trusted. Furthermore the rotor solidity should be limited and no extreme values should be used, causing unrealistic results. However, the analysis is mainly performed around the optimum TSR, which was mostly in the range of three to four (based on the C_p graphs obtained during iterations), and the limitations of high TSRs were therefore mitigated. Furthermore very high solidities were also not considered, since according to literature the optimal solidity factor is between 0.2 and 0.6 [36, 37]. This limitation of the model was hence also mitigated. No exact maximum values were given for the TSR and rotor solidity, however it is documented that the limitation is shown in the results when large "kinks" in the power curve are present [30]. Therefore care was taken in analyzing the power curves obtained for weird kinks and unexpected shape of the curve. Aerodynamic influences of the airflow around auxiliary turbine structures like tower, struts and guy ropes are neglected in the model. Struts have a large effect on the performance by causing drag though and thus a 10% loss factor was added to take this effect into account (based on a 12 kW turbine design in [38]).

The DSM model is not able to correctly predict the effect of changing the fixed pitch angle, as explained in [39]. Iterating the pitch angle using QBlade was therefore not possible, as this would not have resulted in correct results. However, optimizing the fixed pitch angle is something that should be looked into in later design phases when more accurate models are used.

To solve some of the imperfections of the DSM model used in QBlade, two correction factors can be included in the analysis. The first one is a tiploss factor. Since the pressure on the bottom of an airfoil is lower than on the top of the airfoil, a pressure difference exists. This results in tip vortices, causing downwash and a spanwise velocity component of the flow. The tiploss factor in QBlade accounts for this effect by changing the angle of attack, relative wind velocity (as seen by the blade) and lift and drag coefficients [30]. The explained effect however also introduces the limitation of the software. The spanwise velocity which is induced, would cause the streamtubes, as defined for the DSM model, to expand in spanwise direction. The spanwise velocity is not included in the software and will therefore cause a small inaccuracy of the model. The second correction factor is the variable interference factor. The most simple DSM model assumes constant interference factors for the front half of the rotation and back half of the rotation, which is a rough assumption. The interference factor is the ratio between the free-stream velocity and the induced velocity behind the blade. The variable interference factor option in QBlade makes sure the iteration as explained earlier is performed for every azimuth angle. This means that for every specific position of the blade, the

interference factor is calculated separately. It also means that the induced velocity of the air behind the blade (so after losing energy due to the interference with the blade) is calculated for every blade position, making the model more accurate.

QBlade contains one more simplifications which causes an inaccuracy in the results. The simplification is that dynamic stall is not modelled. During a cycle of the blade, the angle of attack and Reynolds number vary substantially. The effect of this is that the aerodynamic loading fluctuates and a series of flow separations and re-attachments occur [40]. This phenomenon is called dynamic stall, causing the lift and drag coefficients to change vastly and depends on many parameters such as turbulence, three-dimensional flow effects and the rate at which the angle of attack changes [33]. Not including dynamic stall in the model causes the performance results to be higher than in reality, since dynamic stall degrades the performance of a VAWT [41]. Dynamic stall is a complex phenomenon and more advanced models exist to account for that. These should be used in later design phases to investigate the influence of this effect on the performance of the turbine.

Concluding, QBlade does contain quite some simplifications which causes some uncertainty in the results produced. However for the current preliminary design it is a suitable tool to use and see the effect of changing design parameters. As explained in Subsection 4.3.1 a more advanced model such as the actuator cylinder model should be used in future design phases. Furthermore the feasibility of the results is checked in verification in Subsection 4.3.5 and the results will finally be validated as explained in Section 7.3.

4.3.3. Design Considerations

In this section the design considerations to optimize the turbine are explained. To optimize the turbine, a high power coefficient C_p is desired, which is a function of TSR. In the following subsections each parameter that influences the C_p curve and the overall performance of the turbine are discussed.

4.3.3.1. Number of Blades

A starting point in designing a VAWT is selecting the number of blades. In theory they can be build with only one blade, however this would require the need for a counteracting weight, which increases the drag. Furthermore self-starting of the turbine would not be possible, since the blade does not generate positive torque at every position in the revolution [42]. Therefore one blade was not considered. From literature the optimum number of blades with respect to efficiency appears to be two, three blades bring quite some further advantages [33, 42]. Turbines with two blades in particular have large fluctuations in torque and the aerodynamic force generated by the two blades peak at about the same time with the resultant force in the same direction. This can cause resonant vibration in the system which is not desired. Having three blades which are evenly distributed at angles of 120° cause a more constant force and torque [33, 42]. Increasing the number of blades further has the effect that the optimum power coefficient is reached at lower angular velocities, however the efficiency will decrease [43]. Therefore, a next design choice (see Figure 7.1) was done: for this design the optimum number of blades was chosen to be three, which is in the end the optimum number of blades according to literature including more criteria than efficiency [33, 42, 44].

4.3.3.2. Design Parameters

To optimize the aerodynamic performance, three main sizing parameters should be investigated.

Rotor solidity σ: The rotor solidity is, as explained in Subsection 4.3.1, defined by $\sigma = \frac{Nc}{R}$, where N is the number of blades, c is the chord length and R is the rotor radius. According to several studies [36, 37], the optimal rotor solidity is in the range $0.2 \leq \sigma \leq 0.6$. Furthermore, $\sigma \geq 0.4$ allows for a self starting turbine [45], which eliminates the need for a an electrical motor which is further discussed in Subsection 4.4.3.

Blade aspect ratio H/c: The blade aspect ratio is the blade height over the blade chord. According to a study by Ahmadi-Baloutaki et al. [36] the optimum ratio lies between $10 \leq H/c \leq 20$, where a larger ratio results in lower tip losses and thus a better performance. However, a larger ratio also means longer blades, which results in a higher weight, thus an increase in cost and larger bending moments.

Ratio height over diameter H/D: In a study by Brusca et al. [46] the effect of H/D is investigated and it was concluded that a smaller ratio leads to a higher efficiency. The optimal ratio is in the range $0.5 \leq H/D \leq 2$, where the lower limit results in smaller blades, thus a lower cost and a smaller bending moment. The upper limit, however, provides an advantage if the space is limited and a smaller radius is required.

4.3.3.3. Airfoil Selection

The next design choice which needed to be made (see Figure 7.1) was which airfoil is most efficient. The blade cross-sectional area is a crucial factor for a more efficient design for the VAWT. A distinction should be made between the classic symmetric NACA airfoils and asymmetric airfoils. NACA airfoils were used since these are the most commonly used symmetrical airfoils in VAWTs [33]. The main advantage of asymmetric airfoils is that they have better aerodynamic characteristics at low Reynolds numbers, thus being able to self-start [33]. However, symmetric airfoils have the advantage that both sides provide lift during a revolution. This means that regardless of the wind direction the airfoil will provide lift and there is no need to re-adjust the airfoil during the rotation. Research has proven that symmetric airfoils have higher power coefficients than asymmetric airfoils at tip speed ratios higher than three [47]. Since the most optimum tip speed ratio is in the range from three to four, it was decided to implement a symmetric airfoil in our design. The most frequently used airfoils, the NACA0012, NACA0015 and NACA0018, will be further investigated. In addition, as a thicker airfoil has structural benefits due to its higher bending capability, the NACA0021 will also be analyzed. The performance of the airfoils can be seen in Figure 4.2.

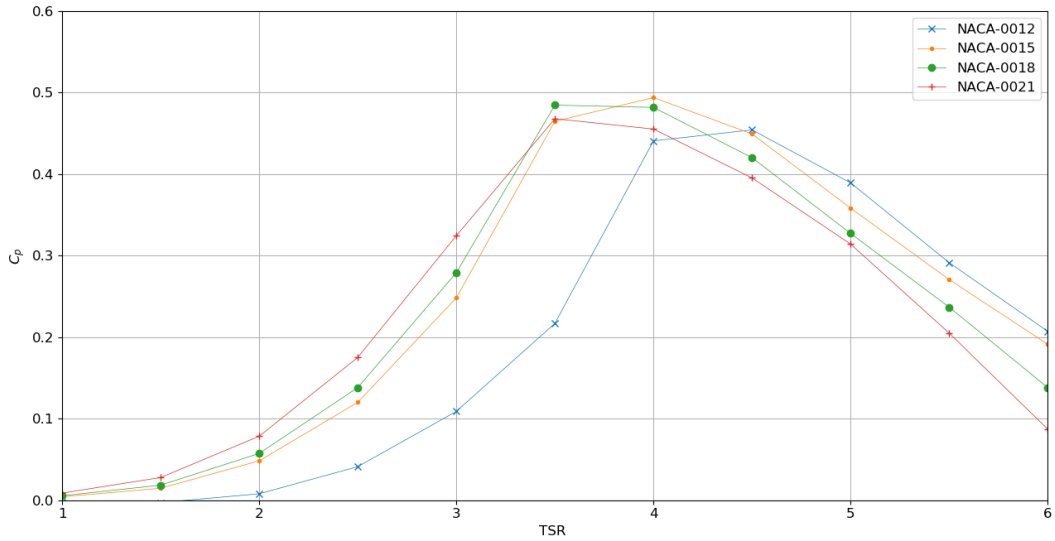

Figure 4.2: C_p curve for different airfoils with the same dimensions: $H = 6m$, $R = 3m$, $c = 0.3m$.

Figure 4.2 shows the effect on performance of a thinner airfoil at higher TSRs. The NACA0015 has the highest C_p with the NACA0018 as close second. However, as the NACA0018 is thicker than the NACA0015 it will result in structural advantages. Therefore, the NACA0018 will be used in further sections.

4.3.3.4. Cut-on and Cut-out Speed

The cut-on speed is the minimum wind speed at which the turbine operates. From the user requirements given in Section 4.2 the turbine shall have a cut-on speed of 3 m/s. The cut-out speed is the maximum wind speed at which the turbine operates [36]. The turbine structural components of the turbine are then not designed to sustain the loads above the cut-out speed. An advised maximum cut-out speed is 25 m/s [37] as this represents storm conditions. As was described in Subsection 2.4.3 the wind distribution is normally distributed over 10 m/s and wind velocities above 18 m/s are very rare. The turbine will therefore be designed with a cut-out speed of 18 m/s. However, in further sections the loads for a 20 m/s turbine will be taken into account as a safety margin.

4.3.3.5. Fixed and Variable Wind Conversion System

Wind energy systems can operate under fixed-speed or variable speed conditions [48]. For fixed-speed turbines, the rotor speed is fixed and directly connected to the grid. This has the advantage of being a simple, reliable and robust option but at the cost of only operating at maximum efficiency at a particular wind speed [48]. The other option is using a variable-speed wind system. This allows for a controlled generator speed for maximum efficiency at various wind speeds and a decrease in mechanical stresses. This comes at an increase in cost and an increase in complexity

of the electrical system [48]. However, as described in Section 2.4 the turbine will operate in a large range of wind conditions. A variable-speed system is then favourable as the output power will overcome the increase in cost and complexity.

4.3.3.6. Power Control

To limit the excess power in case of stronger winds, a power control mechanism is needed. There are different power control mechanisms with each their advantages and disadvantages. Pitch control uses an electronic controller to measure the power output from the turbine and a pitching mechanism to adjust the blades to optimize power output. The efficiency of the turbine increases as it can maintain a constant power output above the rated wind speed, but at the cost of increased complexity and system cost.[1] Stall-regulated turbines make use of the aerodynamic performance of the turbines blades. The blades are designed such that, once the rated wind speed is achieved the blades are stalled causing the power output to decrease.[2] Two types of stall-controlled turbines exist. On the one side the active stall-control which uses a pitch mechanism to increase the angle of attack of the rotor blades such as to make the blades go into a deeper stall, which reduces the power.[3] However, this requires additional moving parts increasing complexity and cost. On the other hand, passive control has a fixed pitch designed such that the stall will occur after the rated power. A significant decrease in power output will occur but no additional moving parts are needed which limits the complexity and cost of the system.[4] Due to the strict budget for this wind turbine, passive stall will be used for power control. However it should be noted that passive stall does lead to a complex aerodynamic design if stall induced vibrations want to be limited.[5] This is beyond the scope for a preliminary design, but should be investigated in further design phases.

4.3.4. Optimization of Aerodynamic Performance

In order to obtain the best design for the given requirements, an iterative design process was performed. The first step in this design process was to analyze the aerodynamic performance. A first estimation of the rated power was done in Section 2.5. To start the optimization, an estimate for the required swept area was necessary. Using Equation 4.1 and assuming sea-level conditions, a rated wind speed of 10 m/s and a power coefficient, $C_p = 0.35$ [49], the total swept area was found to be 78.5 m^2.

$$P = 0.5\rho C_p V^3 A \tag{4.1}$$

4.3.4.1. Optimization Process

After all main parameters for the design process were defined, the iterative process could start. As three turbines will be used for the design, the swept area of each turbine is 26.2 m^2. From there, the dimensions of the turbine were defined such that it was in the range of optimized parameters as discussed in Subsubsection 4.3.3.2. The design was optimised for the highest C_p and the highest power for the range of wind conditions the turbine will be subjected to.

As was described in Subsection 4.3.3, a variable speed wind turbine system will allow for a better power performance. The rotational speed will then be adjusted to perform at maximum efficiency for each wind velocity. To determine the maximum rotational speed, the maximum tip velocity was constrained. From [38], a recommended maximum tip speed of 40 m/s was used, which will result in a limitation of centrifugal forces and emitted noise. Nevertheless, a reiteration was needed if the emitted noise or structural stresses are too high (Section 4.5 and Section 4.6). The rotational speed was then adjusted according to the optimal design TSR which was found at the $C_{p_{max}}$ value.

The C_p-curve and power curve were plotted for different designs, as can be seen in Figure 4.3. The figure shows that the design with a higher blade aspect ratio performs best. This is mainly due to the reduced tip losses. The turbine will operate mostly at wind velocities around 10 m/s and therefore, the design which has the highest rated power around 10-12 m/s should be further investigated. This is because if the maximum rated power occurs at a higher wind speed but the power at wind velocities 10-12 m/s is lower, the annual energy production will be lower due to a lower probability of wind speeds above 12 m/s.

[1] http://xn–drmstrre-64ad.dk/wp-content/wind/miller/windpower%20web/en/tour/wtrb/powerreg.htm [cited 11 June 2020].
[2] http://researchhubs.com/post/engineering/wind-energy/pitch-regulated-and-stall-regulated-wind-turbine.html [cited 11 June 2020].
[3] See footnote 1
[4] wind.nrel.gov [cited 11 June 2020].
[5] See footnote 1

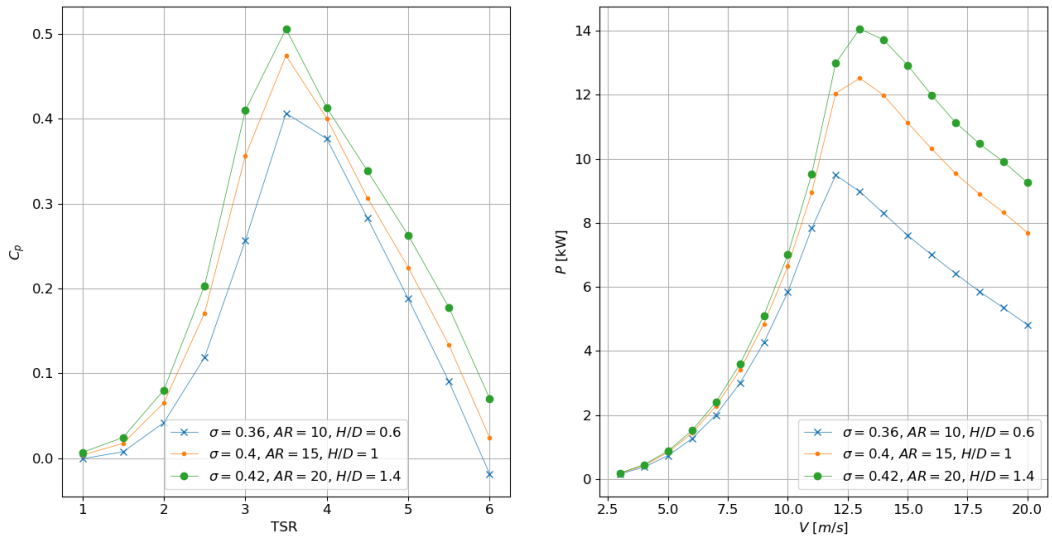

Figure 4.3: C_p in function of tip speed ratio (left) and power in function of wind speed (right) for different designs with rotor solidity (σ), blade aspect ratio (AR), and height to diameter ratio .

A reiteration was done for the best design with the new C_p values calculated, each iteration optimizing the design parameters. It should be noted that the C_p values in Figure 4.3 are way above usual C_p values for VAWTs, which are around 0.25-0.4 [49]. Firstly, the loss due to the connecting arms to the blades was not taken into account. According to [38] a 10% loss can be assumed. Furthermore, as described in Subsection 4.3.1 the DSM model presents some inaccuracies in predicting the aerodynamic performance. In [50], the QBlade model is compared to experimental data and a the QBlade model was found to over-predict the power by 10% for low wind speeds (< 10 m/s) and presents good agreement for higher wind speeds. In addition, in a comparison of the predicted C_p-curve calculated with the DSM model for a straight bladed turbine in [38] with the measured C_p-curve described in [51], the DSM model over-predicted the C_p-curve by about 5%. Therefore, a 10% contingency was used. The $C_{p_{max}}$ of the designed turbine was finally reduced from 0.5 to 0.4 which is a more feasible value.

The next step was to verify that the design meets the annual energy requirement of 50 MWh. To do so, the power curve was multiplied with the load hours described in Section 2.5. If the three turbines were not meeting the requirement, a reiteration was done. The design was reiterated until the requirement of 50 MWh was met with a safety factor of 1.1, which also accounts for electrical losses and wind variance.

4.3.4.2. Turbine Design and Performance

The iteration process discussed above led to a final turbine design for which the main dimensions and parameters are given in Table 4.2.

Table 4.2: Main dimensions and parameters for one turbine.

Parameter	Value	Unit	Parameter	Value	Unit
Swept area	27.97	m^2	Rotational speed	151	RPM
Height	5.55	m	$V_{tip_{max}}$	40	m/s
Radius	2.52	m	Airfoil	NACA0018	-
Solidity	0.33	-	Power control	Passive stall	-

The aerodynamic performance and forces for the design described above are given in Figure 4.4 and Figure 4.5 respectively.

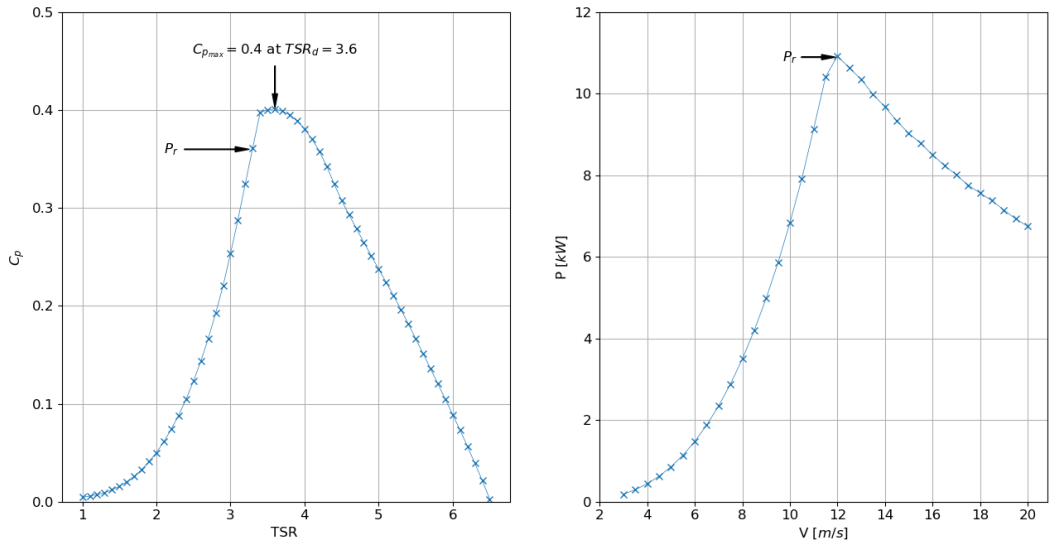

Figure 4.4: C_p curve in function of TSR (left) and power curve in function of wind speed (right) for final turbine design.

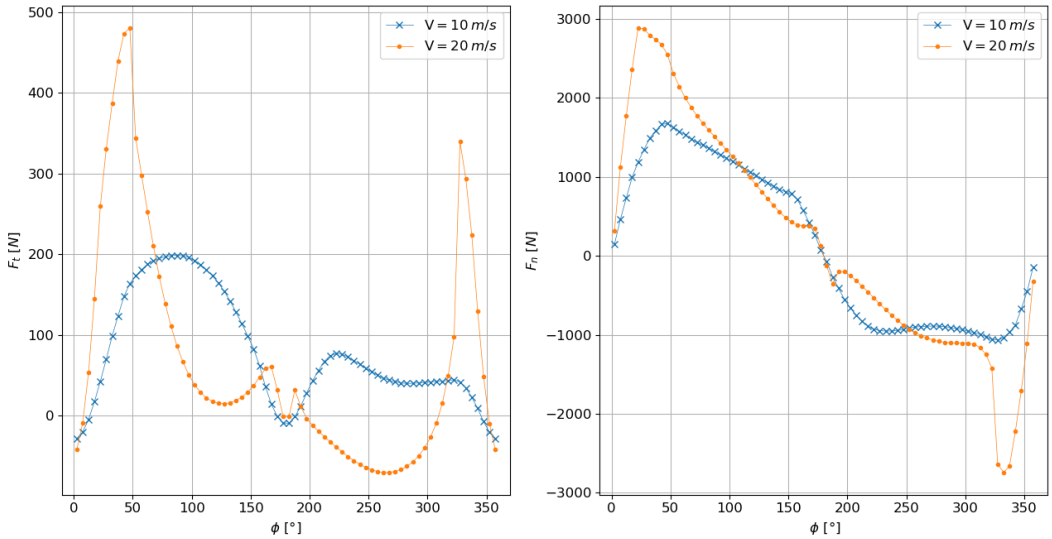

Figure 4.5: Tangential force F_t (left) and normal force F_n (right) on blade in function of azimuth angle ϕ for final turbine design.

In Figure 4.4 it can be seen that the optimal C_p was found at the designed TSR of 3.6. This means that the turbine will keep its designed TSR by changing the rotational speed as was discussed in Subsubsection 4.3.3.5. Once the designed TSR is reached and the incoming wind velocity increases, the TSR will decrease. The rated power is achieved at 12 m/s for a rated power of 11 kW.

It can be noted that the C_p curve shown in Figure 4.4 is sharp. However, it is generally recommended to have a broader peak such that the rotor speed does not have to be closely controlled in order to achieve optimal power output [52]. For this preliminary design phase the turbine performance presented above was considered the most suitable and is further used in this report. However, if at a later development stage, the turbine is found to have a C_p curve with a too sharp peak and difficult controlability, three main further investigations can be made. Firstly, the thickness of the aileron can be increases such that the peak becomes broader. If the thickness increases significantly, the peak will become broader but at the cost of a decreased $C_{p_{max}}$ [52]. The NACA0021 presented earlier would be a suitable choice for further investigation. Secondly, the rotor solidity could be decreased to broaden the C_p curve, decrease the blockage of the flow and parasite drag. However, as was discussed in Subsection 4.3.3 the rotor solidity should remain in its optimal range such as to achieve a higher power output. Finally, a negative preset pitch between

$-2°$ and $-7°$ to the blades could be set which could allow for a broadening of the C_p curve in addition to an increase in peak power [52, 53].

To get the annual energy production for the three turbines, the power curve in Figure 4.4 was multiplied with the load hours described in Section 2.5, which resulted in a yearly production of 56 MWh. This is excluding all the electrical losses which will be further discussed in Section 4.4

In this section, a mostly non-dimensional analysis had been performed in QBlade. In order to get the dimensional forces on the blades, which were of further use in Section 4.6, Equation 4.2 was used (where C_t and C_n are the tangential and normal coefficient respectively, ρ the air density, A_b the area of the blade and U_0 the local velocity of the blade). Both the normal and tangential coefficients were found by the analysis in QBlade and the relative velocity could be computed for each azimuth angle. The tangential and normal force on one blade could then be plotted such as in Figure 4.5. As can be seen from the graph, as the incoming wind speed increases, so do the forces on the blades. In further sections the maximum forces on the blades corresponding to an incoming wind speed of 20 m/s will be used.

$$F_t = C_t\left(\frac{1}{2}\rho A_b U_0^2\right) \qquad F_n = C_n\left(\frac{1}{2}\rho A_b U_0^2\right) \tag{4.2}$$

4.3.5. Verification

As stated in Subsection 4.3.1 QBlade was used for the aerodynamic analysis of the turbine. Several previous studies [50, 54] have verified and validated the results of the aerodynamic performance of VAWTs in QBlade. To verify the results presented above, a comparison was made with already existing straight balded H-rotor. The reference turbine had a rated power of 12 kW and had some differences in dimensions which are extensively described in [38]. The reference turbine had a slightly higher rotor diameter of 3 m, with a lower blade height of 5 m.

Firstly, a comparison of the two turbines was made in QBlade and is presented in Figure 4.6. For this an additional 10% loss was applied to account for the supporting arms.

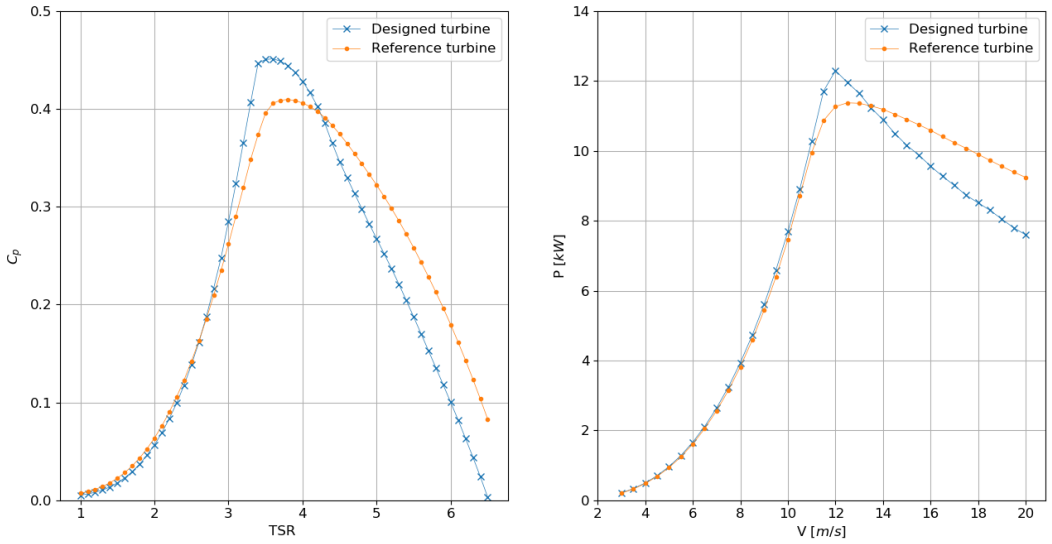

Figure 4.6: Comparison of C_p curve (left) and power curve (right) between designed turbine and reference turbine presented in [38] in QBlade.

In Kjellin et al. [51] the reference turbine shown in Figure 4.6 was tested and the $C_{p_{max}}$ was found to be 0.29. This is significantly lower than the predicted $C_{p_{max}} \approx 0.4$ as shown in Figure 4.6. According to the same study, this significant decrease is mostly due to the blade and supporting arms profile. With some profile improvements, the $C_{p_{max}}$ was able to get to 0.39 which corresponds better to the curve shown in Figure 4.6 for the reference turbine.

From Figure 4.6 it can be seen that the designed turbine can achieve better performance than the reference turbine. Therefore, it can be assumed that with the additional 10% contingency taken as described in Subsection 4.3.4 the results presented for the designed turbines in Subsubsection 4.3.4.2 where a $C_{p_{max}} = 0.4$ was estimated are achievable. Adjustments or improvements of the blade or supporting arms might be needed to achieve the optimal C_p. However, for this more accurate tests should be performed to validate the results.

Secondly, the aerodynamic forces of the designed turbine were compared with measurements of the reference turbine described above. These measurements are described in Rossander et al. [55] and were done for sea level conditions with a constant TSR of 3.5 and a rotational speed of 50 Revolutions per Minute (RPM). The aerodynamic forces of the designed turbines were then plotted for the designed glstsr of 3.6 and rotational speed of 72 RPM, which was for approximately the same incoming wind speed and can be seen in Figure 4.7.

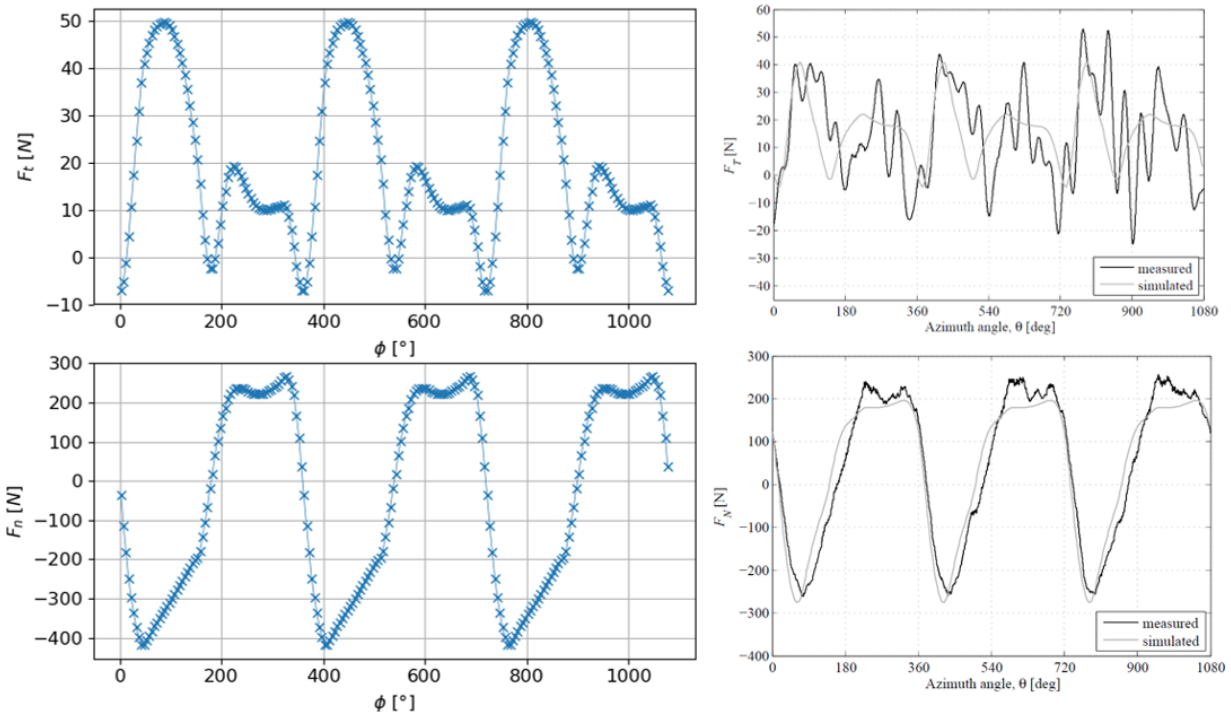

Figure 4.7: Comparison tangential force F_t (top) and normal force F_n (bottom) in function of azimuth angle ϕ of designed turbine (left) and reference turbine (right) from [55].

In Figure 4.7 it can be seen that the tangential force correlates well with the measured data in literature [55]. The QBlade model predicts constant tangential forces between a minimum of -10 N and a maximum of 50 N. The maximum tangential force oscillates between 40 and 50 N while the minimum tangential force oscillates between -10 and -20 N. A maximum over prediction with a factor 1.25 was thus made by the QBlade model. The discrepancies between the model and the results can be explained by the difference in dimensions of the two turbines. Furthermore, the model does not accurately model the complex aerodynamic phenomena that occur in the downstream wake of the upstream blade but also the mechanical oscillations of the blades which results in deviations in tangential force [55].

The modelled normal force presents a good agreement with the measured data. The normal force presented by QBlade presents a minimum force of -410 N while the measurements show a minimum force of -250 N. The model thus over predicts by a factor of about 1.6. This can be explained by the difference in dimensions of the reference turbine. The tip speed ratio for both turbines shown in Figure 4.7 are similar however, the rotational speed of the designed turbine is higher in this specific case and results in higher tip speeds. This results in larger normal forces. From the comparison described above it can be concluded that the results presented in this section present a good first estimation for the designed turbine. The results can thus be used for further calculations.

4.4. Power Train

To generate electricity the wind harvest system needs a generator, which converts mechanical energy to electrical energy. Different types of generators already exist which work on alternating or direct current, synchronous or asynchronous and with or without permanent magnets [56]. An extensive explanation of the working principles and the characteristics of the different types of generators can be found in [56–59]. According to several studies researching small-scale wind energy systems, the Permanent Magnet Synchronous Generator (PMSG) is the best suited and also the most widely used [56, 60–62]. This is mainly due to their high efficiency and low cost maintenance. Furthermore, HAWTs often require a gearbox to match the RPM and the torque of the turbine with the required ones for the generator. As the RPM of VAWTs are usually higher and because smaller turbine sizes were chosen, resulting in lower torque, a gearbox in not required. Hence a direct drive system was chosen as also indicated in Figure 7.1. Direct drive generators eliminate mechanical losses, have less issues due to wear and tear due to the absence of gears, increasing the reliability and emit less noise from the running gears [56].

4.4.1. General Overview of Permanent Magnet Synchronous Generators

PMSGs are direct drive (gear-less) generators. Compared to other generators the PMSG has as advantages that it contains a high power density, a high performance and low maintenance cost [61]. However, at the cost of these advantages, the PMSG has a higher manufacturing cost due to the use of permanent magnets. In addition, the permanent magnets are made out of rare Earth materials which results in a less sustainable design [61]. However, the materials can be recycled after usage, so no waste is produced.[6] For synchronous generators such as the PMSG the output frequency is proportional to the rotational speed n_s and the available rotor poles P [57]. To derive the number of poles required for the PMSG, Equation 4.3 is used.

$$P = \frac{120f}{n_s} \tag{4.3}$$

The grid in the Netherlands is a three phase alternating current circuit and has a frequency of 50 Hz. In Subsection 4.3.4 it was defined that the rotational speed from the wind harvest system will be 151 RPM. Using Equation 4.3 it can then be determined that the generator will need 40 rotor poles.

4.4.2. Generator Sizing

After thorough research into generators, not one was able to meet all requirements on rpm, power and torque requirements. Therefore it was decided that the team will create it's own generator and will contact a company to produce this. A first sizing was done by creating a linear regression on different off-the-shelf generators which can bee seen in Table 4.3. [7,8] Section 4.3 showed that the rated output of the harvesting system will be 11 kW and the rated torque will be 900 Nm. The values in Table 4.3 are then used to create a regression line as can be seen in Figure 4.8a and Figure 4.8b. The regression equations are then used to get a weight estimation on the PMSG. The two equations for power and torque result in respectively weight of 290.6 kg and 341.4 kg. It is decided to take 341.4 kg as the right mass estimation, this was the largest thus taking more margin then the other. Secondly, this regression formula had a R-Squared of 0.8591 which verifies the estimation. All of the generators had a voltage output of 380 V, which needs to be transformed down to 230 V for the grid in the Netherlands.[9]

[6] https://cordis.europa.eu/article/id/415387-recycled-permanent-magnets-provide-a-source-for-rare-earth-elements [cited 12 June 2020].
[7] http://www.qm-magnets.com/index.htm [cited 12 June 2020].
[8] http://www.xindaenergy.com/ [cited 12 June 2020].
[9] https://www.power-plugs-sockets.com/netherlands-holland/ [cited 12 June 2020].

Table 4.3: Small scale generators and their specifications.

Generator	Rated Power Out [kW]	Rated Speed [RPM]	Torque [Nm]	Weight [kg]	Voltage [V]
QM-AFPMG700	5.0	150	318.3	135	380
QM-AFPMG770	7.5	150	477.5	165	380
FD-5000	5.0	200	238.7	170	380
FD-10000	10	200	477.5	240	380
XDSHF700-5 KW	5.0	100	477.5	120	380
XDSHF770-10 KW	10	150	636.6	180	380
XDSHF770-20 KW	20	300	800	180	380
10KW100 RPM	10	110	500	222	380
5KW100 RPM	5.0	100	567	120	380
15KW 150 RPM	15	150	1000	300	400
20KW 100 RPM	20	100	1910	640	400
20kw 100 RPM VA	20	100	1910	990	400

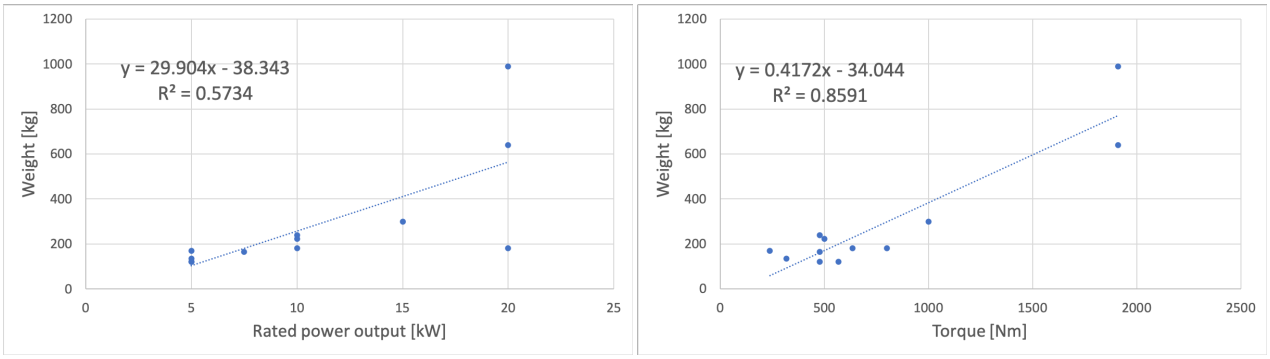

(a) Linear regression of generator mass and rated power output.

(b) Linear regression of generator mass and rated torque.

Figure 4.8: Weight estimation of the generator by means of a linear regression.

Due to lack of available cost data for existing generators, a preliminary cost estimation is done according to the cost of the materials. In Table 4.4 the typical share of materials and their respective specific costs are given. The cost is later estimated to be $921.44, which is €829.3. The WES has three VAWTs thus will need three generators which result in a total budget of €2,500 for the generators. As mentioned before, a generator with the required parameters was not found, thus the team is obligated to find a company that can produce the new design of the generator.

Table 4.4: Material weight breakdown and specific cost [63].[10, 11]

Material	Weight breakdown [%]	Weight breakdown [kg]	Cost/weight [$/kg]	Cost [$]
Iron	56.5	192.89	0.1	19.29
Copper	12.5	42.68	5.5	234.71
Aluminium	29	99.01	1.5	148.51
Neodymium Magnet	2	6.83	76	518.93
				$ 921.44

All generators from Table 4.3 have an efficiency of around 95%, this value is assumed as efficiency for the generator of the design. This results in a new power distribution in function of the wind speed from Subsubsection 4.3.4.2, the results of this can be seen in Figure 4.9 where the old and new power distribution are plotted against the corresponding wind speeds.

[11] https://www.dailymetalprice.com/metalprices.php?c=fe&u=kg&d=1 [cited 15 June 2020].
[11] https://www.prnewswire.com/news-releases/roskill-neodymium-prices-surge-as-permanent-magnet-demand-looks-set-to-take-off-669905463.html [cited 15 June 2020].

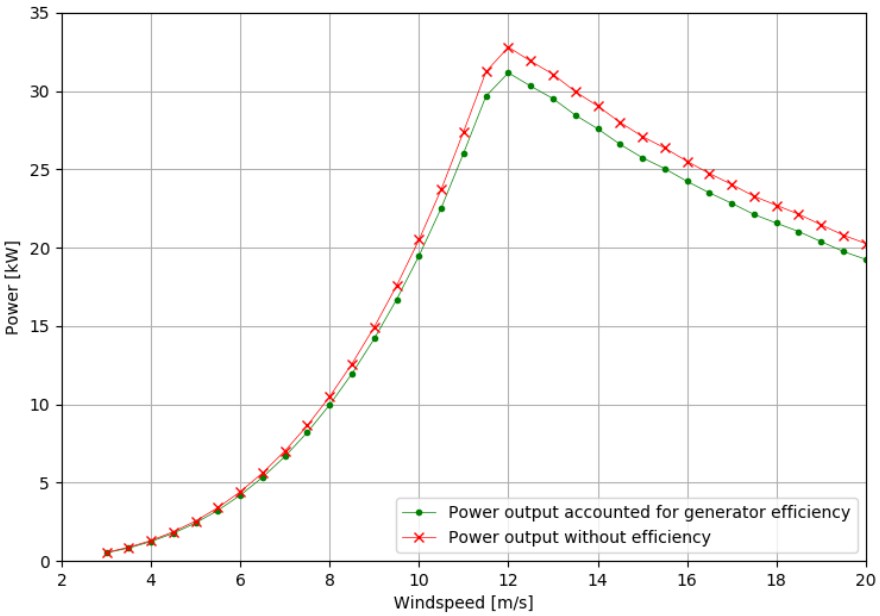

Figure 4.9: Power distribution in function of the wind speed.

4.4.3. Starting Performance

One of the problems with a VAWT is the poor self-starting ability. The main cause is that for low TSR, the angle of attack of the blades becomes really high causing stall. Several options to improve the self-starting performance of a VAWT have been researched, such as using a hybrid design (as was already suggested in Subsection 3.1.4) using a Darrieus and a Savonius rotor or using a variable pitch angle for the blade [64]. However, having a variable pitch angle would greatly increase the complexity of the design, which would lower the reliability and increase the cost. Since these two factors are very important in the design this option was not considered. Having a hybrid solution would increase the complexity and would also increase the cost since an extra system needs to be included.

The most simple solution to start the turbine is by using the generator as a motor to drive the turbine. This costs energy, however the needed energy is very limited. Based on a test performed on a 12kW wind turbine it was estimated that roughly 10.5 Wh was needed to start up the turbine to an angular velocity of 24 rpm [65]. Based on the fact that the WHS design consists of turbines of about 11 kW and the optimal angular velocity based on the cut-on velocity of 3 m/s is about 43 rpm. It can be concluded that the required power per startup will be about two times as high since the rotational speed is about twice as high. It is therefore assumed that on average a startup would cost 20 Wh. Making a rough assumption on the system having to start up two times a day (based on the fact that you would expect the system to be started up about once per day and having some safety margin of one extra start up per day) and taking into account the system consists of three turbines, the required amount of energy would be $2 \cdot 3 \cdot 365 \cdot 20 = 43.8$ kWh per year. Since the average energy price is €0.22/kWh [12], the cost per year will fluctuate around €9. Since this cost is negligible, the decision was made to use the generator to start the system and not design a Savonius rotor for startup. Furthermore since the cost is so low, it can be seen that even if the assumption about the amount of start-ups of the system per day was too low, the cost will still be negligible. Active startup does create the need for wind speed sensors to know when the system should be started up. However due to safety requirements (shutting down the system in case of extreme wind speeds), such a system was already in place. The only drawback of having the generator power up the system is the need for electricity when the system is not generating energy. This energy could be obtained from a battery which saves energy during production, however it was argued in Subsection 2.3.7 that an energy storage system was not needed. Furthermore the amount of energy to startup the system is so small that taking this energy from the regular grid was considered the best possibility. This does decrease the sustainability of the design a tiny bit, however the magnitude of the needed energy is very limited and it was therefore not considered feasible to include such a small battery.

[12] https://www.pricewise.nl/energieprijzen/kwh-prijs/ [cited 9 June 2020].

4.4.4. Brake System

A brake system is one of the most crucial components of a WHS for a reliable and safe operation. The IEC 61400-1 international standard specifies for a braking system used in a wind turbine the following requirements: "The braking system shall be able to bring the rotor to idling mode or complete stop from any operation condition. Means shall be provided for bringing the rotor to a complete stop from a hazardous idling stage in any wind speed less than the wind speed limit defined for maintenance and repair" [66]. Furthermore: "It is recommended that at least one braking system operates on an aerodynamic principle, as such acting directly on the rotor. If this recommendation is not met, at least one braking system shall act on the rotor shaft or on the rotor of the wind turbine" [66]. The need becomes even more relevant when placing a WHS in an urban environment. Therefore, one brake system is not enough. Redundant brake systems are standard in many industries to ensure safety. Also for wind turbines it is required to have two independent fail safe braking systems [67].[13] Before selecting a suitable brake system it is necessary to understand the different scenarios in which a braking system is required to stop the system.

4.4.4.1. Braking Scenario

In case of a VAWT, the brake should reduce the rotational velocity of the turbines blades, axle or bring it to a full stop. This may be the case when the wind velocity is too high, causing disproportionate values for RPM which could lead to too high voltage, temperature, stresses and vibrations in the WES [68–70]. Furthermore, it could damage the generator, the electrical system or other structural components. All impose risks to people in the proximate environment. In an extreme case of an incident, emergency braking would need to be performed, which would impose higher loads to the WHS. Even when the system would shut down, a fail safe brake will ensure stopping the turbine. The brake is coupled with a limit switch where data from multiple sensors evaluating wind speed, maximum RPM, torque exerted on the shaft and the generator temperature is taken into account. If limits are exceeded, appropriate braking will be initialized. Next to this, the braking could also be executed due to a control input from the user, for example in case of maintenance.

4.4.4.2. Braking Technologies

There are three main braking technologies, which act at different components and locations in a WES[69]. First of all the turbine speed can be limited through aerodynamic braking. For that also different methods exist for example passive stall, active pitch control, spoiler, sledge, flaps and others (as was discussed in Subsubsection 4.3.3.6. However, these technologies are mainly used for larger WESs, are more complex and hence more maintenance is required for trustworthy and reliable functionality. Next to that, the popular yaw braking systems as used for HAWTs are not an option for a VAWT, as they will work for any wind direction. Furthermore, it is possible to use the generator also as a brake as is done in electric rheostatic braking. Through switching the generator to a resistor bank, the load on the generator is increased exerting a braking force on the drive shaft. In that way, kinetic energy from the generator will be mainly transferred into thermal energy at the resistor bank. Therefore, an appropriate cooling system would be required. Lastly, the most common brake system is mechanical braking. Two main different systems exist: drum brakes and disc brakes. Drum brakes usually act directly on the shaft or a special designed part of it. In case of a disc brake, brake calipers push braking pads onto a brake disc, which is connected to the shaft[71]. An example of this is shown in Figure 4.10a. Both systems can easily be implemented as fail-safe system - also the reason why those systems are compulsory for a WES. The actuation can be done hydraulically, electromagnetically or through springs.

Table 4.5: Advantages and disadvantages of different brake systems [68–70].

Brake System	Advantage	Disadvantage
Aerodynamic brake	+ longer brake intervals possible	- more complex system
	+ no high temperatures on system	- more prone to component failures
Electric rheostatic brake	+ contactless	- cooling required
	+ very power efficient	- only at lower RPM
Mechanical brake	+ cheap and reliable	- high temperatures
	+ easy to maintain	- high wear of brake pads
	+ compulsory back-up system	

4.4.4.3. Brake Choice

Based on the mentioned braking methods and characteristics, a redundant system of one mechanical disk brake and a dynamic generator braking was selected. The disk brake consists of multiple brake calipers, which will be partially

[13] https://isaacbrana.wordpress.com/2010/07/12/brake-systems-in-wind-turbines/ [cited 22 June 2020]

optimized for high and low speeds respectively[71] as can be seen in Figure 4.10b. Care must be taken in brake pad selection, optimized for the specific loads and brake frequencies [72]. On the brake disc, there will be acting fail-safe brakes based on a pre-compressed spring. An active brake for the normal braking of the system is present as well as an emergency brake. The passive aerodynamic stall control, acts as another safety brake if turbine's RPMs will exceed their limit.

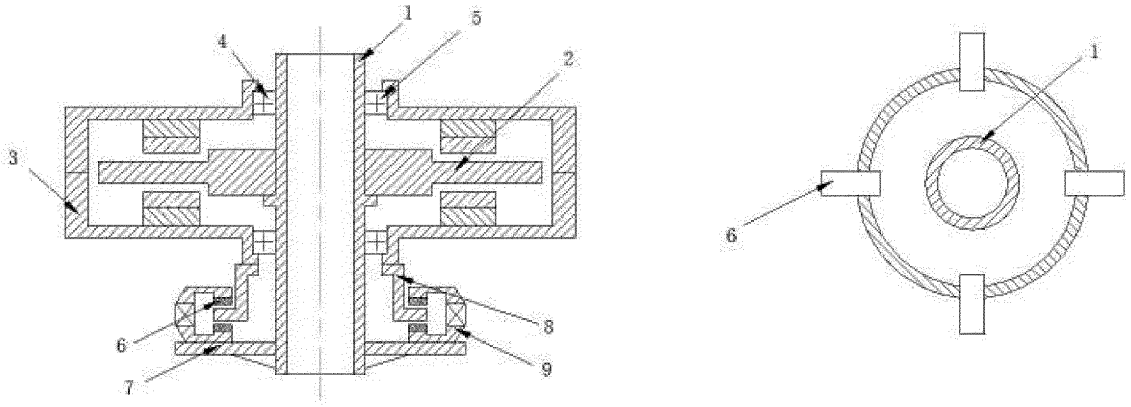

(a) Cutaway view .

(b) Top view: distribution of multiple calipers along the brake disc circumference.

Figure 4.10: Example of a VAWT installed with a disc braking device [71]. (1) drive shaft, (2) generator stator, (3) generator rotor, (4) and (5) bearings, (6) brake shoes, (7) brake support, (8) brake disc and (9) caliper jaws.

Electrical wind turbine brakes are good for small systems and well suitable for cyclic usage, which means slowing down the turbine in intervals to prevent it from spinning too fast and releasing too much energy to brakes at once.[14] The system will include a resistor bank with according cooling system that needs to be sized later as it would be beyond the scope of the project. As the WHS will be placed at higher altitudes (see Section 2.4) it may be possible to use cold air ventilation as a cooling system. Next to that, the maximum torque applied to the shaft and the induced vibrations of all braking methods should be further investigated.

Lock System

A rotor lock system has its main purpose for maintenance. When the turbine was brought to halt and should stay at rest for a longer period, the mechanical disc brake system should be relieved to avoid unnecessary wear. Therefore, a redundant double bolt system is used to lock the disc connected to the turbine shaft. An example is shown in Figure 4.11 which illustrates how maintenance can be executed safely.

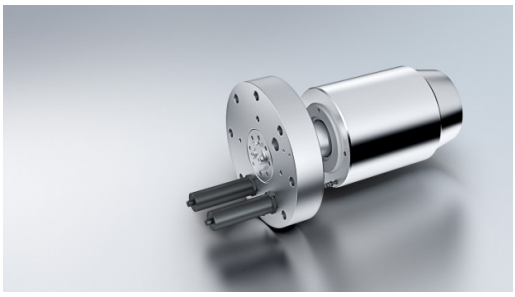

Figure 4.11: Example rotor lock system by Dellner Brakes. [15]

4.5. Airborne Noise

As stated in Section 4.2 the requirements WES-OP-MU-03 and WES-OP-MU-04 require a maximum noise output (L_{den}) of 47 dB(A) during the day and 41 dB(A) during the night. A model needed to be generated in order to be able

[14] https://kor-pak.com/need-good-wind-turbine-brakes/ [cited 19 June 2020].
[15] www.dellner-brakes.com/wp-content/uploads/2018/09/jhs_r200_154.jpg [cited 19 June 2020].

to analyse the noise behaviour of the VAWT. Various types of noise VAWTs produce are tonal noise, airfoil self-noise and inflow turbulence noise. These different types are addressed first explaining the most dominant noise sources.

The requirement is set on L_{den}, which stands for day-evening-night Level. This is a weighted sound level averaged per day and averaged over a year. This can be calculated using Equation 4.4 [73].

$$L_{\text{den}} = 10log\left(\frac{1}{24}\left[12\cdot 10^{\frac{L_{\text{day}}}{10}} + 4\cdot 10^{\frac{L_{\text{evening}}+5}{10}} + 8\cdot 10^{\frac{L_{\text{night}}+10}{10}}\right]\right) \tag{4.4}$$

Where L_{day} is the A-weighted average sound level between 7.00-19.00 local time, L_{evening} is the A-weighted average sound level between 19.00-23.00 local time and L_{night} is the A-weighted average sound level between 23.00-7.00 local time. For noise produced between 19.00-23.00 local time, a penalty of 5 dB(A) is added and a penalty of 10 dB(A) is applied to noise emitted between 23.00-7.00 local time.

Using the analysis of Subsection 2.4.3 it was found that the system is on for approximately 7.7 hours a day. Assuming the wind to be uniformly distributed over a day, this means that the system is on (and thus produces noise) for 3.85 hours during the day period, 1.28 hours during evening and 2.57 hours during night. This assumption is not entirely true, since normally wind speeds are a bit higher during the day than at night,[16] however it was in this analysis only of interest when wind was present (and thus when the system is turned on) and not what the wind speed was. The wind speed was already taken in to account by the fact that the noise is calculated as a weighted average over the different wind speeds resulting from the wind distribution in Subsection 2.4.3. In future design phases an extensive analysis of when during the day what wind speeds are expected could be performed. The rest of the day the system would not experience wind (on average) and therefore would be turned off, not producing noise. Using this analysis the allowable average noise production of the turbine could be calculated by using Equation 4.4 in the reversed direction, since the requirement states L_{den} should be limited to 47 dB(A) (WES-OP-MU-03). This resulted in a maximum allowable Overall Sound Pressure Level (OASPL) of 45.5 dB(A). Requirement WES-OP-MU-04 states that L_{night} has to be below 41 dB(A), but using the same analysis of the system being on for 2.57 hours during night (and thus off for 5.43 hours) results in a maximum allowable OASPL of 45.9 dB(A), which means that this requirement is not critical. Therefore the maximum average noise the system produces should be below 45.5 dB(A).

4.5.1. Tonal Noise

Tonal noise is defined as discrete frequency noise and it is characterized by its spectral tones. It is generated by rotating equipment, such as the blades of the VAWT, at predictable frequencies dependent on the rational speed of the shaft and the amount of blades. However, it is considered to be negligible with respect to the broadband component of noise produced by the VAWT [74]. This tonal noise is mainly emitted in the low frequency spectrum below a 100 Hz, since the human ear is less affected by noise with a low frequency the consequences are minor. Since it is not a dominant source and therefore will not have a large influence on the total decibel output, it was disregarded.

4.5.2. Inflow-Turbulence Noise

This type of aerodynamic noise is produced once airfoil blades interact with inflow turbulence. This type of noise can be analyzed with the Paterson and Amiet's noise model which defines the incoming turbulence using the von Karman spectrum, Buck et al. [75] suggests the Kolomogrov spectrum. However due to resource limitations no investigation was conducted in this type of noise. It would be of great importance in the future to take inflow-turbulence noise into account to accurately predict the total noise output more precise.

4.5.3. Airfoil Self Noise

Airfoil self-noise is produced once, if for example an airfoil, moves through a fluid medium. The scattering of turbulent energy within the boundary layer the airfoil due to the trailing edge is called turbulent boundary layer noise [74]. This energy propagates as an acoustic signal far away from the created pressure side. Since it was chosen to use a symmetric airfoil for the VAWT, only the trailing edge noise estimated by the Brooks, Pope and Marcolini (BPM) model, was taken into consideration. Other self-noise models are not required as they mainly improve noise prediction on cambered airfoils [74].

[16] http://xn--drmstrre-64ad.dk/wp-content/wind/miller/windpower%20web/en/tour/wres/variab.htm#:~:text=wind%20speed%20is%20always%20fluctuating,the% [cited 29 June 2020].

4.5.3.1. BPM Model

The BPM model is the most commonly used to model airfoil self noise. The acoustic signal at the trailing edge is related to the flow over an airfoil. This is done by estimating the boundary layer displacement thickness over the airfoil. The main limitation of the model is that only one type of airfoil was considered [74]. A distinction was made between three parameters that contribute to the overall airfoil noise, namely; pressure side noise ($W_p(f)$) Equation 4.5, suction side noise ($W_s(f)$) Equation 4.6, and high angle of attack noise(W_α(f)) Equation 4.7.

$$W_p(f) = 10log_{10}\left(\frac{\delta_p^* M_0^5 dD_h}{z^2}\right) + A\left(\frac{St_p}{St_1}\right) + (K_1 - 3) + \Delta K_1 \tag{4.5}$$

$$W_s(f) = 10log_{10}\left(\frac{\delta_s^* M_0^5 dD_h}{z^2}\right) + A\left(\frac{St_s}{St_1}\right) + (K_1 - 3) \tag{4.6}$$

$$W_\alpha(f) = \begin{cases} 10log_{10}\left(\frac{\delta_s^* M_0^5 dD_l}{z^2}\right) + B\left(\frac{St_s}{St_2}\right) + K_2 & \alpha < 25° \\ 10log_{10}\left(\frac{\delta_s^* M_0^5 dD_l}{z^2}\right) + A'\left(\frac{St_s}{St_2}\right) + K_2 & \alpha \geq 25° \end{cases} \tag{4.7}$$

The sum of these contributions becomes the following logarithmic Sound Pressure Level (SPL):

$$W_{BPM}(f) = 10log_{10}\left(10^{W_p/10} + 10^{W_s/10} + 10^{W_\alpha/10}\right) \tag{4.8}$$

$W_{BPM}(f)$ is the SPL in third octave bands. Third octave bands are a way of dividing the frequency domain in bins and integrating the noise within that bin to one value for the sound pressure level corresponding to that bin.[17] Third octave bands were used in the entire noise analysis performed in this chapter. In Equation 4.5, Equation 4.6 and Equation 4.7, δ^* is the boundary layer displacement thickness for either the pressure or suction side (subscript p for pressure, s for suction), M_0 is the mach number of the inflow, d is the blade span, D is the directivity function and z is the distance to the receiver. The symbol St represents the Strouhal contributions, A and B are interpolation functions and K is a function to correct the amplitude. All these functions are described in detail in Jason et al. [74]. The directivity function is a function that takes into account the relative position of the observer with respect to the blade and is given in Equation 4.9 [74]. If the location of the observer would just be at a 90° angle with the airfoil, the directivity would be equal to one.

$$D_h = \frac{2\sin^2(\Theta_e/2)\sin^2\phi_e}{(1 - M_0\cos\xi_e)^4} \qquad D_l = \frac{\sin^2\Theta_e\sin^2\phi_e}{(1 - M_0\cos\xi_e)^4} \tag{4.9}$$

Where D_h is the directivity function for the pressure side and D_l is the directivity function for the suction side. M_0 is the mach number, Θ_e and ϕ_e are defined in Figure 4.12 and ξ_e is the angle between the blade chord inflow velocity to the line from the source to the observer [74].

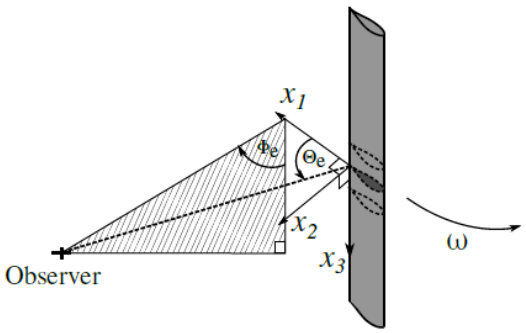

Figure 4.12: Definition of angles used for the directivity functions [74]

[17] http://apmr.matelys.com/Standards/OctaveBands.html [cited 20 June 2020].

4.5.4. Noise Model

The BPM model described above was implemented for the used noise model. To be able to calculate the noise at every azimuth angle, the effective angle of attack and the local velocity needed to be calculated. This was done by taking the free stream velocity and the radial velocity of the VAWT into account. The different velocities and angles are defined and shown in Figure 4.13.

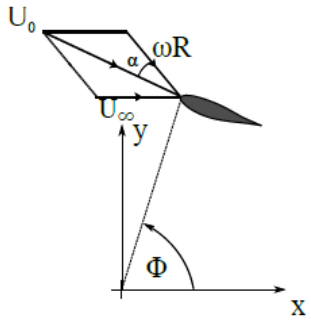

Figure 4.13: Definition of angles and velocities for a VAWT. U_0 is the incoming flow velocity, U_∞ the free stream velocity, α the angle of attack, ω the angular velocity, R the radius and ϕ the azimuth angle. [74]

The effective angle of attack was calculated using Equation 4.10.

$$\alpha = tan^{-1}\left(\frac{sin(\phi)}{cos(\phi)+\lambda}\right) + p \tag{4.10}$$

In which ϕ is the azimuth angle and λ the relation between the radial velocity, the free stream velocity and the tip speed ratio. Parameter p is the fixed pitch angle, which was set to 0 for the given design case. The local velocity of the blade was calculated using Equation 4.11. Where U_∞ is the free stream wind velocity and the other parameters are the same as in Equation 4.10.

$$U_0 = U_\infty\sqrt{1+2\lambda cos(\phi)+\lambda^2} \tag{4.11}$$

The values for the boundary layer displacement thickness (δ^*) were calculated using semi-empirical equations for the NACA0012 as given in [74]. As explained in Subsubsection 4.3.3.3 the NACA0018 was selected for our design. The assumption of using the boundary layer displacement thickness for the NACA0012 therefore introduced an inaccuracy to the model. The effect of this simplification is explained in more detail in Subsection 4.5.5.

While fixing the observer, the noise perceived at that location was calculated as a result of a full rotation of the blade. This was done by calculating the noise generated by the blade (using the BPM model) for a full rotation by taking steps of 10° in azimuth angle, which was then summed up over one rotation. This of course included taking into account the change in distance between the blade and the observer and taking into account the relative velocity between the blade and the observer, causing a Doppler frequency shift. The Doppler correction was calculated by means of Equation 4.12 and the integration over a full rotation was done using Equation 4.13 [74].

$$\frac{f}{f_0} = \frac{c_0+U_r}{c_0+U_s} \tag{4.12}$$

$$G_{\mathrm{BB}}(f) = \sum_{b=1}^{s_n}\frac{n}{\mathrm{n}_\phi}\left(\frac{f}{f_0}\right)_b\left[G(f)\right]_b \tag{4.13}$$

Where c_0 is the speed of sound, U_r is the relative velocity of the observer relative to the noise source (positive if the observer moves towards the source and negative for the other direction) and U_s is the relative velocity of the noise source to the observer (positive if the noise source moves away from the observer and negative for the other direction). Since in the developed model the observer was fixed, U_r is equal to zero. $G_{\mathrm{BB}}(f)$ is the overall acoustic pressure signal, n is the amount of blades, n_ϕ is the amount of angular discretization points in a revolution (so 36, since steps of 10° were used), $\frac{f}{f_0}$ is the Doppler correction of Equation 4.12 and $G(f)$ is the acoustic pressure at the location of the observer for a specific angular position of the blade. The subscript b denotes the summation over the angular

positions of the blade.

A-weighting was then applied to mimic the response of the human ear to noise. A-weighting is a factor applied to the SPL for each frequency. Especially lower frequencies are less audible for human ears and therefore a negative weighting was applied to these respective frequencies. Some other frequencies received a positive weighting.[18] The equation for the A-weighting is shown in Equation 4.14 and Equation 4.15.[19]

$$R_A(f) = \frac{12194^2 f^4}{(f^2+20.6^2)(f^2+12200^2)\sqrt{(f^2+107.7^2)(f^2+737.9^2)}} \tag{4.14}$$

$$A(f) = 20log_{10}(\frac{R_A(f)}{R_A(1000)}) \tag{4.15}$$

The next step was to calculate the OASPL, which was done by integrating over the frequency domain to get one value for the noise, as this is also how the requirements were set. Since the results of the BPM model are in third-octave bands, this integration was performed using Equation 4.16. Where the summation was performed over the SPL_i corresponding to all the third octave bands.

$$OASPL = 10log_{10}\left(\sum_{i}^{N} 10^{SPL_i/10}\right) \tag{4.16}$$

Finally the wind speed needed to be taken into account. The requirements were set on the averaged noise produced per day and averaged over a year [27, 73]. The analysed wind speeds range from 3 m/s to 20 m/s as is explained in Subsection 4.4.3. The noise was calculated for all wind speeds and a weighted average was derived based on the probability of the wind speeds, the explanation for this can be found in Subsection 2.4.3. This results in an average OASPL produced by the WHS.

4.5.5. Limitations

The model used to predict the noise generated was the BPM, as stated before. However, this model does have some limitations which influence the outcome of broadband noise. These limitations are important to keep in mind as they influence the outcome of the model. First of all the limitations of the BPM model are

- In the model, tip effects of the blade are neglected. Each airfoil operates as a 2D airfoil, neglecting noise from tip effects and vortices [74].
- The interaction between following blades and their effect on the flow is not accounted for. Also the interaction between the blades and the support structure is assumed to be negligible. Additional confluent noise sources are neglected [74].
- The directivity is assumed to be two dimensional, not emitting noise in the z-direction, axis perpendicular to the Earth's surface. However since the most critical point for the noise is directly at the building at the height of the turbine, the two dimensional analysis of the directivity leads to the worst case scenario making this a valid assumption.

Furthermore, some general assumptions were made while making the noise calculations. These assumptions also have an influence on the total noise output.

- The BPM is based on statistical relationship created for a NACA0012 airfoil. As stated in Subsubsection 4.3.3.3 the most efficient for this design is the NACA0018. This means that for the design a thicker airfoil has been used. It is expected that this thicker airfoil will create different boundary layer conditions. However, as can be seen in Figure 4.14 the noise behaviour for an applicable frequency range of the NACA0012 and NACA0018 is almost equal and will therefore only introduce a small inaccuracy in the model [76].
- For the noise calculations only the airfoil self-noise was taken into account and the inflow-turbulence noise and tonal noise were disregarded at the beginning. This was validated by the fact that these are not the most dominant noise sources for a VAWT, however they still produce some amount of noise [74]. But, since sound pressure levels are expressed on a logarithmic scale, the addition of two smaller noise sources does not have a significant influence on the total noise output.

[18] https://www.sciencedirect.com/topics/engineering/a-weighting [cited 17 June 2020].
[19] https://stason.org/TULARC/physics/acoustics-faq/8-1-Formula-for-A-weighting.html [cited 17 June 2020].

- The effect of the noise coming from the different turbines had not been taken into account for the analysis. This effect needs a more detailed analysis and furthermore the effect was expected to be minimal, since the turbines are placed several meters from each other. In addition, the noise was analyzed at the most critical point, which is at a 90° angle of the turbine to the building. At this location the noise coming from the turbine closest by will be dominant, so only taken this turbine into the analysis is a good approximation. Finally, since the turbines emit approximately the same frequencies the noise of the turbine could interfere, causing an increase in noise or damping the noise. This effect also needs a more detailed analysis because this effect could maybe even be used to decrease the total noise.

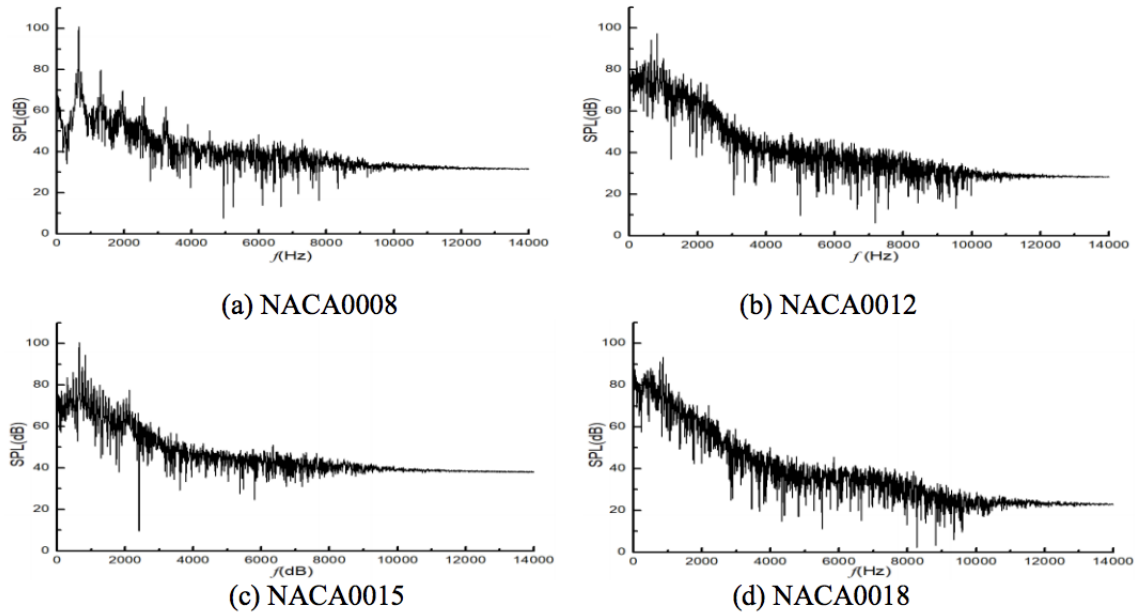

Figure 4.14: Sound pressure level on trailing edge of four different NACA airfoils [76].

4.5.6. Verification

The code used to estimate the noise produced needed to be verified to be used with certainty. First coding errors were removed by running the code and fixing the errors. Several small subsystem checks were performed by testing small parts of the code of what the results are known. For example the function calculating the A-weighting was tested for several frequencies and compared to the correct A-weighting for that frequency as can be found in literature.[20] As the results were consisted, these small parts were verified. Furthermore larger parts of the code were verified such as the functions A and B in Equation 4.7. These were verified using a previously created code for the BPM model. By putting the same input in both programs it could be verified that the formulas were implemented correctly since the same output was produced. The next step was verifying the function that integrated the noise over one rotation and over different air speeds. The Doppler frequency shift was easily checked by checking the magnitude, which should be lower than 1 when the blade is moving towards the observer and larger than 1 when moving away from the noise source. Also the exact number was checked by changing the relative velocity. The integration over a rotation was checked by plotting the SPL versus the frequency for every position in one revolution. Later this was integrated to verify the results. Integration was tested by integrating two distinct locations first separately and checking the results by hand, after which integration over the full rotation was performed. Finally the full results were verified for one specific input case (observer at a distance of 1 meter distance and free stream velocity of 10 m/s) with the results from a numerical model created by Livia Brandetti (PhD candidate at TU Delft) which can model the noise from the BPM model using an actuator cylinder model. The results are shown in Figure 4.15. The results are both plotted with the directivity function on and with the directivity function set equal to 1, such that immediately the directivity function of our model could be verified.

[20] https://www.nti-audio.com/en/support/know-how/frequency-weightings-for-sound-level-measurements [cited 15 June 2020].

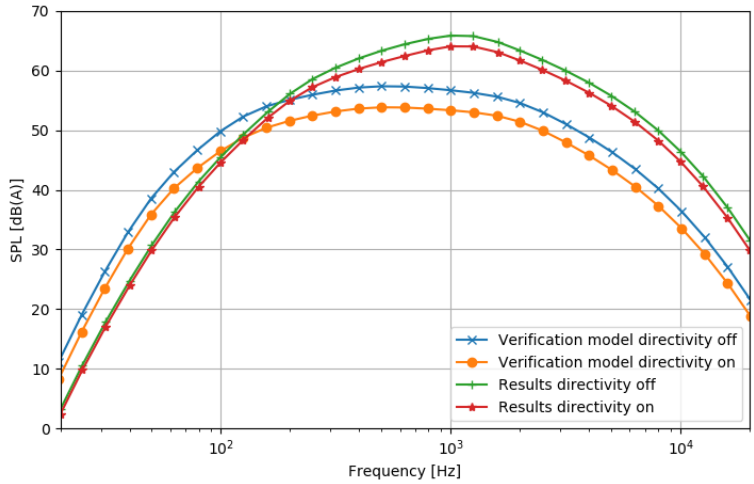

Figure 4.15: BPM model noise prediction of our model and verification model. Sound pressure level at 1 meter distance to the blade plotted versus frequency. Plotted in third octave bands.

From Figure 4.15 it can be seen that the results are comparable, but not entirely match. The developed model overshoots the results from the verification model quite a bit. It can be seen that the implemented directivity function does work properly, since the effect of using this function has the approximate same effect for the verification model. One of the differences between the models is, that the verification model uses the actuator cylinder model to estimate the relative velocity of the blades and the angle of attack. Furthermore, phenomena like dynamical stall are also included in the verification model. In contrast, the generated model calculates the angle of attack and relative velocity only based on geometric relations as explained in Subsection 4.5.4. However this does not explain the differences in Figure 4.15, since for this plot the relative velocity and angle of attack from the actuator cylinder model were used as an input for our model. This was done to verify the rest of the developed model without having the inaccuracy of the angle of attack and local velocity induced.

The effect of the difference in angle of attack and local velocity can be seen in Figure 4.16, and shows that the effect is minimal. The change in the input only influence the results for the low frequencies but the peak remains the same, while the main difference between the used model and the verification model occurs in the peak. The effect of the different input data for angle of attack and local velocity could therefore be neglected, however the difference in Figure 4.15 cannot be neglected.

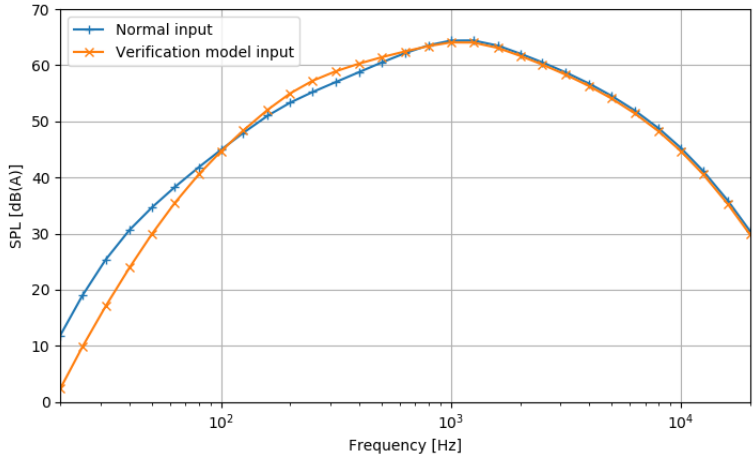

Figure 4.16: Effect of the relative velocity and angle of attack input form verification model on our model. Directivity function is turned on. Sound pressure level at 1 meter distance to the blade plotted versus frequency. Plotted in third octave bands.

The differences between the verification model and the generated model in Figure 4.15 can be explained by the way the boundary layer thickness displacement is determined. In the used model this was done by analytical equations for the NACA0012 [74], causing an inaccuracy since the NACA0018 is actually used. The verification model uses XFOIL to obtain the boundary layer displacement thickness for the NACA0018. However the effect of the different airfoil can probably not explain the entire difference between the two models. For this reason the code used cannot be entirely verified and more verification on the model should be performed. The verification model however verified and tested extensively and was therefore considered more correct than the self developed model. The main goal of the noise analysis is to obtain an estimation for the A-weighted OASPL. This was calculated for the verification model and our model (both with directivity function on). The results are shown in Table 4.6.

Table 4.6: A-weighted OASPL produced estimated by our model and verification model.

OASPL our model [dB(A)]	**OASPL verification model [dB(A)]**	**Difference [dB(A)]**
72.9	64.3	8.6

Due to limited available resources, the verification of the noise model could not be performed more thoroughly. Therefore the exact cause of the differences between the two models was not found. Since, based on the verification, the generated model overestimates the OASPL by about 8.6 dB(A) (as can be seen in Table 4.6, it was decided that a factor should be subtracted for now from the results of the used model. Based on the 8.6 dB(A) difference and taking into account contingency and a safety margin, the results at a distance of 1 meter could be compared to the verification model. It was concluded to subtract 7 dB(A) from the results of the developed model. This of course is a rough estimation and therefore further noise investigation and verification of the model needs to be performed in later design phases. However subtracting this factor does give a more realistic approximation of the noise generated than if the result of the model would just be used.

4.5.7. Results for Expected Noise

Based on the verification the noise estimation of the program is overestimated by about 7 dB(A) due to the simplifications explained. Only the airfoil self noise is estimated, since this is the most dominant noise, but in reality other noise sources are also present. Apart from the noise generated by the airfoil this also includes noise from the generator. However as explained in Section 4.4, a PMSG was selected which does not have brushes or a gearbox and therefore produces a limited amount of noise.[21] Furthermore the noise of the generator can be easily dampened by adding insulation to the nacelle of the generator. Due to the definition of decibels the most dominant noise source is largely influencing the OASPL and therefore these other noise sources are not of high importance for now. For later stages in the design process it is of course important to investigate all noise sources into detail and take them into account. The noise needs to be analysed at the location on the walls of the building and four meters above the ground. These requirements are based on the regulations made by the European parliament and Council of European Union [73]. This means at a distance of four meters (distance to wall of closest building), 20.96 meters (distance to the other of the two buildings) and 144 meters (distance to four meters above the ground). These distances, to the building and the height above the ground, were determined in Subsection 2.4.1. Based on the method described above, the average OASPL was estimated at these locations and summarized in Table 4.7. The A-weighted SPL plotted versus frequency for the various distances is shown in Figure 4.17. This plot however does not contain any adjustment based on the verification, so approximately the same error in shape as in Figure 4.15 should be expected for these graphs.

Table 4.7: Average OASPL produced by the turbine with and without corrections after verification.

Distance [m]	**OASPL [dB(A)]**	**OASPL adjusted due verification [dB(A)]**
4	63.9	56.9
20.96	51.7	44.7
144	35.5	28.5

[21] http://www.regenpowertech.com/42/technology#:~:text=Lower%20maintenance%20costs,due%20to%20few%20moving%20parts [cited 16 June 2020].

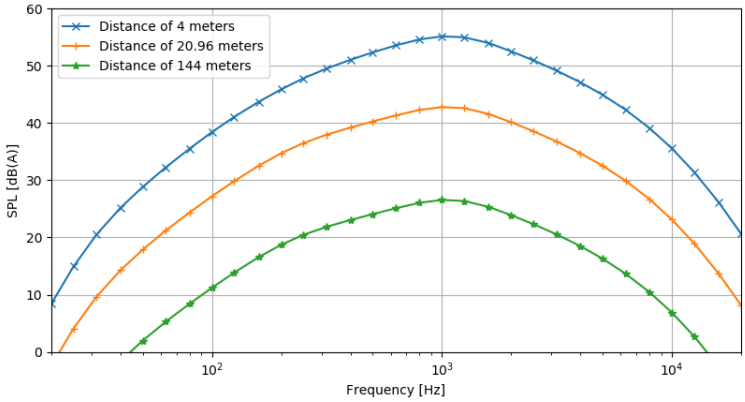

Figure 4.17: Sound pressure level at several distances to the blade plotted versus frequency. Directivity function is turned on. Plotted in third octave bands.

Concluding, the noise requirement is violated only at the nearest building, since the noise received there is 56.9 dB(A), which is more than 45.5 dB(A). Therefore noise reduction methods were analyzed, to meet the noise requirement. An average noise production of 56.9 dB(A) would result in L_{den} = 58.3 dB(A) and L_{night} = 51.9 dB(A) using the amount of hours explained above and Equation 4.4, meaning both the noise requirements are violated for this design. To limit the amount of noise produced, the tip speed was limited to 40 m/s as explained in Subsection 4.3.4. Further reduction of the tip speed would off course reduce the noise, however this would cause a big decrease in the power production efficiency.

4.5.8. Noise Reduction Methods

As was stated before, the noise emission of the WHS are higher than allowed. Noise is of high concern in an urban environment, where people live. It is very annoying and can even cause health issues. Especially the varying frequency are problematic to the human psych [77]. To reduce the noise exposition and to meet the legislation requirements multiple noise reduction options were considered.

There are different methods to reduce airborne noise. Especially for high frequencies Passive Noise Cancellation (PNC) methods like optimizing the airfoil geometry, using porous material or adding serrations at the trailing edge are effective [78]. The airfoil geometry was already optimized for performance and should not be altered. Adding porous material at the trailing edge would also impact the performance undesirably [79, 80]. Therefore, only serration was considered and explained in Subsubsection 4.5.8.1. As the effect of adding serrations is limited, further noise cancellation methods needed to be investigated done in Subsubsection 4.5.8.2, Subsubsection 4.5.8.3 and Subsubsection 4.5.8.4. These solutions will be briefly addressed, however to use them as a reliable solution at this stage is not possible and therefore something which would need to be taken into account for future research.

Besides these noise reduction methods, the entire system design could also be resized and reiterated. This would effect all different system components and may require to change the design philosophy. The impact of that was assessed to be too extensive for the scope of the project and available resources. Hence it was not considered a viable option. Noise was already taken into account in the design in several ways, by not having one big turbine but three smaller turbines, limiting the tip speed to 40 m/s and having some space between the building and the turbines. Also extending the support structure to bring the turbines further away from the buildings would not be an effective option either. This is due to the nature of how the sound level reduces with distance (6 dB per double distance). Even if the system would be placed exactly in the middle of the two buildings, the 15 m would not be enough to reduce the noise level. Besides, the noise level at the other building would then not be met anymore and the complexity and cost of the support structure would increase a lot.

4.5.8.1. Serrations

The first step in reducing noise is to add serrations on the trailing edge of the airfoil. Serrations have been proven to work as a passive noise reduction device and a lot of research has already been conducted. In Figure 4.18 it is shown how the serrations look like, once added to the NACA0018 airfoil.

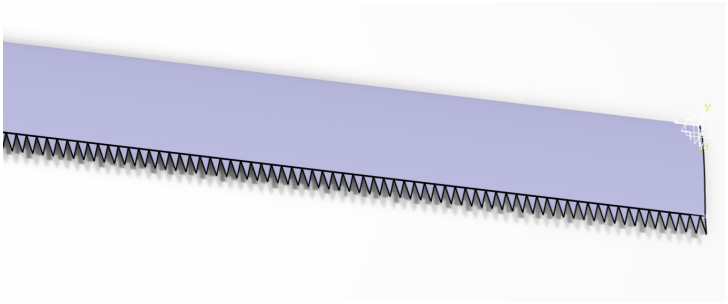

Figure 4.18: NACA0018 with integrated serrations at the trailing edge to reduce airborne noise.

Serrations are a passive noise reduction device for most of the frequencies, but after a certain frequency limit is exceeded noise will be added to the total output. Therefore, it should be known what that limit is before the sizing of the serrations can start. This limit is defined by Equation 4.17.

$$St_i = \frac{f\delta_i}{U_0} = 1 \tag{4.17}$$

It is the point where the Strouhal numbers, on either the pressure or suction side go above 1. The Strouhal number (St_i) have a subscript of i to indicate at which of the airfoil the analysis is done. The same applies to boundary layer conditions (δ_i). The last parameter U_0 is the local flow velocity. This point is reached somewhere around a frequency of 20,000 Hz, and therefore not a problem for this design. As can be seen in Figure 4.16 the noise peak is at a frequency of 1,000 Hz.

The serrations have been sized based on Mayer et al.[81] and Leon at al [82] . The NACA0018 was modeled under different flow conditions and the noise reduction was determined by using different types of modelling. The first model applied, was the serrated trailing edge noise model (STE) and it assumes the airfoil to be a flat plate, introduced by lyu et al. [83]. The model introduced by Howe's [84] is used for comparison against the STE model. Both models were extended with a wave number-frequency spectra. This was needed for the far-field noise calculations using the STE and Howe's model. The calculation of the far-field noise become rather difficult as the boundary layer surface pressure fluctuates, this effect is accounted for via the implementation of the wave number frequency models. The STE model is extended with both the TNO model, devised by Parchen [85], and the Chase model [86]. Howe's model only uses the extension created by Chase. In Figure 4.19 the results can be seen of the various different models.

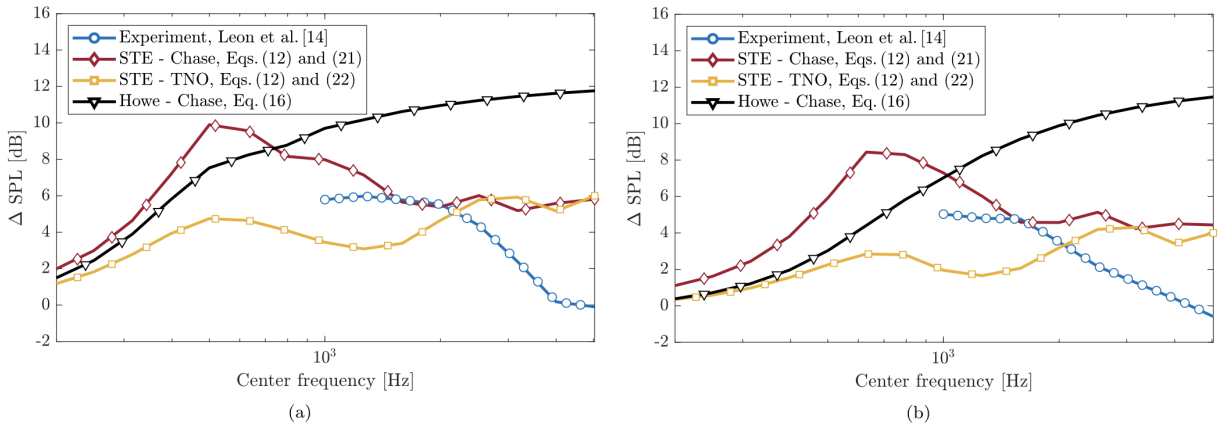

Figure 4.19: 1/3 octave band noise reduction for a NACA0018 airfoil with λ = 2 cm and h = 2 cm; experimental data from : (a) U_∞ = 30 m/s at α = 0.0° (b) U_∞ = 40 m/s at α = 6.6° [81]

In the figures four different curves can be seen representing the different models and the experimental data. A positive Δ SPL means a reduction in noise output. It was concluded that the STE-TNO model under predicts the noise output. Furthermore, the Howe's model shows a continues increase in noise reduction, but it was stated that this is

incorrect as already explained above.

As can be concluded from Figure 4.19 the noise reduction is within the same frequency domain as the VAWT produces noise. The model is reliable as the airfoil used for the system is the same as the airfoil used for the computations. The main difference comes from the fact that the computations have been conducted for higher free stream velocities with respect to the maximum free stream velocities the system will encounter, as determined in Section 2.3. This effect needs to be researched in a future stage, for now the serrations are sized accordingly [81].

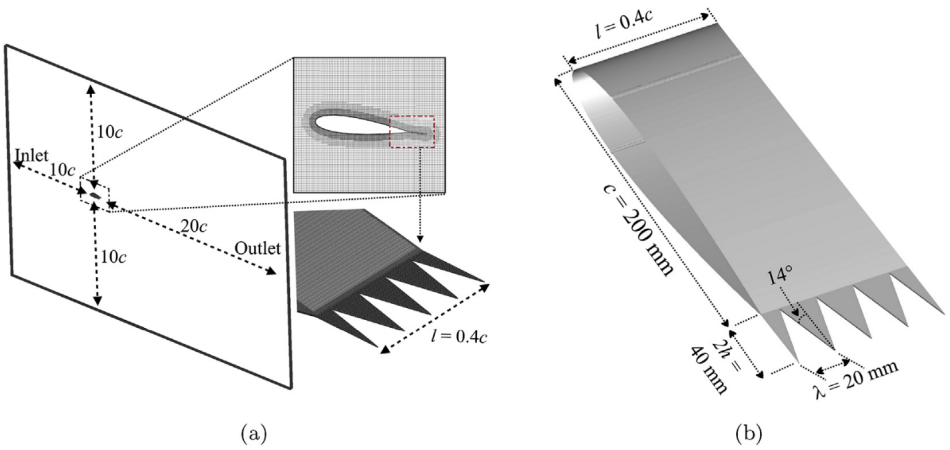

Figure 4.20: Sizing of serrations on trailing edge of NACA0018 airfoil [81].

So, as can be seen each serration for the system in development has a width of 0.1c and a height of 0.2c. The airfoil of the system in development shown in Figure 4.20 has a smaller chord, however the sizing is still applicable as explained. There is no flap angle introduced at this stage, mainly because that would cause the airfoil to be cambered and it was decided as stated in Subsubsection 4.3.3.3 that the airfoil should be symmetric in order to assure a simple design. The noise reduction caused by these serrations is estimated at 3 dB(A). This was concluded after looking at the STE-chase graph and the experiment performed by Leon et al. [82] and taking into account a contingency. The STE-chase model predict a reduction of around 7 dB(A), and the experiment 5 dB(A) at peak output. This peak noise output is at 1000 Hz as can be seen in Figure 4.17. Since it is known that the velocities the system will experience are significantly lower than the ones modelled a contingency of 50% is applied. Leaving an averaged 3 dB(A) decrease at peak noise output.

Table 4.8: Average OASPL produced by the turbine with and without implementation of serrations.

Distance [m]	**OASPL without serrations [dB(A)]**	**OASPL with serrations [dB(A)]**
4	56.9	53.9
20.96	44.7	41.7
144	28.5	25.5
13	48.5	45.5

From Table 4.7 shown in Subsection 4.5.7 it was clear that at four meters distance the requirement of an average noise emission of 45.5 dB(A) is still not yet reached. An average noise emission with serrations of 53.9 dB(A) results in L_{den} = 55.3 dB(A) and L_{night} = 48.9 dB(A), meaning that both the requirements are not yet reached. Therefore further analysis of noise reduction methods was required. However, since serrations lower the noise emission and are easily implementable in the design, serrations are added to the final design. Table 4.8 also shows that for at a distance of 13 meters the requirements of 45.5 dB(A) is reached when serrations are added. This distance is important for the further analysis of noise reduction methods, since this can be used to see what part of the building is exposed to noise exceeding the regulations.

4.5.8.2. Noise Cancelling Panel

One option to reduce noise would be a noise absorbing panel between the WHS and the building. Moreover, the panel should not obstruct the view and hence should be transparent. Glass and acrylic glass are possible materi-

als. Acrylic glass has many advantages over glass and was therefore used for a first sizing (Plexiglas® Soundstop XT BirdGuard[87]).

Based on the setup described in Figure 4.22 a minimum size estimation for such a panel could be done. Given the noise requirement of 45.5 dB(A) at the building facade, a minimum distance of l = 13 m needed to be achieved. Assuming a circular panel centered at half the turbine height with the a structural layout shown in Figure 4.21 a preliminary sizing was performed.

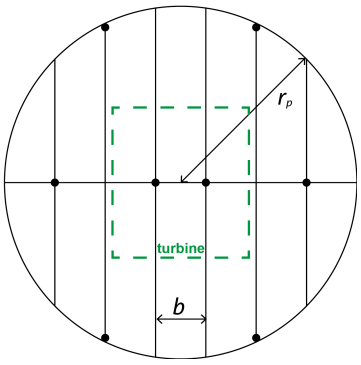

Figure 4.21: Noise panel layout and characteristic dimensions (front view).

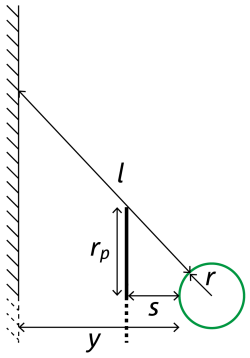

Figure 4.22: Noise panel location, distance and dimension relation (top view).

With a panel spacing s = 0.5 m to the blade path and the rotor dimension and location, r and y respectively, the minimum panel radius r_p was determined through simple trigonometric relation shown in Equation 4.18.

$$r_p = tan\left(cos^{-1}\left(\frac{y+r}{L+r}\right)\right)(s+r) \tag{4.18}$$

For a mass estimation the material properties of aluminum and Plexiglas® were used as given in Table B.1 and Table B.2 respectively. A summary of all parameters is shown in Table 4.9. As a panel per turbine would be required, it clearly shows that such a system is not feasible to be implemented and would also surpass the project budget. Furthermore, such an implementation would also complicate the accessibility of the turbines for maintenance.

Table 4.9: Possible noise reduction panel data.

Parameter	**Value**	**Unit**
Minimum required distance, l	13.00	m
Spacing Building-Blade path, y	4.00	m
Spacing Panel-Blade path, s	0.50	m
Turbine radius, r	2.53	m
Panel radius, r_p	6.52	m
Panel area, A_p	133.7	m^2
Panel thickness, t	12.0	mm
Panel mass, M_p	1909	kg
Frame length, l_f	78	m
Frame spacing, b	1.86	m

4.5.8.3. Active Noise Cancellation

As another method Active Noise Cancellation (ANC) could be used. This technology tries to cancel out the blade's self-noise by emitting the same noise pattern but 180° phase shifted. It is a very complex use case for that technology and in order to function efficiently, extensive further research would be required by analyzing the turbine in more detail. If not well optimized, it has the risk of increasing the noise, rather than diminishing it. Multiple methods already exist and research results are promising [78]. In any case, hardware components as acoustic sensors and sound sources would need to be added and integrated into the WES. The cost for such a system were estimated to be high, but mainly due to large development costs – the hardware costs would be manageable as well as the mass of the system. However, the required power for the sound producing units would need to be considered. Nevertheless,

an ANC system is recommended to be implemented in a future development phase and the best option to meet the noise requirement.

4.5.8.4. Facade Optimization

One other method would deal with altering the facade capabilities to shield the inside from noise. However, this solution to reduce the noise is not really a solution to fulfill the requirement of 45 dB at the building surface. Nevertheless, it is a way to deal with the actual concern of too high noise levels affecting the residents of the building. There is not really an interest in having the maximum noise level reached at the facade, but rather that there is no noise getting inside. As opening windows at a height of the system placement above 148 m, as explained in Section 2.4, is not done anyways. Ventilation systems should ensure that no noise will get inside. The facade and the windows could be optimized for better noise protection. Examples would be facade panels as mentioned before and improved glazing and windows like the Trosifol® Sound Control. When the buildings are made from scratch, these measures could be incorporated, however, if the WES is added to an exiting building this is not economically viable. Again, it is not really a solution to fulfill the noise requirements stated by Dutch legislation.

4.6. Structural Analysis

In this section the structural analysis on the WHS will be performed. First some general stress formulas will be stated and explained, then a material trade-off for the WHS is performed. With these findings firstly the blades will be sized, then the connectors and finally the shaft will be sized. Afterwards, the results will be verified.

4.6.1. General Stress Formulas

Although the need for the following formulas will not be explained until further in this section, however as these will be reused multiple times, they will be stated once at the beginning of this section in their general form.
The following formula, Equation 4.19, will be used to calculate stresses due to normal forces.

$$\sigma_{normal} = \frac{F_z}{A} \tag{4.19}$$

The following formula, Equation 4.20, will be used to calculate stresses due to perpendicular moments.

$$\sigma_{bending} = \frac{(M_x I_{yy} - M_y I_{xy})\,y + (M_y I_{xx} - M_x I_{xy})\,x}{I_{xx} I_{yy} - I_{xy}^2} \tag{4.20}$$

The following formula, Equation 4.22, will be used to calculate stresses due to shear forces.

$$q_s = -\frac{V_y I_{yy} - V_x I_{xy}}{I_{xx} I_{yy} - I_{xy}^2} \int_0^s t y ds - \frac{V_x I_{xx} - V_y I_{xy}}{I_{xx} I_{yy} - I_{xy}^2} \int_0^s t x ds \tag{4.21}$$

$$\tau_{shear} = \frac{q_s}{t} \tag{4.22}$$

The following formula, Equation 4.23, will be used to calculate stresses due to torsion.

$$\tau_{torsion} = \frac{T}{2At} \tag{4.23}$$

The last formula related to stress stated, Equation 4.24 will integrate all other formulas into a single stress: Von Mises Stress.

$$\sigma_{vms} = \frac{1}{\sqrt{2}} \sqrt{[(\sigma_{xx} - \sigma_{yy})^2 + (\sigma_{yy} - \sigma_{zz})^2 + (\sigma_{zz} - \sigma_{xx})^2 + 6\sigma_{xy}^2 + 6\sigma_{yz}^2 + 6\sigma_{zx}^2]} \tag{4.24}$$

To calculate the deflection some general formulas are used. The first equation for deflection, Equation 4.25 is used to calculate the the deflection due to an intermediate load on a cantilever as can be seen in Figure 4.23a. The second equation is also used for a cantilever, however this formula is used for a distributed load as can be seen in Figure 4.23b. The last equation is used for two point loads with an equal distance to the edge, shown in Figure 4.23c.

$$\begin{aligned} \delta &= -\frac{Fx^2}{6EI}(3a - x) \qquad (0 \le x \le a) \\ \delta &= -\frac{Fa^2}{6EI}(3x - a) \qquad (a \le x \le L) \end{aligned} \tag{4.25}$$

$$\delta = -\frac{wx^2}{24EI}(6L^2 - 4Lx + x^2) \tag{4.26}$$

$$\begin{aligned} \delta &= -\frac{Fx}{6EI}(3aL - 3a^2 - x^2) \qquad (0 \le x \le a) \\ \delta &= -\frac{Fa}{6EI}(3Lx - 3x^2 - a^2) \qquad (a \le x \le L - a) \end{aligned} \tag{4.27}$$

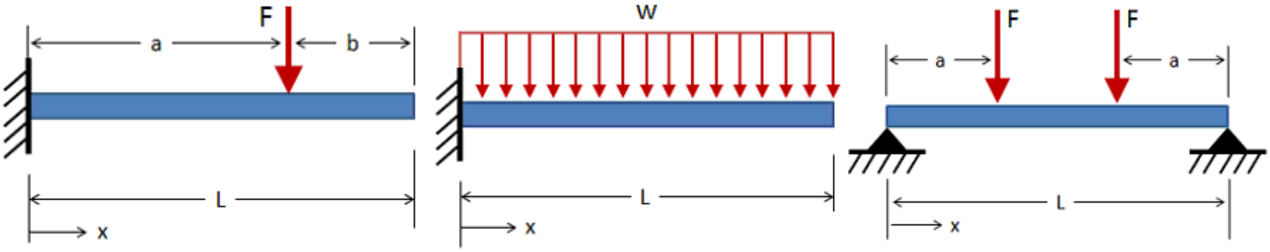

(a) Deflection due to an intermediate load for a cantilever.[22]

(b) Deflection due to a distributed load for a cantilever.

(c) Deflection due to two equal loads for a supported beam.

4.6.2. Safety Factor

For fatigue analysis, National Renewable Energy Laboratory, showed that based on IEC 1400-I a safety factor of at least 1.265 should be considered. Based on Germanischer LLoyd this would somewhere between 1.485 and 1.96[88]. A safety factor of 1.5 will be used in this section as this fulfills the minimum of both requirements.

4.6.3. Wind Harvesting System Material Trade-off

It was necessary to compare multiple materials for the structural components. In the following section a general trade-off is presented.

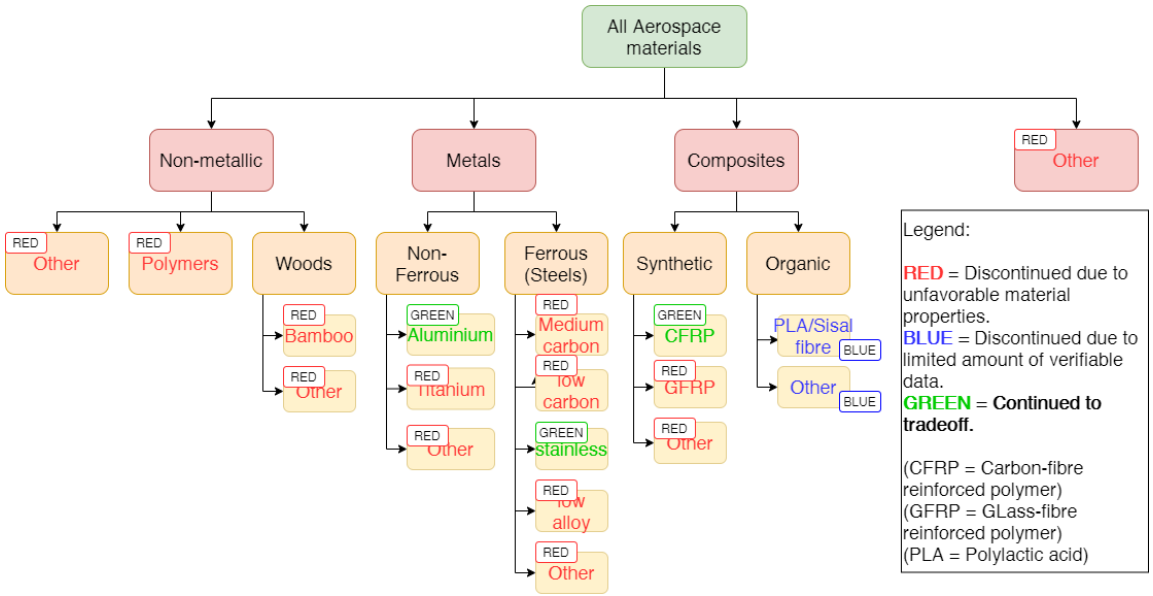

Figure 4.24: The aerospace materials considered for the trade-off.

The Wind Harvesting System is going to be suspended so it was very important for the supporting structure that the turbine consisted of light-weight structures. Because of this, aerospace materials were considered in a design option

[22] https://mechanicalc.com/reference/beam-deflection-tables [cited 19 June 2020].

tree (see 4.24). To be more clear: Titanium was not considered due to it's difficulty to manufacture and material cost. Glass Fiber Reinforced Polymer (GFRP) was not considered further because it has the adverse recyclability characteristics that Carbon Fiber Reinforced Polymer (CFRP) suffers from but at a much lower structural strength. Lastly, both synthetic composites were considered isotropic and with generic epoxy as a matrix [89]. The materials chosen for this trade-off are aluminium 7075-T6 and CFRP for their lightweight properties, and stainless steel for its resistance to the elements and stiffness. For the turbine a material was needed that can sustain a variety of load cases after many cycles. In general, materials are tested for at least 10^7 cycles and this was the load case that must be designed for [89]. However, only the fatigue normal stress was not enough to constitute a load limit. A redundancy factor was added of 1.5 to ensure the endurance of the system under all loads for the entire 10-year lifetime, as shown in Equation 4.28.[23]

$$\sigma_{Allowed} = \frac{\sigma_{Fatigue}}{1.5} \tag{4.28}$$

4.6.3.1. Criteria and Weights

Several criteria played a role in selecting the proper material for the WHS. They are explained here, and a weight is assigned to criterion based on the priority for the design.

Specific strength: As explained earlier, the maximum stress was based on the fatigue load and a safety factor. Additionally, to account for the different weights of materials, this maximum stress was adjusted to each material's density. This value will henceforth be referred to as the specific strength. Shear strength could not be used for the trade-off since there are no agreed-on standard shear force tests, due to the many variables involved in testing shear strength. After the trade-off, however, for all parts it was checked if the internal shear loads were less than $0.6\tau_{allowed}$, a common industry practice, and none of the internal shear loads exceeded this value.[24] The weight for this criterion was set at 35%. This was because the material properties largely drive the design, and a working design is a driving requirement.

Specific cost: The cost of materials is taken into account. Low cost is one of the driving requirements of this project and thus needed to be represented in the material trade-off. The cost was adjusted for the volume of the material to help reflect the importance of a lightweight structure. This criterion was assigned a weight of 35%. This was done to inhibit the choice of a material that would eventually make the WHS break the system cost requirement.

Resistance to environment: Apart from resisting the large cyclic loads, the WHS had to resist the environmental conditions it would operate in throughout its lifetime. Corrosion and degradation resistance is therefore important when designing for 10+ years. The resistance to the environment was based on the average of three values gained from data in the CES edupack [89]. Each materials' performance in UV-light, industrial and rural environments was averaged to arrive at a resistance score. This criterion was assigned a weight of 15%. This value was chosen to reflect that half of the lifetime provisions were already accounted for in the specific strength criterion.

Sustainability: The criteria stated above were mainly based on requirements, however the sustainable goals should also be taken into account. Following this projects six sustainability strategies (see Section 2.6), and considering the recyclability and emission of the materials, the following calculation was devised to test sustainability. The production of the raw materials has a CO_2-output value, measured in $kgCO_2/kg$. This value was multiplied by the percentage of material that is not recycled, to arrive at a final sustainability value.

$$Sustainability = CO_2(1 - \%_{recycled}) \tag{4.29}$$

The sustainability was assigned a weight of 15%. this weight was chosen to reflect the importance of the sustainability goal while still not being a driving requirement of the design. Each material was assigned a rating for each of these criteria. This rating was based on the values each material had for each criterion, see Table 4.10, values taken from the Appendix B.

[23] https://www.nrel.gov/docs/legosti/old/23257.pdf[cited 11 June 2020].
[24] https://www.indfast.org/about/faq.asp?#15 [cited 10 June 2020].

Table 4.10: Material values for criteria.

Criterion	Aluminium 7075-T6	Stainless Steel	CFRP	Unit
Specific Strength (adjusted for density)	0.058	0.052	0.14	MPa· m^3/kg
Volumetric Cost	10138.4	20782	48515	€/m^3
Environmental Resistance	4	4	3.67	-
Emission	7.57	3.43	47.7	kg_{CO_2}/kg

Because all of the criteria could be compared quantitatively, all materials could easily be ranked 1st, 2nd or 3rd for each criterion. This led to the trade-off table as seen in Table 4.11.

Table 4.11: The trade-off table of the WHS material trade-off.

	Material:	Aluminium		Stainless Steel		CFRP	
Criteria	Weight	Rating	Score	Rating	Score	Rating	Score
Specific strength	0.35	2	0.70	1	0.35	3	1.05
Specific cost	0.35	3	1.05	2	0.70	1	0.35
Environmental resistance	0.15	3	0.45	3	0.45	1	0.15
Sustainability	0.15	2	0.30	3	0.45	1	0.15
Final score			2.50		1.95		1.7
Position			#1		#2		#3

The conclusion that followed up from the trade-off is that aluminium 7075-T6 would be most optimal for the built of the turbine. Each component can be made from this material and is accessible for manufacturer. The material characteristics of this material are listed in Table 4.12, values taken from Appendix B.

Table 4.12: Material data of aluminium 7075-T6.

Parameter	Value	Unit	Parameter	Value	Unit
Tensile yield Strength	503	MPa	Compressive Strength	530	MPa
Fatigue strength (> 10^7 cycles)	159.5	MPa	Shear Strength	95.7	MPa
Young's Modulus	72	GPa	Shear Modulus	26.7	GPa
Density	2755	kg/m^3	Cost	3.68	€/kg
Environmental Resistance [rating]	4	-	Recyclable [yes/no]	yes	-
Emission	13.05	kg_{CO_2}/kg	Workability [rating]	3.7	-

4.6.4. Blade

The WHS blade is under a lot of stress from aerodynamic and centripetal loads. This means a structural analysis was necessary to ensure proper functioning of the blade throughout its lifetime and to choose a proper material. The distributed loads acting on the blade are:

- A normal distributed load in the direction of the axle of the WHS, W_n, consisting of the aerodynamic and centripetal forces.
- A tangential distributed load perpendicular to the normal load, W_t.
- A distributed torsional load arising from the pitching moment in the airfoil M_0.

To perform a static structural analysis, several assumptions were made (see also the free body diagram in Figure 4.25):

- The blade is modelled as a circular thin-walled beam (thickness t, radius R) to better resist torsional stresses.
- Reaction forces act at the beam's centroid at two locations, ($x1$ and $x2$), representing the clamping of the connectors to the blade. Due to the symmetry of the connectors, the reaction forces ($R_{n_{blade}}$, $R_{t_{blade}}$ and $M_{r_{blade}}$) at the clamping locations are equal.
- The distributed loads are assumed to be constant over the length of the blade, L_{blade}.
- The structural analysis was performed for the worst case scenario loads in all cases, meaning maximum RPM of the rotor, and at the angle with the highest aerodynamic load.
- The gravitational load of the blade is assumed negligible compared to the aerodynamic and centripetal forces.

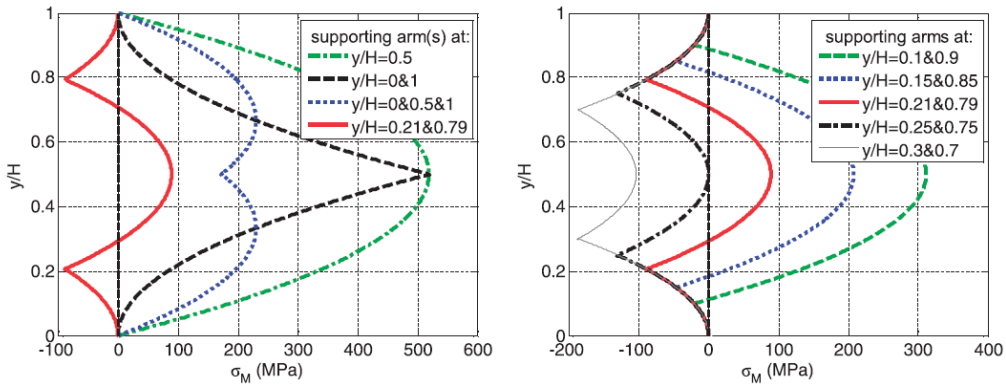

Figure 4.26: Data from [33], illustrating the normal bending stress distribution for various connector placements. The thick red line shows a stress distribution with similar connector placement to this design.

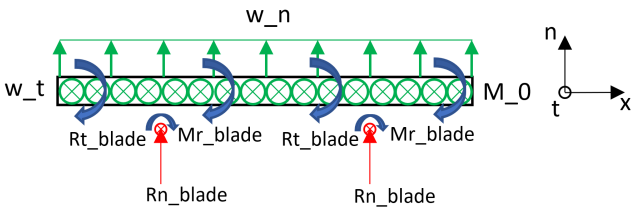

Figure 4.25: The free body diagram of the blade, showing the loads and reaction forces and moments on the blade.

The first step in performing the structural analysis was simplifying the blade as a free body diagram. Using the methods in R.C. Hibbeler's Statics [90], the reaction forces at the connectors were assessed (with at this point a placeholder value for the centripetal force). The next step in this process is to calculate the internal loading of the blade. To calculate this, the blade was cut into three sections and the internal forces were calculates using the methods from Subsection 4.6.1. The normal forces from the bending load and tangential loads were superimposed. The shear forces from the normal and tangential loads were superimposed. This leads to critical points along the length of the blade, but also a critical point along the circular cross-section of the blade. The locations of the critical points depend on the angle between the normal and tangential load vectors. By varying the longitudinal location of the connectors, the ideal attachment location was determined, at 21% and 79% of the length of the blade. These coincide with the Bessel points, validating the location of the connectors.[25]

Using the cross-sectional area determined by the aerodynamic analysis and a place-holder value for the thickness of the skin and the density of the material, the maximum internal stresses could be calculated at the critical points (these are shown in Figure 4.27). The stress level at these critical points was taken into account for the material trade-off for the WHS, as explained in Subsection 4.6.3. The distribution in Figure 4.27 could be verified with data from [33], as seen in Figure 4.26, which again also validates the choice for the connectors' locations.

After aluminium was selected as the proper material for the blades, definite outputs could be established to be used in the further design. A structural weight of 4.81 kg was calculated. Because this produced a final value for the centripetal force, the final reaction forces could also be calculated, as well as the final normal stress distribution in the blade (see Figure 4.27). The maximum shear stress was calculated at the critical points by superimposing the torsional shear stress and the shear stress imposed by the distributed loads. The maximum shear stress was found to be 31.1 MPa, or about 1/3 of the shear strength adjusted for fatigue and was thus within bounds. Additionally because aluminium is assumed isotropic, the Von Mises stress needed to be calculated. The Von Mises stress was considered with Equation 4.24.

It was assessed along the length of the blade at the cross-sectional critical point. Assuming a uniform, circular cross-section, geometric considerations could be used to simplify the localised shear flows and normal stresses as sets

[25] https://en.wikipedia.org/wiki/Airy_points [cited 11 June 2020].

of squared normal and tangential components and thus as sets of hypotenuses by the Pythagoras formula. This simplifies to the Von Mises stress in Equation 4.30, where α_{cr} is the angle of the critical point in the cross-section and the subscripts n, t and T correspond to normal, tangential and torsion, respectively. The distribution is also displayed in Figure 4.27, showing that the Von Mises stress remains within bounds. Finally, the important input and output values of the model are shown in Table 4.13.

$$\sigma_{vms,blade} = \sqrt{0.5(\sin\alpha_{cr}\cdot\sigma_t + \cos\alpha_{cr}\cdot\sigma_n)^2 + 3(\sin\alpha_{cr}\cdot(\tau_t+\tau_n+\tau_T))^2 + 3(\cos\alpha_{cr}\cdot(\tau_t+\tau_n+\tau_T))^2} \tag{4.30}$$

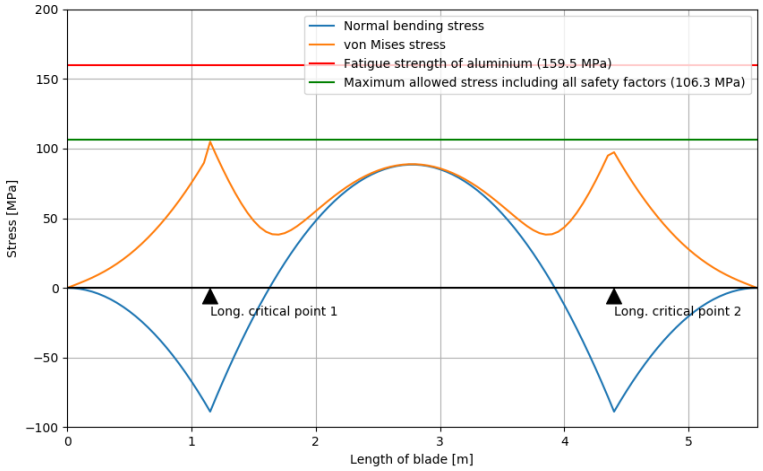

Figure 4.27: The bending stress distribution in the turbine blades. Two limits are drawn to illustrate the safety margin (the asymmetry seen in the figure is due to a counting inaccuracy in the model, and the second peak should be equal to the first).

Table 4.13: Important input and output values for the blade.

Input	Value	Unit
Length	5.55±0.2	m
x1	1.15 ±0.1	m
x2	4.4 ±0.1	m
r	0.0504	m
ρ	2755	kg/m^3
E	72	GPa
G	26.7	GPa
Distr. torsion	199.3	N
W_n	1039	N/m
W_t	86.6	N/m

Output	Value	Unit
Normal load on each connector	2885.9	N
Tangential load on each connector	240.3	N
Bending moment on each connector	553.2	Nm
Mass	4.81	kg
t	0.001	m

4.6.5. Blade connector

The connection between the blade and shaft has the purpose to withstand and carry the aerodynamic and gravitational loads of the blade. Therefore, structural analysis is performed to review and finalize the cross-section of this arm.

In Subsection 4.6.3 a material trade-off was performed and as a result aluminium 7075-T6 will be used as the material for the connectors. Assumptions are proposed to simplify the equations for the structural analysis of the component. A suggestion for the general outline of the connectors is to cover the cylinders by a symmetric airfoil to reduce drag. This analysis only focuses on the structural part and the imposed weight increase by this extra airfoil shape will be negligible. The following assumptions are used:

- The arm is a cantilever beam, with the end that is free to move being attached to the blade.
- All aerodynamic forces from the blade are then divided by two and attached to those ends.
- The aerodynamic forces are the maximum aerodynamic forces at 20 m/s and the centrifugal forces are based on a rotational speed of 151 RPM.
- The hollow circular cross-section is assumed to be superior on strength versus weight. Therefore no other cross-sectional shapes were investigated.
- The forces only result in normal stresses through the z-axis and shear stresses in the xy-plane because the length of the connector is considerable long compared to the width.
- Due to the amount of rotations this system will make, the fatigue strength of the material is the maximum stress the connector should experience.
- The final product would be manufactured without any imperfections in the material.

The structural analysis for the hollow circular connector that functions as a connection between the blade is based on the inputs coming from the blade. Inputs are the normal force, tangential force and the pitch moment produced by the blade. Furthermore, the mass of the blade and the connector itself are creating a moment and therefore also of importance, while the angular velocity of the connector is creating a centripetal force. To finalize the inputs for this section, also the material properties are needed to conclude the cross-sectional area. The parameters of the cross-section are thickness and radius.

As the goal of this section is to simulate the stresses over the connector a python program was developed. There are a few dependencies between the parameters of the formulas used in this program, therefore a first cross-section had to be assumed. This cross-section has an area, which is needed to calculate the mass of the connector. In turn the mass of the connector influences the forces and moments experienced by the connector, while these forces and moments introduce stresses into the structure whose goal it is to not fail and be lightweight. To create the data structure necessary to compute the diagrams, Python Data Analysis Library: pandas is used. Calculations are done over the length of the connector in steps of one centimeter. The model of the stress analysis over the cross-section was performed in steps of 0.02 r over a $2\pi r$ circumference.

A free body diagram showing the stated forces and moments is shown in Figure 4.28. The figure shows that the connector is modelled as a cantilever beam with the moving end attached to the blade. All forces and moments the blade introduces are attached at this end of the connector and taken into the account. The coordinate system in place for this component can be also be seen.

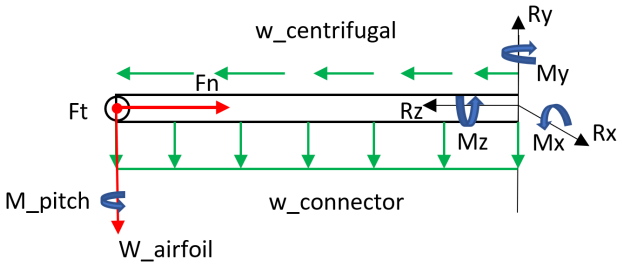

Figure 4.28: Free body diagram of connector.

With the cross-section radius and thickness, which are discussed later in this section, the force diagrams can be computed. They are shown for the normal forces in Figure 4.29a and the shear forces in Figure 4.29b and Figure 4.29c.

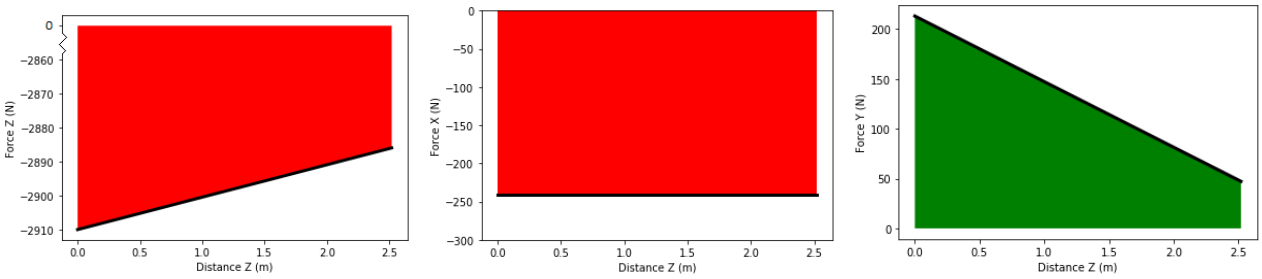

(a) The normal force in the connector.

(b) The shear force in x-direction in the connector.

(c) The shear force in y-direction in the connector.

Figure 4.29: The force diagrams of the connector.

The above figures show the magnitude of the forces in each axial direction along the length of the connector. Out of these results, the following moment diagrams are constructed as shown in Figure 4.30a and Figure 4.30b.

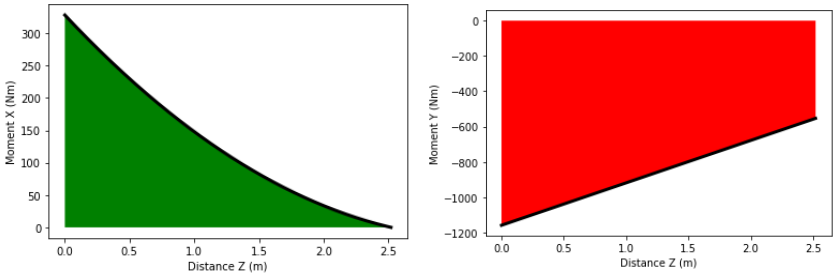

(a) The moment around the x-axis in the connector.

(b) The moment around the y-axis in the connector.

Figure 4.30: The moment diagrams of the connector.

With these force and moment diagrams, the forces and moments for the entire cross-section over the connector are known. As all these forces are known, all stresses can also be calculated over the connector. However, first a better sense of the geometry is needed. The moment of inertia in x- and y-direction will be labelled as by I_{xx} and I_{yy} respectively. The I_{xy} can be set to zero since the cross-sectional area is symmetric. The analysis was performed in the cylindrical coordinate system to simplify some of the stress equations. Therefore x and y can be transformed as shown in Equation 4.31 and Equation 4.32 respectively. The area for a cylinder is Equation 4.34, with r being the radius of the circular section with the thickness t.

$$x = r\cos\theta \tag{4.31}$$

$$y = r\sin\theta \tag{4.32}$$

$$I_{xx} = I_{yy} = \frac{\pi}{4}\pi(r^4 - (r-t)^4) \tag{4.33}$$

$$A = \pi(r^2 - (r-t)^2) \tag{4.34}$$

Having made these clarifications the stresses can be analyzed and the following three different types of stresses will be looked at:

- Normal stresses
- Bending stresses
- Shear stresses due to shear forces

The normal stress is computed with a derivation of Equation 4.19, combined with Equation 4.34. F_z is the force acting along the length axis of the connector. This becomes, Equation 4.35.

$$\sigma_{normal} = \frac{F_z}{2\pi r t} \tag{4.35}$$

The bending stress is calculated using the equation used for transformation of the coordinate system (Equation 4.31 and Equation 4.32) and the moment of inertia (Equation 4.33) and substituting this in Equation 4.20. This results in Equation 4.36.

$$\sigma_{bending} = \frac{M_x r \sin\theta + M_y r \cos\theta}{I} \tag{4.36}$$

The last type of stress that was considered is the shear stress due to the shear forces and is derived from Equation 4.21. The shear force is represented by the capital V in both tangential directions. The integral includes the position where the shear flow is measured in x and y, and the length s that it acts on. After substitution of Equation 4.31, Equation 4.32 and Equation 4.33 into Equation 4.21 and using $\tau = \frac{q_s}{t}$, Equation 4.37 is found.

$$\tau_{shear} = (-V_y \sin\theta - V_x \cos\theta)\frac{2\pi r^2}{I} \tag{4.37}$$

These three stresses should be combined as this measures the stress the connector is really experiencing. The equivalent Von Mises stress can bring these stresses together and is shown in Equation 4.24. As explained before, only tensile stresses in z-direction and shear stresses on the x-y plane are considered, which results in Equation 4.38

$$\sigma_{vms,connector} = \frac{1}{\sqrt{2}}\sqrt{2(\sigma_{normal} + \sigma_{bending})^2 + 6(\tau_{shear})^2} \tag{4.38}$$

The deflection should also be looked at as there are building requirements limiting the amount of deflection that is allowed. The 2018 International Building Code states that aluminum structural members have a maximum deflection [91]. By rule, the maximum deflection of a part is 60 times less than the complete length. This means that for the connector with a length of 2.52m, the maximum deflection is 4.2cm. Taking a safety margin of 1.5 into account, the connector will be designed to not deflect more than 2.8cm.

The connector is a cantilever beam and deriving Equation 4.25 and Equation 4.26 results in Equation 4.39 and Equation 4.40.

$$\delta_x = -\frac{F t z^2}{6EI}(3L - z) \tag{4.39}$$

$$\delta_y = -\frac{W_{airfoil} z^2}{6EI}(3L - z) - \frac{W_{connector} z^2}{24EI}(6L^2 - 4Lz + z^2) \tag{4.40}$$

Most of the variables stated in these equations are stated earlier. z is the distance from the axis and L is the length of the beam. Pythagoras is used to determine the total deflection.

As stated before, the process is a process of iteration. The connector should be optimized for weight, at the same time it should be producible and the Von Misses stresses and deflection should be within a margin. In the end, the model was optimized to a radius of 3.81 cm and a thickness of 6.3 mm, which can be produced.[26] The maximum stress for this geometry was 55.22 MPa and the maximum deflection 2.2 cm. The resulting figures are shown in Figure 4.31a and Figure 4.31b. The characteristics are summarized in Table 4.14.

[26] https://www.metals4u.co.uk/materials/aluminium?product_list_mode=list&shape=70633&product_list_limit=96 [cited 17 June 2020].

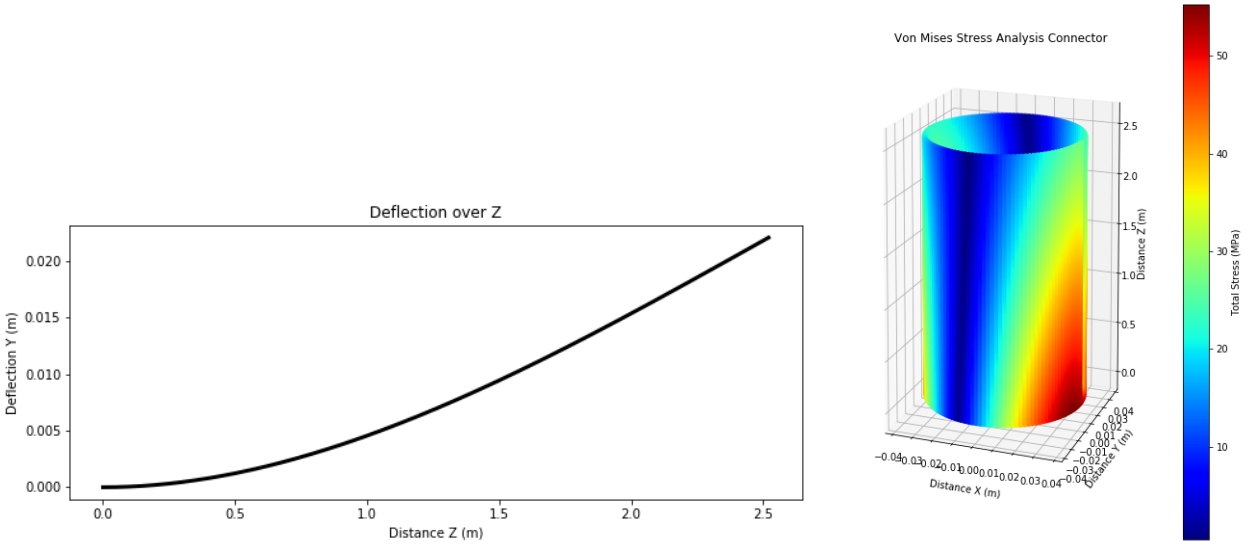

(a) The deflection of the connector.

(b) A three-dimensional Von Mises stress analysis of the connector.

Figure 4.31: The deflection and Von Mises stress through the connector as a result of its geometry.

Table 4.14: Important input and output values for the connector

Input	Value	Unit
Length	2.52	m
ρ	2755	kg/m^3
r	0.0381	m
t	0.0063	m
Mass	9.60	kg
E	72	GPa

Output	Value	Unit
Deflection$_{max}$	0.022	m
Von Mises-stress$_{max}$	55.2	MPa

4.6.6. Central Shaft

For the shaft in the middle of the turbine, the procedure to find the geometry has a lot of similarities as for the connector. The cross-section is also a hollow circle and therefore all equations are applicable. In this subsection only the differences and additions to the explained method are mentioned. First the new part of torque is discussed. Later the tensile stress is discussed.

For the shaft, aluminium 7075-T6 is used, resulting from Subsection 4.6.3. Assumptions are proposed to simplify the equations for the structural analysis of the component.

- The hollow circular cross-section would be superior on strength versus weight. Therefore no other cross-sectional shapes were investigated.
- The forces only result in normal stresses through the z-axis and shear stresses in the xy-plane because the length of the connector is considerable long compared to the width.
- Due to the amount of rotations this system will make, the fatigue strength of the material is the maximum stress the connector should experience.
- The final product would be manufactured without any imperfections in the material.
- The shaft is fixed at both ends and the translated forces and moments are equal on both sides.
- The length of the shaft is taken as the length of the blade, see Table 4.2, plus a contingency of 10 cm on both sides, to account for deflection.
- Each blade is connected with two connectors at a height determined in Subsection 4.6.4 These blades are at a 120-degree configuration.
- The aerodynamic force again will be divided by two and introduced at the height of the connectors.

The forces from the connector are introduced to the edge of the shaft. As the forces on the different connectors were assumed to be maximum and equal, the forces R_z will cancel each other out. This is accounted for by introducing F_{res}, as this is the maximum aerodynamic force all blades together exert on the structure. F_{res} also includes the force R_x introduced by each connector to the shaft. Next to this, R_x also creates torque in the shaft. The F_{res} vector is found with QBlade. M_x is cancelled out, R_y and M_y are introduced in the center to ease calculations. As the shaft has a mass, this introduces a distributed force. To finalize the inputs for this section, also the material properties are needed to conclude the cross-section area. The parameters of the cross-section are thickness and circle radius.

A free body diagram showing the stated forces and moments is shown in Figure 4.32e. The figure shows that the connector is fixed at both ends and the coordinate system starts at the bottom of the shaft. With a python program the stresses on the shaft will be simulated. The program to simulate the shaft is really similar to that of the connector. As the length of the shaft is larger than the length of the connector, the steps in the program are also increased a bit. The normal force diagram is shown in Figure 4.32a, the shear force diagram in Figure 4.32c and the moment diagrams in Figure 4.32b and Figure 4.32d. The free body diagram in Figure 4.32e represents the reaction forces of the connector due to the aerodynamic forces, their respective direction can be seen in Figure 4.28. Therefore, the axis in Figure 4.32e do not represent the axis implied by the forces.

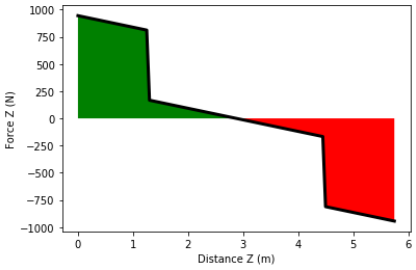

(a) The normal force in the shaft.

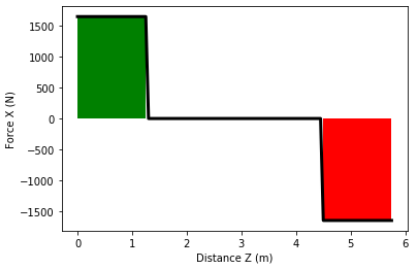

(c) The shear force in x-direction in the shaft.

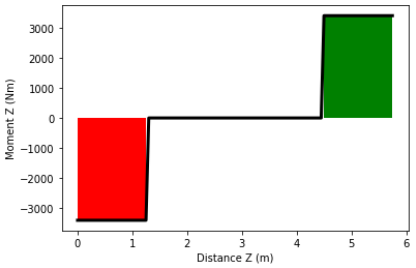

(b) The moment around the z-axis in the shaft.

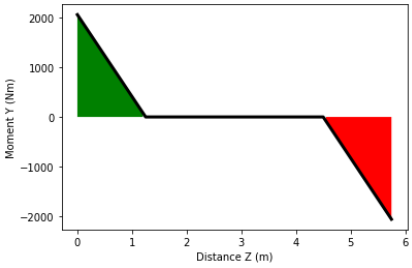

(d) The moment around the y-axis in the shaft.

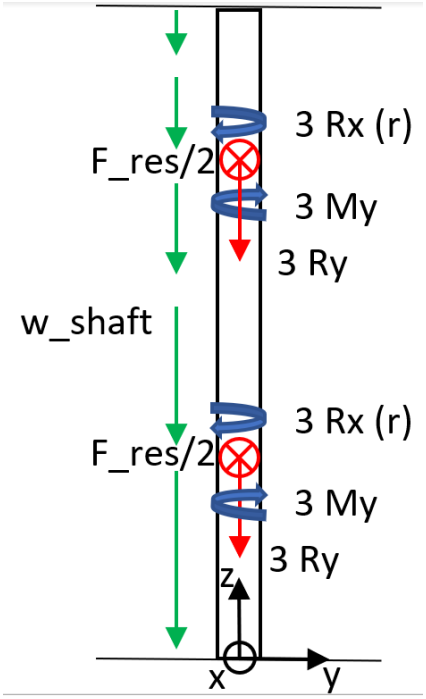

(e) Free body diagram of the shaft.

Figure 4.32: The FBD of the shaft with the resulting force and moment diagrams.

Equation 4.31, Equation 4.32 and Equation 4.33 will be used again for the stress calculations. This time four different types of stresses are looked at:

- Normal stresses
- Bending stresses
- Shear stresses due to shear forces
- Shear stresses due to torsion

The derivations of the normal stress, bending stress and shear stress due to shear forces are the same as for the connector and are therefore given in Equation 4.35, Equation 4.36 and Equation 4.37. The derivation for the shear stresses due to torsion results from Equation 4.23 and becomes Equation 4.41

$$\tau_{torsion} = \frac{T}{4\pi r t^2} \tag{4.41}$$

When the stress due to torsion is incorporated in the Von Mises Stress formula, it results in Equation 4.42.

$$\sigma_{vms,shaft} = \frac{1}{\sqrt{2}}\sqrt{2(\sigma_{normal}+\sigma_{bending})^2 + 6(\tau_{shear}+\tau_{torsion})^2} \tag{4.42}$$

In the analyses of the connector it was stated that a maximum deflection of 60 times less than the length of the part was a building requirement for aluminium structural members [91]. The maximum bending will be at the center of the shaft and for a shaft length of 5.75 meter the maximum deflection, including a safety margin of 1.5, is 3.2cm.

The shaft is fixed and deriving Equation 4.27 results in Equation 4.43.

$$\begin{aligned} \delta &= -\frac{F_{res}/2z}{6EI}(3aL - 3a^2 - z^2) \qquad (0 \le x \le a) \\ \delta &= -\frac{F_{res}/2a}{6EI}(3Lz - 3z^2 - a^2) \qquad (a \le x \le L-a) \end{aligned} \tag{4.43}$$

Where L is the length of the shaft, a is the distance to the first connectors, which is 1.25m and z is the distance from the axis.

Twist was also calculated. The formula for the rate of twist is Equation 4.44.

$$\frac{d\theta}{dz} = \frac{T}{4A^2}\int\frac{ds}{Gt} = \frac{T}{4(\pi r t)^2}\frac{2\pi r}{Gt} \tag{4.44}$$

$$\theta = \frac{d\theta}{dz}z + C \tag{4.45}$$

To get the twist using Equation 4.45, C has to be found and this can be done by aligning the twists with each other.

As stated before, the process is a process of iteration. The shaft should be optimized for weight, at the same time it should be produceable and the Von Misses stresses, deflection and twist should be within a margin. In the end, the model was optimized to a radius of 6.35 cm and a thickness of 6.3 mm, which can be produced.[27] The maximum stress for this geometry was 34.5 MPa, the maximum deflection 2.5 cm and the maximum twist 0.91°. The maximum stress is a lot smaller than the allowable fatique stress, that is because the shaft was designed to tolerate the maximum allowable deflection. The resulting figures are shown in Figure 4.33a, Figure 4.33b and Figure 4.33c. The characteristics of the connector are summarized in Table 4.14.

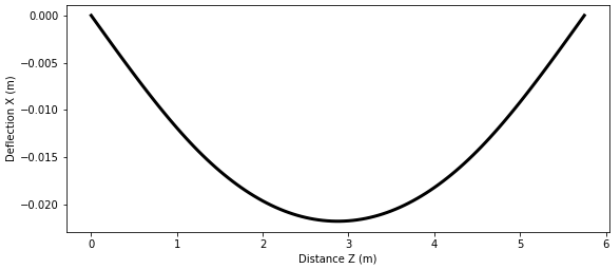

(a) The deflection of the shaft.

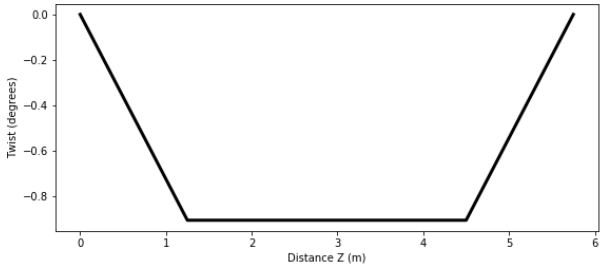

(b) The twist of the shaft.

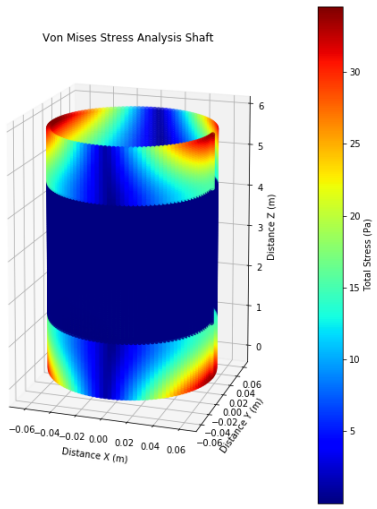

(c) A three-dimensional Von Mises stress analysis of the shaft.

Figure 4.33: The deflection, twist and Von Mises stress over the shaft, due to its geometry.

[27] https://www.metals4u.co.uk/materials/aluminium?product_list_mode=list&shape=70633&product_list_limit=96 [cited 17 June 2020].

The torque induced by braking should be countered by this part of the turbine. Since the shaft of the turbine is not designed for torque, determining the speed at which the turbine can be slowed down depends on the structure of the turbine. The value for the maximum allowable torque in the structure is 35.8 kNm. This results in a maximum braking torque of the same value. This value is found by substituting Equation 4.46 into the first part of Equation 4.47. Where J is the polar moment of inertia for a circular shaft, r the radius of the cross-section and D and d the diameter of the outer and inner circle respectively. Again τ is the maximum allowable shear stress.

$$J = \frac{\pi(D^4 - d^4)}{32} \tag{4.46}$$

$$T = \frac{J\tau}{r} = \frac{\pi}{16}\tau D^3(1 - \frac{d^4}{D^4}) \tag{4.47}$$

Table 4.15: Important input and output values for the shaft.

Input	Value	Unit
Length	5.55 ±0.2	m
x1	1.15 ±0.1	m
x2	4.4 ±0.1	m
r	0.0635	m
t	0.0063	m
Mass	37.84	kg
ρ	2755	kg/m^3
E	72	GPa
G	26.7	GPa

Output	Value	Unit
Deflection$_{max}$	0.025	m
Twist$_{max}$	-0.91	°
Von Mises-stress$_{max}$	37.8	MPa

4.6.7. Natural Frequency

The complete turbine will rotate during the operational time of the system, introducing vibrations. The turbine consists of three different modelled components, and for each, the natural frequency is calculated in this section. All assumptions will be stated per part, and finally a table with all eigenfrequencies is shown. The table will show the first three modes of the eigenfrequency for the three components.

4.6.7.1. Eigenfrequency Wing

For the eigenfrequency analysis of the wing the component is modelled as an overhanging beam, due to two connectors attached to the wing. An illustration of this can be seen in Figure 4.34a. However, literature shows experimental data on overhanging beams where overhanging beams are modelled as seen in Figure 4.34b. For this preliminary analysis the experimental data found from [92] is used for the calculations. This resulted in Equation 4.48 with different constants that can be found in Table 4.16.

(a) Free body diagram of the wing modelled pin supported with difference in lengths.

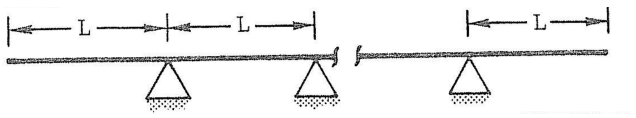

(b) Free body diagram of the wing modelled pin supported with the same lengths.

Figure 4.34: Two different free body diagrams used for the wing.

$$f_i = \frac{\lambda_i^2}{2\pi L^2}\frac{EI}{m}^{0.5} \tag{4.48}$$

Where L is the length of the span of the beam between pinned connections, E and I are Young's modules and moment of inertia of the cross-section respectively and m the linear density. By substituting the values from Table 4.16 into Equation 4.48 the natural frequency is found for the wing, which can be seen in Table 4.19.

Table 4.16: Constants for Free-Free Multispan Beam with Pinned Intermediate Supports [92].

Eigenfrequency mode, (i)	**Constant, (λ)**
1	1.412
2	1.648
3	3.580

4.6.7.2. Eigenfrequency Connector

Finding the eigenfrequencies for the connector is done with a similar method to that of the wing. The connector is modelled as a cantilever beam and therefore Equation 4.48 applies. The constant λ_i is the only thing that differs for the first three modes of eigenfrequency. The corresponding values can be found in Table 4.17, and the final values in Table 4.19.

Table 4.17: Constants for cantilever beam.

Eigenfrequency mode, (i)	**Constant, (λ)**
1	3.516
2	22.03
3	61.70

4.6.7.3. Eigenfrequency Shaft

The final part of the frequency analysis is on the shaft. The shaft is modelled as a beam pinned at its ends. Because of this, the calculations are done differently. Equation 4.49 displays the equation for the shaft. Constants applied for this can be viewed in Table 4.18 and the frequencies are stated in Table 4.19.

$$f_i = \frac{\lambda_i^2}{L^2}\frac{EI}{m}^{0.5} \tag{4.49}$$

Table 4.18: Constants for final pinned beam.

Eigenfrequency mode, (i)	**Constant, (λ)**
1	$\frac{\pi}{2}$
2	2π
3	$\frac{9\pi}{2}$

4.6.7.4. Final frequencies

All final values for eigenfrequency discussed in previous sections can be seen in Table 4.19. The frequency that comes out of the rotor was calculated using Equation 4.50.[28]

$$\text{RPM} = 151 \Longleftrightarrow f = 151/60 = 2.517Hz \tag{4.50}$$

The generated frequency is three times as high due to the presence of three blades, resulting in a frequency 7.55 Hz. All values are higher than the 7.55 Hz the turbine creates and resonance will therefore not occur in the structural part of the turbine. Assumptions are made, and these values may thus differ from reality, and therefore further research is suggested to investigate and find a value that fits better to reality.

4.6.8. Verification

All values obtained in the structural analysis should be verified and verification is performed in the following subsection. First the wing and connectors will be verified, and lastly the obtained values for the shaft are checked.

[28] https://www.convertunits.com/from/RPM/to/hertz [cited 13 June 2020].

Table 4.19: Natural frequencies of all parts and each mode.

$\mathbf{Part_{node}}$	**Value [Hz]**
f_{wing_1}	16.9
f_{wing_2}	23.0
f_{wing_3}	108.6
$f_{connector_1}$	27.5
$f_{connector_2}$	127.5
$f_{connector_3}$	483.1
f_{shaft_1}	17.4
f_{shaft_2}	69.8
f_{shaft_3}	157.0

4.6.8.1. Wing and Connectors

To verify whether the design and the structural analysis of the WHS are correct, the mass of a single blade and support arms is compared to [55]. The reference turbine has a radius of 3.24 m, which results in a longer and therefor heavier connector. In the model to compare the reference data the same radius is used. In Subsection 4.3.5 it is stated that the model for the forces seems correct, so it is assumed that the same forces can be used to recalculate the mass of the connector. As deflection was the limiting factor in minimizing mass, the connector will again be sized for this. A radius of 3.81 cm and a thickness of 6.3 mm was obtained, resulting in a mass of 12.4 kg for the connector. The new mass for a single blade with two support arms will be 29.61 kg. The reference turbine has a mass of 35.79 kg. This difference is acceptable as they make use of a more complicated structure, as can be seen in Figure 4.35. The main advantage of this structure is that the length of the shaft is shorter and can be made lighter. However, the connectors have to be placed diagonal instead of horizontal, which will increase their length and make them heavier. They counteracted this somewhat by including two small struts between both support arms. Also a different safety factor could be used, which would also result in a different mass. Therefore it can be concluded that the results presented in this section present a good first estimation for the designed blade and connector.

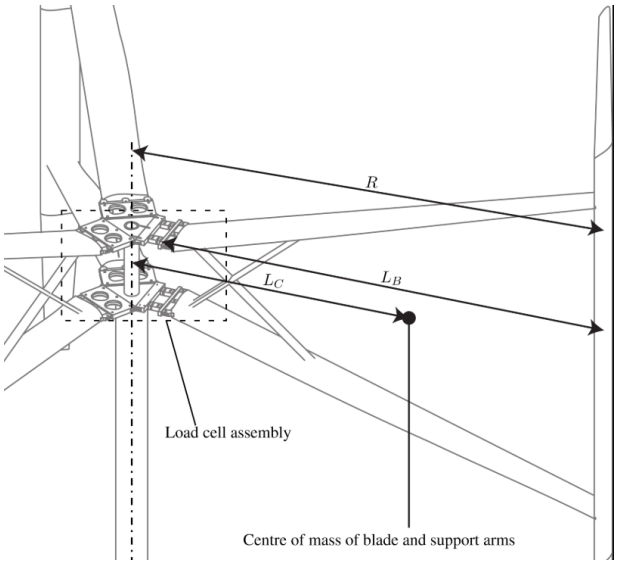

Figure 4.35: The design of the reference Turbine.

4.6.8.2. Shaft

Comparing the shaft to reference data is more complicated, as this is a rare example of a shaft fixed at both sides. The model for the shaft and the connector share a lot of similarities, so one could say that because it was proven that the model for the connector is correct, the model for the shaft should also be correct. An order of magnitude verification can be done, if the shaft is modeled as a cantilever beam, with a fixed bottom. This model would then share enough similarities to compare it with reference data [17]. As the size and amount of connectors is totally different, the tower will be compared to the blades. To make this comparison work a major assumption is that the ratio between the

mass of the blade and that of the shaft is similar for different designs with a different rated power.

The reference model has blades with a length of six meters and a tower of nine meters. Therefor the shaft of the WHS was also modeled to be three meters longer. Sizing this for deflection, making use of Equation 4.25 and Equation 4.26 instead of Equation 4.27, resulted in a radius of 12.7 cm and a thickness of 9.27 mm for the shaft. Which meant that the shaft had a mass of 170 kg. The blades have a mass of 14.43 kg. This gives a ratio of 11.8. Compared to the reference which has blades with a mass of 26.3 kg and a shaft of 243.4 kg. This gives a ratio of 9.2. As the comparison is based on a lot of assumptions, the comparison will not be further analysed and it is concluded that the order of magnitude is correct.

4.6.9. Survival Speed

The survival speed and other strong wind speeds were not considered in designing the structure of the WHS. Mainly because of the difficulties in modelling the aerodynamic forces. Besides Subsection 4.4.4 discusses the ability to completely lock the rotation of the WHS.

4.7. Resource and Sustainability Overview

The mass breakdown will first be shown, afterwards a cost breakdown is done and finally the sustainability of the WHS is discussed.

4.7.1. Mass Breakdown

The mass breakdown consists of the individual part masses of one turbine discussed in this chapter is summarized in Table 4.20.

Table 4.20: Mass breakdown of a WHS.

Part	**Mass [kg]**	**Explanation**
Blades	5 (3x) = 15	Calculated based on the dimensions of the blades and the material density
Connector	10 (6x) = 60	" "
Shaft	38	" "
Generator	341	
Maintenance Platform	250	
Brake	-	Negligible
Total (3x)	**2,110**	

4.7.2. Cost Breakdown

The WHS subsystem total cost depends on two parameters; The cost of the raw materials needed to produce the parts and the labor cost needed to manufacture the parts. The material cost of the three WHSs was calculated to be €1250. The production cost of the wind harvesting system was also estimated at €1250, as explained in Subsection 8.2.3. The generator and blades are prefabricated. The cost breakdown of a WHSs is tabulated in Table 4.21.

Table 4.21: Cost breakdown of the WHSs.

Part	**Costs**	**Explanation**
Material Blades	€250	Raw material cost
Production Blades	€250	Manufacturing cost
Material Shaft + Connector	€1000	Raw material cost
Production Shaft + Connector	€1000	Manufacturing cost
Generator (3x)	€2,500	see Subsection 4.4.2
Brake + Cooling (3x)	€500	Based on relative cost in [16]
Total	**€5,500**	

4.7.3. Wind Harvesting System Sustainability Score

In accordance to the sustainability goals and strategy for this project, a sustainability strategy for the turbine was created as explained in Section 2.6. The turbine can be evaluated based on this and a sustainability score for the subsystem can be established. The turbine is a lightweight structure made of a single material. This means that in

the manufacturing of the turbine, all scrap can be easily recycled. Additionally, it is quickly assembled in a flexible, quick, low-waste assembly line (see also Section 8.2). As the mining of the elements in and processing of aluminium 7075-T6 cannot be done locally and the material is recycle, local suppliers will be contacted and opportunities will be discussed in which way they can assist us in obtaining recycled material. To only use green energy during the manufacturing process is a matter of cost. The power train parts are prefabricated, meaning the environmental impact of their manufacturing cannot be easily obtained. The transportation and integration of the turbine is not based on clean energy, but it is quick, and many materials are locally sourced from recycled resources. The turbine is more noisy than allowed, it has a kind of interesting shape and low shadow impact. The turbine has a very positive impact on the environment, as it emits very little (only during production) and has a clean energy output. The system is highly modular, highly durable and quite reliable. It is very difficult to reach so maintenance is challenging. All components except for the drive train can be easily recycled. The drive train is quite complex, and would require more energy to recycle.

5
Structural Support System

Following from the design of the WHS, the SSS needed to be designed. First a functional analysis is performed in Section 5.1, followed by the functional requirements in Section 5.2. Section 5.3 elaborates on the overall shape of the support structure. The design process of the support structure is then explained in Section 5.4. This is followed by an analysis of vibrations in the structure performed in Section 5.5. Finally, the non-technical aspects such as the mass, cost and sustainability of the SSS are discussed in Section 5.6.

5.1. Functional Analysis

As mentioned in Subsection 3.1.1, Figure 5.1 shows a more detailed functional flow for the structural support subsystem and reaches three levels down. An extensive functional break down structure with one more lower level can also be found in Appendix A.

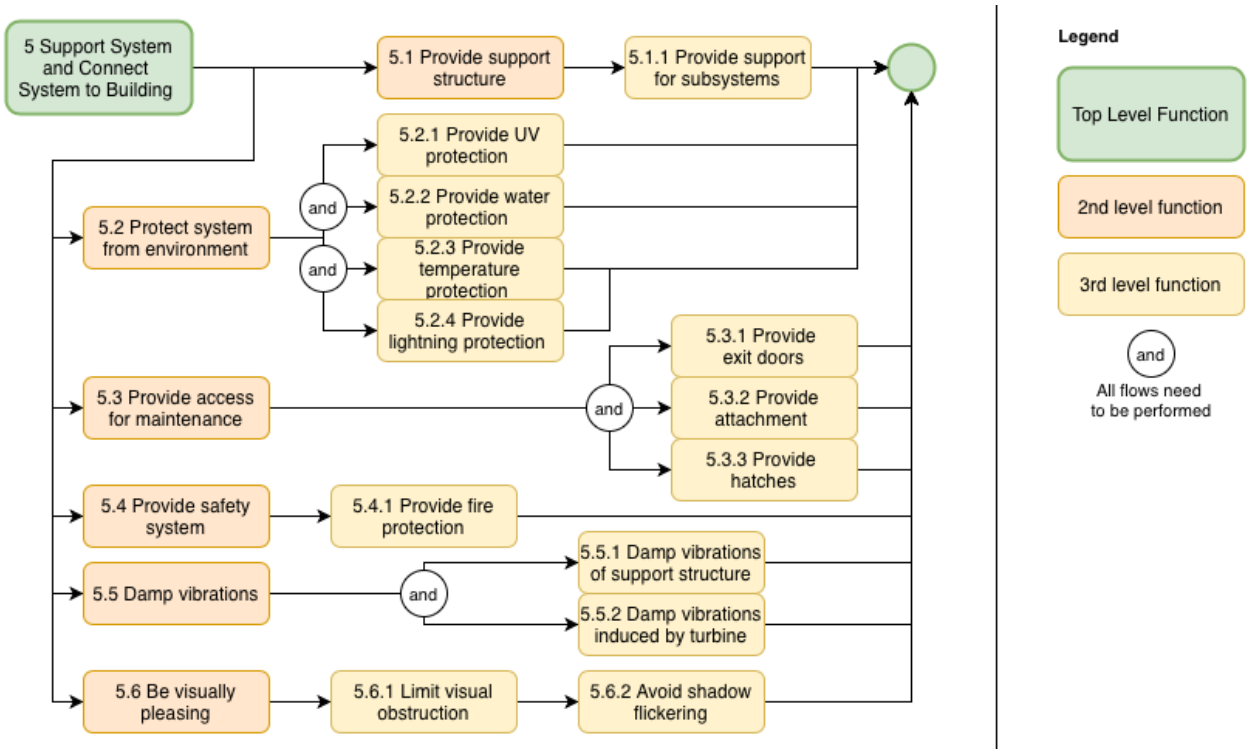

Figure 5.1: Functional flow diagram of the structural support system.

5.2. Functional Requirements

The requirements which are determined to be most driving for the structural integration, are listed in Table 5.1, to function as a guide through this section.

Table 5.1: Main requirements for structural support design.

Requirement code	Requirement
WES-A05	The system shall absorb the turbine generated vibrations in a way that they will not be noticeable to the high-rise buildings.
WES-A09	The system shall not require a technical inspection before 5 operating years.
WES-A10	The system shall not damage the high-rise buildings in case of failure.
WES-A11	The system shall not damage the area in between the high-rise buildings.
WES-A17	The system shall have an overall unit cost below €75,000.
WES-A18	The mechanical safety system shall be controlled by software.
WES-A22	The system shall be integrated into a 30-meter space between two buildings of which the parallel sides have a rectangular shape with a height of 200 meters and a width of 30 meters.
WES-WF-STR-01	The buildings shall carry the support structure.

5.3. Support Structure

The first step is to create a structure to support the WHS on the side of the building, after the trade-off result in [3], outside the boundary layer of that same building. Thus as mentioned before in Subsection 2.4.1, the VAWT could not be inside 4 meters of the building, starting from the side and measuring towards the other building. This created some limitations and high bending loads. As was mentioned in Section 3.2, three turbines will be implemented in between the buildings to meet the energy requirement. Only one trade off was used to decide what kind of support structure would be implemented. To get to this trade off, first the structures needed to be seen and judged.

(a) Option 1. [1]

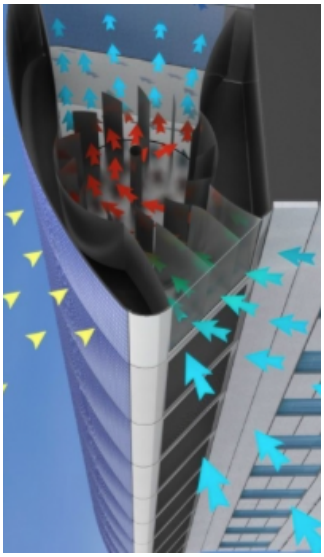

(b) Option 2. [2]

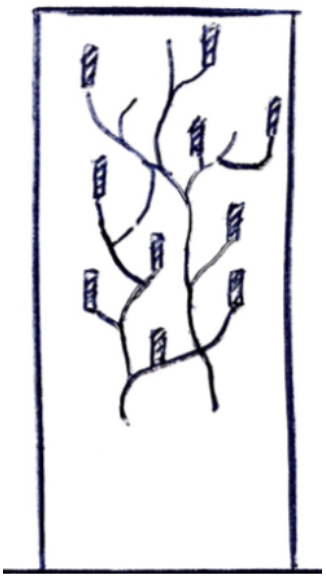

(c) Option 3.

Figure 5.2: Possible support structures.

Three different structures were placed next to each other and by analyzing the option and taking the aesthetics into account, it was decided the implementation of the tree structure, option 3, was the most innovative and efficient. This had mainly to do with its organic and aesthetically pleasing shape. To be able to create a nice and unique tree structure, two concepts were considered, both having an organic shape of a tree as shown. The main difference is the way the VAWT is attached. For the first option, the turbine is attached on one end, while for the second it has

[1] pinterest.com [cited 5 June 2020].
[2] insafeenergy.blogspot.com [cited 2 June 2020].

two ends fixed. The first option caused way higher stresses, while the other one was therefore more prone to be a success.
A structural analysis was done on these attachments to get a better understanding of the loads on the structure and WHS. The analysis was also performed to create a trade-off to be used in the final structure. It was checked for the same dimensions and cross sectional area in the structure. The highest bending/displacement would give the least suitable setup as the structure would have strength and stiffness, and thus weight of the structure and cost, would have to be increased to sustain all the loads. From this analysis the the thickness and optimal size of the beams and trusses were obtained.

5.4. Structural Analysis

First the attachment of the VAWT was checked and narrowed down to four kinds depicted in Figure 5.3. Calculations were done to see where the highest bending loads would originate. To do this, assumptions had to be made in terms of loads. The system was seen as a hanging VAWT (Figure 5.3a), standing VAWT (Figure 5.3b). A combination of these two was checked by having a single VAWT attached on the bottom and top of its axis, as shown in Figure 5.3d. The last checked was the VAWT attached such that the axis becomes horizontal in Figure 5.3c, meaning it would be perpendicular to the side of the building. The list of assumptions used for the trade-off are listed below.

- The translation and rotation, around the right side of each free body diagram, in all directions are considered fixed. This creates reaction forces in all directions and reaction moments around every axis, as shown in Figure 5.4. This originates at the cross section of the wall and the beam.
- A straight cantilever beam was considered with constant cross-section and thickness.
- The materials are assumed to be the same for all cases.
- The wind is a distributed force (Wwind) acting parallel to the buildings and perpendicular on the beams in positive x-direction. It was not taken into account that the wind would be varying the further it acts from the building.
- The weight of the system acts as a point load (Wwhs) downwards in the center of the WHS in negative y-direction.
- A resultant force (Fresultant) was added to the VAWT in the middle of the WHS. This load will act in the same direction as the wind. This force was determined with usage of QBlade.
- The weight of the beam/rod itself is considered as a rectangular distributed load, but is depicted as a point load(Wbeam) downwards in the center of the beam.
- For the double attachment, it was assumed that the forces created on the top beam would be the same as the bottom beam. Thus halving the reaction forces acting on it.
- l1 is the length for all the beams in z-direction, l2 is the distance added in the relevant direction of the VAWT.
- The coordinate system is determined by the right hand rule.

Using these assumptions, four free body diagrams of the attachements were created as displayed in Figure 5.3.

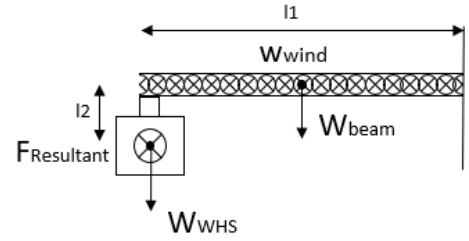

(a) Hanging WHS system.

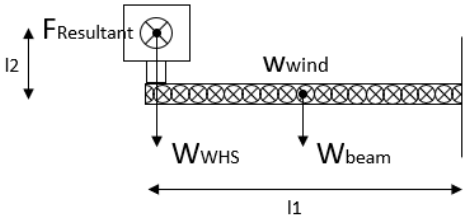

(b) standing WHS system.

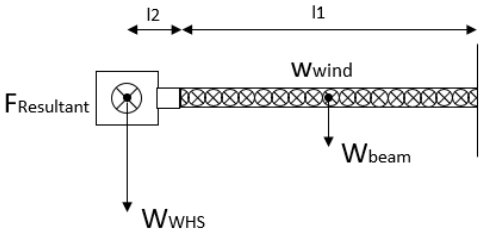

(c) Horizontal WHS system.

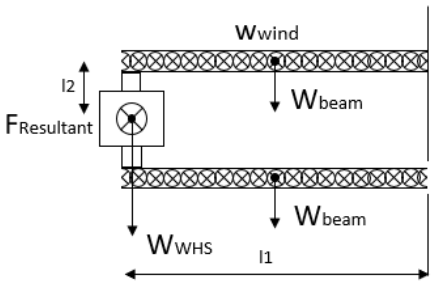

(d) Double attachment WHS system.

Figure 5.3: WHS attachments.

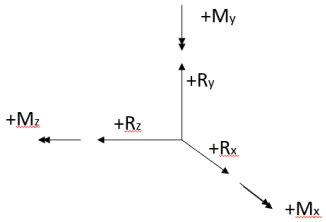

Figure 5.4: Reaction forces and moments

Out of these four, two kinds of attachments could already be discarded by applying logic. First, the hanging VAWT could be dropped as a possibility as it would have the same loads as the standing one, only having the turbine hanging from the generator. It was decided that having a WHS hanging would be negative in terms of efficiency and operational life duration. Next, the horizontal WHS would also be ignored, as it will create a higher moment on the beams and the generator. This would increase fatigue as well as possible failure of the system due to the moment on the generator. Now only Figure 5.3d and Figure 5.3b remain as possible design choices. The following step is to check what kind of bending occurs and where it would be the most critical. This was done by using basic structural analysis techniques with a python code. This way not only the bending was checked, but also the displacement, the stresses and eventually the optimal thickness and area could be determined and used for further iteration.

First, all reaction forces and moments were determined, conform to static analysis. These were used to determine the maximum bending moment, stress and deflection caused due to all load cases. The program was written such that the width/height would vary from 0.01 m to 0.13 m in steps of 0.01 m. The next step was to vary the thickness from 0.001 m to 0.02 m with a step size of 0.001 m.

It should be noted that for the double attachment, another assumption was made, mentioned in Section 5.4. Namely, the forces on the system are equally divided over the both attachments. Thus the reaction forces for both attachments are equal. Leading to the results only being calculated for one beam instead of two. The results for the case of the standing VAWT are compared to those of the singular beam of the double attached VAWT.

The load cases used are shown in Table 5.2 and the trade-off table is given in Table 5.3.

Table 5.2: Input parameters the trade-off of the attachments for one load case.

Parameter	Case 1	Unit
Wind speed	55	m/s
Weights of turbines	780	kg
Resultant force per turbine	3500	N

Table 5.3: Attachment trade-off table.

Parameter	Standing	Double attached	Unit
Maximum stress	119.57	118.43	MPa
Height	0.11	0.08	m
Thickness	0.018	0.018	m
Mass	885.75	625.85	kg
Deflection in y	-0.0477	-0.0621	m
Deflection in x	-0.0194	-0.0305	m

While the thicknesses are the same for nearly the same maximum stress value, there is a large difference in deflections. The singular beam of the double attached has a much higher deflection than the standing VAWT. It was expected to be lower instead of higher. This is mainly because of the cross section and the height difference. To make a good comparison, the height of the cross section of the double attached was changed to the optimal height of the standing VAWT. Now the attachments contain the same cross section. All results found subsequently are better to compare the best setup and are shown in Table 5.4.

Table 5.4: Improved attachment trade-off table.

Parameter	Standing	Double attached	Unit
Maximum stress	119.57	118.43	MPa
Height	0.11	0.11	m
Thickness	0.018	0.018	m
Mass	885.75	885.75	kg
Deflection in y	-0.0477	-0.02385	m
Deflection in x	-0.0194	-0.01179	m

The stresses are again expressed as Von Mises stresses shown in Figure 5.5.

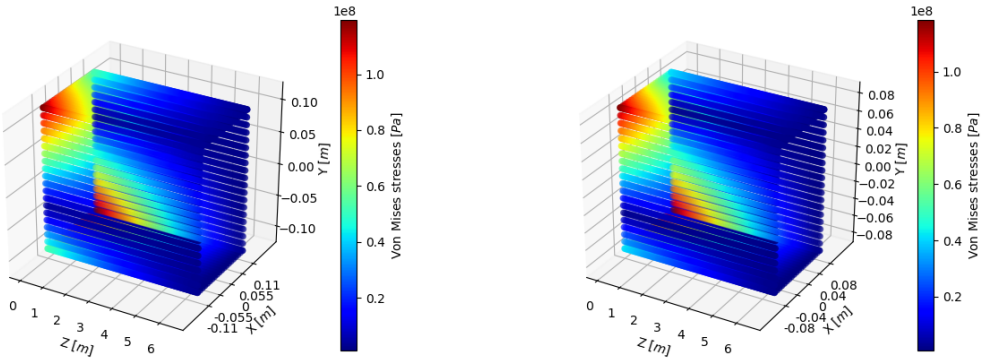

(a) Single attachment.

(b) Double attachment.

Figure 5.5: Von Mises stresses for different attachments.

It is clear that the deflection of the double attached is much lower than the deflection of the standing. Although the weight will be higher, lifetime will be elongated significantly, keeping maintenance at a minimum. This will reduce costs eventually that much more. Do notice that the deflection will be the same for the whole double attached system as well as a singular beam in that system. This means that the deflection on the whole structure will be a lot lower than for a single attachment. So the decision is made to use a double attached VAWT tree structure as the support system for the WHS, as shown in Figure 5.3d.

5.4.1. Structural Analysis of Tree Structure

As mentioned in Section 5.3, the tree structure was chosen because of its organic and aesthetically pleasing shape. The fact that VAWTs work better in numbers, using most of the lost wind energy from other systems, is used when considering a tree structure. The system will be attached to the side of one building, due to the higher score in the trade-off in [3]. Furthermore, the tree structure would simplify the scalability of the whole system. Adding extra turbines would not need a very extensive structural analysis. The supports can be added with almost no additional calculations, however due to possible increased vibrations, Section 5.5 would need a revision. Now that a choice is made for the structural integration to the building, a structural analysis of the tree structure can be made. In order to perform the structural analysis the Euler-Bernouilli beam theory will be used as it is a simple tool and provides a good first estimation for a structural analysis [93]. The fundamental equations for the Euler-Bernouilli beam theory were already given in Section 4.6. The support structure will be subjected to different loads: the weight of the support structure itself, the weight of the turbines, the wind loads and the resultant force of the turbines. A free body diagram of the support structure and its respective forces are shown in Figure 5.6, where four truss structures connect the vertical support structure to the building.

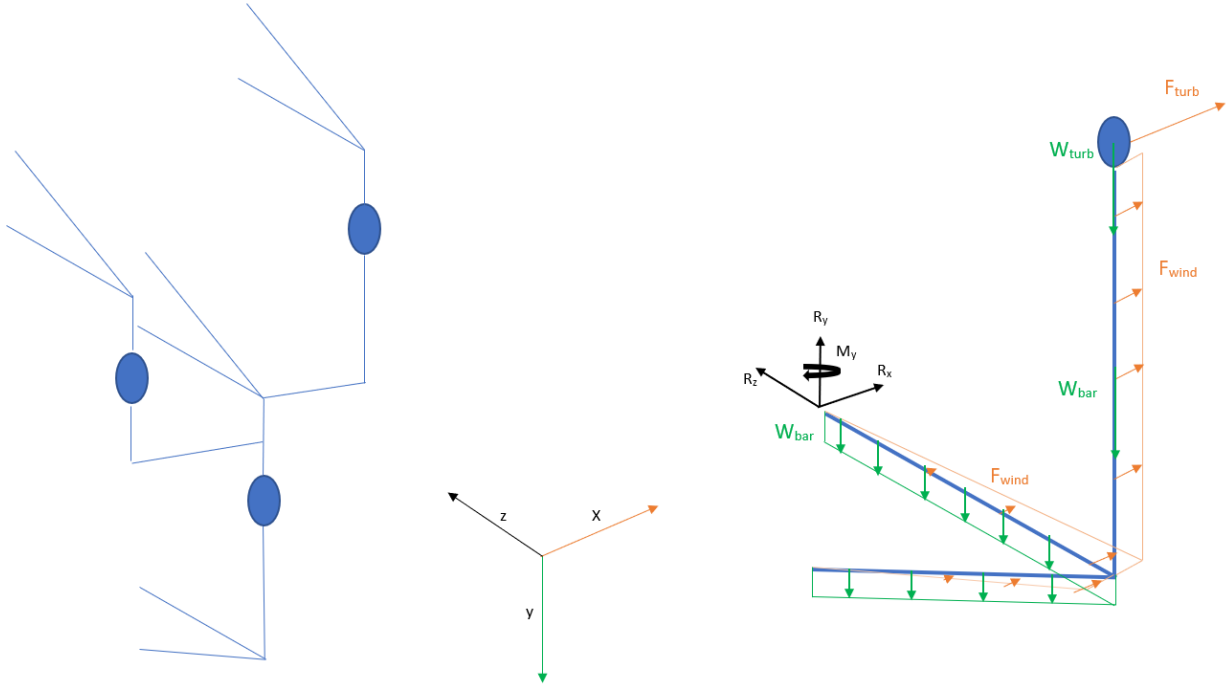

Figure 5.6: Free body diagram of the support structure with global overview of support structure (left) and forces on support structure (right).

The length dimensions of the support structure are estimated to minimize length dimensions and avoid the turbines to be in the wake of an upstream turbine. The exact length dimensions of the turbine can be found in Figure C.1 and Figure C.2. For the length of the truss structure, the constraint was that the turbine should be entirely outside the boundary layer of the building, which reaches a width of four meters when the wind is coming parallel to the axis of the space between the two buildings.It was also chosen to use a simplified truss structure instead of a cantilever beam as the stresses on a cantilever beam will be too high due to the forces acting far from the building. The angle in the truss structure is set to 45°.

To perform a structural analysis of the structure shown above, a few assumptions are taken to simplify the calcula-

tions:

- All cross-sections are assumed to be symmetric and consistent throughout the applied forces.
- The beams are assumed to be rigid with no deformations due to the loads.
- Distributed loads act on the symmetry axis, thus not causing torsion.
- The wind turbines and the loads from one member to another are assumed to be point loads.
- The wind velocities are linearly increasing in the boundary layer, that is zero wind speed at the building to free stream velocity at the rotor blade closest to the building. The wind speed at the turbines is equal to the free stream velocity.
- No buckling or torsion will occur in the members.
- Stress concentrations and possible cut-outs are not considered.
- Wind loads and resultant turbine loads are parallel to the building.
- Loads are equally distributed over the four attachment truss structures to the building.
- The horizontal bar of the truss is connected to a smooth pin with no moment in the x-direction.
- The diagonal bar of the truss is connected to a smooth pin with an assumed equal force in the y and z-direction and no moment in the x-direction.
- The forces and moments in x-direction and y-axis respectively are assumed to be equally distributed over the horizontal and diagonal bar of the truss structure.

The assumption to have pin connected structures to the building is a rough assumption as no moment is carried by the pins. The assumption was made as the structure would otherwise be three degrees indeterminate. Therefore, the results for such an assumption will most likely differ from reality, in which the beam will be clamped to the building. This will be taken into account and further discussed in Subsubsection 5.4.1.5. In addition, it should be noted that as the velocity between the building and the turbines increases linearly, the wind loads then increase quadratically as can be derived from Equation 5.1.

5.4.1.1. Load Cases

As the support structure is located in an open environment in-between two high-rise buildings it will be subjected to various wind loads. In Section 2.4 the wind distribution was described to be mostly around 10 m/s and in Subsection 4.3.3 the cut-out speed was determined to be 18 m/s. However, for the highest turbine loads, the loads at 20 m/s will used as a safety margin. Even though extreme wind speeds above 20 m/s are very rare, they are possible and the structure should be able to withstand these extreme loads without failing. According to [94] a survival wind speed of 55 m/s should be designed for.

Another load case that should be designed for is for the maintenance of the turbines. During the maintenance phase the load at the turbines will increase due to the working personnel and working gear. The maintenance operation will be further discussed in Section 7.4. An additional load of 750 kg at the turbines will be used for low wind conditions (< 10 m/s).

In addition to extreme cases described, the support structure will have to meet the yield criteria. To do so the Von Mises yield criterion will be used as described in Section 4.6. However, as the support structure will be subjected to high loads for a long time, failure modes such as fatigue should be taken into account. Fatigue occurs when the material is subjected to repeated cycles of stress or strain, leading to fracture even though the stresses are below the yield strength. However, if the stress is limited to the so-called endurance or fatigue limit, it is assumed the material has an infinite lifetime [95]. Therefore, for each material the fatigue limit will be used. Creep is another failure mode when the material has to support a load for a very long time . However, for metals, creep is normally only considered when the structure is subjected to high temperatures , which means it can be neglected for this structural analysis as the temperatures of the support structure will not attain very high temperatures [95]. In addition, a safety factor of 2 will be used on top of the fatigue yield strength to ensure safe operation of the structure over its lifetime [96].

5.4.1.2. Optimization Process of Support Structure

Since all the load cases and the different failure modes are defined an optimization process can be done to find the optimal dimensions of the beams such as to minimize stresses and cost.

The first step is to define different beam cross-sections possibilities. As the different parts of the support structure are subjected to different loads, the optimal beam cross-section will vary. Three shapes of beams will be considered: rectangular, circular and I-beams as shown in Figure 5.7. Each shape performs differently when it comes to bending,

which is due to their different moment of inertia [95]. The rectangular beam will perform better if bending in both the y and x-direction will occur. The I-beam is a better option if bending in only one direction occurs, as the weight decreases compared to the rectangular box. The circular beam performs worse than the two others when it comes to bending. For the support structure tension cables have not been considered as they result in a more flexible design, where in this case a rigid support structure is preferred.[3]

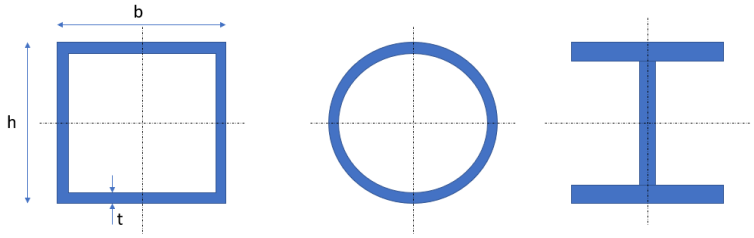

Figure 5.7: Different shapes of beams considered for the support structure with constant thicknesses and symmetrical.

The support structure will be subjected to wind loads which can be described by Equation 5.1. The different shapes described above have each different drag coefficient which results in different wind loads. The I-beam, rectangular and circular beam have drag coefficient of 2.75, 2.05 and 1.3 respectively. The I-beam and rectangular have significant higher drag coefficients, which will result in higher wind loads. Therefore, the case of adding a thin circular sheet around the I-beams and rectangular beams will also be investigated. Another problem that can occur with an I-beam in wind conditions is torsional flutter which is extensively explained in Daito et al. [97]. Adding a circular sheet around the I-beam could also limit this effect. Wind loads in low wind speed conditions (<10 m/s) are negligible. However as the wind speed increases to above 30 m/s, even though rare, the wind loads become very significant as the wind loads increase quadratically with the wind speed.

$$F = \frac{1}{2} C_d \rho A V^2 \tag{5.1}$$

The next step is optimize the dimensions such that the lowest cost is achieved while the Von Mises stresses do not exceed the yield criterion. To do so, an optimization algorithm is used which calculates the maximum stresses for each beam according to the loads shown in Figure 5.6. The stresses are calculated with respect to the equation for axial stresses, bending stresses and shear stresses extensively described in Hibbeler et al. [95]. The Von Mises stresses are then calculated in a similar fashion as discussed in Section 4.6. If the maximum stresses do not exceed fatigue yield strength with safety factor, the dimensions of the beam are stored. Then by using the specific cost of material, the total cost of the support structure is estimated. From there, the cheapest beam structure can be found.

5.4.1.3. Material Selection

The primary requirement on the support structure is of course that it properly supports the WHS. This means most of all that a rigid, strong material was necessary. Multiple types of material were considered. Steel was chosen as the best type of material for this purpose. It is easy to manufacture, recyclable and cheap, yet very strong and rigid. It is essentially the most used load carrying material for construction purposes.[4] Three steels were considered for the support structure. Low-carbon steels, which are cheap and ductile, medium carbon steels, which are rigid and strong, and stainless steel, strong and resistant to the environment. The criteria to perform a trade-off are listed below, to start with the cost criteria.

Cost: Material cost is considered as one of the driving requirements for this relatively bulky structure. This is why material cost per Kg material was taken into serious consideration. The weight for this criterion was set at 0.40.

Producibility: Another important factor of in producing such a large structure was it's producibility. The material cost is of course only one of the considerations to be made. Another is actually assembling the material. To accurately represent the producibility of the materials, their elongation at fracture were used as a measure of their ductility.[5] The weight of this criterion was set at 0.40 to represent the need for practical production.

[3] https://www.pearsonhighered.com/assets/samplechapter/0/1/3/2/0132803208.pdf [cited 12 June 2020].
[4] https://www.cdmg.com/building-faqs/most-used-metals-in-construction [cited 11 June 2020].
[5] https://www.productionmachining.com/articles/ductility-as-measured-by-tensile-testing [cited 11 June 2020].

Material strength: The material needs to carry the entire weight of the system. The material strength was therefore assessed in the form of the yield strength of each steels. Although supporting the system is a driving requirement of the subsystem, steels are considered very strong materials. This meant that cost considerations were placed at the foreground of this trade-off, and this criterion was assigned a weight of 0.20.

This trade-off could be performed numerically. All the ratings for each criteria per steel type are listed in Table 5.5. These ratings are based on the values taken from Appendix B, unless specified otherwise.

Table 5.5: Material values for criteria.

Criterion	Stainless Steel	Low-carbon steel	Medium carbon steel	Unit
Cost	2.685	0.655	0.655	€/kg
Ductility	29.5	35	20.5	%ϵ at fracture
Yield strength	698.5	305	652.5	MPa

The materials were scored 3-1 based on this value, which was multiplied by the weight to arrive at a final score for each material, as seen in Table 5.6.

Table 5.6: The trade-off table of the SSS material trade-off.

	Steel type:	Low-Carbon		Medium-Carbon		Stainless	
Criteria	Weight	Rating	Score	Rating	Score	Rating	Score
Cost	0.4	3	1.2	3	1.2	1	0.4
Producability	0.4	3	1.2	1	0.4	2	0.8
Yield strength	0.2	1	0.2	2	0.4	3	0.6
Final score			2.6		2		1.8
Position			#1		#2		#3

Low-carbon steel was chosen as the material for the support structure based on this trade-off. The material data of low-carbon steel can be found in Table 5.7, a complete overview of material properties can be found in Appendix B.

Table 5.7: Material data of Low-carbon steel.

Parameter	Value	Unit	Parameter	Value	Unit
Specific Strength	305	MPa	Compressive Strength	305	MPa
Fatigue strength ($> 10^7$ cycles)	240.5	MPa	Shear Strength	144.3	MPa
Young's Modulus	210	GPa	Shear Modulus	81.5	GPa
Density	7810	kg/m^3	Cost	0.665	€/kg
Environmental Resistance [rating]	2.33	-	Recyclable [yes/no]	yes	-
Emission	2.44	kg$_{CO_2}$/kg	Workability [rating]	4.2	-

However, unprotected carbon alloyed steels are very prone to corrosion after long periods of environmental exposure. To prevent this from happening to the support structure, a coating would be applied to the the support structure. To guarantee the recyclability of the support system, and to enhance the aesthetic design, this coating was chosen to be a polymer, adhered to the surface through polymer powder coating, a cheap, effective and proven method By M. Ashby [89]. The chosen polymer for this application was Thermoplastic Polyvinyl Chloride (tpPVC) as it is more resistant to UV-light than other options, but is still recyclable. A structure made of low-carbon, polymer coated steel is thus the best option for the SSS.

5.4.1.4. Optimized Support Structure

The support structure is optimized to achieve minimal cost and should withstand the loads for two extreme cases. From the material selection low-carbon steel was selected for the support structure. In Table 5.8 the two load cases and input parameters are given.

Table 5.8: Input parameters for optimization of support structure for two load cases.

Parameter	Case 1	Case 2	Unit
Wind speed	55	5	m/s
Weights of turbines	780	780	kg
Extra weight	0	750	kg
Resultant force per turbine	3500	500	N

Parameter	Value	Unit
Fatigue yield	240	MPa
Material density	7810	kg/m^3
Youngs modulus	210	GPa
Specific cost	0.668	€/kg

Following the optimization process discussed in above, the optimal beam shapes and dimensions were found and are reported in Table 5.9. It should be noted that the horizontal I-beams between the turbines will have the girders parallel with the ground, while the vertical I-beams will have the girder perpendicular to the incoming wind between the buildings. This is due to the transverse loads only being in one direction. In addition, all the beams will have an additional circular thin sheet to decrease the wind loads. Buckling and deformation of the sheet is not taken into account as it is assumed that the structure inside the circular beam provides sufficient reinforcement. The Von Mises stresses for the truss structure are shown in Figure 5.8 and Figure 5.9 for the two extreme cases respectively.

Table 5.9: Shapes and dimensions of beams in support structure.

	Shape	t [mm]	h [mm]	b [mm]
Two member frame	Rectangular beam	11	140	140
Beams between turbines	I-beam	10	100	80
Surrounding beam	Circular beam	3	130-200	130-200

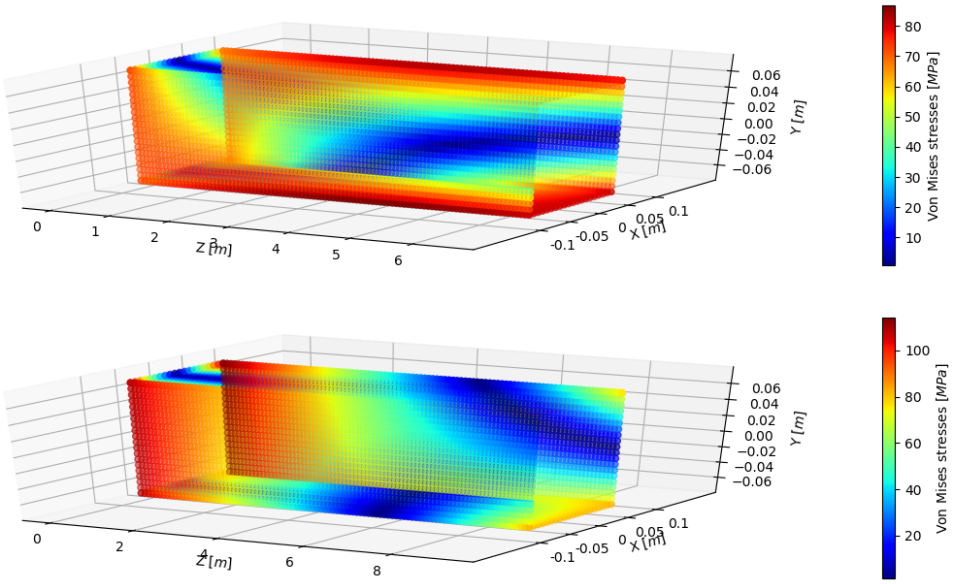

Figure 5.8: Von Mises stresses for Case 1 for the horizontal beam (top) and diagonal beam (bottom) of the truss structure.

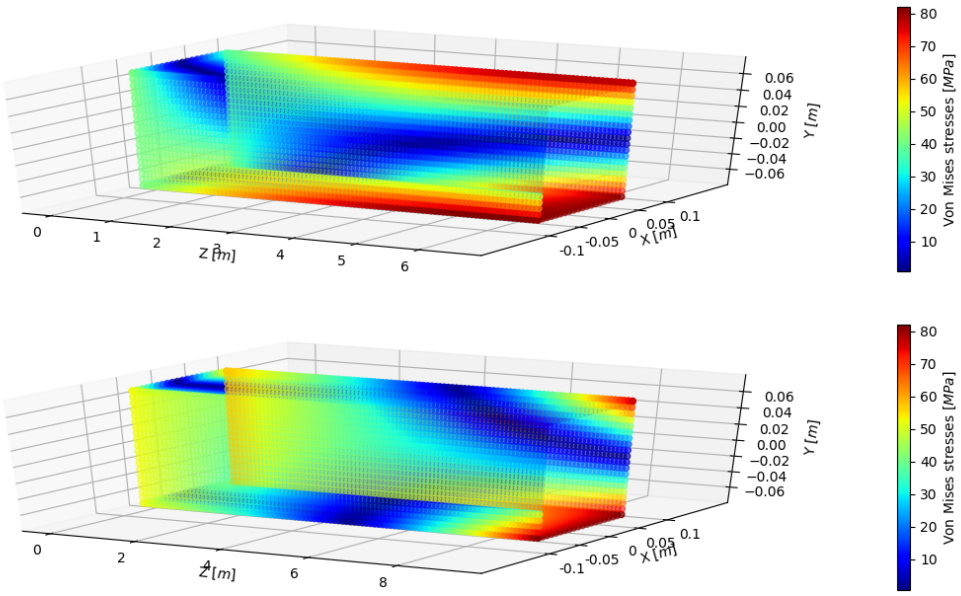

Figure 5.9: Von Mises stresses for Case 2 for the horizontal beam (top) and diagonal beam (bottom) of the truss structure.

As can be seen in Figure 5.8 and Figure 5.9, the limiting case is for extreme wind speeds for which a maximum stress of 115 MPa, which takes a safety factor of 2 above the fatigue load into account, can be found at the base of the diagonal beam on the side of the beam. This is due to the fact that the wind loads at the end of the beam create a significant moment at the building, which results in increased local stresses. The fact that adding weight does not change the stresses significantly can be explained by the fact that thanks to the truss structure the compression forces due to the added weight are distributed through the truss structure into the building. Therefore, an addition in weight will not result in the failure of the support structure. However, the loads might be too important for the building to hold. Therefore, an in depth analysis of the capability of the building to support the loads of the structure should be done at a later stage. The forces that occur at the building from the support structure for the two extreme cases are given in Table 5.10. These are the limiting loads from the two extreme cases the building should be able to support in order to install the structure. It should be noted that this assuming that no moments around the x-axis occur and should be revisited in more detailed design phase.

Table 5.10: Reaction forces on the building for the horizontal beam and diagonal beam.

Horizontal beam	**Value**	**Unit**
R_x	3	kN
R_y	4.7	kN
R_z	14	kN
M_y	16	kNm

Diagonal beam	**Value**	**Unit**
R_x	3	kN
R_y	14	kN
R_z	14	kN
M_y	18	kNm

5.4.1.5. Verification

In Subsubsection 5.4.1.4, the results presented were for an assumed pin connected structure. It was therefore assumed that the pins at the building did not carry any moments. However, as the support structure will most likely be a fixed connection where a moment is carried, an analysis of a clamped structure should be made.[6] By means of a Finite Element Analysis (FEA) in CATIA[7], the pin will be replaced with a fixed constraint. The predicted stresses discussed above will therefore shift as the moment is now largest at the fixed constraint. The stresses should however

[6] http://web.mit.edu/4.441/1_lectures/1_lecture13/1_lecture13.html [cited 15 June 2020].
[7] https://www.academia.edu/36174242/CATIA_V5_Structural_Analysis_for_the_Designer [cited 15 June 2020].

remain in the same range.

For the stress analysis in CATIA, Case 1 will be used (see Table 5.8. The input parameters are the same as for the stress analysis done above. Table 5.11 provides an overview of the forces used in the CATIA model. The stress analysis from CATIA can be seen in Figure 5.10.

Table 5.11: Input parameters for FEA in CATIA.

Forces	**Value**	**Unit**	**Dimensions**	**Value**	**Unit**
Distributed weight on horizontal beam	3.9	kN	Height	140	mm
Distributed weight on diagonal beam	5.5	kN	Width	140	mm
Point load in y-direction	7.4	kN	Thickness	11	mm
Distributed wind loads	4.2	kN	Length of horizontal beam	6.5	m
Point load in x-direction	3.4	kN	Constraints	Clamped	-

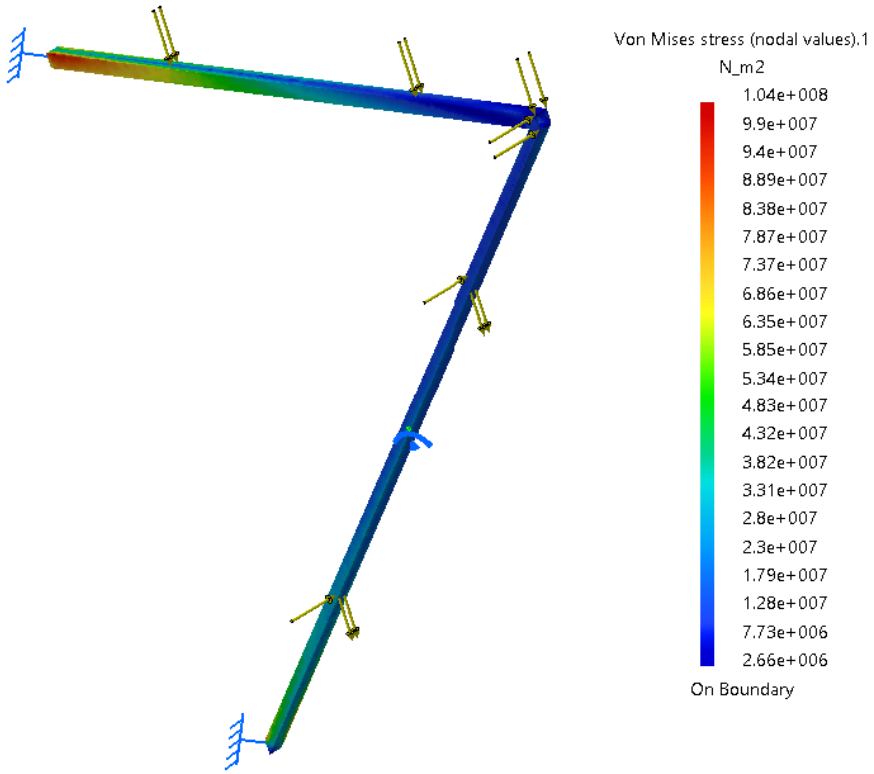

Figure 5.10: Finite element analysis of truss structure in CATIA with clamp constraint for Case 1.

As can be seen in Figure 5.10, the range of stresses correlates well with the predicted stresses in the section above. However, as was assumed earlier, the locations of the maximum stresses have moved towards the clamped connections as the moments are highest there. The highest stress is however not on the diagonal beam as was predicted in the section above. This can be explained by the fact that for the optimization process, it was assumed that the resultant force in the x-direction would be equally distributed over the two beams. In CATIA, this resultant force was distributed over the edge connecting the two beams and the greater part of that force is taken up by the horizontal beam. The maximum stress is however on the side of the beam as was predicted in shown in the previous section. Another verification that can be made is comparing the maximum deflections.

The results from the FEA show that the assumptions taken for the optimization process do not entirely reflect the reality as the stress distribution over the beams change with the assumptions taken. However, the range of stresses and location of stresses on the beam calculated in the optimization process do correspond to the FEA. It can then be assumed that the simplified optimization process gives a good first estimation for the ideal support structure. As the

the ideal structure was also verified by means of a FEA, it can be concluded that the described support structure will not fail.

5.5. Vibrations in Structure

In this section the vibrations of the structure will be analyzed. An introduction to structure born noise is given as well, this is not finished as it was deemed out of the scope for this design phase and will be put into further recommendations.

5.5.1. Vibrations and Natural Frequency

In this section the natural frequency of the structure will be compared with the frequency that comes out of the rotor. The frequency that comes out of the rotor can be calculated by using Equation 5.2.[8]

$$\text{RPM} = 151 \Longleftrightarrow f = 151/60 = 2.517Hz \tag{5.2}$$

Because there are three blades the aerodynamic and centripetal forces alternate three times per cycle, as shown in Section 4.3, the f in the above equation should be multiplied by three. This results in an operating frequency of 7.55 Hz from the rotor. It is assumed that the three different turbines operate in-phase with each other, in real life this will not be true and there will be parts where the frequency will reach levels of maximum $3 \cdot 7.55 = 22.65$Hz. The natural frequency of the beam will be calculated by taking the following assumptions:

- The structure will work as a cantilevered beam
- The total mass of the turbines will be a point mass
- The point mass will be placed at the end of the cantilevered beam

In vibrations it is important to realize the following; a beam actually has an infinite number of natural frequencies, so there are many 'Eigenfrequencies'. For structural design purposes, it is important to only pay attention mostly to the first few modes (lowest frequencies) [98]. The natural frequency is calculated by assuming that the tree wind turbines are one big mass that is held high by four cantilever beams. A sketch of this assumption can be seen in Figure 5.11 where the 2 other beams are hidden behind the two visible beams.

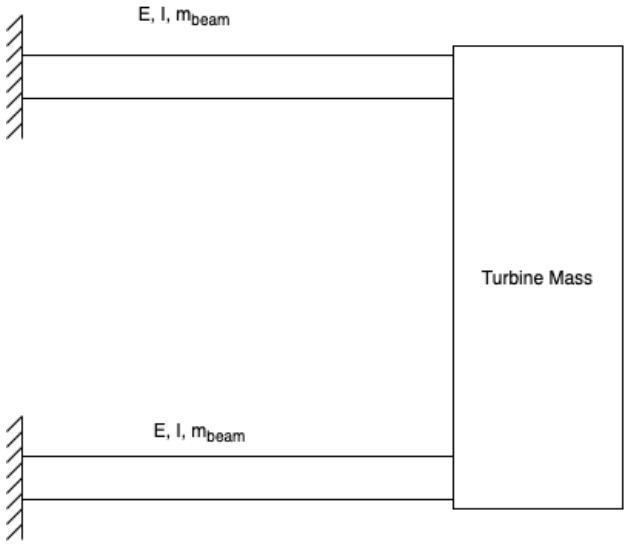

Figure 5.11: Sketch of the cantilevered beams assumption.

The natural frequency will be calculated by using Equation 5.5. Where k_{eq} is the stiffness of the beam and m_{eq} to total mass of the turbine and beam mass combination. k_{eq} can be calculate by using Equation 5.3 [98]. Whereas the m_{eq} can be used by using Equation 5.4 [98]. Using the values from Table 5.8, Table 5.9, Table 5.11 and Table 5.12 Equation 5.3, Equation 5.4 and Equation 5.5 can be filled in. The total mass of the support structure will be divided over the two beams in Figure 5.11.

[8] https://www.convertunits.com/from/RPM/to/hertz [cited 13 June 2020].

$$k_{eq} = 2 \cdot \frac{3EI}{L^3} \tag{5.3}$$

$$m_{eq} = m_{turbines} + 0.23 m_{beams} \tag{5.4}$$

$$\omega_n^2 = \frac{k_{eq}}{m_{eq}} \longrightarrow \omega_n = \sqrt{\frac{12EI}{m_{eq}L^3}} \tag{5.5}$$

The natural frequency of the structure is 15.13 Hz. As the natural frequency of the structure is higher then the operating frequency of the turbine there will not be any resonance. Because the difference between the operating frequency and the natural frequency of the structure is found big enough it can be concluded that the support structure will not experience problems due to vibration of the turbine. It can now be said that the support structure is in compliance with user requirement WES-A05: "The system shall absorb the turbine generated vibrations in a way that they will not be noticeable to the high-rise buildings" [2]. It should be noted that this is in compliance because of the in-phase assumption that was stated in the beginning of the section. In a further design phase, the assumed model to calculate the natural frequency should be improved.

5.5.2. Structure-borne Noise

Noise is an important factor in the development of building mounted wind turbines. In Section 4.5 the effects and the results of the airborne noise that resulted from the turbine were discussed and analyzed. In addition to this, there is also the potential that the residents of the building experience problems with structure-borne noise. Structure-borne noise is noise that starts off as vibrations which are then transferred through the building structure which then can result in noise inside the building. As this noise cannot be analyzed nor predicted with the methods from Section 4.5, a new method was found in [99]. The goal is to plot the noise level in function of the rotational speed of the VAWT.

The first step is to recognize the VAWT as the source of the structure-borne noise. The next step is tho calculate the blocked forces of the systems. For this report the blocked forces are by definition: "They can be taken as the hypothetical dynamic forces that a given Building Mounted Wind Turbine (BMWT) would apply to a perfectly rigid base when operating under given conditions. The higher the blocked force, the greater the excitation of the building." [99]. The blocked forces were calculated using Equation 5.6 where v_b is the operational velocity, $Y_{C,cb}^T$, the mobility matrix of the structure and f_{bl} the blocked forces[100]. The mobility matrix was calculated using the method described in [101].

$$v_b = Y_{C,cb}^T f_{bl} \tag{5.6}$$

The output of the teams model can be seen in Figure 5.12a and is then compared to the output of the model from the paper Figure 5.12b [99]. When comparing the two plots it can be seen that indeed for rotational speeds up to 151 rpm the blocked forces stay around the same magnitude and only increase around 250 rpm.

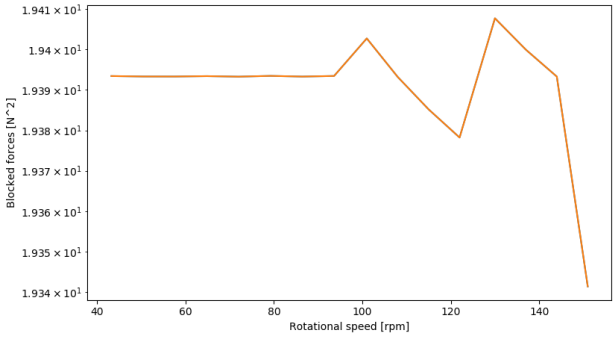

(a) Blocked forces for the designed WES.

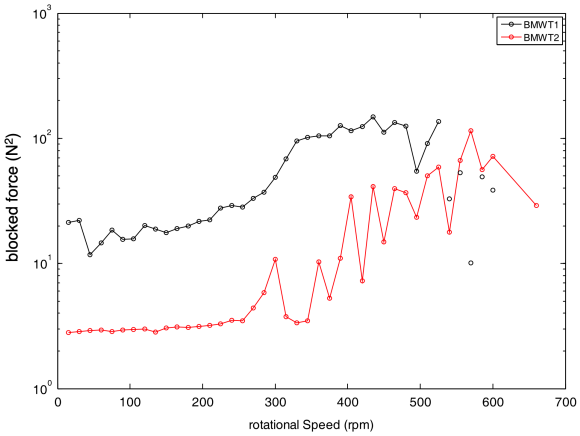

(b) Blocked forces from [99] for small turbines (Diameter MWT1: 1.7 m, MWT2: 1.1)

Figure 5.12: Blocked forces

At this point it was decided that the further analysis of the structure-borne noise was out of the scope of the DSE. Because the blocked forces in the design team's model showed similar behaviour as the one in paper [99], it was decided that for this moment the results of paper [99] can be used as an estimation for structure-borne noise of this design. The field results can be seen in Figure 5.13, where data for two different building mounted wind turbines is shown.

In Figure 5.13 both wind turbines do not reach higher noise levels then 35 dB(A) for rotational speeds up to 151 rpm. Since this is way below the noise generated at the building by the turbine as analyzed in Subsubsection 4.5.8.1 (which is equal to 53.9 dB(A)) and due to the way decibels are defined, this will not change the OASPL (35 dB(A) + 53.9 dB(A) $\approx$ 53.9 dB(A)). The assumption on the structure-borne noise is off course very rough for now and this noise source should therefore be analyzed into more detail and with the help of experts in a later design phases [102].

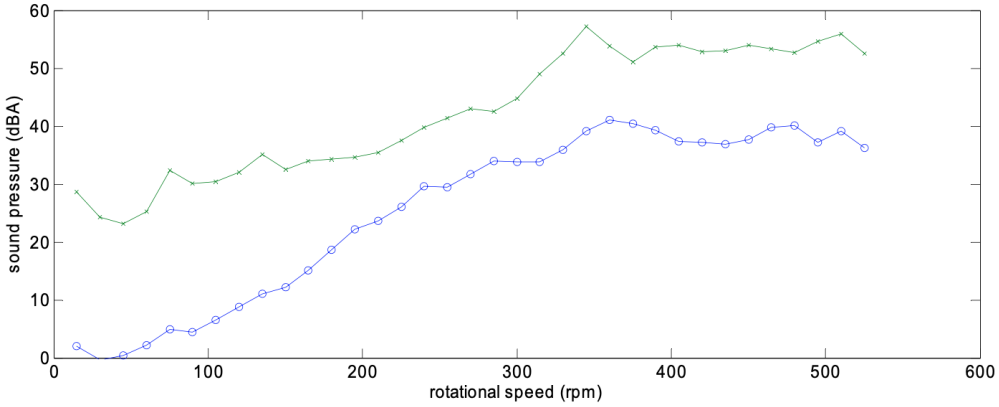

Figure 5.13: Structure-borne sound pressure in function of rotational speed of two different BMWT [99].

5.6. Resource and Sustainability Overview

The entire support system has now been designed, but a few parameters still need to be assessed. First is the mass breakdown of the structure, considered in Subsection 5.6.1, which offers a definitive value of the total mass of the subsystem. Afterwards, a cost breakdown of the subsystem in Table 5.13 which includes the material costs and manufacturing costs to arrive at a definitive value of the subsystem. Finally, the sustainability of this subsystem is analyzed, in Subsection 5.6.3.

5.6.1. Mass Breakdown

In Table 5.12, the subsystem parts can be found. Listing each individual member would be repetitive so the total weight is shown. The mass of the coating is estimated based on cost considerations.[9, 10] The definitive values of the mass of this subsystem can now be used in the mass budget in Table 8.1.

Table 5.12: Mass breakdown of a SSS.

Part	**Mass [kg]**
Steel Members	4,575
Polymer Coating	100
Total	**4675**

5.6.2. Cost Breakdown

The cost of producing the structural support system is a combination of the material costs, see Table 5.7 and production costs based on Subsection 8.2.3. The final values of the cost of this subsystem are used in the cost overview in Table 8.2 and help in creating a total cost analysis for the entire system.

Table 5.13: Cost breakdown of the SSSs.

Part	**Costs**	**Explanation**
Material Steel Members	€3,000	Raw material cost
Production SSS	€3,000	Manufacturing cost including polymer coating
Total	**6,000**	

5.6.3. Support Structure Sustainability Analysis

In accordance to the sustainability goals and strategy for this project, a sustainability evaluation of the support structure was composed. The resources of the manufacturing of the support structure will be sourced from recyclable sources. First production steel is wasteful, but due to the economy of scale, the emissions are lower than, for instance, aluminium (see Appendix B) .The manufacturing, which will include a lot of welding, will be quite wasteful, due to gasses expelled from the welding of the steel. The polymer powder coating can be done in a clean way, though, by collecting all waste powder for recycling. The logistics and integration are very standard, but do not involve many complicated steps. The integration in the building will require much energy, however. For more information on the production of the support structure see Section 8.2. The social and economic impact of the support structure is positive. The shape is intriguing and the structure does not create much noise. The environmental impact of the support structure is neutral, there is no energy output, but some fumes are emitted in the manufacture of the members. The lifetime of the support structure is high, the design is modular, durable, reliable but difficult to maintain, because of the installation height. Lastly, all materials can be recycled, but the coating needs to undergo some treatment to be recycled.

[9] https://www.pfonline.com/articles/how-to-calculate-the-cost-of-powder-coating [cited 15 June 2020].
[10] https://www.steelconstruction.info/Cost_of_structural_steelwork#Key_cost_drivers [cited 15 June 2020].

6
Electrical and Control System

In this chapter, the design of the electrical control system is described. The subsystem should perform multiple functions categorized as data handling and electricity management. This division separates the chapter. First, the functional analysis is given in Section 6.1, followed by the functional requirements in Section 6.2. The data handling systems are then described, consisting of a control unit, an external measurement unit, and an internal measurement unit. The systems respectively oversee the data handling, monitor the environment, and collect data on the different parts of the wind energy system. A further elaboration can be found in Section 6.3, Section 6.4 and Section 6.5 in that same order. Next, managing electricity is discussed. This consists of the electrical grid sizing, which also necessitates a transformer to transform the voltage from the generator to the grid level. Additionally, the cabling from the wind harvesting system up to the building is designed. To finish up the sizing of the electrical grid, the intermittency of the system is discussed, and an overview of the electrical grid is given. A thorough description is documented in Section 6.6. Finally, the non-technical aspects such as the mass, cost, and sustainability of the ECS are discussed in Section 6.7.

6.1. Functional Analysis

As already mentioned in Subsection 3.1.1, in Figure 6.1 and Figure 6.2 a more detailed functional flow for the external measurement unit, the data handling and control subsystem is presented respectively. Both FFD reach three levels down while in Figure 6.2 also an optional function is included. This is the possible add-on solution for a battery storage system as explained in Subsection 2.3.7. A functional break down structure can also be found in Appendix A.

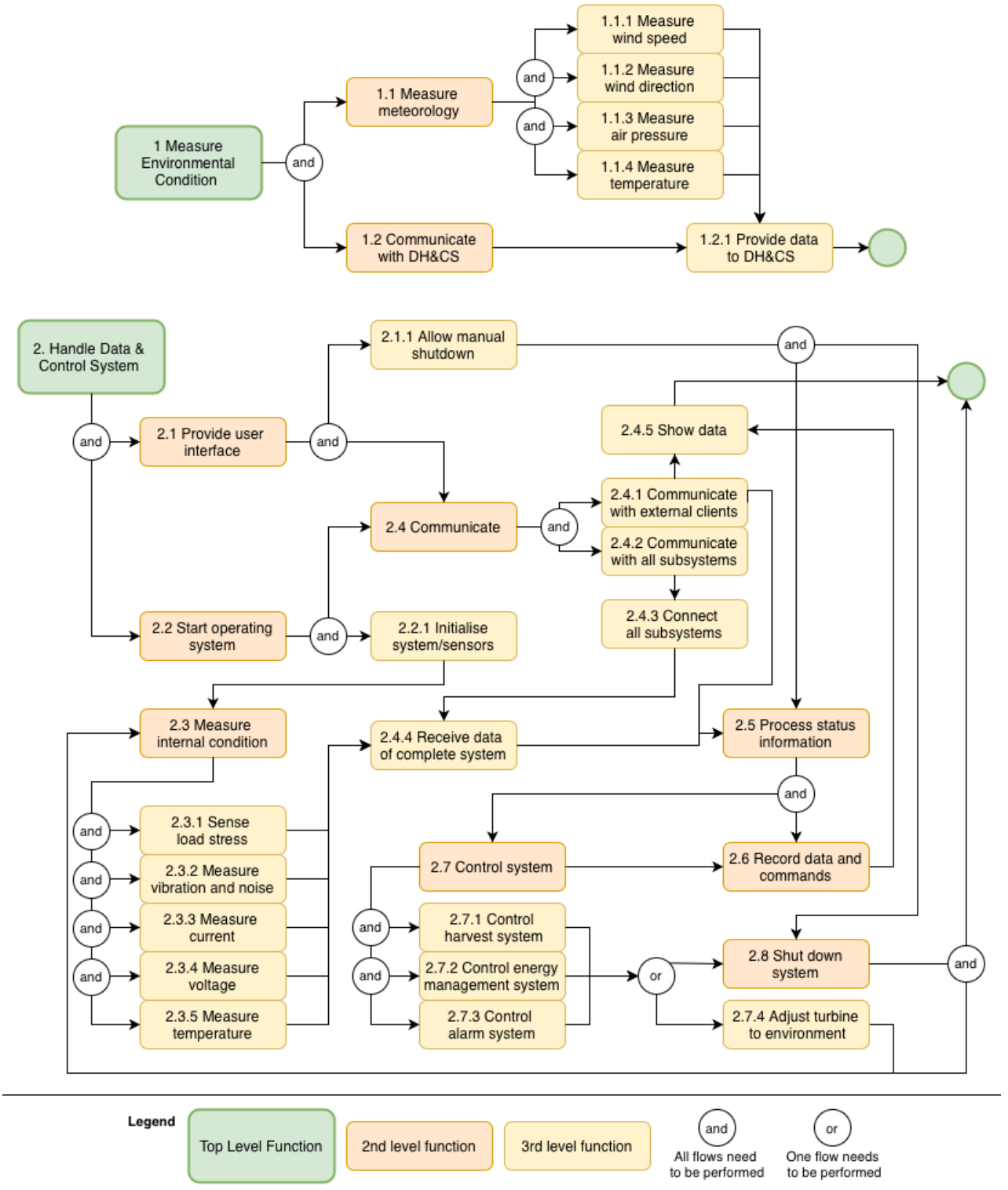

Figure 6.1: Functional flow diagram of the external measurement unit.

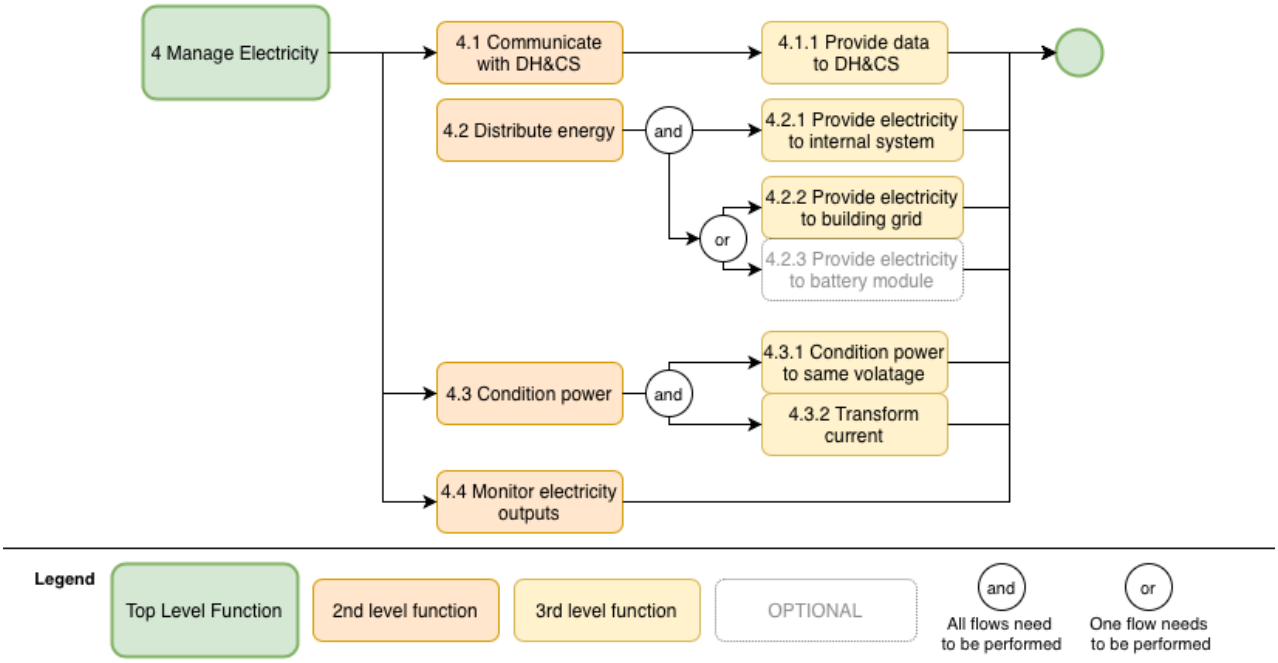

Figure 6.2: Functional flow diagram of the energy management system.

6.2. Functional Requirements

The main requirements for the electrical control system design are listed in Table 6.1.

Table 6.1: Main requirements for electrical control system design.

Requirement code	Requirement
WES-A09	The system shall not require a technical inspection before 5 operating years.
WES-A13	The system shall stop working automatically in case of failure.
WES-A17	The system shall have an overall unit cost below €75,000.
WES-A18	The mechanical safety system shall be controlled by software.
WES-OP-SC-03	The system shall be able to measure wind speed.
WES-OP-SC-06	The system shall be able to control the energy outflow to the building.

6.3. Control Unit

The entire system has to be controlled by a central system. This controller will have to analyze inputs from the turbines and communicate with the building and grid about the amount of power that will be delivered. In this case the DEIF's Advanced Wind Turbine Controller, AWC 500 will function as this system.[1] With the ability to calculate the energy and power, combined with the inputs from the connected sensors, discussed in Section 6.4 and Section 6.5, it will be able to adjust the operations of the system to favorable operations.

The controller can operate in extreme temperatures from -40 °C to +70 °C while being immune to electrical noise. Electrical noise is the result of electrical signals getting coupled into circuits where they should not be and can disrupt information-carrying signals. This of course should be prevented. It conforms to IEC 661131-3 programming and operates on Linux, with 3-phase 690 V voltage and 1/5 A current measurement.

[1] https://www.deif.com/products/awc-500?sgm=wind+power [cited 14 June 2020].

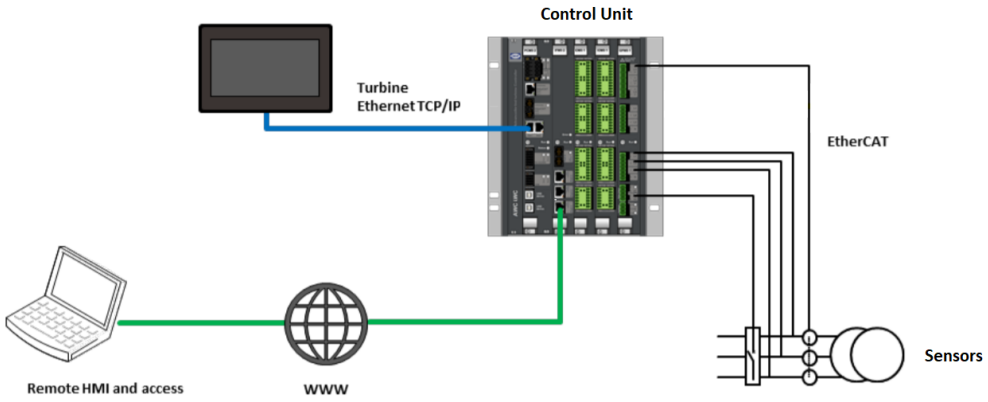

Figure 6.3: The system diagram of the control unit.

The controller as shown in Figure 6.3 contains a rack, including motherboard, with four different modules (from left to right):

- **Power and control module:** These contain a CPU, used for logging the data. They can store and analyze this data as well and have a connection to the interface for the local operator.
- **Four-port Ethernet twisted-pair and fiber module:** This makes communication with a remote office possible, by sending data via the fiber optical Ethernet.
- **Input and output modules (2x):** These highly flexible input and output modules can read the most commonly used sensor signals and send this as digital data to the control module and vice versa.
- **Grid protection module**: This can measure the current, power, voltage, etc. with an ANSI C12.20 accuracy class of Class 0.5. If these measurements are faulty the system will take the appropriate safety measures.

As the protection of the WES is assumed to be more similar to older systems and less advanced compared to most modern wind turbines, this system can help reduce this risk. It helps to mitigate the consequence of not having power by uninterrupted continuing operations during the beginning of this scenario. If power is still absent, it will enter its safe shutdown cycle in which it will prioritize that all data from the application is sent to the power-loss protected data storage and will be available to the application when power supply returns. This ensures for a fail-safe working. Another finding that will be taken advantage of is that the company tries to personalize its hardware and software to the desired configuration. With a lifetime of no less than 20 years, it conforms to the requirement of at least 10 years. As this system is of utmost importance a hot standby controller is available within the control unit as redundancy. Besides DEIF secures full traceability on all units in all production, which helps with sustainability. The system consumes at maximum 30 W. This means the total energy losses due to the control unit will be 0.219 MWh per year. The cost of the AWC500 was not obtained, however, the cost for a AEOLOS-V-5kW Grid-on Controller was around €2,000, which would mean if the price scales linear, that for the WES that would be around €14,000.

All data found by the sensors is handled and can give feedback for maintenance or an emergency stop. A clear example is an electronic circuit which can obtain a larger resistance due to disturbances. This can be detected due to the current sensors and maintenance can be applied instead of waiting for a burn through. Sensors should be chosen such that there is an overlap in dependencies. Meaning that an increase of values in one sensor should also increase the values of other sensors. These dependencies provide a dataset necessary for a smart system. Besides the real-life data, during testing, all produced data by the sensors are recorded. This will help make the dataset more robust and reliable, especially in the beginning when there is a lack of real-life data. Emergency stops can be applied because outliers should be detected by the system. For this, a good dataset plus a detection algorithm is needed.

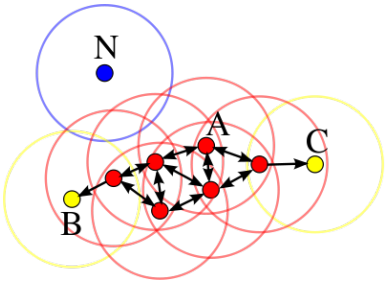

Figure 6.4: Visualisation of dbscan method to detect outliers (N).[2]

Detection Technique: Density Based Spatial Clustering of Applications with Noise (dbscan) [3] will be used to cluster the data and understand the relations between data better. Dbscan is a density-based clustering algorithm and focuses on finding neighbors by density (MinPts). Meaning that for some radius around a datapoint it looks at the number of other data points. It defines three different classes of points: core points (A), border point (C), outlier (N). A data point is a core point (A) when its neighborhood has the same or more points than the parameter for the entire cluster, MinPts. A data point is a border point (C) when the amount of data points in its neighborhood is less than MinPts and the data point is an outlier (N) when its neighborhood does not have other data points. This is visualised in Figure 6.4. How the value for the radius and the MinPts should be defined depends on the dataset, however, there are Python tools that can assist with this.

6.4. External Measurement Unit

The freestream flow before entering the area of the buildings needs to be analyzed. This is done by either obtaining public information on the internet or by the system itself. Both options are used for the design that is chosen. Pressure, temperature, and rainfall are parameters that can be found on the internet and the accuracy of these numbers is of less importance. However, the wind speed and direction are of great importance to the harvesting system and therefore are both measured real-time on the ground.

Industrial sensors that would be able to measure this with a lot of precision are too expensive for this kind of system. As this system is less dependent on wind direction and performance can be less optimized for precise wind speed, standard sensors were selected shown in Table 6.2. With an accuracy of three degrees direction wise and 0.3 m/s speed wise it is assumed that the measurements are accurate enough. These sensors are in place to validate data from other sensors in real-time. For example, the wind speed will influence the braking system, and the average power generated and the measurements from the sensors should be correlated.

6.5. Internal Measurement Unit

The measure of performance of key components in the system is monitored constantly, to assure failure is detected beforehand. For this reason, multiple sensors are placed in different locations as can be seen in Table 6.2. Next to this, the desired sensors are stated. The selected sensors are inspired by amongst others the sensors of TE, shown in Figure 6.5. Cheaper options for the sensors are chosen instead of state of the art machinery. The main reason for this is the budget stated in requirement WES-A17. Table 6.2 also shows the amount of each sensor.

The sensors that verify performance and ensure safety measure either the stress and strain, the acceleration, the temperature, the current, and the voltage at that specific location. When the blades rotate they are expected to experience extreme stresses while being designed lightweight. To ensure safety, stresses at the most critical positions of the blade are measured as well as the acceleration. The acceleration will help to validate the measurements of the stress and the control unit. The same sensor is used to measure the acceleration of the SSS as extreme vibrations that translate to the building are catastrophic. The stresses on the SSS and other parts of the WHSs will also be monitored, to detect irregularities. The current and voltage are measured in the cables and the temperature is measured in components that are expected to see an increase in heat due to operations. Spikes in current, voltage, and temperature could indicate a malfunctioning. The temperature in brakes is measured as bad performance of this mechanical system often translates to heat.

[2] https://towardsdatascience.com/a-brief-overview-of-outlier-detection-techniques-1e0b2c19e561 [cited 22 June 2020].
[3] see footnote 2

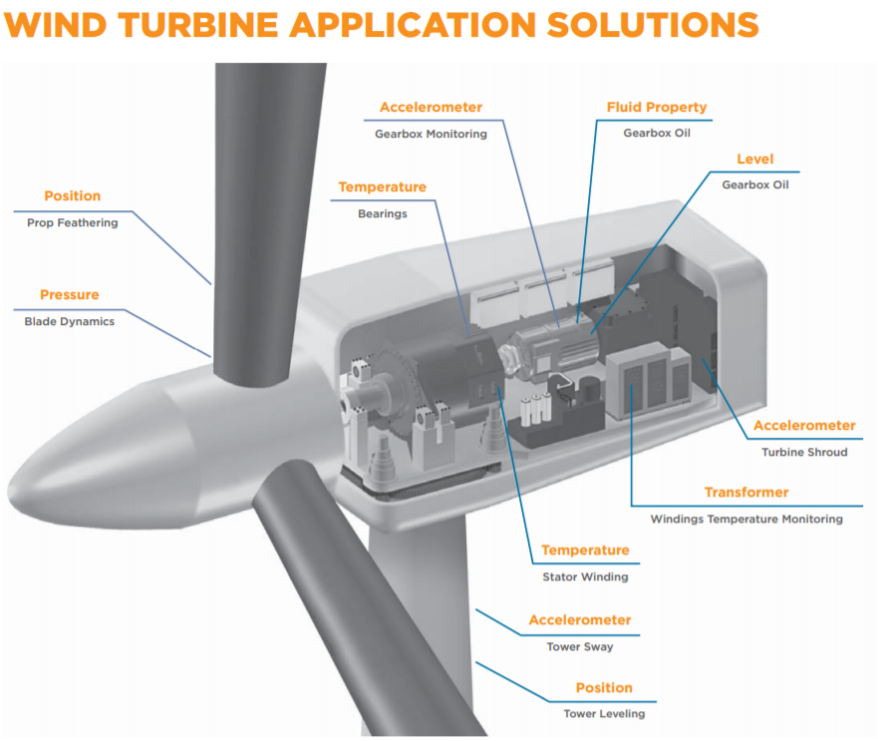

Figure 6.5: A sensor diagram of TE.[4]

Table 6.2: Instrumentation used to perform different measurements.

Location	Type	Amount	Total Cost
Blade	RS PRO Wire Lead Strain Gauge	18	€170
Shaft	RS PRO Wire Lead Strain Gauge	6	€55
Connector	RS PRO Wire Lead Strain Gauge	18	€170
SSS	RS PRO Wire Lead Strain Gauge	9	€80
Blade	ADAFRUIT INDUSTRIES 3-Axis Accelerometer	9	€85
SSS	ADAFRUIT INDUSTRIES 3-Axis Accelerometer	2	€15
ECS	TE Connectivity PT1000 Sensor	3	€10
Brakes	TE Connectivity PT1000 Sensor	3	€10
Generator	TE Connectivity PT1000 Sensor	3	€10
Cooling	TE Connectivity PT1000 Sensor	3	€10
Cables	Non-Invasive Current Sensor	10	€95
Cables	TE Connectivity Measerement Specialties EPM-4001	10	€20
External Measurement Unit	Mumusuki Wind Speed Meter	2	€55
External Measurement Unit	Mumusuki Wind Direction Meter	2	€55
		Total	**€1,000**

6.6. Grid sizing

In this section, the sizing of the electrical grid of the WES is performed. The electrical diagram shows an overview of the electrical system. At the end of this chapter, the total cost and mass estimation are given.

[4]https://www.te.com/content/dam/te-com/documents/sensors/global/TE_SensorSolutions_Wind-Turbines.pdf [cited 14 June 2020].

6.6.1. Step-down Transformer

In Section 4.4 the generator was sized, this generator had an output voltage of 380 V alternating current. The grid voltage in the Netherlands is 230 V [5], this means this 380 V needs to be converted to a lower 230 V level. To do this a step-down transformer will be needed in the electrical circuit of the system.

It is perfectly possible to use an off the shelf step-down transformer for this design. For this design the Siemens 3-phase transformer [6] is chosen and can be seen in Figure 6.6. This transformer has a cost of around €600 and has dimensions of 219x168x168 mm. The transformer will be stored in a box where it is safe from the environment and it also is not easily accessible by people. This box will be placed on the support structure.

Figure 6.6: The Siemens step-down transformer. [7]

6.6.2. Cabling

The WES electrical grid needs to have cabling that transfers the generated power to the building circuit. From Subsubsection 4.3.4.1 it is known that the output of one wind turbine is 11 kW which means the whole system has an output of 33 kW, and as previously said in Subsection 6.6.1 the voltage is 230 V. This means the electrical wires need to be able to withstand a certain level of current [103]. Equation 6.1 calculates the current (I) that flows through the wires, the next thing is to find a wire that can handle that high of a current level. Where P is the power output of the system and V is the voltage level.

$$P = IV \leftrightarrow I = \frac{P}{V} \approx 143A \tag{6.1}$$

For this level of Amps, four kinds of wires were selected, the AWG 1/0, AWG 2/0, AWG 3/0 and AWG 4/0.[8] In Table 6.3 an overview of the maximum Amps level, the resistance, and the cost per meter is given. These values will be used to calculate cost and power losses. The wire will be chosen after these are calculated.

Table 6.3: Considered cables for the grid.

Wires	**Maximum amps level [A]**	**Resistance per meter [$m\Omega$/m]**	**Cost per meter [$/m]**
AWG 1/0	150	0.161	4.76
AWG 2/0	175	0.203	5.25
AWG 3/0	200	0.256	6.56
AWG 4/0	230	0.323	8.20

Before calculating this an estimation of the needed wire length is made. Using Figure 5.6 it can be estimated that a wire length of 25 m is needed for the harvesting system, the other lengths are estimated by sketching them like Figure 6.7, which results in a total length of 250 m. Where 50 m extra will be taken as a safety margin, this is the length that will be used in the cost and power losses calculations.

As all the cables in Table 6.3 are protected with a tough, polyamide, nylon outer covering, the cables can be brought down to ground from the system by adding it to the outside of the building. Thanks to this cover the cables are

[5] https://www.power-plugs-sockets.com/netherlands-holland/ [cited 12 June 2020].
[6] https://www.elektramat.nl/siemens-ag-4ap20428bc400ha0-sie-trans-sitas-ph-3-pn-pn-s6/ [cited 12 June 2020].
[7] https://www.elektramat.nl/siemens-ag-4ap20428bc400ha0-sie-trans-sitas-ph-3-pn-pn-s6/ [cited 12 June 2020].
[8] http://www.aic-controls.com/wire-size [cited 13 June 2020].

also fire-safe in case of short-circuiting. If possible the cables can be brought inside the building but for this more information on the building is needed.

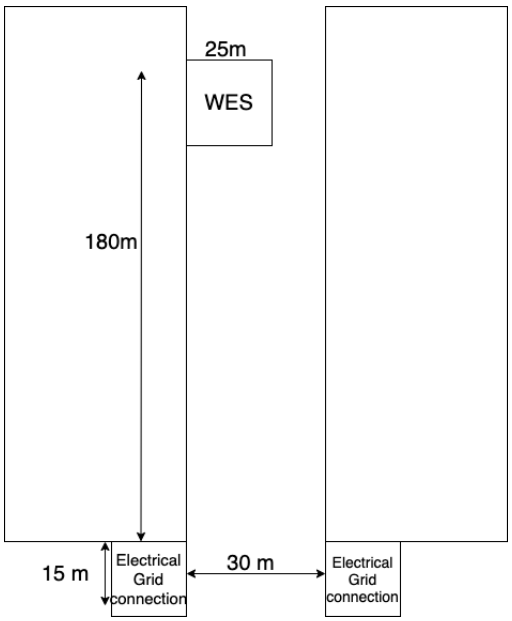

Figure 6.7: Cable length estimation.

The power loss, P_w, is calculated with Equation 6.2. The resistances per meter for the cables can be seen in Table 6.3 these then need to be multiplied by 300 meters to get the resistance of the cable.[9] Using Equation 6.2 the maximum power losses are 1994.8 W, 1581.0 W, 1253.7 W and 994.3 W respectively for AWG 1/0, AWG 2/0, AWG 3/0 and AWG 4/0.

$$P_w = I^2 R \tag{6.2}$$

The 1/0, 2/0, 3/0 and 4/0 wires had a dollar per meter cost of respectively 4.76\$/m, 5.25\$/m, 6.56\$/m and 8.20\$/m.[10] In Figure 6.8a the power losses are plotted in function of the cost, it can be seen that here it is decided to go with the highest cost and thus the AWG 4/0 cable as this is only around €1,000 more expensive but has twice less power loss. The total cost for the cabling will, therefore, be €2,200.

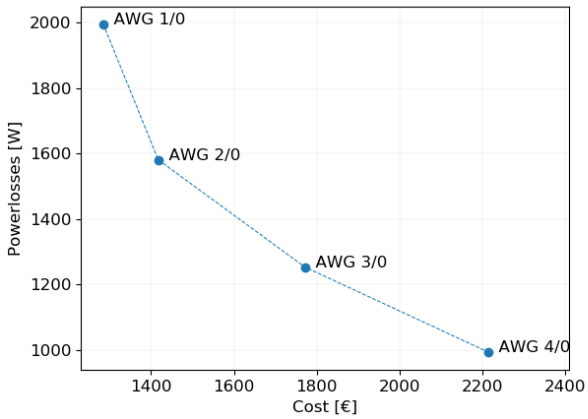

(a) The cost vs the power loss.

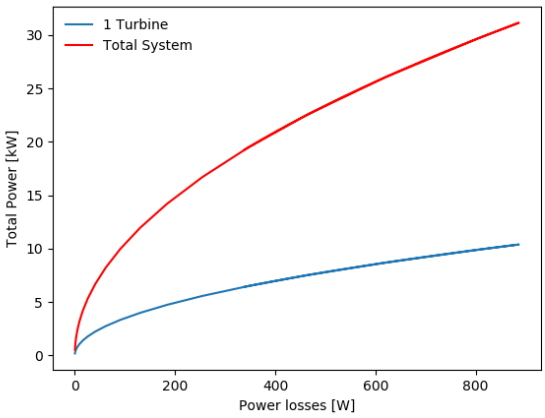

(b) The power output from the system with the respective power losses.

Figure 6.8: Weight estimation of the generator by means of a linear regression.

[9] https://www.daycounter.com/Calculators/AWG.phtml [cited 13 June 2020].
[10] https://www.wireandcableyourway.com/thhn-thwn/ [cited 13 June 2020].

This results in a maximum power output for the system of 30.27 kW at the wind velocity of 12 m/s. The relationship of the power output from the power train, Section 4.4, and the power losses due to cables can be seen in Figure 6.8b. The power loss changes with the power output because for example at lower power, the Amps through the cable will be less, this results in an exponentially lower power loss as can be seen in Equation 6.2. In Figure 6.9 the final power distribution in function of the wind speed can be seen. In this figure, it can also be seen how much the new distribution is changed in comparison with the power distribution after there was accounted for the losses due to the generator in Section 4.4.

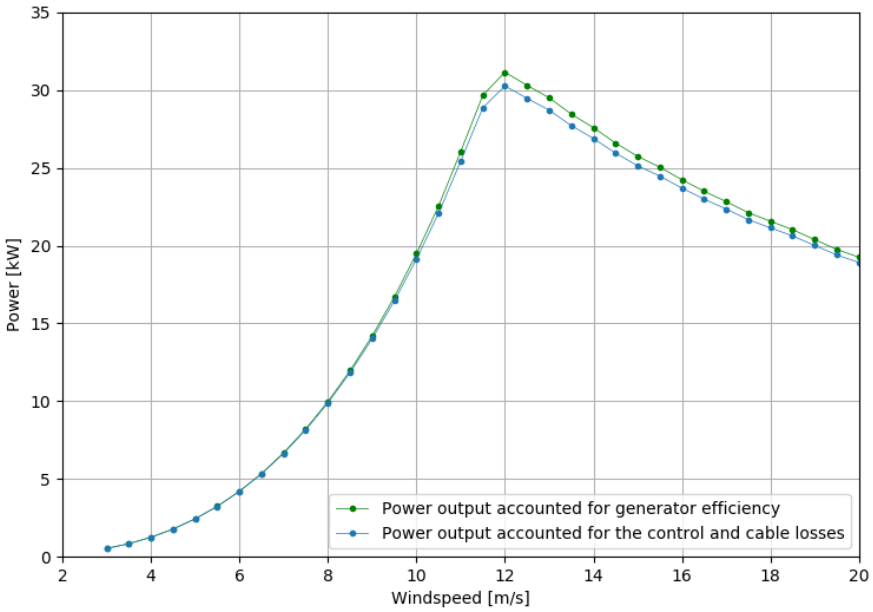

Figure 6.9: Power distribution in function of the wind speed.

6.6.3. Intermittency

Intermittency is something that every kind of renewable energy source needs to deal with. Intermittency is the term that is used to describe that systems like solar panels and wind turbines do not produce energy around the clock. These systems of course only produce energy when it is sunny and there is enough wind. This intermittency introduces the challenge to balance the supply and demand for energy. Intermittency is something that will not be a big problem for this project but it is however something that needs to be addressed.

Intermittent renewables like the WES make it difficult for grid regulators to predict and adjust the day-ahead operating procedures. This is because it is not very easy to predict exactly how much wind is expected in the coming days, meaning that if there is no wind the grid needs to be able to handle the extra demand. Luckily the wind depends on a natural system which can be modeled and predicted with a reasonable accuracy which makes it possible to manage hour to hour predictions.[11] As said before, this intermittency will only form a problem on a bigger scale. In the case of a day with low wind velocities, the electricity company should be able to easily handle the extra demand that is created.

6.6.4. Electrical Overview

In Figure 6.10 an overview of the electrical grid of the building is given. In this overview, the process of how power is delivered to the buildings is shown. The generator gives an alternating current power output, P_t, at a voltage of 380V. This is then converted to 230V by the step-down transformer which is represented by the two red lines. The power is then transferred through the cables which results in a power loss, P_w, due to the cabling and control units. The two buildings are now supplied by a power of P_e from the harvesting system and the main grid, where the main grid supplies the demand that the WES cannot fulfill. The main grid is represented in Figure 6.10 by the pylons.

[11] https://blogs.scientificamerican.com/plugged-in/renewable-energy-intermittency-explained-challenges-solutions-and-opportunities/ [cited 19 June 2020].

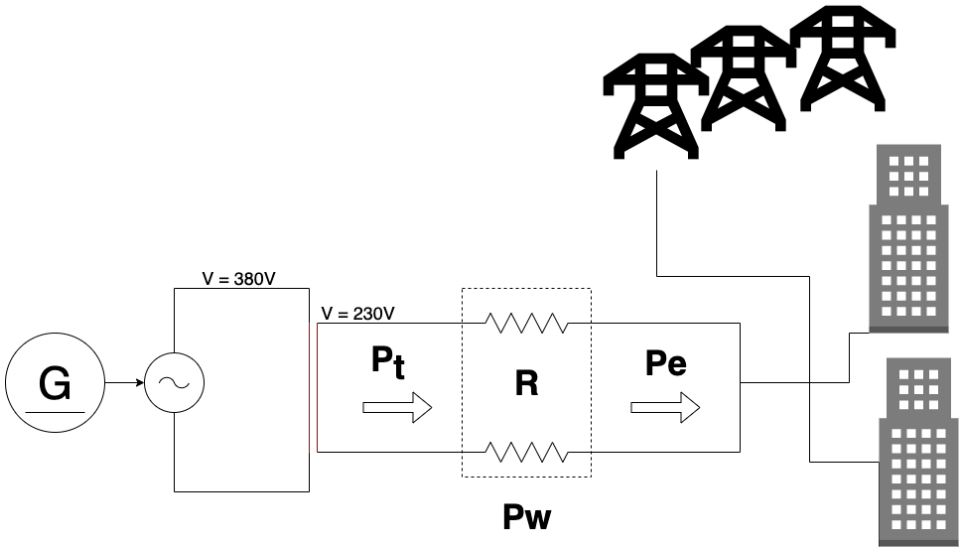

Figure 6.10: Electrical diagram overview.

6.7. Resource and Sustainability Overview

The entire electrical subsystem has now been designed, but not all of the final values have been determined. In this section, those details are explained. First, the mass breakdown of the subsystem, or rather lack thereof, is discussed. This is followed by a cost breakdown of the subsystem. Finally, the sustainability of the subsystem is analyzed.

6.7.1. Mass breakdown of Electrical Control System

Since the sensors of the ECS are negligibly lightweight and because the heavy parts are located in the building, the mass of this subsystem does not need to be considered and will be neglected for the rest of the mass breakdown.

6.7.2. Cost Breakdown

The cost breakdown of a ECS is tabulated in table 6.4. These values are then used in the total cost overview, see Table 8.2.

Table 6.4: Cost breakdown of a ECS.

Part	**Cost**	**Explanation**
Sensors	€1000	All products are prefabricated
Control Unit	€14,000	–"–
Voltage Transformer	€600	–"–
Cabling	€2,200	Determined from cable length
Total	**€17,800**	

6.7.3. Sustainability Analysis of Electrical Control System

A sustainability analysis of this subsystem needs to be performed to make sure the sustainability goals of the project are reached. Because many of the components in this subsystem differ in function and are off the shelf, they will be analyzed one by one. The internal and external measurement units consist of low energy use equipment that can all be purchased in the Netherlands. The CPU is manufactured in Denmark. It is made specifically for wind turbines, and is, therefore, fail-safe and built for long life. The transformer is manufactured in Mexico. It lacks most environmental protection and reliability if not enclosed because of its Ingress Protection IP00 rating [12], Placing the transformer inside a box can mitigate this. Using a step-down transformer to raise the current in the cabling does increase cable losses. The in the cabling energy is lost due to electrical resistance. The choice of a thicker cable mitigates this. The cabling is, however, manufactured in Georgia, USA. The cabling can be fully recycled.

[12] https://www.elektramat.nl/siemens-ag-4ap20428bc400ha0-sie-trans-sitas-ph-3-pn-pn-s6/ [cited 12 June 2020].

7
Final System

During the entire system sizing process explained in Chapter 4, Chapter 5 and Chapter 6 respectively, many design decisions were done. An overview is shown in Figure 7.1. After each subsystem sizing was performed, the whole system layout became more clear. Due to its purpose, location, and appearance, the WES was given the name:

Urbanergy WindVine

The organically looking support structure, resembling a vine growing on the building, structurally connected via tendrils, and the turbines as flowers showing off its beauty and drawing the attention to the WindVine's core technology.

In this chapter, the focus lies on the full system integration of the Urbanergy WindVine. First the performance analysis is presented in Section 7.1, followed by a sensitivity analysis and a validation plan in Section 7.2 and Section 7.3 respectively. Subsequently in Section 7.4 the results of reliability, availability, maintenance, and safety (RAMS) analysis are provided. At the end of this chapter both the final internal and external layout are shown (Section 7.5). This section includes the main system diagrams as well as visual renders of the Urbanergy WindVine.

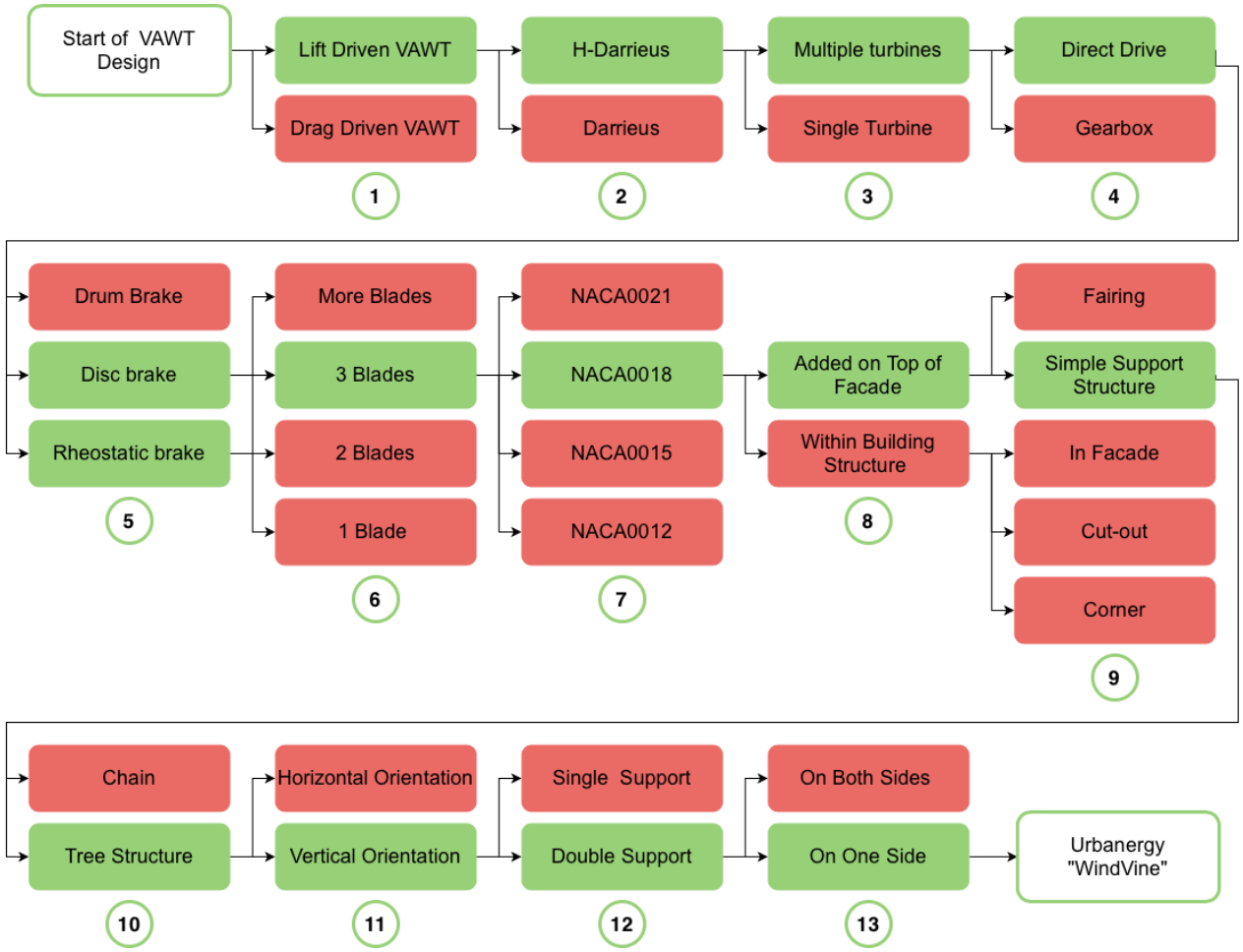

Figure 7.1: Design choices throughout the entire design process with references to the according sections in this report: (1) and (2) Subsection 3.1.4, (3) Section 3.2, (4) Section 4.4, (5) Subsection 4.4.4, (6) Subsubsection 4.3.3.1, (7) Subsubsection 4.3.3.3, (8), (9) and (10) Section 5.3, (11) and (12) Section 5.4, (13) Section 5.3

7.1. Performance Analysis

In Subsubsection 4.3.4.1 the power distribution as a function of the wind speed was given for the first time. An update of this distribution was given in Section 4.4 and Subsection 6.6.2, in the first distribution losses due to the generator were not accounted for yet. Where in Subsection 6.6.2 the final power distribution was given after accounting for the power losses due to the cabling. The final power distribution can be seen in Figure 7.2. This graph is the one that was produced after accounting for the power losses in the cables.

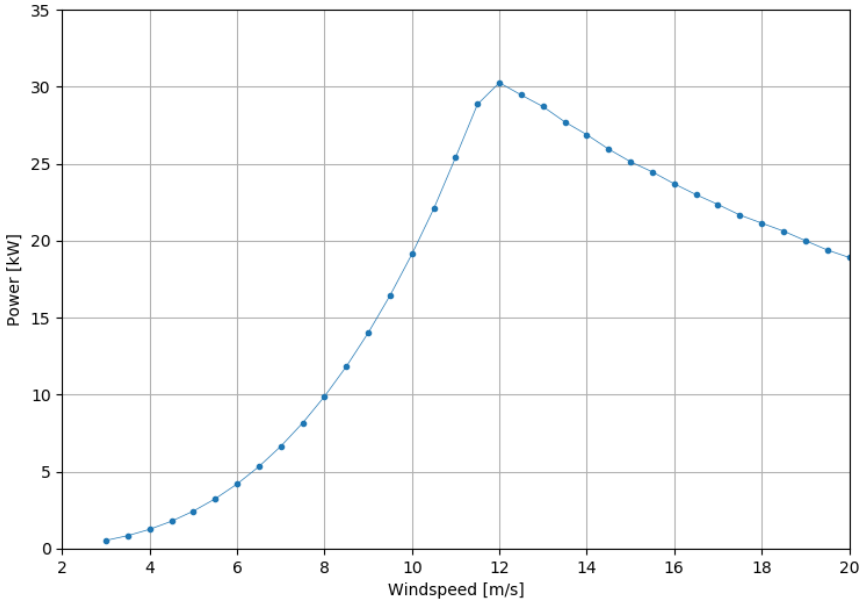

Figure 7.2: The power distribution of the WES.

In Table 7.1 the yearly energy production of the WES is given. This shows that the first estimation that was made from the QBlade data was multiplied with 0.8. The reason for this is that a margin of 10% was taken because the strut could not be modeled well and the other 10 % was taken as a contingency. This was all explained further in Subsubsection 4.3.4.1. The generator had an efficiency of 95 % which is explained in Section 4.4. Lastly the losses due to the cables and the control unit needed to be accounted for which resulted in a final value for the amount of energy harvested every year, 51.96 MWh. This value is calculated using a weighted average of the energy produced for the wind speed distribution as explained in Subsection 2.4.3. This is also in compliance with user requirement WES-A02: "The system shall provide 50 MWh at a rated velocity of 10 m/s with free-stream turbulence of 50% distributed with Gaussian law."

Table 7.1: This shows the energy that is harvested per year, based on a weighted average over the expected wind speeds.

	One turbine	**Total system**
Energy after QBlade analysis [MWh]	23.38	70.15
Energy after margin factor [MWh]	18.71	56.12
Energy after generator losses [MWh]	17.77	53.32
Energy after cable losses [MWh]	17.39	52.18
Energy after the control system losses [MWh]	17.32	**51.96**

7.2. Sensitivity analysis

In this section, the effect of input parameter changes on the behavior of the system is evaluated. This is done to identify critical parameters that the design is sensitive to. By changing the critical parameters it can be checked how robust the design solution is and if the driving requirements are still met. Furthermore, the flexibility of the system in less-than-ideal conditions is checked by changing the parameters.

7.2.1. Changing Average Wind Speeds

The first parameter to be varied was the average wind speed. The average wind speed has been assessed as a normally distributed curve around 10 m/s with a $\sigma = 2.5$ standard deviation. A shift in the average wind speed to 12 m/s and 8 m/s was evaluated. The generated power and emitted noise for these different wind speeds are given in Table 7.2.

Table 7.2: Power and noise output for different average wind speeds.

Output \ Wind speed	8 m/s	10 m/s	12 m/s
Power Output [MWh]	33.15	51.96	66.14
OASPL [dB(A)]	51.1	53.9	55.6
L_{den} [dB(A)]	52.6	55.3	57.0
L_{night} [dB(A)]	46.2	48.9	50.6

The change in average wind speed to 8 m/s roughly accounts for the change in wind speed if the WindVine is not placed between two buildings, but simply on the side of any building [9]. The change to 12 m/s corresponds to an increase in installation height of about 100 m as can be seen in Subsection 2.4.1. These different wind speeds can off course also be experienced if the system would be integrated at other locations in the world, with different wind conditions. As can be seen from Table 7.2, the system is very sensitive to a change in average wind speed. This is of course logical since it was designed for an average speed of 10 m/s. The system is analyzed and able to operate at speeds around the average of 10 m/s as was also analyzed in Section 4.3, since the wind speed was assumed to be normally distributed around the average speed. However, an increase of 2 m/s on the average is quite a big deviation. Logically, a wind energy harvesting system produces the required amount of power only at the rated wind velocity. From the noise results, it is clear that the noise requirements are not met for any of the wind speeds. This means that even when the average wind velocity changes, still additional noise reduction methods are required as described in Subsection 4.5.8.

All structural considerations are based on the worst-case scenario wind situation (55 m/s). This would not change if the average wind speed changes. A stronger maximum wind would increase the weight of the wind harvesting system, but the effects of this are discussed in the next section.

7.2.2. Changing the Weight of the Wind Harvest System

If a sudden structural change is needed to compensate for some unforeseen load on the turbine, its weight may be changed. In this section the weight of each turbine is increased to account for sudden sizing changes and whether the structural support system would respond appropriately to this.

As explained in Chapter 5, truss structures are used to sustain the weight of the support structure. Increasing the weight would not lead to a failure of the support structure as the compression loads would be distributed over the structure into the building. With the same calculations as in Chapter 5, it was found that increasing the weight of the turbines by a factor 6 would result in an increase in maximum stress of 7%: from 104 MPa to 112 MPa. However, it should be noted that even though the support structure would be able to withstand the loads, the building and the attachment points may not. Therefore, an analysis of the capability of the building to sustain increased weights should be done at a later stage.

7.3. Validation Process in Further Development Phase

In the previous chapters, the design process to get to the final design was described. Verification methods were used to ensure that the results presented are achievable and correlate with existing data. However, to make sure the system fulfills all the technical and safety requirements a validation process needs to be performed in further development phases. The three main subsystems that need to be validated and certified will be briefly described below.

Wind harvest system: For the wind harvest system, two main things will need to be analyzed. On the one hand the aerodynamics and on the other hand the structures. For the aerodynamics, the turbine will have to be tested

for the flow conditions it was designed for. A wind tunnel test will need to be done in order to determine the flow over the blades and the resulting performance of the turbine. From these tests, modifications to the design may need to be done. An example would be that the tip-losses are too important, therefore wing-lets might need to be added. In addition, the loss due to the supporting arms should be investigated. A loss of 10% was assumed for this study for airfoil-shaped support arms. However, this loss might be more significant due to the induced drag and flow separation near the connection point. In this study more complex phenomena such as dynamic stall and turbulent behavior of the blades in the wake of the upstream blades [104] have not been investigated. An in-depth analysis followed by test measurement should be performed to understand the flow behavior of the turbine. Not only should the performance of the turbine be analyzed in a wind tunnel, but a more realistic test with turbulent wind should also be performed since this can largely influence the performance of a wind turbine. Furthermore, the noise produced by the turbines will have to be tested in order to validate the results provided above. It should be noted that in this study only the airfoil self-noise has been modeled for. Other types of aerodynamically induced noise discussed in Section 4.5 will have to be tested for. Furthermore, the interaction of the noise coming from the three different turbines has to be researched.

For the structural validation of the turbine the varying loads should be investigated. As VAWTs are prone to fatigue loads [23] due to the large variation in normal forces, the stresses along the blades should be analyzed in detail. Furthermore, the turbine should be tested such as to validate its survival speed. As the turbine will be integrated between two high-rise buildings, failure due to strong winds should be looked into and validated in order to get a certified system.

Support structure: In this study, a preliminary investigation on the flow in-between two buildings has been performed. However, this is one of the most crucial points to make the design profitable as less favorable wind conditions will result in a significant decrease in annual energy production. Therefore, in-depth analysis and test measurement for the local wind conditions around a given shaped building should be done in order to certify the acceptable wind conditions.

For the support structure itself, a validation procedure for the attachment points should be done. It should be verified that the building is in fact capable of supporting an added structure that will be subjected to varying loads. In addition, using more accurate engineering models external loads, aeroelasticity, and failure modes should be investigated to certify the system.

Electrical system: In order to connect the turbine to the electrical grid, several technical and safety requirements need to be met.[1] Therefore, test such as power quality test, control performance test, low-voltage ride through test, voltage/frequency response test and anti-islanding protection tests should be performed such as discussed in [105].

7.4. RAMS and Risks

Reliability is closely linked to availability, cost, and revenue. First early failures due to infant mortality, then random failures and later failures due to wear and tear [106] will occur.[2] This can be seen in Figure 7.3. However, there is no standardized definition of failure. In the following the reliability is elaborated and the resulting expected availability discussed in Subsection 7.4.1 and Subsection 7.4.2 respectively. Maintenance and its accompanied requirements on the subject are explained in Subsection 7.4.3. In Subsection 7.4.4 the safety is addressed and the technical risks and their mitigation in Subsection 7.4.5.

[1] https://www.energy.gov/energysaver/grid-connected-renewable-energy-systems [cited 18 June 2020].
[2] https://www.weibull.com/hotwire/issue21/hottopics21.htm [cited 22 June 2020].

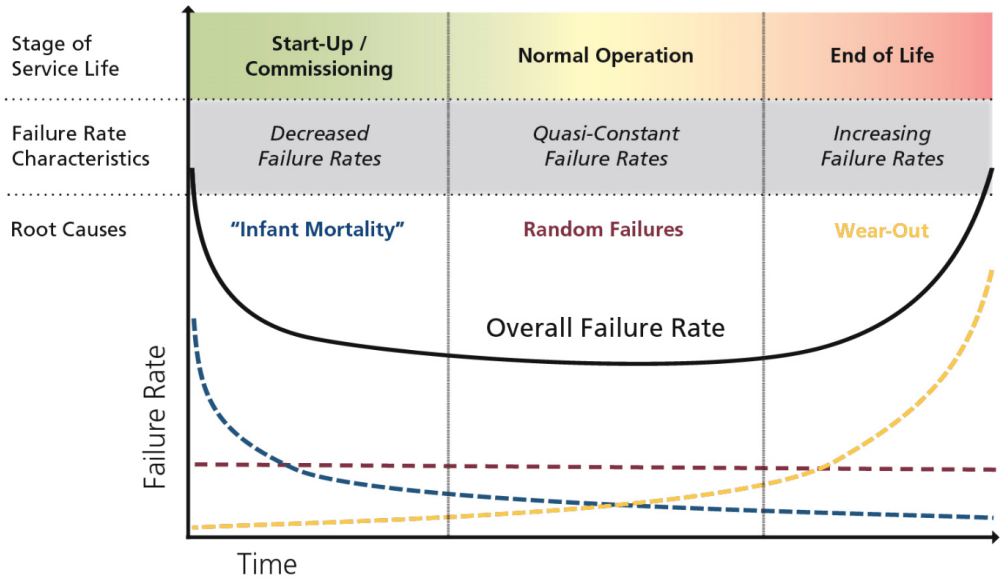

Figure 7.3: Bathtub curve for failure over lifetime.[3]

7.4.1. Reliability

Failure rates of onshore wind turbines are investigated intensively, and the reliability that comes along with that. A recent analysis (Ozturk,2019) [107] provides statistical insights into turbine reliability based on the German database WMEP (Wissenschaftliches Mess- und Evaluierungsprogramm). According to different classification (power rating, environment condition), the data was presented. To obtain an indication for the reliability and downtime of the Urbanergy WindVine average historic data from 1989-2006 was assumed. Unfortunately, no useful data could be obtained for more recent years. Furthermore, the provided data originates from horizontal axis wind turbines, which means the values should be assessed with care. The results are shown in Figure 7.4 indicating the annual failure rate and average downtime for different parts of a wind turbine. These values are as mentioned average values and therefore related closer to the main operation phase as described in Figure 7.3. The gearbox, yaw, and hub systems were omitted as they do not apply to the vertical WindVine turbine which is direct-driven, as shown in Section 4.4. This design decision results in higher reliability, as a gearbox is the most vulnerable component in most turbines [107, 108].

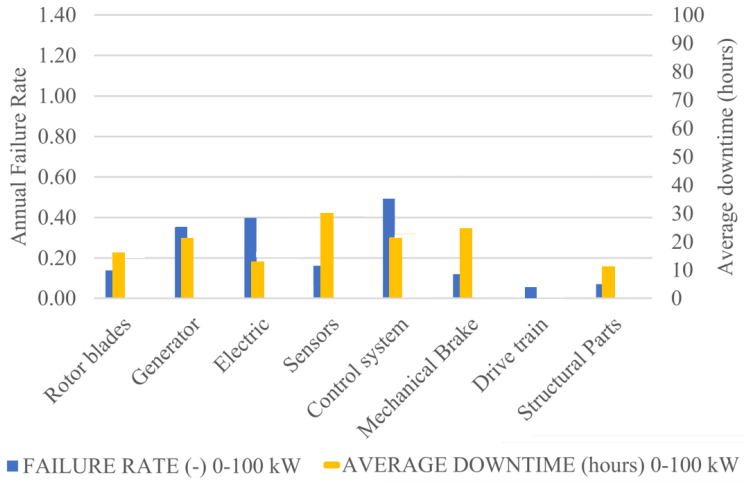

Figure 7.4: Annual failure rate and average system down times of 112 turbines (<100 kW) documented in the WMEP database (2006)[107].

[3]https://www.osihardware.com/quantifying-bathtub-curve/ [cited 22 June 2020].

As can be seen from Figure 7.4 the electrical and control system is the most vulnerable system including the electronic control unit, relays, switches, converters, cables, and connections. To reduce the downtime, most of these components are placed inside the building for a better environment and faster access. Lower capacity turbines have in general higher reliability which is an advantage for the three turbine configuration of the Urbanergy WindVine [107]. Furthermore, according to Hahn [106] the failure rate of wind turbines below 500 kW is not expected to rise before 15 years of operational life-time and stay more or less constant. The causes of failure for different parts were very diverse and the main issues are summarized in Table 7.3. Here also the respective failure effects and quantified values for the failure rates and downtimes are given.

Table 7.3: Failure locations and respective failure causes and effects for different turbine parts as documented in the WMEP database (2006)[107] and an indication if the part is associated with a WindVine turbine (T) or the entire Urbanergy system (S).

	Failure Location	Failure Cause	Failure Effect	Failure Rate	Downtime [h]
S	Structures	High wind	Overspeed	0.07	10.6
T	Drive Train	Icing	Vibration	0.05	0.00
T	Mechanical Brake	Lightning	Noise	0.12	24.5
T	Control System	-	-	0.49	20.7
S	Sensor	Other causes	Other consequences	0.16	29.5
S	Electrical System	-	-	0.39	12.4
T	Generator	Component wear or failure	Causing follow-up damage	0.35	23.1
T	Rotor Blade	Grid failure	Overload	0.13	15.8
Total per turbine				**1.14**	**84.1**
Total for system w/o turbine				**0.62**	**52.5**

7.4.2. Availability

The system availability depends heavily on the reliability of the system (time-to-failure or failure rate) and the maintainability effort (time-to-repair or downtime)[107, 109]. As described in Subsection 7.4.1, the failure rates and associated downtimes were shown in Figure 7.4. Summing up the failure rates per WindVine turbine resulted in a total failure rate of $FR = 1.14$ and an associated downtime of $DT = 84.1h$. As the structure, system sensors, and the electrical system can be considered independently of a WindVine turbine, the failure rate and downtime for those components are $FR = 0.62$ and $DT = 52.5h$ respectively. In case these parts fail, it is assumed, that the entire system is down, while in the other case, only the power output is reduced of that specific WindVine. The Urbanergy system consists of three WindVine turbines, which has a positive effect on the availability, as the probability of a full system failure gets reduced. However, the risk of one turbine failure is multiplied by the numbers of turbines. As was explained in Section 2.4, only a fraction of the total year is suitable for operation at full capacity. Therefore, to increase the availability, all check-ups and maintenance should be scheduled as much as possible based on the weather forecast and long time prediction.

7.4.3. Maintainability

Maintainability is necessary for the system to remain operational in the required 10 years of harvesting. Different methods and variations exist that can be applied to the WHS. In this subsection, multiple studies are discussed that elaborate on maintaining wind turbines, either on- or offshore.

Maintenance can be subdivided into preventive and corrective maintenance, where preventive is later divided into the condition and scheduled [107]. All should be considered while the WHS system is operational. Corrective maintenance is by rule always too late - something broke and should now be repaired. Especially since the requirements hold that all components should be produced locally, corrective maintenance would ramp up cost while the system is not operational (see Subsection 7.4.1). Corrective maintenance is covered in the contingency plan. To stay ahead of corrective maintenance, preventive maintenance is introduced. Scheduled maintenance can be a regular check-up or replacement of a degrading part in the system. Degrading parts in the system are found by monitoring the turbine condition, where the Internal Measurement Unit measures critical parameters. Measuring the current status of the system is further explained in Section 6.5. In the first five years of operation, no scheduled maintenance is allowed. Therefore, all sensors are heavily monitored, to still prevent failure before happening. Figure 7.5 visualizes all different options for maintenance and how they relate to each other.

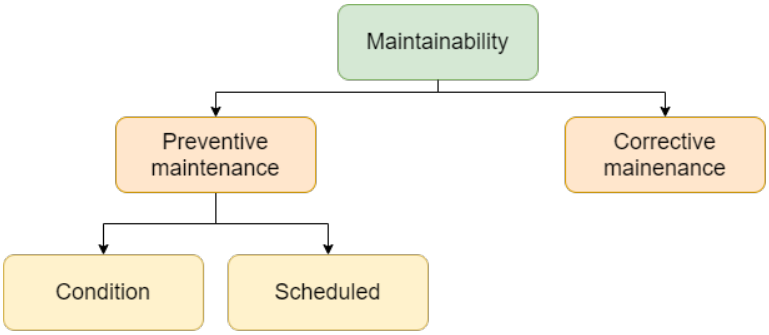

Figure 7.5: All maintenance options subdivided

7.4.3.1. Accessibility

The WES is a system integrated into a building. Part of the system lays outside of the building, namely the turbine, the generator, the external measurement unit, and of cause the support structure. However, there is also a part that is installed inside the building. The user interface, energy converter, and main system controller for example. The system components that are inside are easily accessible, but for the component outside this is more difficult.

The support structure was designed with an accessibility concept in mind. Although all the turbines are spaced apart from each other, the tree structure contains branches above each turbine. At the bottom of these branches, there will be a slide system to which an inspection cradle can be connected. This is a common way to maintain, inspect, and clean high-rises. Most buildings are already equipped with systems like that and could be used. Whether there will be additional doors integrated at closer locations to the WES should be investigated.

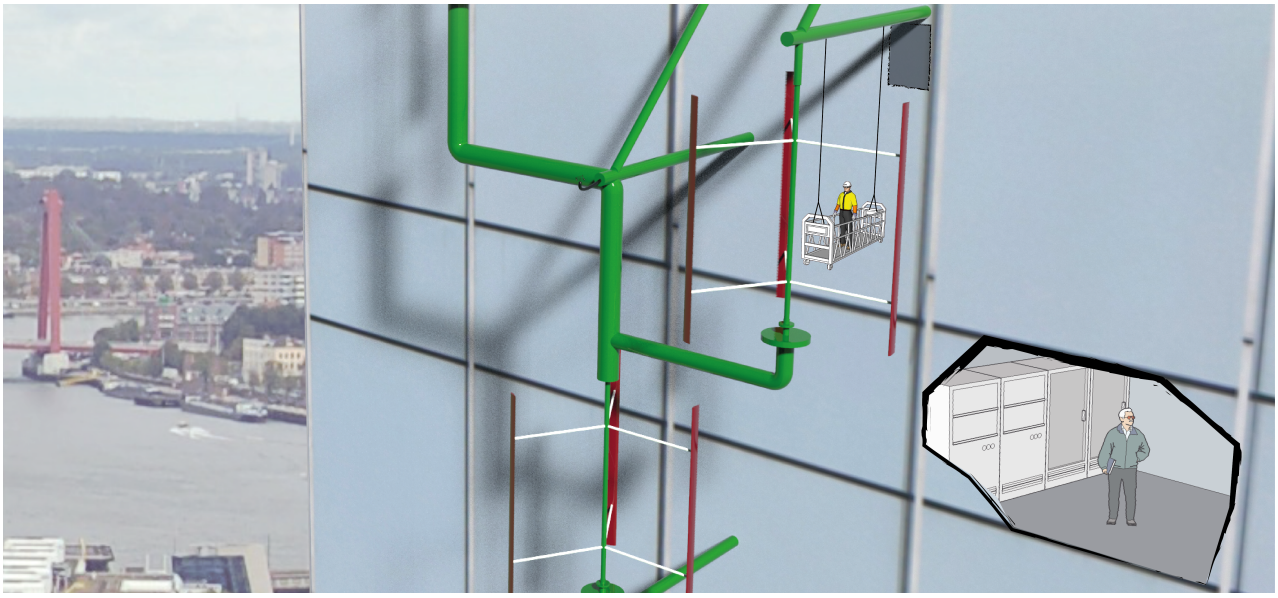

Figure 7.6: Visual representation of possible maintenance method

7.4.4. Safety

Safety is one of the main requirements since the high-rise buildings will be populated during the complete operational time of the harvesting system. Besides being harmful to residents of the building, the operation is not supposed to harm the environment or other facilities nearby either. The build-in safety measures for this are reviewed.

Structural safety is of great importance and assured by implying a safety factor. The safety factor of 2 is used for the structural integration, besides the safety factor of 1.5 for the structural analysis for the turbine. The choice of both is well argued in their respective sections. Also, the design of the structure enhances safety, as the system is attached at different locations adding reliability. Two connections to the blades and a possible internal safety cable reduce the

risk of blades flying off in case of external impact or structural failures due to cyclic loading (fatigue). Especially for VAWTs, the blades experience cyclic varying loads due to continuous changing angles of attack throughout a revolution. Fatigue failures are therefore one of the most critical ones.

A fail-safe braking system is in place for emergency stops when a failure occurs in one of the turbines components. Braking can be conducted by the generator and the mechanical brakes as seen in Subsection 4.4.4. Also, a lock system was integrated to keep the turbine in a safe fixed position.

7.4.5. Risk Assessment

Risks are an ongoing conversation, and risks can be added or changed during a design and production process. This section will handle the technical risks that can be encountered from this report until the system is taken down after ten years of operation. It should be mentioned that most of the risks are already mentioned in earlier reports [2, 3]. Subsubsection 7.4.5.1 will state all risks regarding the system and in Subsubsection 7.4.5.2 the respective mitigation and risk map are discussed.

7.4.5.1. Risks

The risks that have been added are given a different identification. The table is now split up in risks regarding structure, safety, budget, operational risks, measurement unit, production, aerodynamics, turbine, and others. Risks regarding support are given the acronym SUP, MES is for measurement unit, HAR is linked to harvesting, PROD is for production and TUR is the last acronym affiliated to risks for the turbine section of the system. The complete list with all risks is shown in Table 7.6

To define the *Impact* and *Probability* of the risks to the project, a scale is in use. The scale and the meaning are defined in Table 7.4 and Table 7.5 [3].

Table 7.4: Scale for *Impact*.

1	Negligible
2	Moderate
3	Significant
4	Severe
5	Catastrophic

Table 7.5: Scale for *Probability*.

1	Very small
2	Small
3	Neutral
4	Large
5	Very large

Table 7.6: Technical risks of complete System.

# ID	Risk	*P*	Impact
STRUCTURE			
1.1-01	Structure of WES is not able to support Wind Harvesting System	3	4
2.2-01	Connection and integration of the SSS to building not feasible	2	5
3.3-01	Natural resonance occurs in system	3	5
SUP-01	Material fail at the joints of supporting structure	2	4
SUP-02	Performance of material is lower than expected	2	5
SUP-03	Stresses are modelled incorrectly	3	4
SAFETY			
2.5-01	Safety system fails	3	5
3.1-03	During operational time, cabling fails and systems fall to the ground	2	5
BUDGET			
1.2-02	Technologies are too expensive	3	4
FC-BU-01	The chosen configuration is not possible within the budget	5	5
FC-BU-03	The interest rates are not dropping as expected and the system never becomes profitable	4	3
OPERATIONAL			
3.1-01	Operating systems do not start up	3	4
3.1-02	Extreme environmental conditions prevent the system from working	3	4
3.2-01	Control systems are not adjusting properly	3	4
3.4-02	Energy is not provided to the grid	2	5

3.5-01	Harvesting system is not shutting down during failure/emergency	2	5
FC-HW-01	Failing of turbine blades destroys WES	3	4
FC-HW-02	Failing of turbine blades destroys high-rise buildings	3	4
MEASURE UNIT			
4.1-01	Documentation of experiences get lost	2	2
MES-01	Sensor stops working or faulty results are produced	2	4
PRODUCTION			
1.5-01	Material shortage	2	4
4.4-01	Components intended for upcycling or reusing are not usable anymore	2	3
PROD-01	Components that were intended to be bought recycled are unavailable	2	3
AERODYNAMIC			
HAR-01	Noise produced is above regulations	5	4
HAR-02	Estimated noise production is below actual noise produced	5	4
HAR-03	Noise of the different turbines interfere and cause amplification of the noise	3	4
HAR-04	Power produced is lower than expected	4	3
HAR-05	Wind speeds are lower during a year, causing less energy produced	3	3
HAR-06	More power produced than the rated power output	3	2
TURBINE			
TUR-01	Breaks overheat structure, deform and damage of other system components	3	5
TUR-02	Brake subject to high wear	4	4
TUR-03	Brake system failure	2	5
TUR-04	Shaft is not able to withstand the applied braking torque	1	5
TUR-05	The two connectors per wing deflect at a different rate and cause unexpected stresses	2	4
TUR-06	Overheating of generator	2	4
TUR-07	Failing of turbine injures people	2	5
OTHERS			
1.1-02	Location is unfeasible	2	3
1.2-01	Technological Readiness Level of concepts is too low	4	3
1.2-03	System is too complicated to develop	4	5
1.3-01	Testing facilities are not available	3	1
2.1-01	Installing the system / subsystem takes longer than predicted	3	3
2.1-02	Permissions are not granted	2	4
2.4-01	Efficiency of conversion of energy is lower than expected	4	5

7.4.5.2. Mitigation

For each risk in Table 7.6 exists a mitigation process that states the measures in place for reducing the probability and impact of the risk. Each mitigation is stated below and is structured in the same manner as found in Table 7.6.

STRUCTURE

1.1-01: Set realistic requirements which the building can fulfill and analyse the loads at the connection points, so these don't fail

2.2-01: Perform 3D-designs, load modelling and do quality checks

3.3-01: Model the natural frequency of the whole system before building

SUP-01: All joints are welded together by contracted professionals. Their track record is good, and these manufacturers can be trusted

SUP-02: Comply with regulations, as regulations are in place to reduce this risk. In the case of deflection, regulations of UP 1604.3 Serviceability are complied with, which states that aluminum structural members shall not exceed //60 and floor members shall not exceed //360. [4] IEC 1400-1 requires a total safety factor of 1.485 in the case of ultimate strength analysis and 1.265 for fatigue analysis

[4] https://up.codes/s/serviceability [cited 19 June 2020].

SUP-03: Stress testing of components should be done

SAFETY

2.5-01: Validation, verification and quality checks should assure steady operation

3.1-03: Verification, validation and safety measures are done to prevent

BUDGET

1.2-02: Continuously check budget requirements

FC-BU-01: Propose a new budget or check whether another configuration can still be chosen that fulfills all other requirements

FC-BU-03: Thorough research into the economic market to predict the future better

OPERATIONAL

3.1-01: Mechanics are in place in case of problems

3.1-02: Thorough analysis should be performed on the location and its conditions all year round

3.2-01: Verification, validation and testing should reduce risk

3.4-02: Check connections and control software

3.5-01: Verification, validation and testing should reduce probability of risk

FC-HW-01: Create fail safe environment for blades, so that it can not harm the system further

FC-HW-02: Create fail safe environment for blades, so that it can not harm the buildings

MEASURE UNIT

4.1-01: Create back-ups regularly, which will lead to better technological improvement for next products

MES-01: The control unit and the sensor network are designed in such a way that faulty results can be measured and after losing a sensor other sensors are able to cover the absence of this data. In practice patterns can be detected between sensors, for example, a relation between the acceleration of the blade and the pressure is expected. The acceleration on its part is expected to depend on the wind speed and wind direction. And if there is a change in the measured power and energy output, while the acceleration data seems correct, that would indicate that there is a loss in the turbine, which should be measured by either the current or the temperature sensors

PRODUCTION

1.5-01: Use local, recyclable and non-scarce materials

4.4-01: Design with durability in mind and perform regular maintenance

PROD-01: Start early with finding all the material that is needed for the components. Moreover, availability should considered in the material trade-off

AERODYNAMIC

HAR-01: Several noise reduction methods are looked into and possibilities for further research have been given

HAR-02: Most dominant noise is estimated and due to the definition of decibels, other less important noise sources won't change the estimation much. More research has to be performed on noise later in the design stage, and also the possibilities of adding an aeroacoustic fearing needs to be looked into in the further design phases

HAR-03: This effect could also be used to actually dampen the noise of the turbine with one another. The exact working of this should be looked into in the following design phases

HAR-04: A safety factor is applied and the model is verified

HAR-05: The wind cannot be influenced and therefore this cannot be mitigated. However, the system only partially provides the energy needed for the buildings, so more energy can always be extracted from the grid when the system is producing less

HAR-06: Due to the fact that the system only provides part of the power consumption of the buildings, this will not be a problem and all the energy will be able to be used. In extreme cases (for example when the power consumption is extremely low) energy could be sold back to the grid, however, this is in the current design not expected to occur

TURBINE

TUR-01: Make efficient use of brake systems: brake not for too long times and start braking at the right moment, not too late. More can be found in Subsection 4.4.4

TUR-02: Analyze braking cycles and investigate wear, to design the brake system accordingly. Establish regular maintenance and replacement plans. Size WHS for the correct environmental condition to limit the brake usage

TUR-03: Have a redundant brake system and implement a fail-safe brake system

TUR-04: Strain gauges are applied on the rod and if the maximum value is reached, the brakes need to be stopped

TUR-05: Placement is accurately performed and during testing, the placement of the rods to the wing is verified

TUR-06: Let generator operate with safety margins. Furthermore, a temperature gauge is applied to the generator per turbine

TUR-07: Structural analysis of the turbine considers the failure stresses while calculating for the dimensions of the cross-section

OTHERS

1.1-02: The airflow conditions are investigated at the location based on public data. The airflow is modeled with assumptions that maintain the accuracy necessary to get the desired results. These assumptions are compared to earlier stated requirements and changes in the requirements are made when this was deemed necessary. Another solution might be to come up with another possible location

1.2-01: Use existing components

1.2-03: Break system down into smaller parts, such as the turbine, which is split up into three different components

1.3-01: Contract testing facility early on in the design process

2.1-01: Include a safety factor in the time management for construction

2.1-02: Receive confirmation of the needed permissions long before building. In addition, lawyers can be contracted regarding legal issues, such as contracts

2.4-01: Validation and test should foresee this before implementation

Table 7.8 represents all risks with their respective probability and impact on a risk map. After mitigation methods have been applied to all risks, probability and/or risks are reduced. This is again visualized, as seen in Table 7.9. The colored cells in Table 7.8 show severe risks and are especially in need of mitigation. A few risks are still severe to the project after mitigation and are identified as key risks. These risks should be monitored closely by the risk manager.

Table 7.8: Risk map overview

Probability \ Impact	1	2	3	4	5
1					TUR-04
2		4.1-01	1.1-02, 4.4-01, FC-BU-03	1.5-01, 2.1-02, 3.6-01, SUP-01, MES-01, TUR-05, TUR-06, PROD-01	2.2-01, 3.1-03 3.3-01, 3.4-02, 3.5-01, SUP-02, TUR-03, TUR-07
3	1.3-01	HAR-06	2.1-01, HAR-05	1.1-01, 1.2-02, 3.1-01, 3.1-02, 3.2-01, 3.4-01 FC-HW-01, FC-HW-02, SUP-03, HAR-03	2.5-01, 3.3-01, TUR-01
4			1.2-01, HAR-04, FC-BU-03	TUR-02	1.2-03, 2.4-01
5				HAR-01, HAR-02	FC-BU-01

Table 7.9: Risk map overview after mitigation

Probability \ Impact	1	2	3	4	5
1		1.1-02, 4.1-01, 4.4-01, FC-BU-03	2.1-02, 3.6-01, SUP-01, TUR-06	2.2-01, TUR-04, TUR-05	3.1-03, 3.4-02, 3.5-01, SUP-02, TUR-03, TUR-07
2	1.3-01	1.5-01, 3.1-02, 3.2-01, 3.4-01, HAR-06	HAR-05	1.1-01, 1.2-02, 2.1-01, 3.1-01, SUP-03, MES-01, HAR-03, PROD-01	2.5-01, FC-BU-01, TUR-01
3	FC-HW-01, FC-HW-02	1.2-01, FC-BU-03	HAR-01, HAR-04, TUR-02	1.2-03, HAR-02	2.4-01
4					
5					

7.5. Final Design Summary

In this section, the final design is summarized and shown. Firstly the three main subsystems are discussed in Subsection 7.5.1 to 7.5.3. Then in Subsection 7.5.4 the system block diagrams describing the different components and relations between the subsystems are given. Finally, in Subsection 7.5.5 a summarizing table with all the important specifications of the system is given.

7.5.1. Wind Harvesting System

With the VAWT as the chosen system, the main subsystems and parts needed to be designed and analyzed. The system consists of multiple parts: the blades, the struts, the main shaft and the generator. All these parts had to comply to the user requirements described in Table 2.1. Subsequently, sub-requirements were created to be able to start the detailed design. As a starting point the amount of turbines and turbine blades needed to be chosen. From a trade-off process it was decided to have three turbines. Each turbine would have three blades as this would result in smaller fluctuations in torque and force. Furthermore, the most frequently used NACA-series airfoils in wind turbines were considered for this system. Although having a not that much smaller C_p than the NACA0015, the NACA0018 has a higher thickness leading to better structural performance. By performing an aerodynamic optimization process, the optimal turbine design for the given wind conditions was found. With a rated power of 11 kW at 12 m/s the turbines should be able to meet the energy requirement of 50 MWh.

The noise research, in parallel to the design of the turbine, led to having an averaged noise of 56.9 dB(A) which exceeds the noise requirement with 11.4dB(A). To meet the noise requirements, some reduction methods were researched. The only feasible method at this phase of the design was the use of serrations. However, even by using this design improvement, the noise still did not comply to the requirements. The design of the blade with serrations can be seen in Figure C.1.
PMSG, a direct drive gearless generator, is chosen to be the best suited for this application due to its high power density, high performance and low maintenance cost. It does have a higher manufacturing cost, but its recyclable nature makes up for this. There are a multitude of different designs that could be chosen, however it was decided to size and design the generator in-house, using available data from off the shelves generators.
Following this, the poor self-starting performance of the turbine causes a lower power output than expected. This can be mitigated by using the generator as a motor. Electricity from the power grid is then used to start up the turbines.

To support the blades of the turbine, connecting rods were designed and analyzed. By means of an iterative process which computes the bending and shear loads, a rod was found with the dimensions displayed in Figure C.2. This process was repeated to determine the shaft connecting the connectors to the generator. This analysis had to take into account that rod would have to be mounted on the cylindrical part of the shaft. The dimensions found are shown below Figure C.2.

By connecting each blade to two rods and connecting the generator to the low part of the shaft, a full system can be presented as shown in Figure 7.7.

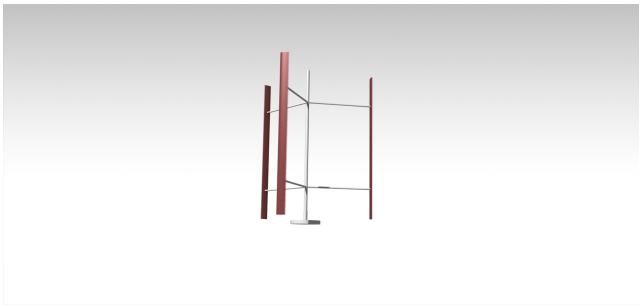

Figure 7.7: Wind energy system assembly.

7.5.2. Structural Support System

The system was required to be built and attached in between two buildings according to WES-A22. The building itself had to be free from vibrations. In addition, it was required for the non structural components to be recyclable and lightweight.

First, it was determined after an aerodynamic analysis that the building boundary layer would be 4 m wide. Thus the system was designed to be outside this limit. As an aesthetically pleasing design was a driving goal for the system, a organic kind of structure was chosen. To be specific, a tree and/or vine-like structure would be most pleasing at the side of, or in between two buildings. Two options were researched and analyzed. The first having the WHS standing on the structure, while the second option would have the VAWT suspended in between two structures. The latter was chosen due to the optimal characteristics and the better analysis possibilities in this projects' time limits.

The cross sections were then analyzed to be able to see what kind would work the best in high bending conditions. Two were chosen, because these would serve different purposes on the support structure. The I-beam was chosen as the best in withstanding bending loads. The structure in-between all the WHSs would be with this beam. Next, square beam were chosen for the structures attachment to the walls of the building leading it out of the high-rises boundary layer. From a material trade-off it was decided to use low-carbon steel as material for the support structure. A render with the different dimensions can be found in Figure C.1 and Figure C.2.

Finally, a vibration analysis is done to see whether the structure emits extra noise and if the building would be able to hold the structure without failure. The conclusion is that no extra noise will be created on top of the noise of the WHS. The vibrations will also not induce more stress on the structure and the building, making it a solid and operational structure.

7.5.3. Electrical and Control System

The WES will be controlled by one central unit. The control unit oversees the data and power flow. It communicates the inputs from sensors to an interface in the building and to a remote location. It also communicates inputs from the interface in the building and the remote location to the controlled components of the turbine. The chosen control unit is a DEIF's advanced wind turbine controller, AWC 500. The controller consists of a motherboard, a power and control module, a four-port Ethernet twisted-pair and fibre module, two input and output modules, and a grid protection module.

Next to the control unit, an external measurement unit, which will measure the wind speed and direction at two different locations in front of the WHS, is added for a price of €220. Subsequently, an internal measurement unit will be installed. These are added to detect possible failures and reduce risk. The sensors applied here are strain gauges, accelerometers, temperature sensors, power sensors and current sensors. These are all represented in Table 6.2. The total cost for all sensors excluding the wind speed and direction meters is €780. Finally, the whole system will be connected to the grid for which the transforming, the cabling and the intermittency need to be addressed. To transform the 380 voltage a/c output of the generator to 230 voltage, a step-down transformer is used of the type Siemens 3-phase transformer. The cables will have a total length of 300 meters, which leads to a cost of up to €600.

7.5.4. System Block Diagrams

The electrical block diagram is shown in Figure 7.8. This diagram shows how the power flows through the different components. The turbine system on the left side of the diagram is present three times in the design. The main energy flow of the harvested energy is displayed by the thick arrows. The arrow going from the energy grid to the turbine controller is there because even when the system is not generating power it should have power available for start-up and control of the system. The power going to the sensors, brakes and cooling is managed by the turbine controller. The power going from the turbine directly to the generator is the power needed to speed up the turbine to start up the VAWT.

The data handling & communication diagram is presented in Figure 7.9. All external en internal sensors and their outputs are shown. The sensors measure wind speed and direction but are also tools to predict failures. The outputs of the sensor give input to the main control unit. The control unit automatically reads the data and can shut down the system manually or automatically during an emergency stop.

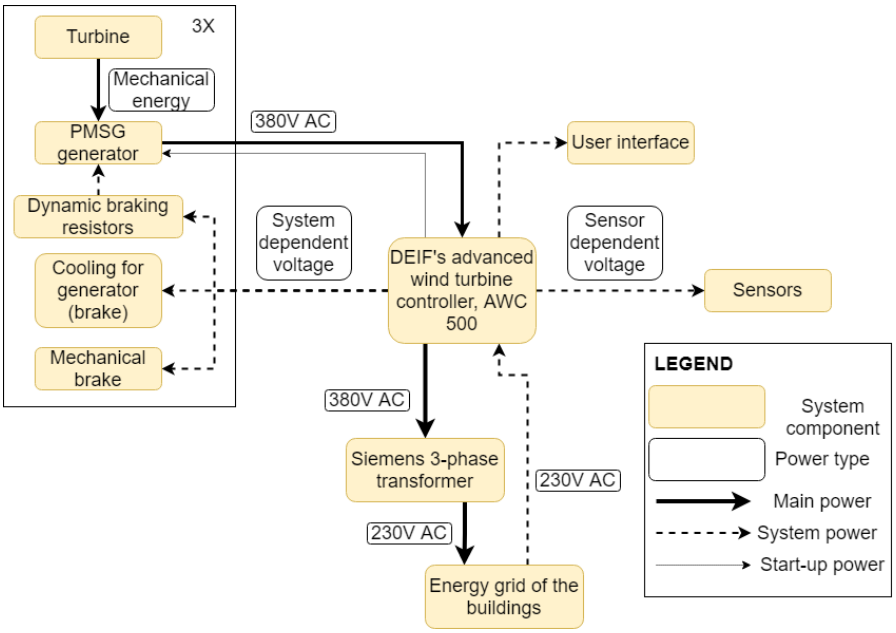

Figure 7.8: Electrical block diagram.

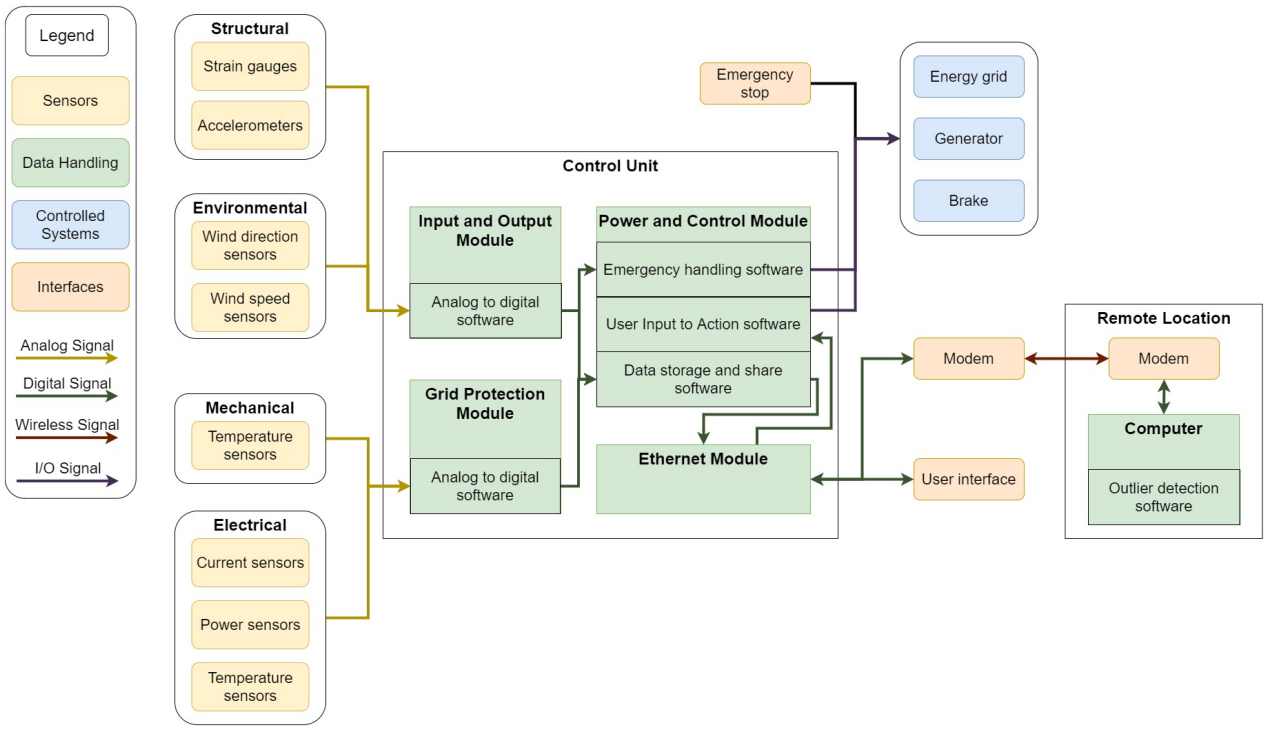

Figure 7.9: Data handling & communication diagram including the hardware and software connections.

7.5.5. Summarizing Urbanergy WindVine

Now that each subsystem has been summarized a render of the whole system can be found in Figure 7.10. In addition, in Table 7.10 all relevant values that define the Urbanergy WindVine can be found.

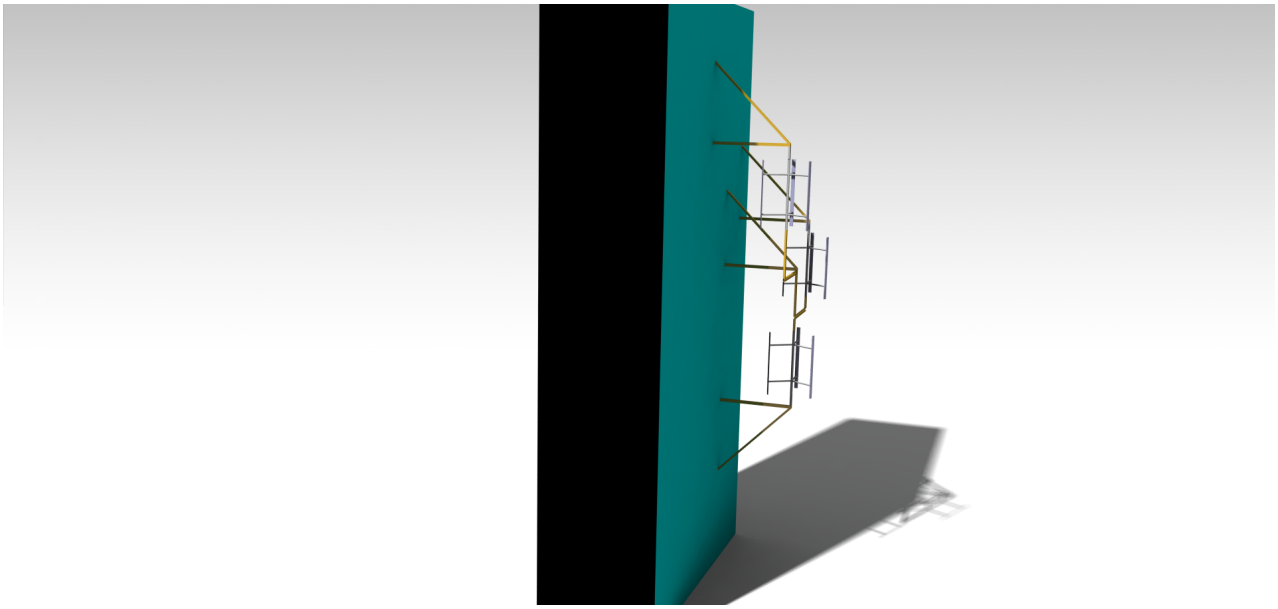

Figure 7.10: Render of the whole system attached to the building.

Table 7.10: Summary table for the Urbanergy WindVine integrated in Rotterdam.

Parameter	Value	Unit
General specifications		
Annual energy production system	51.96	MWh
Rated wind speed	12	m/s
Rated power per turbine	11	kW
Cut-in wind speed	3	m/s
Cut-out wind speed	18	m/s
Amount of turbines	3	-
Blades per turbine	3	-
Building height	200	m
Minimum system height	148	m
Space between building and turbine blades	4	m
Generator		
Type	Permanent magnet synchronous	-
Max. rotational speed	151	RPM
Drive system	Gearless direct-drive	-
Brakes		
Rheostatic	Dynamic generator brake with resistor bank	-
Mechanical	Fail-safe disc brakes	-
	- Cyclic operation	-
	- Emergency brake	-
Noise		
L_{den}	55.3	dB(A)
L_{night}	48.9	dB(A)
Turbine dimensions		
Blade airfoil	NACA0018	-
Blade length	5.55	m
Blade chord	280	mm
Serration width	28	mm
Serration height	55.85	mm
Rod diameter	63.5	mm
Rod thickness	6.3	mm
Rod length	2.52	m
Shaft diameter	127	mm
Shaft thickness	6.3	mm
Shaft length	5.75	m
Main material	Aluminium 7075-T6	-
Support structure dimensions		
Attachment trusses	4	-
Square beam thickness	11	mm
Square beam width	140	mm
Horizontal truss length	6.5	m
Angle trusses	45	m
Turbine connected beams distance	6.5	m
I-beam thickness	10	mm
I-beam width	80	mm
I-beam height	100	mm
Support structure material	Low-carbon steel	-
Unit cost	57,600	€

8
Project Development

In this chapter the project development will be given. First the project design and development logic is given in Section 8.1, including an implementation plan and a post DSE Gantt chart. Then the production plan will be given in Section 8.2. In Section 8.3 the operation and logistics of the design are analyzed. A financial and a sustainability analysis of the final design are performed in Section 8.4 and Section 8.5 respectively. Followed by this is the compliance matrix of the design with the user and driving requirements, given in Section 8.6. Finally the future vision of the Urbanergy WindVine is outlined in Section 8.7.

8.1. Project Design and Development Logic

The project design and development logic is a preliminary plan for the post-DSE realization of the WindVine. The implementation plan, post-DSE Gantt chart and project setting are discussed in the upcoming section.

8.1.1. Implementation Plan

The implementation plan, seen in Figure 8.1 and Figure 8.2, is a 4-phase program that encompasses the entire life of the WindVine, from design to decommission. Phase 1 concerns the post-DSE in-depth design and development of the WindVine. Design, testing and certification are all accounted for. Phase 2 concerns the installation of the system. A rough timeline of phase 1 and 2 can be found in the post-DSE Gantt chart, see Figure 8.3. Phase 3 concerns the operation and maintenance of the system. In Section 4.1, Section 5.1 and Section 6.1, these functions are further elaborated. Phase 4 concerns the decommissioning and recycling of the WindVine. This is further discussed in Subsection 8.3.4.

8.1.2. Post-DSE Process

In Figure 8.3 the Gantt chart is shown and elaborates on the realization of the system. The Gantt chart contains three milestones, symbolizing a finished, certified and realized system, respectively. In the first phase, the DSE is evaluated to determine the focal points for further research after which the environment of the building is thoroughly monitored for a period to determine the local weather. Based on the data gained from this a finished design of the WindVine will be made over a period of eight months. Next, testing and certification will take place. Already before the WindVine is ready for production, most of the detailed production planning will take place. Once the WindVine has been cleared for production, these plans will be put into action and the production can start. Once the WindVine has been completely realized, operation and maintenance will start.

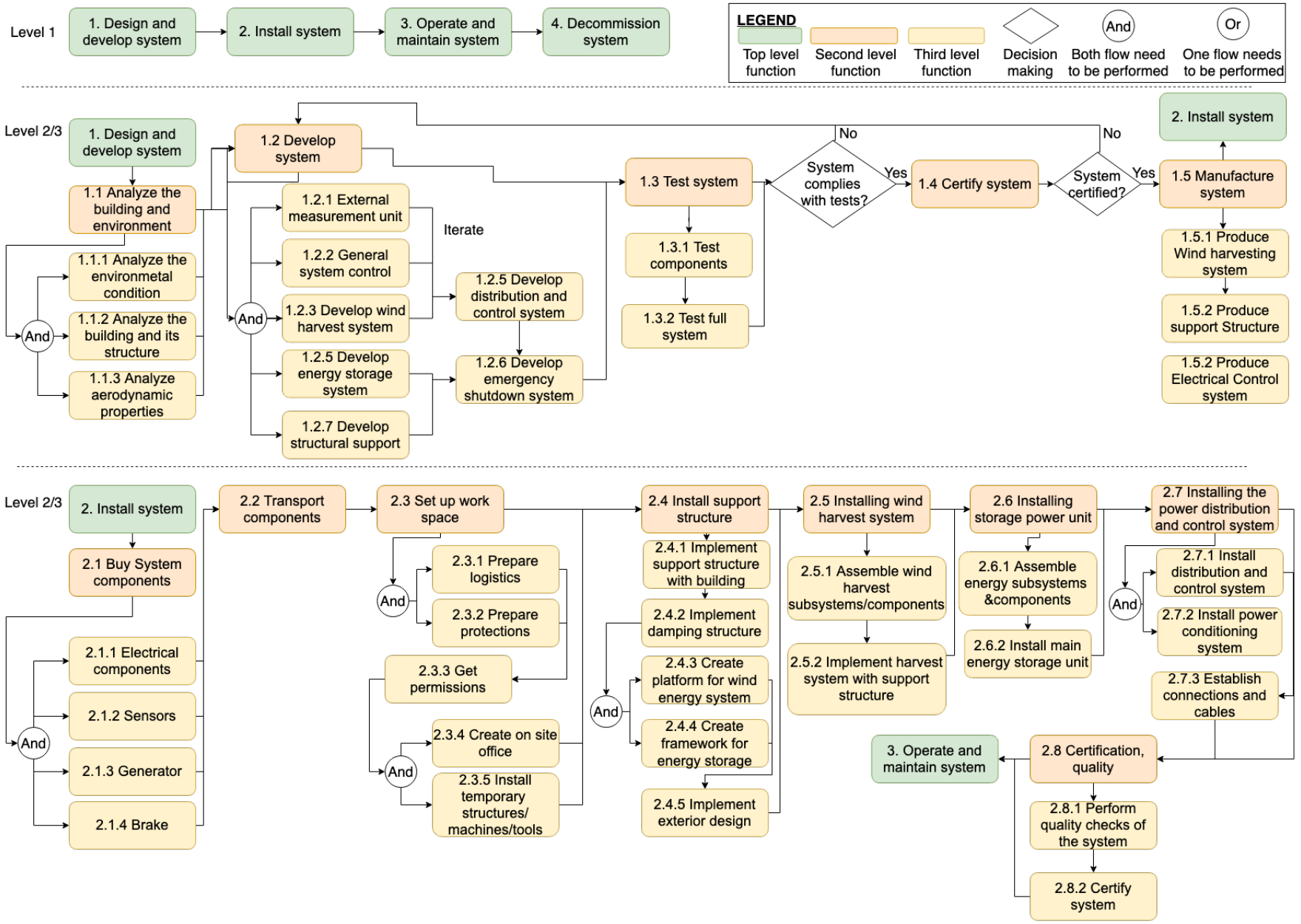

Figure 8.1: Project logic diagram phase 1 and phase 2.

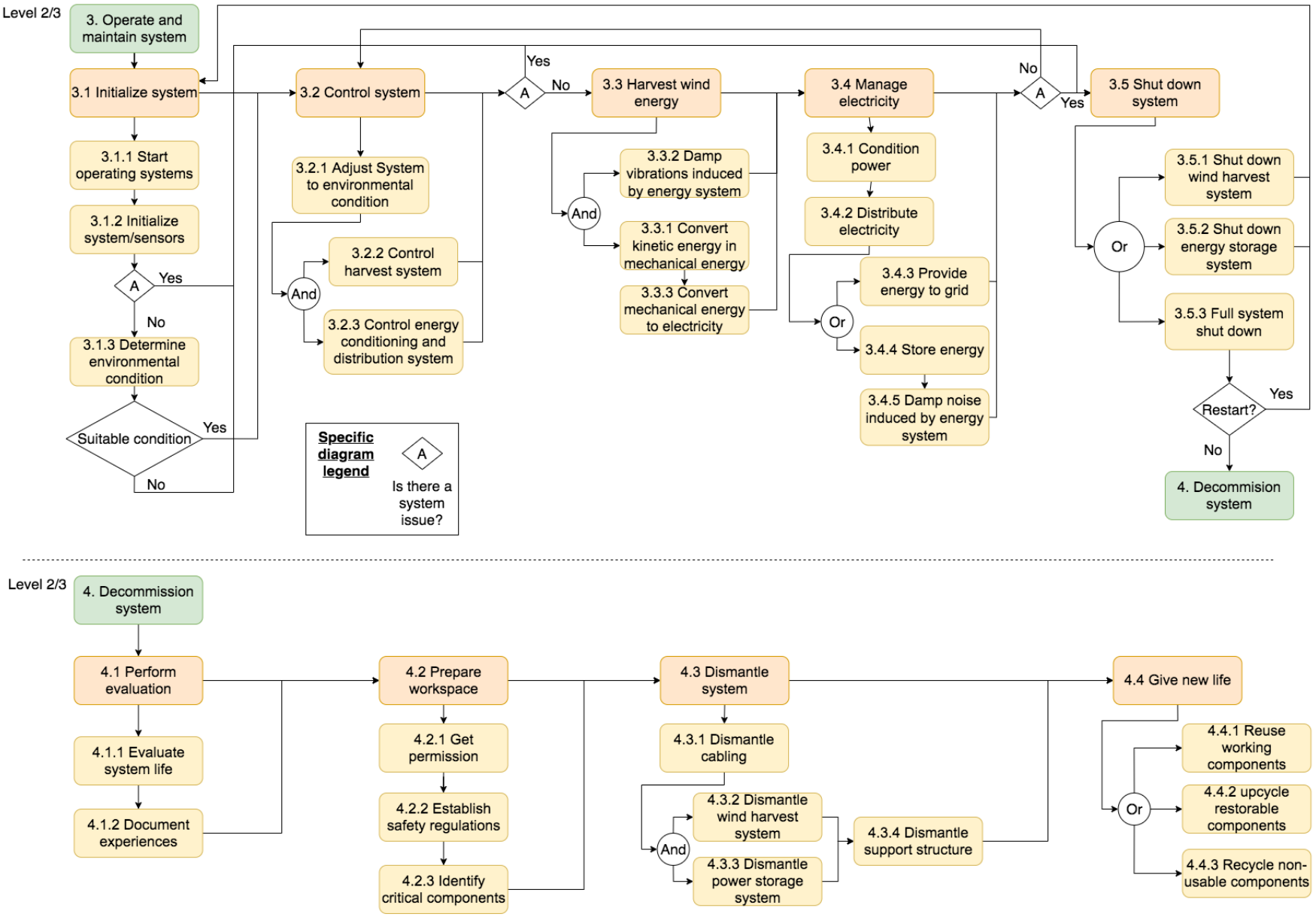

Figure 8.2: Project logic diagram phase 3 and phase 4.

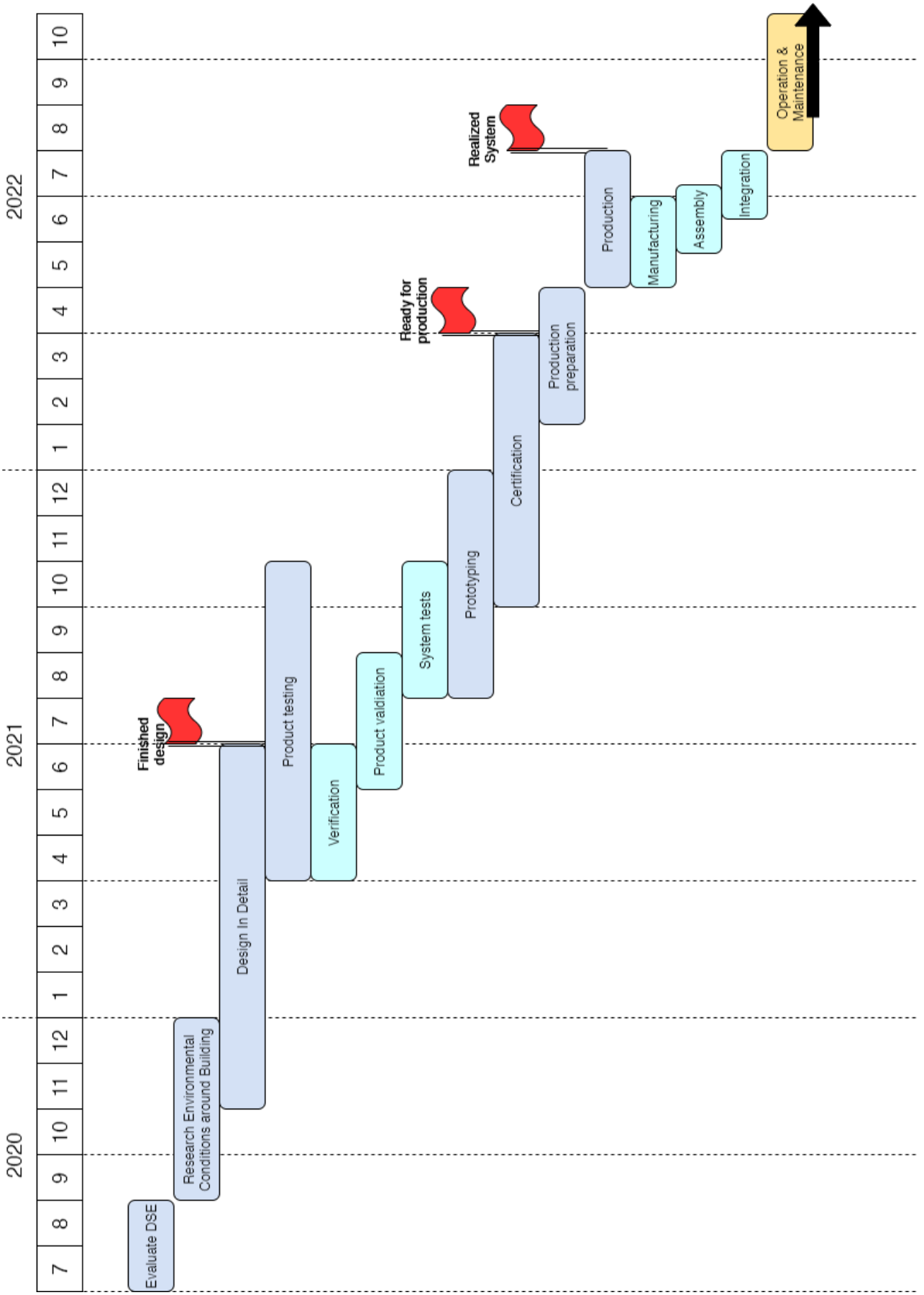

Figure 8.3: The Gantt chart displaying the timeline of activities after the DSE.

8.1.3. Setting

The location where the first WindVine will be placed is discussed in depth in Section 2.3 and Section 2.4. As stated in the midterm report [3], there will be a need for a factory, a warehouse and an office. The company will have access to the property below the skyscrapers only during installation and maintenance. The factory and office will be stationed in the area of Rotterdam, preferably in the industrial area Rotterdam North-West. As this location is ideal for transportation and more companies like Urbanergy are located here. Advantage should also be taken from the excellent geographical location of Rotterdam, with access to the largest seaport in Europe and a great road network. The management will work from the office while having the ability to oversee manufacturing. The office will be responsible for outsourcing customer support and legal expertise. The customer support will function as a way to keep the residents living nearby informed on what is going on during the different phases. These residents can also voice their opinions about the building. Local authorities and charges will be directed to the law firm. The office will also hire a health and safety officer and human resources. The health and safety officer will implement health and safety measures. Human resources will make sure that the social side of the working environment is good and will do the hiring of employees. There will be a need for an office during the different phases 2 to 4 as described in Subsection 8.1.1 and visualised in Figure 8.4.

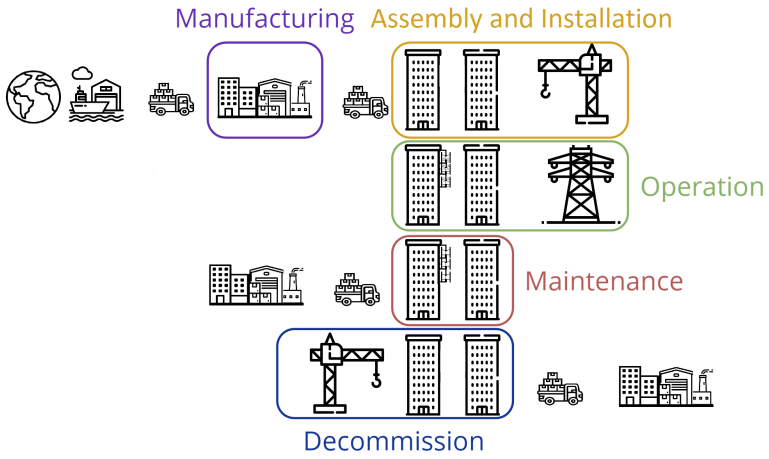

Figure 8.4: Logistics diagram from manufacturing until decommission.

8.2. Production Plan

Now that the entire design and the setting has been explained, the plan for the production of the WindVine needs to be thought out, in the form of a Manufacture, Assembly and Integration (MAI) plan or production plan. This plan is needed once the system is certified.

8.2.1. MAI Flow Diagram

In Figure 8.5 a flow diagram for the MAI plan is shown. The diagram logically shows the steps undertaken to produce a WindVine, divided into the three subsystems. The steps to produce the wind harvesting system need to be undertaken three times to produce thee turbines for the system.

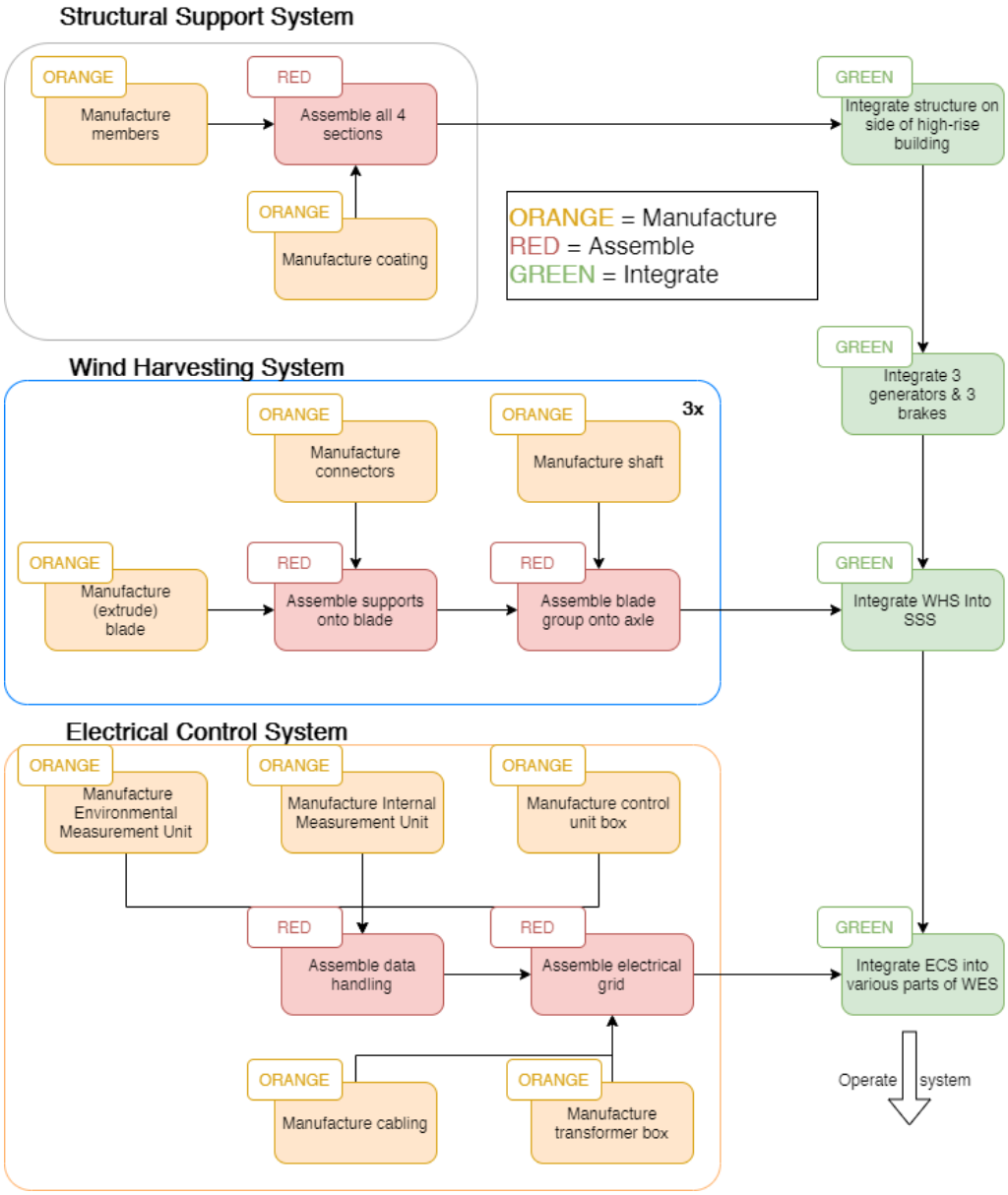

Figure 8.5: The MAI plan shows the manufacture, assembly and integration of a WindVine.

8.2.2. Manufacturing of Parts

Each part is manufactured from plating and prefabricated components to produce the WindVine. The parts are the structural components of the wind harvesting system, the support system and the grid wiring of the electrical control system. In this section the manufacturing process of these parts is explained [110]. The timeframe assumed for this phase is around two months, see Figure 8.3. The manufacturing tools necessary for the manufacturing of all WindVine parts are:

- Aluminium extrusion machine with custom die to extrude the turbine blades.
- Die bending and/or cold-rolling machinery to roll metal plating for the airfoil around the turbine connectors and the circular steel sheet around support beams.
- Welding equipment to weld the circular steel sheets to the support beams.
- Cutting equipment to cut steel and aluminium sections, and wire cutting equipment to cut the electrical wires.
- Powder coating equipment to spray the coating onto the steel members.
- A large curing oven or autoclave to cure the coating at a low temperature.
- Ultra-sonic Non-Destructive Testing (NDT) equipment, to check parts for imperfections in the material.

The I-beams and square steel beams are prefabricated and need to be inspected before manufacturing, in case any

imperfections may be present due to manufacturing. A circular steel covering around the I and square beams of the support structure is made from thin steel plates. The plates are rolled in quarter circles and welded to the corners of the beams. These welds need to be neatly finished. To facilitate access to the WHS and attachment points for the cabling and measurement units, attachment points (rings, etc.) need to be attached to the outside of the members. Once all members are manufactured they can be painted. This requires powder coating gear. The entire member needs to be coated and excess polymer powder needs to be collected and recycled. Once the tpPVC powder covers the entire member, it needs to be cured in an oven at low temperature and cooled in preparation of the assembly.

The blades can be directly extruded into the NACA0018 shape with a custom die.[1] The aluminium 7075-T6 airfoil and connectors, as well as the shaft, need to be visually inspected and checked for discontinuities using ultrasonic NDT testing to guarantee their quality. The ends are bolted or riveted after cure. The connectors are prefabricated circular members, which are extended into airfoils with thin rolled aluminium sheets. The shaft is a prefabricated aluminium circular beam. Most of the parts of the ECS are quite complex and therefore sourced from specialized companies. A separate container needs to be manufactured for the transformer and the control unit, as they come with little protection by themselves, explained in Subsection 6.7.3. Cabling needs to be cut into the correct length.

8.2.3. Assembly of WindVine

Once the parts have been manufactured and all system parts have been inspected for compliance to the design, they are assembled according to the method presented in [110]. The time frame assumed for this is six weeks as shown in Figure 8.3. The equipment needed for assembly is the following:

- Bolting equipment in the factory
- Bolting equipment on site
- Testing equipment for the quality of the bolting
- Electricians and electrical equipment for the assembly of the electrical system

The steel members need to be assembled as much as possible in the factory. This will mostly consist of the four independent assemblies that the SSS is made up of. The size of these assemblies depends on the logistics of transporting these parts to the construction site. The maximum width of parts that can be transported to the construction site is 2.48 m, so it is more efficient if all members are bolted together at the construction site. Bolts will be used, as they create less residual stresses than rivets, and because this system needs to be easily disassembled after decommissioning [110]. The connections need to be inspected after assembly, to make sure all bolts are properly connected. The blades need to be attached to the connectors, and the connectors to the shaft. If this was a weld, it would degrade the T6 cure. The connector thus needs to be bolted or riveted, with a ridge at one end and rings on the shaft in which the other side of the connector can be placed. All connections need to be inspected after assembly.

Most of the various parts of the ECS need to be integrated into the WES. But the connections need to be checked and assembled on the ground beforehand. This consists of connecting all data handling stations and connecting all electrical stations with cabling. The connections need to be checked and the system needs to be tested. The system can be tested by unit testing the connections between individual parts, followed by testing the interfaces between different sections of the ECS. The production and assembly costs are based on general construction costs. The rule of thumb is that the production costs equal the assembly costs.[2]

8.2.4. Integration of WindVine

The integration of the WindVine is the most complicated part of the production of the WindVine, as the integration takes place at such an altitude. The production plan, however, is quite simple. The timeframe assumed for the integration of the WindVine is six weeks, see Figure 8.3. The equipment necessary needed for the integration is:

- A construction crane on the top of the high-rise building, to hoist the sections of the support structure and the Wind Harvesting System into place (should already be available as the building would be under construction, if the WindVine would be installed into an already finished building, a new crane needs to be deployed).
- High altitude construction & safety equipment, for the specialised team that will install the WindVine onto the side of the building.
- Electricians and electrical equipment to integrate the electrical control subsystem.

[1] http://tri-stateal.com/extrusion-guide[cited 15 June 2020].
[2] https://www.steelconstruction.info/Cost_of_structural_steelwork#Key_cost_drivers [cited 15 June 2020].

- In the case that this system is integrated into a completed building, protective scaffolding to protect the building, and other preventive gear is needed to shield the inhabitants from the construction work.

The integration of the SSS requires the individual assemblies to be hoisted up and attached to the side of the building. The members need to be bolted to one another as well. Once the structure has been integrated into the side of the building, the power train of the WHS needs to be integrated at the three attachment points. Once the power train is in place, the turbine needs to be hoisted up to the side of the building and integrated to the power train. Once the WHS and SSS are integrated, data handling parts need to be attached to the SSS and WHS. This consists of integrating the control unit and measurement units and hooking them up. An interface needs to be present to manually control the WHS. This means that the control unit needs to be inside of the building. The transformer needs to be integrated close to the building, and the electrical cabling needs to be hooked up to the connectors. The cabling connecting the WHS and the grid then needs to be attached to the side of the building.

The costs for integration are based on similar sized wind turbines, with a contingency based on the fact that installation takes place at a higher altitude, see Subsection 8.4.2. This height during integration will increase risks. Therefore appropriate safety measures have to be taken, such as placing a safety net below the construction site.

8.3. Operation and Logistic Concept

Once the system is manufactured and integrated between the high-rise buildings, it has to be initialized and operated. After five years of nominal operation, maintenance will be done yearly, which will be discussed in this section. The operations during failure modes are detailed followed by the decommissioning of the system.

8.3.1. Operations

The workings of this operating system are discussed in Section 6.3 and Figure 6.3 shows how the system communicates. The system has three interfaces that can interact with operators. The first interface is near the control unit and will be used to initialize and decommission the system. Near the turbine, an emergency button is also present that can overrule and shut down the entire system. The system can also be operated from a remote location, this interface has similar capabilities as the one close to the control unit. The operator will start the operating system and initialize the subsystems and sensors. When all these systems work, control will be taken over by the control unit. The controllers will share relevant data with the factory and an operator in the factory will oversee this data. Different wind conditions result in different amounts of power that are generated. The control systems should regulate this. During the phase of normal operations, communication with residents is important. Residents will be moving into the high-rise buildings and might have questions, so customer support will always be available. In case a lawsuit is filed against Urbanergy because some residents think the system is dangerous, the law firm will be notified.

8.3.2. Maintenance

Outsourcing the maintenance is faster, safer, and has lower costs for offshore wind turbines [111]. It is expected that this also will be the case for the WindVine. Requirement WES-A09 states that the first technical inspection will be performed after five years, from this time onward it is assumed that maintenance should be done at least once a year and the service party will be paid a fixed amount of money each time. It is wise to keep a spare parts inventory management in the factory. Which parts should be included in the inventory is based on a trade-off balance. This trade-off contains the cost of shortage, holding, and reordering. In consultation with the service party, the parts will be delivered with rented trucks to the on-site location. When it is possible to speak with certainty of broken or defective parts, spares should be easily delivered. In the case that, spare parts are not in the inventory a list of suppliers is available and ready to deliver these parts at a reasonably fast time. It is realistic to assume that the factory will not have the equipment to produce the parts it was able to produce during the manufacturing phase, therefore a competitor is asked to produce these parts.

To schedule this maintenance effectively an understanding of when it is needed is necessary. The system has many sensors in place to check performance. All sensors present in and on the system are already discussed in Section 6.5. The real-time performance and status of the system are monitored by these sensors and with this data, the necessary maintenance can be determined. When the sensors show data that is unacceptable for that part, that specific part of the system will need a check-up. When replacement is necessary the parts are delivered and taken down by the designated cable system. Parts can be stored within the building on the same level of the harvesting system, and

after that brought down or up with the cable system. Failures in the electrical system are detected by voltage measurements. Replacements for burnt cables are available and faulty connection can easily be replaced.

Although the high-rise buildings were yet to be completed during installation, it is assumed that during this phase of the project residents will live in the building. This brings major complications and the service party should be provided with this information beforehand. Although the team will not work on-site during this time, complaints from residents will be directed to the customer service. Licenses from the local authority will be obtained with the help of the law firm and maintenance is done in agreement with the high-rise building managers.

8.3.3. Failure

Failure is one of the modes that should be mitigated to the point of very low probability. This is especially important as this is not a proven concept yet. However, if failure does occur the inhabitants of the building should not be endangered. In the case there is an injury, all injured parties are heard and dealt with politely. The insurance company is contacted after the cause is known and damage to anyone lawfully resolved. Apart from this, in case of system failure, the requirement on the minimum amount of energy produced can also no longer be fulfilled. All parts should be recovered and internally an investigation should be done. An external neutral party will lead an additional investigation to find the cause of failure.

8.3.4. Decommissioning and Recycling

When the WindVine has reached its end of life, the operator will shut down the system, and decommissioning will start. The system life will be evaluated and experiences should be documented. The experience gained in this project might be very useful for next-generation urban wind harvesting systems. Legal expertise and a health and safety officer are necessary to get permission to dismantle the system and establish safety regulations. Therefore, critical components will be identified.

On-site preparations will start again, which means that the same procedures as during installation are executed, with the result that the site is equipped with the machinery, temporary structures, and tools that are needed to dismantle the system. Electricity needs to be cut off so the cabling can be dismantled. Afterward, the structure will be dismantled. Throughout this process, trucks will drive from the high-rise buildings to the factory and vice versa to pick up the dismantled material. As residents are living in the high-rise buildings, there is a need to dismantle the system quickly with little inconvenience. In coordination with the high-rise building manager, dismantling will happen during convenient hours, which will probably mean on weekdays during the day. The dismantled components and subsystems are stored in the factory temporarily. Either a working component/subsystem can be sold directly and be re-used in another project or analysis should be performed to determine how the non-usable component/subsystem can be recycled and what materials can be re-used. A separate section, Section 8.5 will discuss this process in more detail.

8.4. Resource (Class II) and Financial Analysis

This section will provide an insight into the resource and financial aspect of this project. First a mass budget is given, afterwards the expected costs of this project are estimated and shown in a cost breakdown structure. Finally a method to determine the return on investment is described.

8.4.1. Mass Budget

The mass breakdown of the WES follows from the breakdown per subsystem in Subsection 4.7.1, Subsection 5.6.1 and Subsection 6.7.1. There will be three WHS, so that will be accounted for in the breakdown. A contingency over the entire system was added based on aerospace industry standards [18], which results in Table 8.1

Table 8.1: Mass breakdown of the WHS.

Part		Mass	Contingency
Blades		15 kg	
Connector		60 kg	
Shaft		38 kg	
Generator		341 kg	
Maintenance Platform		250 kg	
Brake	+	-	
Wind Turbine (3x)		2,110 kg	
Steel Members		4,575 kg	
Polymer Coating	+	100 kg	
Foundation		4,675 kg	
Electrical Infrastructure		-	25 %
Mass		**6,750 kg**	
Contingency	+	1,690 kg	
Total Mass		***8,470 kg***	

The total mass of the system is 8,470 kg. As sensitivity of 25% is used to see how this value will vary, which results in: 6,780 kg - 10,590 kg. Both these values seem reasonable.

8.4.2. Cost Breakdown

Three different methods are used to determine the cost of all cost items. Each cost item has a contingency and is organised in a category. This results in the total lifetime cost of this system. Three different methods were used to estimate the cost of individual cost items. The first method can be found throughout the report and is done by directly estimating the costs of components based on the characteristics of that component. The unit cost can be found when all these components are added up. A contingency of 30% is included as this project is in a developing phase that has a need for Class 4 or Class 3 cost estimations [15].

The second method in determining the cost is by looking at data on the average cost structures of small wind turbines, where the U.S.. Pacific Northwest National Laboratory defined a commercial small wind turbine as having a rated power of between 21 kW to 100 kW [14]. This data is presented in $/kW and multiplying this with a rated power of three times eleven, see Subsection 4.3.3, gives the average cost for a wind turbine of similar size as the WindVine. It is assumed that the non material cost, such as the cost for Zoning, Permitting, Inspection, and Incentives (ZPII), will be similar as for the WindVine. Converting the values to euros and adding a contingency of 50%, as there is a bigger uncertainty due to this concept being relatively new, results in the cost for the WindVine. For maintenance a yearly maintenance value was stated. For the WindVine it was assumed that the first maintenance required will be after five years and afterwards yearly maintenance is required.

The third method used is to estimate specific costs that were specified all together in the research of Pacific Northwest National Laboratory as Overhead and Profit [14]. This includes the costs for insurance and decommissioning. There was no specific data available for small wind turbines, so the cost of bigger wind turbines was analyzed [112]. Both land-based, fixed offshore and floating offshore wind turbines have an insurance and a decommissioning cost of around one percent of the total project with decommissioning being about 50% more costly. As this project would be on the riskier side, just like floating offshore wind turbines, those percentages were used.

All these costs are summed up in Table 8.2. It can be noted that there are no operational costs present. This is due to the small size of the wind turbine [14]. Furthermore the client has stated that the buildings are still under construction when the wind harvesting system will be installed, while only the structure is in place [3]. It is therefore assumed that most of the infrastructure for construction is still in place, which means that the installation cost would not be exceedingly higher than that of an installation at ground-level.

Table 8.2: The cost overview of the total lifetime of the WES

Category	**Large HAWT**	**Small HAWT**	**WES**	**Contingency**
Material Blades			€250	
Production Blades			€250	
Material Shafts + Connectors WHS			€1000	
Production Shafts + Connectors WHS			€1000	
Generators			€2,500	
Brakes and Cooling	1 % Unit Cost		€500	
Noise Reduction Fund			+ €15,000	
Wind Turbine			*€20,500*	30 %
Material SSS			€3,000	
Production SSS			+ €3,000	
Foundation			€6,000	30 %
Voltage Transformer			€600	
Control Units			€14,000	
Cabling			€2,200	
Sensors			+ €1,000	
Electrical infrastructure			*€17,800*	30 %
Unit Cost			*€44,300*	
Contingency			+ €13,300	
Total Unit Cost			**€57,600**	
Transportation and Logistics		130 $/kW	€4,000	
Customer Acquisition and Qualification		51 $/kW	€1,500	
Engineering, Designing and Testing		30 $/kW	€1,000	
ZPII Processing		274 $/kW	€8,000	
Insurance	1%		€1000	
Decommissioning	1.5%		€1,500	
Assembly and Installation		523 $/kW	€15,000	
Maintenance		16 $/kW	+ €500 (6x)	50 %
Lifetime Cost Incl. Total Unit Cost			*€90,700*	
Contingency Excl. Unit Cost			+ €17,500	
Total Lifetime Cost		6,450 $/kW	***€108,600***	

The cost structured in Figure 8.6 are based on a common method for wind turbines [112]. On a top level the costs are split in capital expenditures and operational expenditures. The capital expenditures contain the capital cost for the turbine, the balance of the system and the financial costs, which are split in seven individual cost items. Requirement WES-A17 is met as the total unit cost is of €57,600. Taking a sensitivity of 25 % into account, the unit cost is found to be in the range €46,100 to €72,000, meaning that the unit cost stays within the cost requirements. When this same sensitivity factor is applied to the total lifetime cost, it results in a range between €86,800 to €135,800.

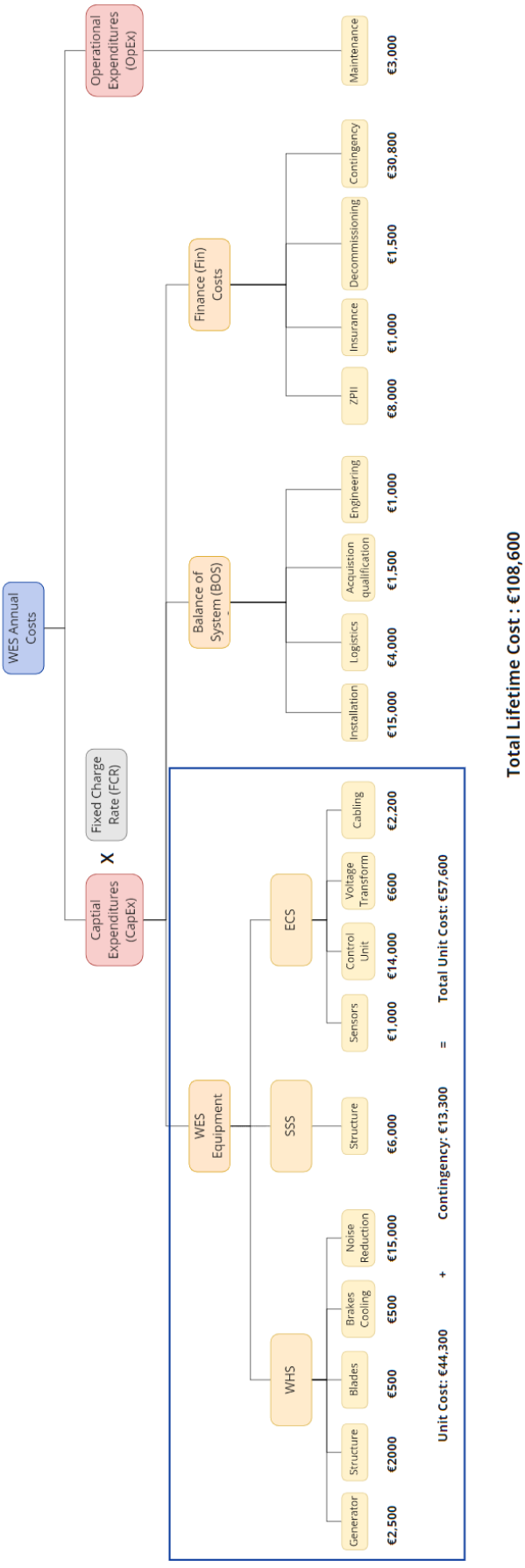

Figure 8.6: The Cost Breakdown Structure of the entire WES.

8.4.3. Levelized Cost of Energy

The Levelized Cost of Energy (LCOE) is defined as the total cost of the system over the total energy produced over the lifetime of the project and can be computed from Equation (8.1). It allows the comparison of different energy production technologies [113].

$$LCOE = \frac{\sum_{t=0}^{T_{life}} C_t (1+r)^{-t}}{\sum_{t=0}^{T_{life}} E_t (1+r)^{-t}} \tag{8.1}$$

where C_t and E_t are the total cost and energy yield respectively for year t, with a real interest rate r for T_{life} service years. The real interest rate represents the interest rate adjusted for inflation over time. The real interest is difficult to predict as it is dependent on the borrower and the risk of the project.[3] Onshore wind farms have a real interest rate in the range of 5-7%, while offshore wind farms have a slightly higher real interest rate around 8% due to their higher perceived risk.[4] As the turbine system will be placed between two high-rise buildings, the perceived risk is assumed to be at least as high as for an offshore wind farm. Therefore, a real interest rate between $8-10\%$ will be assumed. Furthermore, as the client requested a system with a lifetime of at least 10 years, the LCOE will be investigated for lifetimes between 10 and 20 years, which is common for conventional wind turbines [114]. In addition, an annual degradation rate of 1.5% will be assumed [115].

The annual energy yield of the turbines was already estimated in Section 7.1 to be 52 MWh and the cost breakdown over the systems lifetime has been done in Subsection 8.4.2. The system will not have any maintenance in the first five years. Therefore, a yearly operation and maintenance cost from the sixth year onwards will be used. Then by means of Equation 8.1 and the input values described above the LCOE can be calculated to be in the range $0.25-0.4$ €/kWh depending on the real interest rate and lifetime. The minimum value of 0.25 €/kWh corresponds to the most optimistic case with a lifetime of 20 years and a real interest rate of 8%. The maximum value corresponds to the the worst case scenario with a lifetime of 10 years and a real interest rate of 10% According to [116], the LCOE of the most common energy sources is between $0.05-0.18$ €/kWh. This is significantly lower than the LCOE for the designed system. However, comparing with already existing urban wind systems [117] the designed turbine has a favourable LCOE mainly due to its high power output and favourable wind conditions described in Subsection 2.4.3.

As described above, the current estimation of the LCOE for the designed turbines is significantly higher than other existing technologies, which might result in a less favourable interest in investment in the proposed technology. However, the design presented in this report is not as developed as more conventional horizontal axis turbines. This means that several improvements over the years might be achieved which will result in a lower LCOE. The two parameters which are most likely to change, as the technology matures, are the cost of the system and the energy production. For the cost of the system, cost contingencies have now been taken into account which can be estimated to become null over the years. In addition, it will be assumed that noise mitigation fund will be halved as noise mitigation technology and the turbine aerodynamic performance improves. For the energy production, it can be assumed that over the years, the technology will improve in its performance but also that the site location might present better wind conditions. This could be due to rounder buildings, accelerating and enlarging the incoming wind sector. As a first estimation, a 5% increase in energy production will be assumed. The LCOE for the two cases described can be seen in Table 8.3.

Table 8.3: Future LCOE estimation for improvements in cost and energy production. The decrease in cost corresponds to no contingency and a reduction in noise fund by two. The increase in energy production is with respect to the estimated yearly 52 MWh.

Improvements	**LCOE for r = 8%, T_{life} = 20 [€/kWh]**	**LCOE for r = 10%, T_{life} = 10 [€/kWh]**
Decrease in unit cost	0.16	0.24
5% increase in energy production	0.24	0.37
Both improvements	0.15	0.23

As can be seen in Table 8.3, the LCOE could with improvements over time decrease significantly and become competitive with existing offshore wind farms [116]. Further investigations should be made on whether the designed

[3] https://www.investopedia.com/terms/r/realinterestrate.asp [cited 15 June 2020].

[4] https://www.windpowermonthly.com/article/1523677/energy-costs-analysis-why-wind-broke-mainstream-2018 [cited 15 June 2020].

turbines could become more economically profitable than large wind farms. However, een with a slightly higher lifetime cost, the system does have an added value by its sustainable aspect in a urban environment, which will be further discussed in Section 8.5.

8.4.4. Return on Investment

In the previous subsection the total cost over lifetime was calculated to compare with already existing energy generating technologies. In order to determine the economic benefit that could result from this system, the revenues and thus return on investment should be investigated. To do so, an analysis of the cost and revenues of the system is done in this section.

Firstly, the life cycle cost are calculated in a similar fashion as done for the LCOE. All costs presented in Subsection 8.4.2 are given in their present value. However, to perform an economic analysis of the project, the variation in cost due to inflation should be taken into account. Therefore the same real interest rate of 8% as for the calculations of the LCOE will be used. In addition, as for the LCOE a yearly degradation rate of 1.5% will be used [115]. For the revenues, the present cost of electricity for an average household will be used. This corresponds to 22 €c/kWh in the Netherlands.[5] To take into account the inflation over the years, a yearly inflation rate of 2% on the electricity price will be used.[6]

The net present value can then be calculated and plotted as shown in Figure 8.7. It can be seen that for the estimation presented above, the project will break even after 16 years and result in a final net present value of about €10,000 after 20 years. In [118] the pay back time for urban wind projects was estimated to 23 years which is significantly higher than for this project. This is however mainly due to the favourable wind conditions at significant heights which allow for an increased energy production.

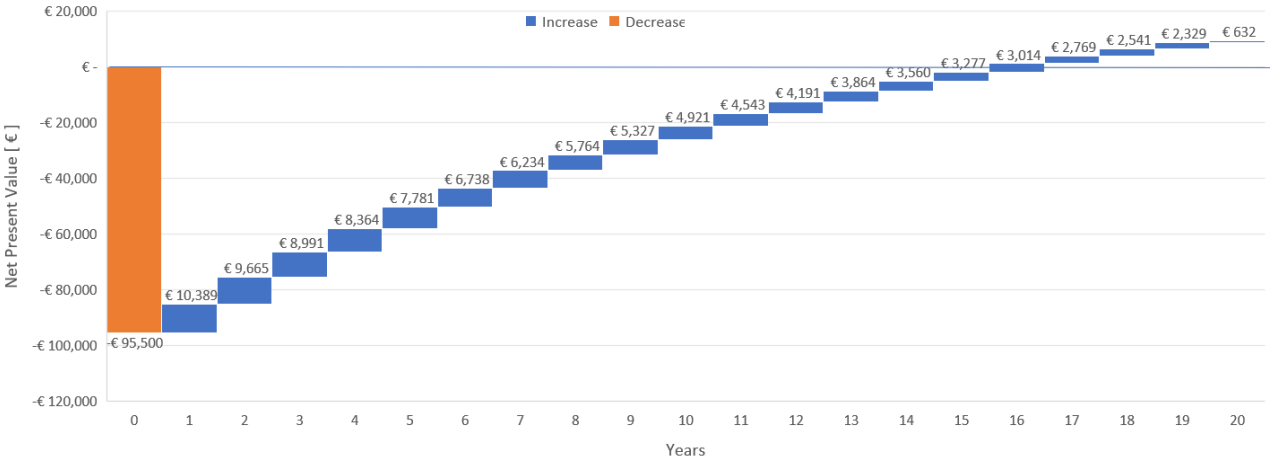

Figure 8.7: Net present value of project for 20 years.

To complete the financial analysis, it should be stated that the internal rate of return is 9.4%.[7] Therefore, any real interest rate lower than the internal rate of return will result in a positive net present value for an estimated life time of 20 years. Finally, the return on investment can be calculated to be about 9% after 20 years.[8]

8.5. Sustainability Score Final Design

As the final design is finished and every component of the WindVine was sized, the sustainable goals stated in Section 2.6 need to be checked. These goals have been a guideline throughout the designing process and therefore it is important to evaluate them and see where any possible improvement is required. In Figure 8.8 a sustainability tree visualizing how to build a sustainable future is shown.

[5] https://ec.europa.eu/eurostat/statistics-explained/ [cited 17 June 2020].
[6] https://tradingeconomics.com/netherlands/core-inflation-rate [cited 17 June 2020].
[7] Method for calculation: https://www.investopedia.com/terms/i/irr.asp [cited 18 June 2020].
[8] Method of calculation: https://www.investopedia.com/terms/r/returnoninvestment.asp [cited 18 June 2020].

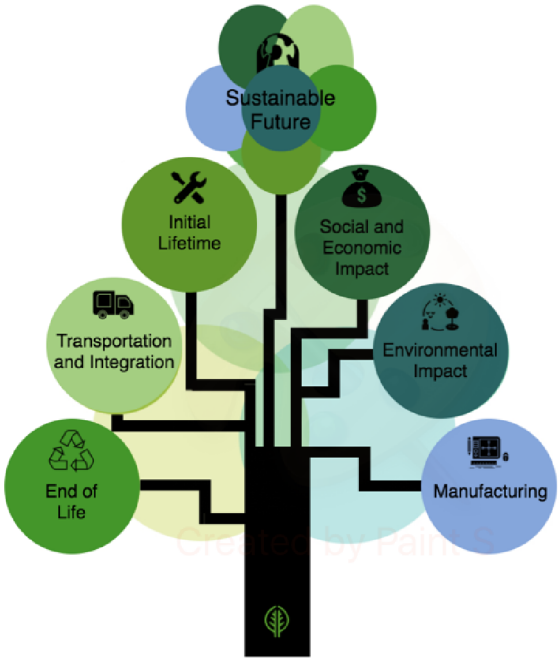

Figure 8.8: Overview of sustainability strategies.

Manufacturing: The first strategy was the optimization of the manufacturing process. The aim for this process was a "+". This process started with the material choice. The entire WHS is made out of aluminium and thus is completely recyclable. This means that requirement WES-A16 is met. For the structural component, steel and a polymer coating are used, which can also be recycled. The production process for the WHS as stated in Section 8.2 is low-waste, flexible and all the scrap created can be collected and recycled as only a single material is used. The production of the steel components are more wasteful, mainly because harmfull gasses are expelled during welding. The coating can be made in a sustainable way. It is known that the process can be harmfull, however if a safe processing is applied by a specialized third party no harm will be done to the environment. Since only three types of material are used, only a few steps are required to produce the system and therefore the amount of waste can be minimized. The structure is very lightweight as this was required by the structural department since it had to be integrated at a height of a 150 meters, which also means that the material use is quite low. To conclude, the team believes that at this stage the aim to optimize the manufacturing techniques is met. Once the actual production of the WindVine starts and the components are being produced by third parties, clear communication is required to notify the sustainability wishes.

Transportation and integration: The next step in the production phase is the transportation of the components to the building site and the integration of the entire system. Since this was a strategy mainly carried out by third parties, a transparent process is difficult to achieve and it was chosen to go for a "-" aim. To keep an overview of what is possible to trace, the transportation is divided in a top-level and a lower level. Throughout the design process it became more clear that a lot of concessions could be made and that even a sustainable transportation and integration was within the possibilities for top-level. The structural components of the WHS and SSS will be assembled on site, but can mostly be obtained from local suppliers. However, these materials are not mined and processed in the Netherlands. The local suppliers will thus be contacted and the possibilities to use recycled AL 7075-T6 and low carbon steel will be discussed. As both these materials can be recycled and because the Netherlands has an extensive database on availability of metals[9], it is expected that this can be done. All the components for the electrical control system need to be bought off the shelf. The transportation for these components can be traced on a top level as the factories of the supplier are often known. The control unit can even be traced on a lower level as stated in Section 6.3. However for the other components and especially the smaller components it becomes harder to know where the materials

[9]https://www.rvo.nl/onderwerpen/duurzaam-ondernemen/circulaire-economie/kennisplein-grondstoffen/grondstoffenscanner [cited 21 June 2020].

come from. Besides, the environmental impact of the transportation of these components will be lower.

The transportation of most components to the factory will be carried out by a third party. The integration of the system is going to be quite challenging, as explained in Subsection 8.2.4 as a crane needs to be installed on top of the high-rise building. Since the integration takes place at height a lot of safety regulations apply as the lives of the workers is the most important. It can be concluded that the integration is going to be an operation which requires a lot of energy. Investigation needs to be applied to look at possibilities to buy green energy to use for the integration. As a result, the team believes that with respect to the optimization of the transportation and integration techniques, the system over performs the initial aim. It was decided to give it a score of "o". However, it must be noted that a lot of extra research has to be done before this can be quantified, but that was beyond the resources at this stage of the process.

Social and economic impact: The social and economic impact of the WindVine was the third strategy created to assure a sustainable design. The tree-structure applied on the three aerodynamically optimized turbines are, in the team's opinion, aesthetically pleasing. But, this shall be validated with a survey of the residents. The applied color can be varied, as easy maintenance, and therefore accessibility was of top priority. The color can be chosen based on the wishes of the residents. The shadow impact is minimized as explained in Section 2.4 the location at which the system is integrated has almost no direct sunlight during the day. The ROI of the total system was calculated to be 16 years, and as the system is to operate more than 10 years it is believed that is possible to reach the break even point under normal circumstances. The system is mainly designed to kick start the implementation of sustainable energy harvesting system in the urban area, and not to generate money. Thus, it can be concluded that reaching the breaking point after 16 years is quite an accomplishment.

The only problem which needs to be dealt with has to do with the noise generated by the system. As described in Section 4.5 the system produces too much noise to meet requirement WES-A4. The noise should be below 47 dB(A) at the nearest building facade, which is not the case for this design. However, three possible solutions are given accordingly. But due to limitation of resources these solutions could not be integrated in the design, and should be therefore researched in future development phases. This means that the sustainable aim at stage for the social and economic impact is not yet met. All the criteria score very well and only have to be validated, but the noise problem is a very dominant criteria for the implementation of the WindVine. For this reason the team gave the social and economic impact a "o" score. However, as can be seen in Figure 8.9, a blue dashed line is added which visualizes the potential the system has, once one of the three provided noise solutions is implemented.

Environmental impact: The next strategy addressed is the environmental impact. As concluded in Section 4.3 requirement WES-A21 is met, which means that the system has an output of more than 50 MWh. This comes at a cost of 43.8 kWh, to kickstart the system, and 219 kWh to power the electrical control unit explained in respectively Subsection 4.4.3 and Section 6.3. Combined, it is less than 1% of the total output, in which also a safety factor was applied. Therefore, it can be concluded that a high clean energy output is reached. Since it is a system working solely on wind energy, no toxic emissions are generated during the harvesting process. This means that the aim set in the beginning for the environmental impact is reached and the system can be scored with a "++".

Initial lifetime: The fifth sustainable strategy created was about the optimization of the initial lifetime of the WindVine. The first important criteria to ensure this is a reliable design. All subsystems communicate with each other and various sensor have been added to provide updates during operation at all times, as explained in Section 6.5. The maintenance of the system will be a difficult operation, but with proper preparations and keeping all the regulations in mind, it can be done. An increase in moving components increases the chance of the system braking. However, as decided in Section 4.4, a gearbox was not necessary and a direct drive system was possible, which increases the simplicity of the system. Throughout the design phase a fair trade-off has been made with respect to increasing efficiency which corresponded to an increase in complexity. The conclusion was, that a smart yet easy system is able to meet the power requirement and therefore any additional features were not really necessary and therefore discarded. Thus, it could be concluded that the aim for the optimization of the initial lifetime is met and can be scored with a "+".

End of life: The last sustainable strategy concerns the end of life process of the WindVine. The generator is made out of a variety of materials which are recyclable as stated in Subsection 4.4.2. The harvesting system is entirely made out of aluminium 7075-T6 which can be recycled. The steel used for the structural component can be reused, after some work has been done on deleting any imperfections. This is also applicable for the coating applied, some treatment

is required before it can be re-used. This will require some money, but is accounted for in the contingency of the total cost breakdown structure in Section 8.4. All the cables and transformers used need to be decommissioned and the recyclable materials need to be extracted. Some waste will be created but no alternative option was found at this stage. The energy use during decommissioning should be optimized with a proper preparation and the knowledge gained over at least 10 years of operation. However, as mentioned before, operating at height will cost a lot energy to ensure a safe process. Still, the team has decided to score the end of life optimization with a "+", as the criteria with respect to the recycling are met.

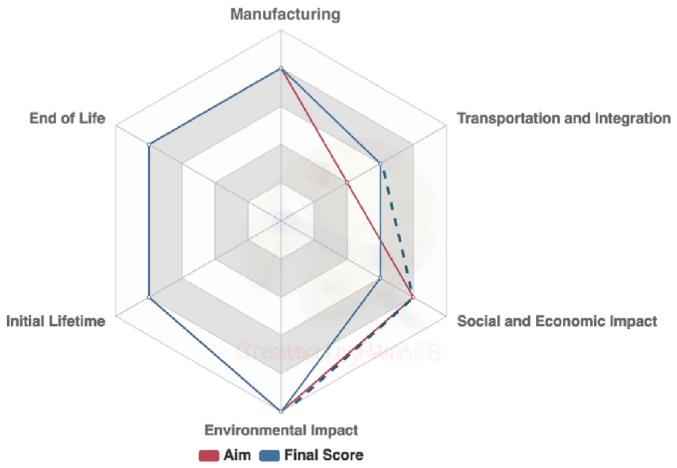

Figure 8.9: Radar diagram of final sustainability score.

An overview has been created in Figure 8.9, it shows that all aims are reached except for the social and environmental. But, as stated before there are possible solution to reach that aim, that are not yet integrated. The main take away from this sustainability analysis is that a lot of things are possible to do as long as enough effort and resources are put into this goal. Thus, time and budget should be allocated to this in future stage to elaborate on these strategies in more detail.

8.6. Compliance Matrix

In this section the compliance of the design with the user requirements is given. The compliance matrix is given in Table 8.4. A few extra requirements that are not user requirements are stated because those provide additional value to the user requirements. If a requirement is not met, the value that design reaches is stated. Furthermore the reason why the requirement is not met and how the design could be improved to meet this requirement is given below the table. The table also contains a reference to the section where the requirement was addressed in the design process.

Table 8.4: Compliance matrix.

Requirement code	Requirement	Compliance?	Reference
WES-A01	The system shall have a cut-on velocity of 3 m/s.	Yes	Subsection 4.4.3
WES-A04	The system shall be within standard noise regulations for conventional wind turbines.	No. See WES-OP-MU-03 & WES-OP-MU-04	Subsubsection 4.5.8.1
WES-A05	The system shall absorb the turbine generated vibrations in a way that they will not be noticeable to the high-rise buildings.	Yes	Section 5.5
WES-A08	The system shall have a minimum lifetime of 10 years.	Yes	Section 7.4

WES-A09	The system shall not require a technical inspection before 5 operating years.	No	Section 7.4
WES-A10	The system shall not damage the high-rise buildings in case of failure.	Yes, see explanation below	Section 7.4
WES-A11	The system shall not damage the area in between the high-rise buildings.	Yes, see explanation below	Section 7.4
WES-A12	The system shall not damage people in case of failure.	Yes, see explanation below	Section 7.4
WES-A13	The system shall stop working automatically in case of failure.	Yes	Section 7.4
WES-A14	The system shall be controlled by a mechanical safety system.	Yes	Section 7.4 & Subsection 4.4.4
WES-A16	The system, excluding structural components, shall be made of recyclable materials.	Yes	Subsection 4.6.3, Subsubsection 5.4.1.3 & Section 8.5
WES-A17	The system shall have an overall unit cost below €75,000.	Yes	Subsection 8.4.2
WES-A18	The mechanical safety system shall be controlled by software.	Yes	Section 7.4 & Subsection 4.4.4
WES-A21	The system shall provide 50 MWh at a rated velocity of 10 m/s with a free-stream turbulence distributed with Gaussian law at a standard deviation of 2.5.	Yes	Section 7.1
WES-A22	The system shall be integrated into a 30-meter space between two buildings of which the parallel sides have a rectangular shape with a height of 200 meters and a width of 30 meters.	Yes	Section 5.3
WES-OP-MU-03	The system shall have an absolute noise limit of 47 dB(A) L_{den} (Dutch absolute noise power limit [27], [28]),[29]).	No. L_{den} = 55.3 dB(A)	Subsubsection 4.5.8.1
WES-OP-MU-04	The system shall have an absolute noise power limit at night, L_{night} (23.00-7.00 local time), of 41 dB(A). [28],[29]	No. L_{night} = 48.9dB(A)	Subsubsection 4.5.8.1
WES-WF-STR-01	The buildings shall carry the support structure.	Yes	Section 5.3 & Section 5.4
WES-OP-SC-03	The system shall be able to measure wind speed.	Yes	Section 6.4
WES-OP-SC-06	The system shall be able to control the energy outflow to the building.	Yes	Section 6.3

As can be seen in Table 8.4 the only requirements that are not yet met are the requirements on noise and maintenance. As described in Subsection 4.5.8, the noise requirement is only not met at the building the system is attached to. The reason these requirement are not met is that the noise requirements in the Netherlands are very strict. To provide a frame of reference of the requirements, 47 dB is comparable to the noise of a refrigerator and 41 dB is comparable to the noise of light rain or the noise of a computer.[10] However several possible solutions are presented, such as implementing noise cancelling panels in the design, using active noise cancellation or optimizing the facade as explained in Subsection 4.5.8. Several opportunities are presented but a more extensive research is needed to design these noise reducing subsystems. It should be noted that all of the proposed methods are able to reduce the noise by the needed amount of 8.33 dB(A) to meet both the requirements for L_{den} and L_{night} as specified in requirements WES-OP-MU-03 and WES-OP-MU-04 respectively.

[10] https://www.soundstop.co.uk/decibel-scale [cited 19 June 2020].

The technical inspection requirement cannot be met. As explained in Section 7.4, the failure rate of WES is still quite high. Having no technical inspection is therefore not realistic at all. It is even recommended to have multiple inspections and maintenance activities in order to reduce operational costs (see Subsection 7.4.3). Furthermore, the requirements WES-A10 to WES-A12 will be met by the Urbanergy WindVine under normal operational conditions with the chances of usual failures. Nevertheless, it is not possible to exclude the risk for damages. Exceptional environmental conditions may cause harm or damage to the surrounding area.

8.7. Future Vision

Having completed and analysed the design, it is time to analyse the possibilities for this project in the future. This section will discuss what the successes of the system are and what the goals are from the first implementation forward.

8.7.1. Evaluation of Success of the System

The system produces as much energy as projected, and the clients are satisfied with the result attached to their high-rise building. There are multiple ways to analyze the success of the system. The outcomes of these analysis will determine whether the continuation of this concept is feasible or not.

Financial success: The capital costs of the system fit inside the budget of €75,000 Section 8.4. Therefore, one can call it financially successful. However, when placing the system on another building, the flow characteristics can vary quite a bit and therefore the efficiency of the system will be lower than expected. In this case the financial success is not yet reached. Each different order will need to have a customized cost, applicable to the relevant building. Afterwards, a plan for financial success can be established. The return on investment by harvesting energy, instead of collecting from the grid, is desired to be larger in the future. When more systems are operational, software updates should maximize the production of sustainable energy and therefore give a higher return on investment.

Public success: The development for renewable energy sources grows each day, however in the building environment, such as a city, no real solutions exist and/or are market ready. Therefore the solution of harvesting wind energy on the side of a high-rise building will gather a lot of attention from the public, pushing companies and governments to invest in these kinds of renewable energy.

Sustainability success: Although the costs of investment are large, the vision on sustainability for this project is leading in its own sector. All buildings that embark in the system will be seen as sustainable. Companies that want to be associated with a green and climate progressive nature will want to be linked to a system pioneering in producing clean energy.

8.7.2. Goals and Priorities

No project evolves by sitting on the sidelines and wait for opportunities. Therefore goals and priorities are set to achieve after the first implementation of the system in The Netherlands. All different aspects that are looked at will be discussed.

Expanding markets: The Netherlands is just the beginning as a huge potential for a market in Asia and the middle east, with less strict restrictions for shadow or noise, could raise awareness in new sustainable technologies. More buildings can be found in this part of the world that the system can be applied to. The unit price can be lowered by selling more systems, because it will be more approachable for lower buildings as stated in Section 8.4. Renewable energy sources and a fossil free future, are two large factors in the growing and expanding market for wind energy systems.

Building a company and brand: To branch out, the first step is to scale up the team from research group to production company. This involves hiring personnel, departmentalizing our company structure, but mostly, building a brand. This entails quality management and assurance for our product, positive press on the first system in Rotterdam, and a professional environment to conduct business in. This phase will most likely take from half to a full year. A brand that is respected and trusted is the most important part when entering the Asian market. The name Urbanergy should be well known on the market for wind harvesting.

Logistics: If branching out is to be facilitated, the production of the different parts should be easily explainable to

local manufacturers. Moreover, in new areas trust persons should be appointed to work as stated in Section 8.3. This person will then help with familiar routes and companies specialized in the installation of systems high above the ground. All the systems that will be implemented are known by many and therefore safety is good for the reputation of the brand. Every step in the logistic process from manufacturing to operation, that trust person will make sure the system shall not be damaged.

Production line improvements: As stated in the logistical part of expansion, production will become a major part of attention. To keep the original sustainable vision, parts will need to be produced in the country and/or city where the system will become operational. Therefore, multiple manufacturers shall be contracted to streamline this process and keep the production of the system as sustainable as possible.

9
Conclusion and Recommendation

This chapter gives the conclusion regarding the project and the final design, which will be discussed in Section 9.1. Later in Section 9.2, recommendations on the design are mentioned, which can be performed in later studies in this field of work.

9.1. Conclusion

From the start of the project, the mission was to "Provide a local sustainable wind-energy harvesting source for urban usage" [119]. A set of driving requirements was given which created a design environment. Early on in the design process, the team realized that the requirement on storage was not necessary as the total required power generation per year was too low in comparison to the average power usage of two 200 meters high buildings. If in the future larger systems are requested, a storage system could be relevant again and the already researched possibilities could be considered.

One of the other important requirements was the noise production, due to the urban environment that the system will be operating in. The requirement on this is not met with the calculations done in the final design phase. Therefore, it is concluded that more in-depth investigation will need to be performed to finalize and improve the noise on WindVine. Any recommendations on this are stated in Section 9.2. After thorough market analysis it is concluded that a large market can be reached when the system is proven in the real world. This is reasoned by two main arguments. Firstly, the designed system is not restricted to the combination of two high-rise buildings close to each other. This opens a large amount of new locations for implementation. Secondly, the designed system is not required to be mounted to a high-rise building of at least 300 meters high, but just needs a minimal height of 148 meters. Again, this enlarges the market.

The last conclusion that can be made on the final design is on the given budget. The requirement for the budget to create a harvesting system below the cost of 75,000 euro is heard and complied with. When storage or more electricity is required, the result will be that the budget also needs to increase.

9.2. Recommendation

Technology is always moving forward and research will not come to an end soon. This also applies to the investigations regarding wind energy harvesting. During the detailed design phase, the final layout of the system is found. All the dimensions of the design have now been preliminary determined. These values are obtained by making various assumptions that do not always reflect with reality. Because of this, and the arguments stated in this section, recommendations are made.

Noise reduction: Regarding noise there are multiple hardware recommendations to the system mentioned in Subsection 4.5.8. One of the software recommendations is to create a program that can predict the vibration and structural born noise more precisely. The current program is not able to provide noise numbers that represent reality completely and more precise final values allow the investigators to make a better decision on the choice of noise reduction hardware.

Sustainable materials: Up until this point of the design, the reliability and certainty of bio materials is not investigated. More conventional materials are used in the production of the system. This option can be researched in a later stadium to, hopefully, find even more sustainable solutions for the production of the turbine.

Brakes: In the design of the shaft the braking torque is not taken into account. The thickness of the shaft is not designed for a maximum braking torque. Due to this, the time of the emergency stop is long. A recommendation for the next phase of designing is to include the maximum braking torque into the structural analysis of the shaft.

Cables: The cabling was not taken into account, but considered during the last week of the final design phase. It would then be possible of creating a fail safe version of the turbine. The fail safe turbine will consist of cables running through the turbine parts. When one of the structural components fails, the cables will ensure that the parts will not fall to the ground. The other end of the cable is namely attached to the building, and are designed to withstand the weight of their respective component if their initial support fails.

Bibliography

[1] P. Irwin, J. Kilpatrick, J. Robinson, and A. Frisque, *Wind and tall buildings: negatives and positives,* The structural design of tall and special buildings **17**, 915 (2008).

[2] DSE Group 03, *Dse: Baseline report – wind energy system integrated between high-rise buildings,* (2020).

[3] DSE Group 03, *Dse: Midterm report – wind energy system integrated between high-rise buildings,* (2020).

[4] M. Terterov, *Investing in St Petersburg* (GMB Publishing, 2005).

[5] V. Bhargava and R. Samala, *Acoustic Emissions from Wind Turbine Blades,* Journal of Aerospace Technology and Management **11** (2019).

[6] H. A. Michael Taylor, Pablo Ralon and S. Al-Zoghoul, *Renewable Power Generation Costs in 2019* (IRENA, 2020).

[7] *Jaaroverzicht van het weer in Nederland*, Klimaatdata en -advies, Koninklijk Nederlands Meteorologisch Institut (KNMI) (Ministerie van Verkeer en Waterstaat, 2010-2019).

[8] S. Emeis and M. Turk, *Comparison of logarithmic wind profiles and power law wind profiles and their applicability for offshore wind profiles,* (Springer, 2007) pp. 61–64.

[9] L. Lu and K. Y. Ip, *Investigation on the feasibility and enhancement methods of wind power utilization in high-rise buildings of hong kong,* Renewable and Sustainable Energy Reviews **13**, 450 (2009).

[10] A. D. Zegeye, *Boundary layer concept,* in *Fluid Mechanics* (Debre Markos Unviversity, 2017) Chap. 6, p. 81.

[11] S. Mertens, *Wind Energy in the Built Environment* (Multi-Science, 2006).

[12] ESDU, *Strong winds in the atmospheric boundary layer. part 1: hourly-mean wind speeds,* (1982).

[13] G. Harding, P. Harding, and A. Wilkins, *Wind turbines, flicker, and photosensitive epilepsy: Characterizing the flashing that may precipitate seizures and optimizing guidelines to prevent them,* Epilepsia **49**, 1095 (2008).

[14] A. Orrel and E. Poehlman, *Benchmarking U.S. Small Wind Costs*, Tech. Rep. (Pacific Nortwest National Laboratory, 2017).

[15] P. Christensen and L. R. Dysert, *Cost estimate classification system – as applied in engineering, procurement, and construction for the process industries,* AACE International Recommended Practice (2005).

[16] B. L. Ennis and D. T. Griffith, *System levelized cost of energy analysis for floating offshore vertical-axis wind turbines.* Renewable Energy (2018), 10.2172/1466530.

[17] Y. Bazilevs, A. Korobenko, X. Deng, J. Yan, M. Kinzel, and J. Dabiri, *Fluid–structure interaction modeling of vertical-axis wind turbines,* Journal of Applied Mechanics **81** (2014), 10.1115/1.4027466.

[18] G. Karpati, T. Hyde, H. Peabody, and M. Garrison, *Resource management and contingencies in aerospace concurrent engineering,* Aerospace Research Central (2012).

[19] J. Diehl, *DESIGN FOR SUSTAINABILITY, A STEP-BY-STEP APPROACH* (UNEP AND Delft University of Technology, 2008).

[20] D. Djairam, *The electrostatic wind energy converter : electrical performance of a high voltage prototype* (Delft University of Technology, 2008).

[21] A. Yusof and M. R. Mohamed, *Vertical axis wind turbines: An overview,* in *InECCE2019* (Springer Singapore, Singapore, 2020) pp. 821–835.

[22] B. Habtamu and Y. Yingxue, *Effect of camber airfoil on self starting of vertical axis wind turbine,* Journal of Environmental Science and Technology **4** (2011), 10.3923/jest.2011.302.312.

[23] M. M. A. Bhutta, N. Hayat, A. U. Farooq, Z. Ali, S. R. Jamil, and Z. Hussain, *Vertical axis wind turbine – a review of various configurations and design techniques,* Renewable and Sustainable Energy Reviews , 1926 (2012).

[24] J. Damota, I. Lamas, A. Couce-Casanova, and J. Rodriguez-Garcia, *Vertical axis wind turbines: Current technologies and future trends,* in *International Conference on Renewable Energies and Power Quality (ICREPQ'15)*, Vol. 1 (2015) pp. 530–535.

[25] R. Kishore, C. Stewart, and P. Shashank, *Wind Energy Harvesting - Micro- to Small-Scale Turbines* (De Gruyter, 2018).

[26] J. Park, H.-J. Jung, S.-W. Lee, and J. Park, *A new building-integrated wind turbine system utilizing the building,* Energies **8**, 11846 (2015).

[27] Marshall Day Acoustics, *Examination of the significance of noise in relation to onshore wind farms,* (2013).

[28] E. Koppen and K. Fowler, *International legislation for wind turbine noise,* (2015).

[29] Ministerie van Volkshuisvesting, Ruimtelijke Ordening en Milieubeheer, *Besluit van 19 oktober 2007 houdende algemene regels voor inrichtingen (besluit algemene regels voor inrichtingen milieubeheer),* (2007).

[30] D. Marten and J. Wendler, *Qblade guidelines,* (2013).

[31] M. Alaskari, O. Abdullah, and M. Majeed, *Analysis of wind turbine using qblade software,* (2019).

[32] H. Madsen, *The actuator cylinder - a flow model for vertical axis wind turbines,* (1982).

[33] M. Ahmadi-Baloutaki, R. Carriveau, and D. Ting, *Straight-bladed vertical axis wind turbine rotor design guide based on aerodynamic performance and loading analysis,* Proceedings of the Institution of Mechanical Engineers, Part A: Journal of Power and Energy **228**, 742 (2014).

[34] O. Günel, *Comparison of cfd and xfoil airfoil analyses for low reynolds number,* International Journal of Energy Applications and Technologies **3**, 83 (2016).

[35] F. Mahmuddin, S. Klara, H. Sitepu, and S. Hariyanto, *Airfoil lift and drag extrapolation with viterna and montgomerie methods,* Energy Procedia **105**, 811 (2017).

[36] M. Ahmadi-Baloutaki, R. Carriveau, and D. S. Ting, *Straight-bladed vertical axis wind turbine rotor design guide based on aerodynamic performance and loading analysis,* Proceedings of the Institution of Mechanical Engineers, Part A: Journal of Power and Energy **228**, 742 (2014).

[37] I. Paraschivoiu, *Wind turbine design: with emphasis on Darrieus concept* (Presses inter Polytechnique, 2002).

[38] A. Solum, P. Deglaire, S. Eriksson, M. Rahm, M. Leijon, and H. Bernhoff, *Design of a 12kw vertical axis wind turbine equipped with a direct driven pm synchronous generator,* European Wind Energy Conference and Exhibition 2006, EWEC 2006 **1**, 122 (2006).

[39] C. Ferreira, H. Madsen, M. Barone, B. Roscher, P. Deglaire, and I. Arduin, *Comparison of aerodynamic models for vertical axis wind turbines,* Journal of Physics: Conference Series **524**, 012125 (2014).

[40] G. Bangga, G. Hutomo, R. Wiranegara, and H. Sasongko, *Numerical study on a single bladed vertical axis wind turbine under dynamic stall,* Journal of Mechanical Science and Technology **31**, 261 (2017).

[41] J. Yen and N. Ahmed, *Enhancing vertical axis wind turbine by dynamic stall control using synthetic jets,* Journal of Wind Engineering and Industrial Aerodynamics **114**, 12 (2013).

[42] B. Kirke, *Evaluation of self-starting vertical axis wind turbines for stand-alone applications,* (1998).

[43] M. Raciti Castelli, D. Betta, and E. Benini, *Effect of blade number on a straight-bladed vertical-axis darreius wind turbine,* World Academy of Science, Engineering and ... **61** (2012).

[44] M. Hameed and S. Afaq, *Design and analysis of a straight bladed vertical axis wind turbine blade using analytical and numerical techniques,* Ocean Engineering **57**, 248 (2013).

[45] W. Tong, *Wind power generation and wind turbine design* (WIT press, 2010).

[46] S. Brusca, R. Lanzafame, and M. Messina, *Design of a vertical-axis wind turbine: how the aspect ratio affects the turbine's performance,* International Journal of Energy and Environmental Engineering **5**, 333 (2014).

[47] M. Islam, D. Ting, and A. Fartaj, *Desirable airfoil features for smaller-capacity straight-bladed vawt,* Wind Engineering **31**, 165 (2007).

[48] M. D. SN, P. Tapre, and C. Veeresh, *A comparative study of constant speed and variable speed wind energy conversion systems,* GRD Journals- Global Research and Development Journal for Engineering **1** (2016).

[49] W. Tjiu, T. Marnoto, S. Mat, M. H. Ruslan, and K. Sopian, *Darrieus vertical axis wind turbine for power generation i: Assessment of darrieus vawt configurations,* Renewable Energy **75**, 50 (2015).

[50] D. Marten, J. Wendler, G. Pechlivanoglou, C. N. Nayeri, and C. Paschereit, *Qblade: an open source tool for design and simulation of horizontal and vertical axis wind turbines,* IJETAE **3**, 264 (2013).

[51] J. Kjellin, F. Bülow, S. Eriksson, P. Deglaire, M. Leijon, and H. Bernhoff, *Power coefficient measurement on a 12 kw straight bladed vertical axis wind turbine,* Renewable energy **36**, 3050 (2011).

[52] C. Pearson, *Vertical axis wind turbine acoustics,* Ph.D. thesis, University of Cambridge (2014).

[53] A. J. Fiedler and S. Tullis, *Blade offset and pitch effects on a high solidity vertical axis wind turbine,* Wind engineering **33**, 237 (2009).

[54] S. Ilin, H. Dumitrescu, V. Cardos, and A. Dumitrache, *A free wake method for performance prediction of vawt,* AIP Conference Proceedings **1479**, 1635 (2012).

[55] M. Rossander, E. Dyachuk, S. Apelfröjd, K. Trolin, A. Goude, H. Bernhoff, and S. Eriksson, *Evaluation of a blade force measurement system for a vertical axis wind turbine using load cells,* Energies **8**, 5973 (2015).

[56] R. Kishore, C. Stewart, and S. Priya, *Wind Energy Harvesting: Micro-to-small Scale Turbines* (Walter de Gruyter GmbH & Co KG, 2018).

[57] C. Anderson, *Wind Turbines: Theory and Practice* (Cambridge University Press, 2020).

[58] C. Nayar, S. Islam, H. Dehbonei, K. Tan, and H. Sharma, *Power electronics for renewable energy sources,* in *Power electronics handbook* (Elsevier, 2011) pp. 723–766.

[59] P. S. Veers, *Wind Energy Modeling and Simulation, Volume 2: Turbine and System*, Tech. Rep. (National Renewable Energy Lab.(NREL), Golden, CO (United States), 2019).

[60] R. I. Putri, S. Adhisuwignjo, and M. Rifa'i, *Design of simple power converter for small scale wind turbine system for battery charger,* in *2018 3rd International Conference on Information Technology, Information System and Electrical Engineering (ICITISEE)* (IEEE, 2018) pp. 169–173.

[61] Y. Yasa and E. Mese, *Design and analysis of generator and converters for outer rotor direct drive gearless small-scale wind turbines,* in *2014 International Conference on Renewable Energy Research and Application (ICRERA)* (IEEE, 2014) pp. 689–694.

[62] S. Tripathi, A. Tiwari, and D. Singh, *Grid-integrated permanent magnet synchronous generator based wind energy conversion systems: A technology review,* Renewable and Sustainable Energy Reviews **51**, 1288 (2015).

[63] M. Lindegger, H. BINNER, B. EVÉQUOZ, and D. SALATHÉ, *Economic viability, applications and limits of efficient permanent magnet motors,* Switzerland: Swiss Federal Office of Energy (2009).

[64] R. Afify, H. Elgamal, and E. Saber, *Performance of sb-vawt using a modified double multiple streamtube model,* Alexandria Engineering Journal **57** (2018), 10.1016/j.aej.2018.07.009.

[65] J. Kjellin and H. Bernhoff, *Electrical starter system for an h-rotor type vawt with pm-generator and auxiliary winding,* Wind Engineering **35**, 85 (2011).

[66] *IEC 61400-1: Wind turbines - Part 1: Design requirements*, International Electrotechnical Commission, 3rd ed. (2005).

[67] J. P. Lyons, A. A. M. Esser, and P. S. Bixel, *Method and system for wind turbine braking,* General Electrics Company (1997), filed: 09 June. United States Patent. Patent no. US5907192A.

[68] Q. Mo, J. Wen, X. Liu, and J. Wang, *The brake system and method of the small vertical axis wind turbine,* (2016).

[69] E. A. Sirotkin, E. V. Solomin, S. A. Gandzha, and I. M. Kirpichnikova, *Backup mechanical brake system of the wind turbine,* Journal of Physics: Conference Series **944** (2018).

[70] J. Clarke, L. Hancox, D. Mackenzie, and M. Whelan, *Design of a Vertical-Axis Wind Turbine Final Report*, Tech. Rep. (MUN VAWT Design, 2014).

[71] D. Jiang and J. Wang, *Braking equipment for vertical shaft wind generator and braking method therefor,* National Wind Energy Co Ltd (2011), filed: 31. January. European Patent Office. Patent no. EP2535560A1.

[72] J. Kang and H. Lee, *The Development of Rotor Brakes for Wind Turbines,* International Journal of Applied Engineering Research **12**, 5094 (2017).

[73] European parliament and Council of European Union, *Directive 2002/49/ec of the european parliament and of the council of 25 june 2002 relating to the assessment and management of environmental noise,* (2002).

[74] J. D. M. Botha, *Predictions of Rotor Broadband Noise* (Trinity College Dublin, 2013).

[75] S. Buck, S. Oerlemans, and S. Palo, *Experimental characterization of turbulent inflow noise on a full-scale wind turbine,* Journal of Sound and Vibration **385** (2016), 10.1016/j.jsv.2016.09.010.

[76] F. Huanhuan, L. Yong, W. Qi, and Z. Sen, *Numerical study on tone noise of different thickness airfoils,* IOP Conference Series: Materials Science and Engineering **538**, 012052 (2019).

[77] A. Skagerstrand, S. Köbler, and S. Stenfelt, *Loudness and annoyance of disturbing sounds – perception by normal hearing subjects,* International Journal of Audiology **56**, 775 (2017).

[78] S. Roy and P. Naik, *Simulation Study of Active Noise Control in Wind Turbines Using FxLMS Adaptation Algorithm,* Journal of Power and Energy Engineering **5**, 72 (2017).

[79] A. Rubio Carpio, R. Merino Martínez, F. Avallone, D. Ragni, M. Snellen, and S. van der Zwaag, *Experimental characterization of the turbulent boundary layer over a porous trailing edge for noise abatement,* Journal of Sound and Vibration **443**, 537 (2019).

[80] M. Herr, K.-S. Rossignol, J. Delfs, M. Mößner, and N. Lippitz, *Specifcation of porous materials for low-noise trailing-edge applications,* (2014).

[81] Y. Mayer, B. Lyu, H. Jawahar, and M. Azarpeyvand, *A semi-analytical noise prediction model for airfoils with serrated trailing edges,* Renewable Energy **143** (2019).

[82] C. A. Leon, F. Avallone, and D. Ragne, *Piv investigation of the flow past solid and slitted sawtooth serrated trailing edges,* AIAA Aero- space Sciences Meeting (2016).

[83] B. Lyu, M. Azarpeyvand, and S. Sinayoko, *Prediction of noise from serrated trailing edges,* J. Fluid Mech. , 556 (2016).

[84] M. Howe, *Aerodynamic noise of a serrated trailing edge,* Journal of Fluids and Structures , 33 (1991).

[85] R. Parchen, *A prediction scheme for trailing edge noise based on detailed boundary layer characteristics,* TNO-Report HAG-RPT (1998).

[86] D. Chase, *Modeling the wavevector-frequency spectrum of turbulent boundary layer wall pressure,* Journal of Sound and Vibration **70**, 29 (1980).

[87] R. GmbH, *Technical information: Plexiglas® soundstop xt birdguard,* Riedbahnstraße 70, 64331 Weiterstadt Germany (2020), ref.No: 232-33.

[88] W. Musial and C. Butterfield, *Using partial safety factors in wind turbine design and testing,* University of North Texas Libraries, UNT Digital Library (1997).

[89] M. Ashby, *CES Edupack* (GRANTA, 2019).

[90] R. Hibbeler, *ENgineering mechanics: Statics* (Pearson, 2017).
[91] International Code Council, *2018 international building code,* (2018).
[92] D. Gorman, *Free vibration analysis of beams and shafts* (Wiley, 1975).
[93] O. Bauchau and J. Craig, *Euler-bernoulli beam theory,* in *Structural analysis* (Springer, 2009) pp. 173–221.
[94] P. Gipe, *Wind power, revised edition: renewable energy for home, farm, and business,* New York, Chelsea Green (2004).
[95] R. C. Hibbeler and S. Fan, *Mechanics of Materials*, Vol. 2 (Prentice Hall Upper Saddle River, 2017).
[96] W. D. Musial and C. Butterfield, *Using partial safety factors in wind turbine design and testing*, Tech. Rep. (National Renewable Energy Lab., Golden, CO (United States), 1997).
[97] Y. Daito, M. Matsumoto, and K. Araki, *Torsional flutter mechanism of two-edge girders for long-span cable-stayed bridge,* Journal of Wind Engineering and Industrial Aerodynamics **90**, 2127 (2002).
[98] D. J.Inman, *Engineering Vibration* (Pearson, 2014).
[99] A. Moorhouse, A. Elliott, G. Eastwick, T. Evans, A. Ryan, S. von Hunerbein, V. le Bescond, and D. Waddington, *Structure-borne sound and vibration from building-mounted wind turbines,* Environmental research letters **6** (2011), doi:10.1088/1748-9326/6/3/035102.
[100] A. Moorhouse, A. Elliott, and A. Evans, *In situ measurement of the blocked force of structure-borne sound sources,* Journal of Sound and Vibration **325**, 679 (2009).
[101] A. Elliott, G. Pavíc, and A. Moorhouse, *measurement of force and moment mobilities using a finite difference technique,* Proceedings Acoustics Paris 2008 , 3339 (2008).
[102] A. Moorhouse, A. Elliott, G. Eastwick, T. Evans, A. Ryan, S. von Hunerbein, V. le Bescond, and D. Waddington, *Noise and vibration from building mounted micro wind turbines* (University of Salford, 2011).
[103] D. C. Giancoli, *Physics for Scientists & Engineers with Modern Physics* (earson Education Inc, 2009).
[104] M. Nini, V. Motta, G. Bindolino, and A. Guardone, *Three-dimensional simulation of a complete vertical axis wind turbine using overlapping grids,* Journal of Computational and Applied Mathematics **270**, 78 (2014).
[105] C. Yongning, L. Yan, L. Zhen, C. Ziyu, and L. Hongzhi, *Study on grid-connected renewable energy grid code compliance,* in *2019 IEEE Sustainable Power and Energy Conference (iSPEC)* (IEEE, 2019) pp. 72–75.
[106] B. Hahn, M. Durstewitz, and K. Rohrig, *Reliability of wind turbines: Experiences of 15 years with 1,500 wts,* Fraunhofer IWES (2006).
[107] S. Ozturk, *Forecasting Wind Turbine Failures and Associated Costs* (Columbia University, 2019).
[108] M. D. Reder, E. Gonzalez, and J. J. Melero, *Wind turbine failures - tackling current problems in failure data analysis,* Journal of Physics: Conference Series **753**, 072027 (2016).
[109] J. Carroll, A. Mcdonald, and D. Mcmillan, *Failure rate, repair time and unscheduled o&m cost analysis of offshore wind turbines,* Wind Energy **19** (2015), 10.1002/we.1887.
[110] J. Sinke, *Production of Aerospace Systems - Reader* (Technische Universiteit Delft, 2019).
[111] M. Shafiee, *Maintenance logistics organization for offshore wind energy: Current progress and future perspectives,* Renewable Energy **77**, 182 (2015).
[112] T. Stehly and P. Beiter, *2018 Cost of Wind Energy Review,* Tech. Rep. (National Renewable Energy Laboratory, 2019).
[113] F. Ueckerdt, L. Hirth, G. Luderer, and O. Edenhofer, *System lcoe: What are the costs of variable renewables?* Energy **63**, 61 (2013).
[114] L. Ziegler, E. Gonzalez, T. Rubert, U. Smolka, and J. J. Melero, *Lifetime extension of onshore wind turbines: A review covering germany, spain, denmark, and the uk,* Renewable and Sustainable Energy Reviews **82**, 1261 (2018).
[115] I. Staffell and R. Green, *How does wind farm performance decline with age?* Renewable energy **66**, 775 (2014).
[116] IRENA, *Renewable power generation costs in 2017,* Report, International Renewable Energy Agency, Abu Dhabi (2018).
[117] M. Gough, M. Lotfi, R. Castro, A. Madhlopa, A. Khan, and J. P. Catalão, *Urban wind resource assessment: A case study on cape town,* Energies **12**, 1479 (2019).
[118] T. Kealy, M. Barrett, and D. Kearney, *How profitable are wind turbine projects? an empirical analysis of a 3.5 mw wind farm in ireland,* International journal on recent technologies in mechanical and electrical engineering **2** (2015).
[119] DSE Group 03, *Dse:project plan – wind energy system integrated between high-rise buildings,* (2020).

A

Functional Breakdown Structure

A functional breakdown structure of the Urbanergy WindVine is given in Figure A.1. It is subdivided into five main parts. Starting from measuring the environmental conditions, the data is then used to effectively start the wind harvest system. The produced electricity then needs to be managed and distributed to the building grid through the supporting structure.

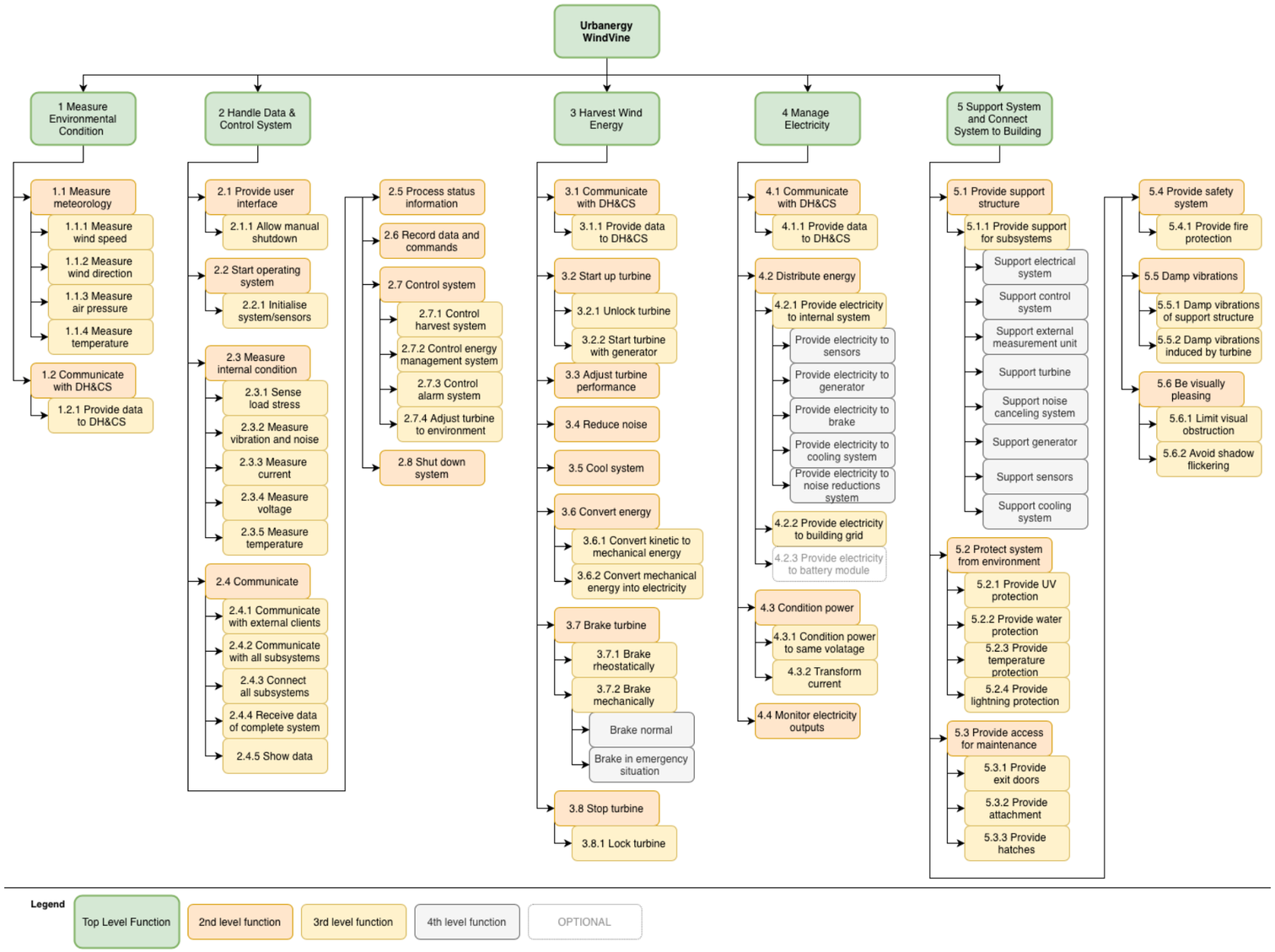

Figure A.1: Functional Breakdown Structure

B

Material Overview

For the design of the WHS aluminium 7075-T6, stainless steel, low and medium carbon steel, isotropic CFRP, GFRP, sisal Polylactic Acid (PLA) (bio composite) and Bamboo were considered. An overview of the respective material characteristics is shown in Table B.1.

Table B.1: Overview of Material Properties [1]

Parameter	Unit	AL 7075-T6	Stainless Steel	Low Carbon Steel	Medium Carbon Steel	Sisal-PLA	Bamboo	CFRP*	GFRP
Yield Strength	MPa	503	698.5	305	652.5	146	39.95	800	151
Compressive strength	MPa	530	726	305	652.5	n/a	79.95	640	172.5
Fatigue Strength (>10^7 cycles)	MPa	159.5	399	240.5	389	73	34.35	225	251
Shear Strength**	MPa	95.7	239.4	144.3	233.4	87.6	23.97	25.31	40
Shear Modulus	GPa	26.7	78	81.5	81	n/a	1.08	44	8.5
Youngs Modulus	GPa	72	200	210	210	15	35	109.5	21.5
Density	kg/m^3	2755	7740	7810	7800	1324	699.5	1550	1860
Cost	€/kg	3.68	2.69	0.66	0.66	1.95	1.44	31.3	23.2
Recyclable	yes/no	yes	yes	yes	yes	biodegradeable		no	no
Resistant to Environment***	$rating$	4	4	2.33	2.33	n/a	2	3.67	3.67
CO2 to produce	kg_{CO_2}/kg	13.05	5.45	2.44	2.49	2.44	1.06	48.15	13.31
Workability****	$rating$	3.7	3.7	4.2	4	3.4	1.1	1.2	1.4******

*Quasi-isotropic layup
**0.6 of yield strength (www.indfast.org/about/faq.asp?#15 and for composites (www.performance-composites.com/carbonfibre/mechanicalproperties_2.asp)
***Average value of rating 0-4 including: Rural and Industrial environment, UV
****Average value of rating 0-5 including: Castability, Formability, Machinability, Weldability, Solder/brazability
*****All values taken from [89], unless otherwise stated

For noise reduction, an extra panel made of Plexiglas® Soundstop XT BirdGuard [87] was considered. The advantages and properties of this material are given in Table B.2.

Table B.2: Advantages and material properties of Plexiglas® Soundstop XT BirdGuard [87].

Advantages	**Properties**	**Value**	**Unit**
Excellent light transmission and brilliance	Light transmission	>92	%
Extremely high weather resistance	Thickness	12-15-20-25	mm
Ease of fabrication	Width	2000	mm
High surface hardness	Length	up to 6000	mm
Low weight – half the weight of glass	Density	1.19	g/cm^3
11 times the impact strength of glass	Sound Reduction	29-35-32-33	dB
100% recyclable	Bird protection	embedded stripes	

C

Catia Drawings of Final Design

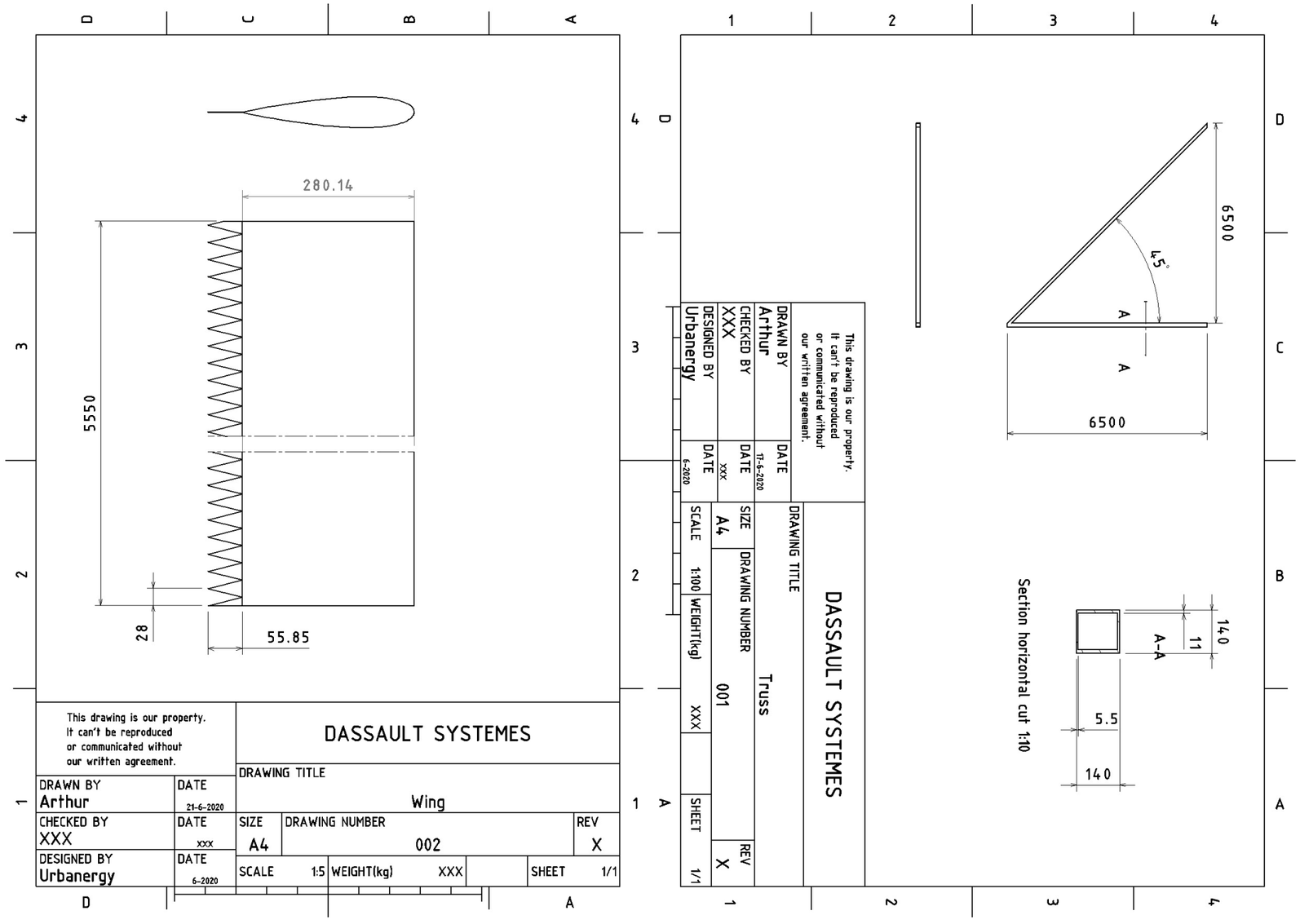

Figure C.1: Technical drawings of the blade and part of the truss structure

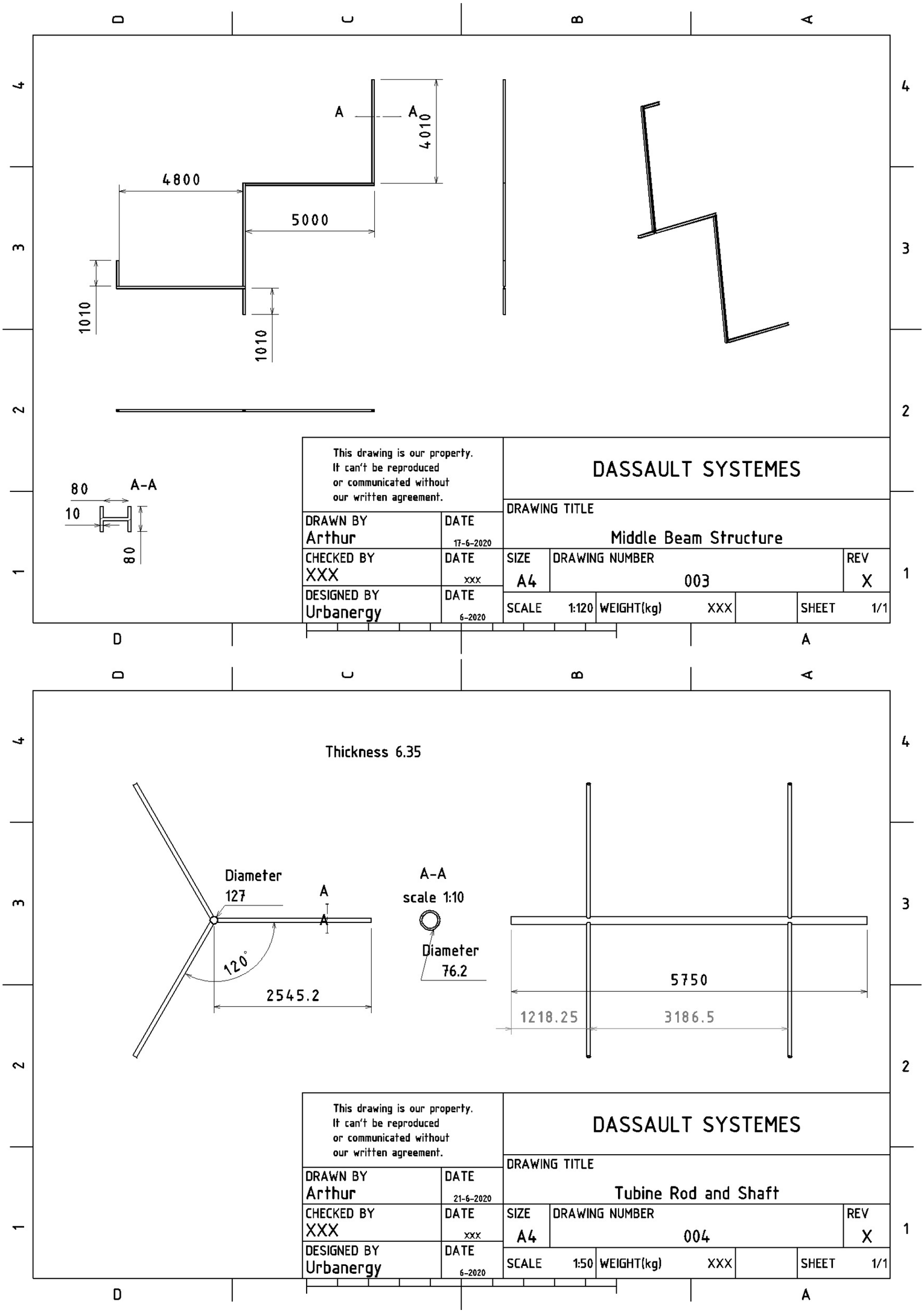

Figure C.2: Technical drawings of the turbine rotor and beam structure